JAERI-Review
98-019

ANNUAL REPORT OF NAKA FUSION RESEARCH ESTABLISHMENT FROM APRIL 1, 1997 TO MARCH 31, 1998

November 1998

Naka Fusion Research Establishment

日本原子力研究所
Japan Atomic Energy Research Institute

本レポートは，日本原子力研究所が不定期に公刊している研究報告書です。
入手の問合わせは，日本原子力研究所研究情報部研究情報課（〒319-1195　茨城県那珂郡東海村）あて，お申し越しください。なお，このほかに財団法人原子力弘済会資料センター（〒319-1195　茨城県那珂郡東海村日本原子力研究所内）で複写による実費頒布をおこなっております。

This report is issued irregularly.
Inquiries about availability of the reports should be addressed to Research Information Division, Department of Intellectual Resources, Japan Atomic Energy Research Institute, Tokai-mura, Naka-gun, Ibaraki-ken, 319-1195, Japan.

編集兼発行　　日本原子力研究所

JAERI-Review 98-019

Annual Report of Naka Fusion Research Establishment from April 1, 1997 to March 31, 1998

Naka Fusion Research Establishment

Japan Atomic Energy Research Institute
Naka-machi, Naka-gun, Ibaraki-ken

(Received October 1, 1998)

This report provides an overview of research and development activities at Naka Fusion Research Establishment, JAERI, during the period from April 1, 1997 to March 31, 1998.
The activities in Naka Fusion Research Establishment are highlighted by high temperature plasma research in JT-60 and JFT-2M, and progress in ITER-EDA, including technology development.

The objectives of the JT-60 project are to contribute to the ITER physics R&D and to establish the physics basis for a steady state tokamak fusion reactor like SSTR.

Improvements and regulation of the facilities and developments of the instruments were performed. The construction for the divertor modification from the original open type to the W-shaped semi-closed type for improving the particle control was finished in May 1997. The modification intends to investigate effects of divertor geometry on divertor functions such as particle and impurity controls, and to realize radiative divertor compatible with good confinement.

With respect to the negative-ion based NBI, input power to the plasma was gradually increased along with improvement of operational optimization to attain 5.2 MW at 350 keV with deuterium negative ion beams and 4.2 MW at 360 keV with hydrogen negative ion beams.

Experiments simulating the helium exhaust in ITER were performed with the W-shaped pumped divertor. Helium atoms introduced in the ELMy-H plasmas for 6 sec by helium neutral beam injection were efficiently exhausted by helium pumping with Ar frosted cryopumps in the divertor. The experiments successfully demonstrate high helium exhaust capability of $\tau_{He}^{*}/\tau_{E} \approx 4$ in steady state, which satisfies the ITER requirement. These results strongly support the divertor design of ITER.

Because long heating time with a total heating energy of 203 MJ was achieved without

---

Editors: Seki, M., Shimizu, K., Seki, M., Nagashima, T., Shoji, T., Okabe, T

harmful increase in impurity and particle recycling, a DT equivalent fusion gain of $Q_{DT}^{eq} \approx 0.1$ was sustained for 9 sec in an ELMy-H mode.

Toward the advanced feedback controls of multiple parameters, the JT-60U started new feedback controls of central line density and divertor neutral gas pressure in addition to the existing controls of off-axis line density, radiation power and neutron production rate. Characteristics of halo current during disruptions were also studied. The NNB-driven current was identified directly from the internal magnetic measurement and driven current profile was confirmed to be consistent with the ACCOME calculation. The current profile control with LHCD successfully sustained the internal transport barrier in reversed shear plasmas. Continuous TAE modes were observed with NNB for the first time in the world as beam-driven TAE modes.

Objectives of the JFT-2M program are (1) advanced and basic researches for the development of high-performance plasmas for nuclear fusion and (2) contribution to the physics R&D for ITER, taking full advantage of flexibility of a medium-size device.

In the closed divertor experiments, it is found that the closer the divertor geometry becomes, the wider the high confinement regime coexistent with a dense and cold divertor plasma results. A compact toroid (CT) injection system has been installed in collaboration with the Himeji Institute of Technology for the development of the advanced fueling for fusion reactors, such as ITER. Encouraging results were obtained with initial CT injection experiments, such that reduction of radiation loss power was observed after the CT injection into OH plasmas. A heavy ion beam probe system, which was developed by the National Institute for Fusion Science has been installed for clarifying mechanism of improved confinement more definitely through fast measurements of the electric field.

The primary objective of theory and analysis is to improve the physical understanding of the magnetically confined tokamak plasma. Remarkable progress has been made on physical understanding of the reduced transport and the stability not only of ideal MHD modes but also of kinetic ballooning mode in reversed shear plasmas. Progress was also made on the neoclassical transport calculation by the Matrix Inversion method and on the scaling law of an offset nonlinear form for the ELMy-H-mode confinement. A five-point model for the scrape-off layer and divertor plasmas was developed and the inside/outside divertor asymmetry was investigated.

The main focus of the NEXT (Numerical Experiment of Tokamak) project is to simulate tokamak plasmas using particle and fluid models on the developing technology of massively parallel computers. A particle-fluid hybrid model was developed for simulation of the kinetic MHD instabilities. The self-generated radial electric field derived by the Reynolds stress and its effect on transport have been studied to contribute to understanding of improvement of the confinement.

R&D of fusion reactor technology has been focused on the ITER/EDA-related area. Major highlights in FY1997 are as follows.

Winding and heat treatment of Nb_3Sn conductors of all eight layers for the outer module of

ITER CS model coil have been successfully completed and the assembling technology for the model coil has been developed. Production of 46 kA cable of Nb_3Al strands for the insert coil was also completed.

Fabrication of two full-scale 1/40-sector models of the ITER vacuum vessel was completed in the end of September 1997. The cross section is D-shape of 15 m high and 9 m wide. Both sectors, each of which uses different fabrication procedures and welding techniques, satisfy a dimensional accuracy of within ±3 mm. Hot isostatic pressing (HIP) technology was developed to fabricate a prototype mock-up of ITER shield blanket modules. Regarding the development of ITER divertor, full scale mock-ups of the vertical plates and the wings were successfully fabricated using newly developed bonding technology. The mock-ups were subjected to thermal cycle tests under an ITER steady-state heat load condition of 5 MW/m^2. The tests prove that all the mock-ups can endure the heat load for a repetition of 10^3 cycles without any damages. As to the development of the ITER blanket handling system, performance tests of the full-scale vehicle system was started for demonstration of remote replacement of 4 ton blanket modules.

A stable negative hydrogen ion beam of 25 mA has been successfully accelerated to 1 MeV with a five-staged accelerator. Development of a gyrotoron has progressed to deliver a maximum energy of 520 kW for 5 sec at 170 GHz with a diamond disk window. A large caisson of 12 m^3 was installed in a room of TPL to investigate tritium behavior released into confinement system and environment.

In the fusion reactor design, the DREAM design activity was focused on the prototype reactor. In the area of safety research, safety evaluation code development, LOVA and ICE experiments using small scale models, and the study of tokamak dust removal methods were also carried out.

The Final Design Report (FDR) of ITER was issued by the Director in December 1997. After the review by the Technical Advisory Committee (TAC) in January 1998, the FDR was presented to the ITER Council at its 13th Meeting held in February 1998. The FDR is composed of various technical documents on the detailed design of plasma parameters, tokamak components, plant system and the tokamak building. The major results of safety analyses described in the Non-site Specific Safety Report (NSSR) -2 was also included in the FDR. The technical review of the FDR is being conducted by the four Parties. The Japanese Home Team contributes to the design progress in the various fields through the conduction of design tasks in close collaboration with the Joint Central Team (JCT). The JCT member built up to 161 including 46 Japanese members as of December 1997.

Keywords: Fusion Research, JAERI, JT-60, JFT-2M, DIII-D, Plasma Physics, Fusion Engineering, ITER, EDA, Fusion Reactor Design, Annual Report

那珂研究所年報（平成９年度）

日本原子力研究所
那珂研究所

(1998 年 10 月 1 日受理)

原研那珂研究所における平成９年度（1997 年４月～1998 年３月）の研究開発活動について報告する。那珂研究所の主な活動は、JT-60 と JFT-2M における高温プラズマの研究及び、工学技術開発を含む ITER 工学設計活動（EDA)である。

JT-60 計画の目的は、ITER 等実験炉の設計に貢献するとともに、SSTR のような定常トカマク炉を実現するための物理的基盤を確立することにある。

本年度は、装置に関しては、W 型のセミクローズ・ドダイバータへの改造が 5 月に完了した。この改造は、粒子制御、不純物制御等のダイバータの機能が、その幾何学的構造によってどのように変化するかを調べること及び、優れた閉じ込め特性の主プラズマと両立する遠隔放射冷却ダイバータの実現を目指すものである。

JT-60 の特徴である負イオン NBI に関しては、運転の最適化を進めることによってプラズマへの入射パワーを徐々に増大させ、重水素負イオンビームで 350keV 時に 5.2MW、水素負イオンでは 360kev 時に 4.2MW を達成した。

W 型ダイバータにより ITER でのヘリウム灰排気の模擬実験を行った。その結果、定常状態において ITER の長時間燃焼維持に必要なヘリウム排気性能を世界で初めて実証したことは特筆に値する。また、長時間のプラズマ加熱を行っても不純物やリサイクリング粒子の増加を抑えることが可能となり、ELMy-H モードのプラズマを等価エネルギー増倍率 Q_{DT}～0.1 で９秒間維持することに成功した。

多重パラメータによる先進的なフィードバック制御に向けて，JT-60 ではこれまでの軸外線密度、放射パワー、中性子生成率に加えて、中心軸線密度とダイバータ中性ガス圧力のフィードバック制御を開始した。ディスラプション時のハロー電流特性の研究も進めた。負イオン源中性粒子入射によって駆動された電流は内部磁場測定によって直接同定し、その電流分布が ACCOME コードによる計算値と一致することを確認した。また、LHCD による電流分布制御により負磁気シアプラズマの内部輸送障壁

那珂研究所：〒311-0193 茨城県那珂郡那珂町向山 801-1
編集者：関　昌弘、清水　勝宏、関　正美、永島　孝、荘司　昭朗、岡部　隆

を維持することに成功した。さらに、負イオン源中性粒子入射による連続的な TAE モードが、世界で初めて観測された。

JFT-2M 計画の目的は、中型装置の機動性を生かした核融合プラズマの先進的及び基礎的研究、ITER 物理 R&D への貢献である。

ITER など将来炉の先進的燃料注入装置の開発を目指し、コンパクトトロイド(CT)入射装置を姫路工大と協力して据え付け、実験を開始した。初期実験の結果、CT を OH プラズマに入射すると放射損失が減少するなどの今後に期待のできる成果を得た。また、電場を高速で計測することで改良閉じ込めのメカニズムをより明確にするために、核融合科学研究所の開発した重イオンビームプローブ装置を設置した。

理論と解析研究の主要な目的は、トカマクプラズマの物理をより深く理解することにある。理想的な MHD モードのみならず負磁気シアの動的バルーニングモードにおける輸送や安定性に関する物理の理解が目覚ましく進んだ。スクレープオフ層やダイバータプラズマに対する 5 点モデルを開発し内外ダイバータの非対称性に関する研究が進んだ。

数値トカマク(NEXT)研究では、粒子・流体ハイブリッド手法に基づく数値アルゴリズムを発展させ、内部崩壊のシミュレーション研究を進めた。乱流発生時の電場形成やそれによる輸送抑制現象のシミュレーションを行い、閉じ込め改善現象の理解に貢献した。

核融合炉工学の R&D は ITER/EDA に関連する分野を重点的に実施してきた。1997 年の主要な成果は次の通りである。

超伝導磁石の分野では、中心ソレノイドモデルコイル外層モジュール全 8 層の巻線と熱処理を完了するとともに、このモジュールをコイルに組み立てる技術を開発した。また、ニオブアルミ(Nb_3Al)撚線を 1 トン製造し、インサートコイル用 46kA ケーブルを製作した。ITER 用真空容器の実機大の 20 分の 1 セクターを製作した。D 型断面で、高さ 15m、幅 9m であるが、いずれの方向も寸法精度±3mm を満足することができた。また、遮蔽ブランケットの原型モジュールの製作も完了した。プラズマ対向機器の開発ではダイバータの開発を進め、実機大の受熱板モジュールを製作し高熱負荷試験を行って 5MW/m^2 の定常熱負荷で 1000 サイクルの繰り返し加熱に耐える機器の開発に成功した。遠隔保守機器の開発ではブランケット保守用ビィークルシステムを組み上げ、性能試験を開始した。プラズマ加熱技術については、中性粒子入射加熱装置の開発において 25mA の水素負イオンビームを 1MeV まで加速することに成功した。ジャイロトロンの開発では、窓材料に熱伝導特性に優れた人造ダイアモンドを採用し、170GHz、520kW で 5 秒間の運転に成功した。トリチウムに関する R&D では、トリチウムの閉じ込め系内や環境での挙動を調べる目的で 12m^3 のケーソンを製作し、トリチウムプロセス研究棟内に据え付けた。

核融合炉設計研究に関しては、発電を実証する原型炉としての DREAM 炉設計を行った。安全性研究については、安全評価コードの開発及び、冷却材喪失／真空破断

事象に関する予備実験を行い、またトカマク炉内に生じるダストの除去に関する検討を進めた。

ITER 工学設計活動の最後の設計報告書である最終設計報告書が完成し、平成 10 年 1 月の技術諮問委員会のレビューを経て 2 月に ITER 理事会に提出された。最終設計は詳細設計をさらに改良・進展させたもので、設備機器の機能や配置上のインターフェイス及び運転状態の定義がなされ、プラント設備や補助設備の運転状態や保守を考慮した設計となっている。技術諮問委員会において最終設計報告書は、ITER の諸元と設計は技術目標を満足しているとの、高い評価を受けた。なお、1997 年 12 月現在の国際共同中央チームのメンバーは日本からの 46 名を含み 161 名である。

Contents

目　次

This is a blank page.

Foreword

Naka Fusion Research Establishment (Naka) of Japan Atomic Energy Research Institute (JAERI) has been conducting fusion experiments on JT-60, JFT-2M and DIII-D (US-Japan collaboration). Engineering activities focus on the R&D's for the International Thermonuclear Experimental Reactor (ITER) Engineering Design Activities (EDA). JAERI, as the Japanese implementing institute for ITER EDA, organized the Japanese Home Team and has been performing technology R&D's and designs in cooperation with the Joint Central Team.

The JAERI fusion program are being conducted based on the Third Phase Basic Program of Fusion Research and Development laid down by the Atomic Energy Commission of Japan in 1992. Present emphases of Naka fusion program are placed on contribution to ITER.

The programmatic objectives of the JT-60 project are to investigate the confinement improvement and the steady-state operation study, including disruption control, divertor study, and energetic particle physics. JFT-2M and DIII-D have been exploring advanced tokamak concepts such as stability control and particle control. Theoretical and computational efforts have been carried out on the topics of confinement analysis, MHD stability and burning physics.

Steady state helium pumping experiments with the W-shaped divertor in JT-60 have revealed efficient helium exhaust capability of $\tau_{He}^{*}/\tau_{E}=4$, which satisfied the ITER requirement. The DT equivalent fusion gain $D_{DT}^{eq}\approx 0.1$ was sustained for 9 sec in an ELMy H-mode discharge with a total heating power of 203 MJ.

As for the ITER technology R&D's, on-going activities cover superconducting magnet, neutral beam heating, radiofrequency heating, plasma-facing components, reactor structure, remote maintenance, blanket and tritium technology. The Center Solenoid model coil winding of 8 layers has been completed the thermal treatments without cracking, and the 1/20 sector of the full scale vacuum vessell (D-shape, 15m × 9m) was fabricated with an accuracy of ±3 mm.

The ITER Final Design Report (FDR) was presented to the ITER Council in February 1998, which is being reviewed by the Fusion Council in Japan.

太田 充

Mitsuru Ohta
Director General
Naka Fusion Research Establishment, JAERI

This is a blank page.

I. JT-60 PROGRAM

Objectives of the JT-60 project are to contribute the design of Experimental Reactor (ITER) and to establish the physics basis for a steady state tokamak fusion reactor like SSTR. The previous open divertor was modified to a W-shaped divertor with pumps from February to May in 1997. The aim of this modification is to investigate effects of divertor geometry and control on divertor functions and to realize radiative divertor compatible with good confinement simultaneously. The W-shaped divertor is characterized by inclined targets and a dome in the private flux region and pumping from the inboard side in the private flux region, which has never been found in other tokamaks. Therefore, divertor performance obtained in this divertor will have strong influence on the determination of divertor structure of future tokamaks like ITER.

The JT-60U experiments in 1997 focused mainly on the steady-state tokamak research with new divertor and the negative ion based neutral beam (NNB) in addition to the existing profile and shape control techniques developed in JT-60U. The research on divertor physics was accelerated under the new divertor system with many of fine diagnostics: Detachment characteristics, pumping control, impurity control, recycling characteristics, etc. In the steady (5s) helium pumping experiment using the core fueling helium beams to model the helium ash, τ_{He}^{*}/τ_{E}~4 satisfying the ITER requirement was obtained.

The main purpose of confinement and stability studies in 1997 was to improve steadiness of high confinement plasmas with the new divertor. Since a long heating time with 203MJ of the total heating energy became possible without harmful increase in impurity and particle recycling, the DT equivalent fusion gain Q_{DT}^{eq}~0.1 was sustained for 9 sec in a ELMy H-mode discharge. The progress in the high confinement reversed shear operation was demonstrated by a quasi-steady sustainment of the internal transport barrier with an ELMy H-mode edge. Researches progressed also for the formation conditions of the internal and the surface transport barriers in the high-βp mode, the reversed shear mode and the H-mode.

Toward the advanced feedback controls of multiple parameters, the JT-60U started new feedback controls of central line density and divertor neutral gas pressure in addition to the existing controls of off-axis line density, radiation power and neutron production rate. Characteristics of halo current during disruptions was also studied. Optimization of NNB operation progressed steadily and injection power increased up to 5.2 MW. The NNB-driven current was identified directly from the internal magnetic measurement and driven current profile was confirmed to be consistent with the ACCOME calculation. The current profile control with LHCD successfully sustained the internal transport barrier in reversed shear plasmas. Continuous TAE modes were observed with NNB for the first time as beam-driven TAE modes.

1. Operation and Machine Improvements

In FY 1997, a total of 2,197 pulses were run during the period of 9-cycle operations and wall conditioning. The total number of shots carried out for the past thirteen years amounts to 25,142 as shown in Fig.I.1-1.

Modification from open divertor to W-shaped pumped divertor was completed in May. Various maintenance works including inspection of high pressure gas facilities such as the NBI cryopump system were also performed in May. Following this shutdown, coil excitation tests were performed for confirming the integrity of the tokamak machine after modification of the W-shaped divertor. Stable W-shaped divertor discharges were obtained in the middle of June. In mid-July, boronization were conducted for wall conditioning. After that, campaign of the divertor studies and negative-shear experiments were started aiming at realization of steady-state operation with high performance.

Annual maintenance of the JT-60 facilities were performed from November through December in 1997. The operation restarted late in January 1998. After boronization conducted in the middle of March, discharge optimization was started for the succeeding high Q_{DT} experiments.

In spite of the operation after modification of the divertor, JT-60 was satisfactorily operated throughout the year. The database obtained in the operation and maintenance was arranged and made useful for maintenance plan and measures for the aged deterioration of the facilities. In particular, an overall revision of the operation manuals for the JT-60 facilities were made for ensuring safety in the operation.

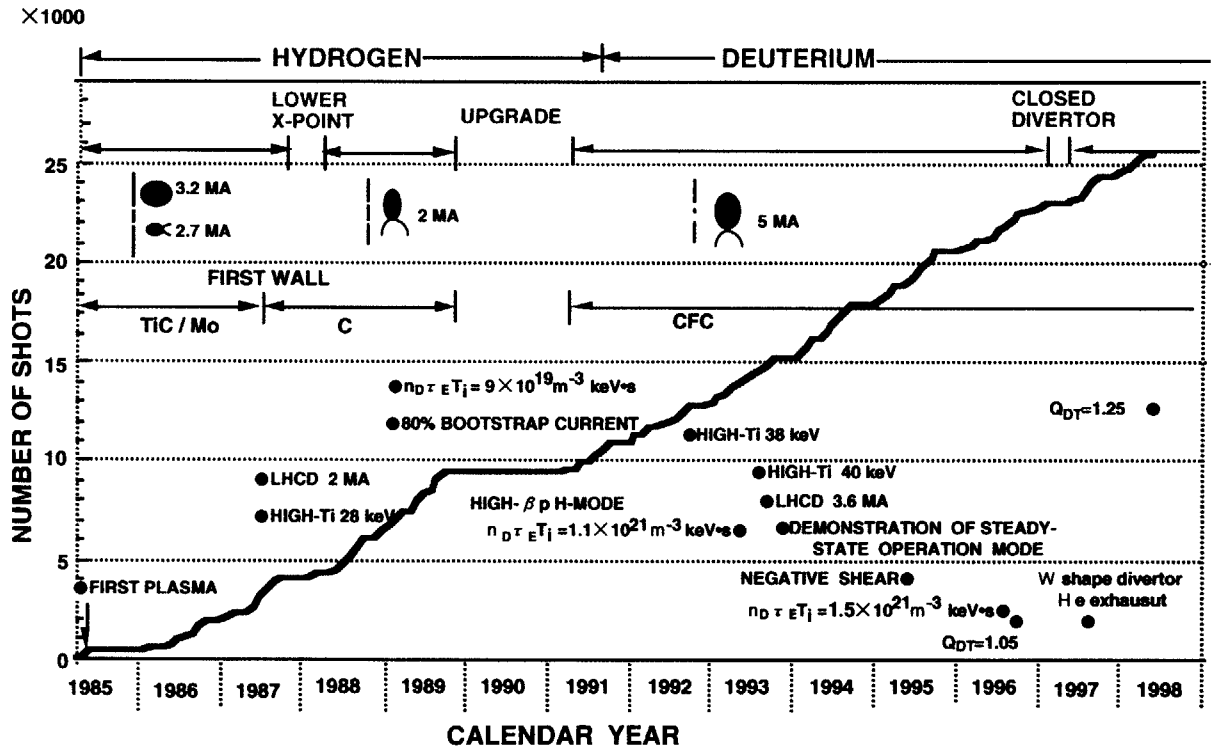

Fig.I.1-1 Progress in JT-60 operation.

1.1 Tokamak Machine

1.1.1 Toroidal Field Coil (TFC) and Poloidal Field Coil (PFC)

Since the occurrence of water leakage of cooling pipes for toroidal magnetic field coils (TFC) in 1992 (TC-9) and 1995 (TC-14), the coil layers with water leakage have been operated without water cooling. The cause for the water leakage was identified as some cracks which were found by a fiberscope observation system. Hence, in every maintenance period, the inside of the cooling pipes with cracks have been investigated by the fiberscope observation system [1.1-1] and airtight testing has been carried out for all the cooling pipes of TFC. By these examinations, it has been confirmed so far that there is no further growth of the cracks and no new cracks. On the other hand, as a protection system of TFC, a short circuit detection system has also been developed. This system aims to find precursor events as early as possible before occurrence of a short circuit between coil layers which finally lead to damage to the TFC. The configuration of the system is shown in Fig. I.1.1-1. This system consists of a Rogowskii coil and a set of six magnetic probes arranged around a TFC. The Rogowskii coil detects the short circuit phenomenon and the magnetic probes complement the Rogowskii coil data. With a successful result of preliminary tests on S/N ratio of the system, construction of this system has started on a full scale. In parallel with this development and taking into account that cracks might occur in neighboring coil layers in the future, influence of Fluorinert (Fluorocarbon) on the TFC construction materials have been examined as an alternative coolant for the TFC with cracks. This is because cooling of these coil layer cannot be expected without some coolant in this situation. The examination of results is favorable for usage of Fluorinert. Corrosion due to Fluorinert, which is a key for long term use as a coolant, was found to be permissible.

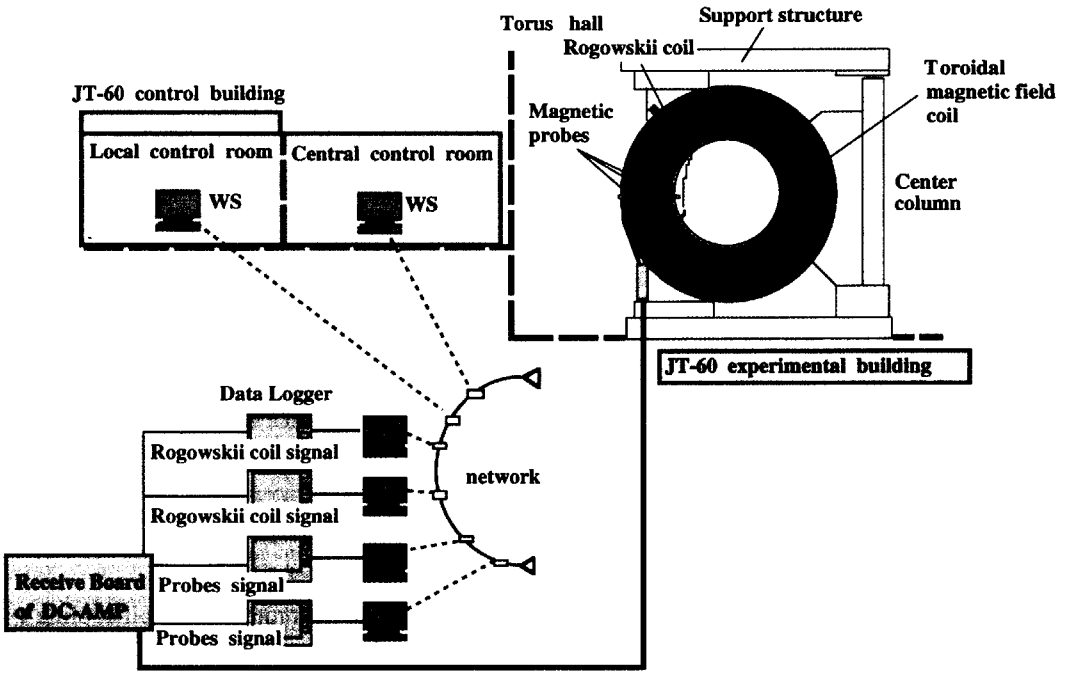

Fig. I.1.1-1 Short circuit detection system.

In long pulse high triangularity operations, there is a risk that temperature of the VT-coil for controlling triangularity of the plasma may rise up to higher than the design value. For safe operation of this coil, interlock system with an optical fiber thermometer was installed in the VT-coil feeder.

1.1.2 In-vessel Inspection

The divertor modification was completed in May 1997. The first experimental campaign was started in June and ended in October. During this experimental campaign, operational parameters of JT-60U with the W-shaped divertor were : number of shots 1753, plasma current of 2.5 MA, NBI heating power of up to 25 MW, toroidal magnetic field of 4 T and number of disruption ~200. After this five months' operation, a routine inspection of the JT-60U vacuum vessel interior was conducted in November.

Severe erosions of outer divertor tiles and dome tiles were found in the routine inspection. These erosions were concentrated at the tile lip. Two outer dome tiles were broken in two, but still stayed on the dome plates. Fine cracks of outer dome tiles were also found. These show that heat flux higher than expected even reached the outer dome tile lip. The designed heat flux to the outer dome tiles was 1 MW/m^2 x 10 sec. These outer dome tiles were fabricated from isotropic graphite which is fragile at lower thermal shock compared with carbon fiber composite (CFC), because high heat flux was not expected on the outer dome tiles. So, the main cause for the tile break and cracks is probably thermal shock. These eroded and broken dome tiles were exchanged for CFC tiles with higher thermal shock resistance. The eroded divertor tiles were tapered according to each erosion.

Thick deposit of carbon was observed on the inner divertor tiles, but no severe erosion was found. Total amount of the deposit estimated by weight measurement was approximately 25g. In the previous divertor, recycling of the inner divertor was higher than the outer one, so exhaust for the divertor pump is located between inner divertor and dome to control recycling with the strong in-out asymmetry. The asymmetric deposit of the carbon must be related to the structure and/or the in-out recycling asymmetry.

Soundness of the W-shaped structure was almost demonstrated by this inspection. Plasma sprayed ceramic could be used as gas-seal between structures without extreme deformation. Insulation resistance of this plasma sprayed ceramic did not deteriorate. Other stainless and Inconel structures were also sound.

References

[1.1-1] Arai T., Honda M., Koike T., et al. , "Inspection techniques for JT-60 toroidal field coil cooling pipes", FUSION TECHNOLOGY 1996 1099-1102 (1997)

1.2 Control system

The control system works in the JT-60 experiments according to the required schedule. The following developments were newly performed in this fiscal year to improve plasma control performances and operational efficiency.

(a) A precise long-time digital integrator, that can be applied to the 2000-s pulse discharge in ITER, has been completed, and 75 sets were built up for JT-60 magnetic measurements. (Refer to 1.2.1)

(b) A new advanced plasma control system has become ready for installation in JT-60. The computational time was greatly reduced to a hundredth of that of the former system. Design and development of a new discharge control system have been started. (Refer to 1.2.2)

(c) To improve the accuracy of plasma X-point height, a new function parametrization formula was introduced, and its new coefficients were derived as a result from the method of least-squares using the JT-60 new equilibrium data base. (Refer to 1.2.3)

(d) Corresponding to the modification of closed divertor, two feedback controls were installed: controls of neutral gas pressure and plasma electron density at the divertor region using an actuator of neutral gas feed into the divertor.

(e) A differential feedback control method was added to the existing neutron feedback control. This modification is a preparation toward high confinement experiments.

(f) A plasma equilibrium prediction code with human-friendly interfaces has been developed: This system calculates the full JT-60 equilibria throughout a pulse discharge to fit the given preprogrammed waveforms such as plasma total current, positions of the plasma geometrical center, etc. Using this tool, a physics operator could know if plasma configuration would be correct, coil currents would not exceed their heat capacity, etc.

For the maintenance of the control system, annual inspections were made on the computer system, control boards, and the signal processing system for plasma control during the shut-down period of November and December.

The workstation, that manages JT-60 discharge condition parameters (discharge conditions server), was superseded by a faster workstation with a large auxiliary memory. This increased the number of discharge conditions which were used in the past experiments. Human-friendliness for the screen layouts on the workstations were also appropriately improved in response to the requests from the JT-60 physics operators.

1.2.1 Development of a Precise Long-Time Digital Integrator for Magnetic Measurements

Magnetic field measurements are indispensable for control and diagnostics of a tokamak plasma. The existing methods for the measurement are (i) integration of time-derivative of magnetic field, and (ii) direct measurements of absolute magnetic field using rotating coils, Hall-element sensors, etc. The latter seems to be incompatible with 14-MeV neutron field, while the

former has a problem of inevitable signal drift in an integrator, and thus it could not work for a long period of discharge (e.g., 2000 s for ITER). We chose the VF (voltage-to-frequency)-UDC (up-down counter) method for the development from the following view points: Its high accuracy is expected equivalent to analog integration. Wider dynamic range is allowed in a large digital accumulator, and drift can be compensated more precisely in a digital system.

We built three trial models with new improvements added to reduce the integral errors in the VFC-UDC system arisen from the following causes: (1) VF conversion non-linearity, (2) production of deadbands, (3) slow base-line drift, and (4) stepped change at plasma instabilities. Finally, the third board showed good integration accuracy even for ITER with suppressing drift speed in the test environments of JT-60 experiments [1.2.-1, 2] .

On the basis of the technical experiences mentioned above, manufacturing of 75 VF converters have been completed. All the old VF converters will be superseded by the newly developed ones for JT-60 experiments in 1998. The outside view of a new VF converter is shown in Fig. I.1.2-1.

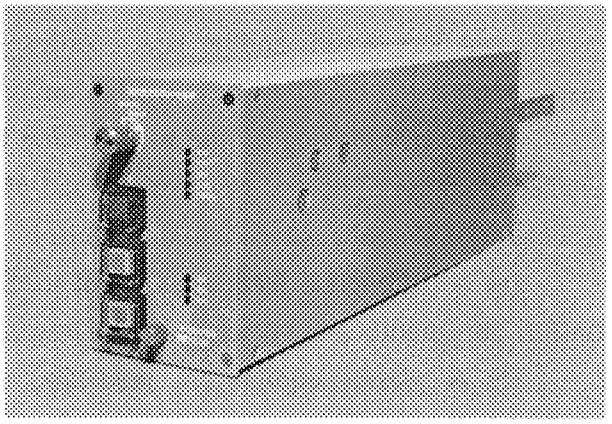

Fig. I.1.2-1 A new VF converter outside view.

1.2.2 Development of the JT-60 New Control Systems

Since requirements for modification of advanced plasma control and efficient discharge control increase, two control systems are being developed. Concerning a new plasma control system, we chose an Alpha-288 VME board (made by DEC. Ltd.) for main processors, and built

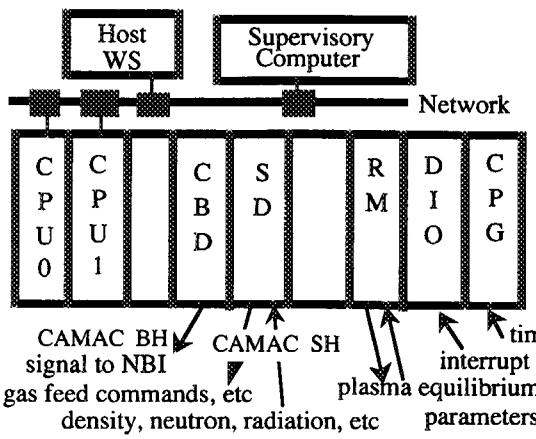

Symbol	Type	Function /Manufacturer
CPU0,1	AXPvme280	DEC 21066A, 288MHz, 64MB/ DEC
CBD	CBD8210	CAMAC Branch Driver / CES
SD	VSHD2992	CAMAC Serial Driver / HYTEC
RM	VMIVME5576	Reflective Memory (256kB) / VMIC
DIO	DSP8230	Digital Input (32 ch) / MTT
CPG	CPG241	Clock Pulse Generator / MTT
WS	Alpha WS 255	UNIX-WS alpha 255MHz / DEC

BH: Branch Highway SH: Serial Highway

Fig. I.1.2-2 Configuration of the plasma realtime control system.

a VME-bus system together with the I/O boards and a reflective memory module as shown in Fig. I.1.2-2. As a result from its performance test, this system can execute the realtime program within 0.1 ms. This period is approximately 100 times faster than the old mini-computer (10 ms). However, slow communication (1.4 ms) with the existing old subsystems through CAMAC highway is an obstacle for minimization of the total execution time.

This system will begin to work for JT-60 in May 1998, after several integration tests with the other subsystems.

Concerning a new discharge control system, we performed system design of the hardware configuration. According to the current design, this system is composed of two parts: one is a supervisor for compilation of discharge condition files and acquisition of result data from all the subsystems (DC/RD-SV), and the other is a supervisor for discharge sequential control (SQ-SV).

DC/RD-SV, as a master for discharge condition files before discharge, distributes the appropriate conditions to the corresponding subsystems after compilation procedures. After discharge, DC/RD-SV works as a master for result data acquisition. This receives result data from all subsystems, and builds an intermediate file before transferring it to the JT-60 database production server.

SQ-SV manages all the actions and events occurred in the JT-60 systems according to the discharge sequence by sending the command messages and receiving the replies. This part will be composed of VME modules due to the required fast on-line communications. DC/RD and SQ-SV's will be expected to come into operation in 1999.

1.2.3 A New Function Parametrization Formula

A function parametrization (FP) method has been adopted for the real-time control of JT-60U plasma position and shape, where sets of linear coefficients in the FP formulas are determined through the method of least squares (LS) on the numerically-prepared equilibrium database. On modification of the divertor structure, the number of linear coefficients was increased from 7 to 33 to improve the control accuracy.

Although the numerical examination using the database had shown a good accuracy (standard deviation σ ~2 cm), the experimental comparison of the FP method and the equilibrium analysis showed considerably large discrepancies of large offset bias and large standard deviation in X-point position for high-elongated plasmas. Investigation of these problems has determined that the following items could be the causes: an ill-posedness in the FP formula coefficients and negligence of ohmic-heating coil (OH-coil) effects.

It was found out that strongly correlated sensors or very insensitive sensors involved in the LS analysis caused the ill-posed problem that small amount of actual sensor noise or error could make large difference from the numerical results on the ideal database. We excluded probes of concern and recalculated the coefficient. As a result, the new coefficients set suppressed that the

offset bias completely.

A lot of experimental results suggested that the effects of OH-coil field have strong influence on the error. We have then developed a new FP formula for X-point position X_P^{FPM} that takes the effects of the OH-coil current (I_{OH}) as well as the divertor-coil current (I_D) as follows,

$$X_P^{FPM} = C_0 + C_1\frac{I_D}{I_P} + C_2\frac{I_{OH}}{I_P} + \sum_{i=1}^{N_\omega}\left(C_{\omega i} + D_{\omega i}\frac{I_D}{I_P} + E_{\omega i}\frac{I_{OH}}{I_P} + F_{\omega i}\frac{I_D I_{OH}}{I_P^2} + G_{\omega i}\frac{I_D^2}{I_P^2}\right)\frac{B_{\omega i}}{I_P} + \sum_{i=1}^{N_\rho}\left(C_{\rho i} + D_{\rho i}\frac{I_D}{I_P} + E_{\rho i}\frac{I_{OH}}{I_P} + F_{\rho i}\frac{I_D I_{OH}}{I_P^2} + G_{\rho i}\frac{I_D^2}{I_P^2}\right)\frac{B_{\rho i}}{I_P}, \quad (1.2.3\text{-}1)$$

where I_P is the plasma current, $B_{\omega i}$ and $B_{\rho i}$ tangential and normal components of magnetic fields at the i-th probe positions, N_ω and N_ρ the numbers of probes, and the C_1, C_2, $E_{\omega i}$, $F_{\omega i}$, $G_{\omega i}$, $E_{\rho i}$, $F_{\rho i}$ and $G_{\rho i}$ the coefficients determined by the method of LS.

The application of the new FP formula to the actual experiments are shown in Fig. I.1.2-3, where X-point positions are certainly detected within 2 cm, as expected in the numerical analysis [1.2-3].

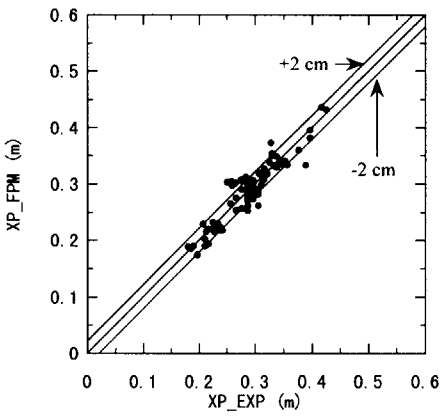

Fig. I.1.2-3 Correlation of X-point positions, X_{P-FPM} and X_{P-EXP}. (X_{P-FPM}: the FP formula on experimental data. X_{P-EXP}: the equilibrium analysis).

References

[1.2-1] Kurihara K. and Kawamata Y., "Development of a precise long-time digital integrator for magnetic measurements in a tokamak," in Proceedings of 17th Symposium on Fusion Engineering, San Diego (USA, 1997).

[1.2-2] Kurihara K. and Kawamata Y., "Development of a precise long-time digital integrator for magnetic measurement in a tokamak," JAERI-Research 97-072 (1997) (in Japanese).

[1.2-3] Miura Y. M., Kawamata Y., Fukuda T. and Kurihara T, "A New Function Parametrization Formula for the JT-60U X-Point Position Control", JAERI-Research 98-039, "Review of JT-60U Experimental Results in 1997" (1998).

1.3 Power Supply System

The JT-60 power supplies were operated on schedule without any serious problems throughout this physical year, though fourteen years have passed since they were completed. In November and December 1997, annual maintenance of the power supplies were performed according to the regulations for electric equipment in Naka Fusion Research Establishment. The following maintenance works were conducted as the measures against aged deterioration of the devices: (1) Insulating supports for thyrister stacks in converters of the vertical filed coil power

supply were replaced. The surface of the supports made by FRP had chemically changed and the electrical insulation resistance had been extremely decreased. (2) All of the insulated-signal transducers for the feedback control of the inverter unit in the un-interruptible power supply were replaced with new ones for preventive maintenance. (3) Water was found on the floor near the DC feeders from the thyrister converters in the poloidal field power supplies due to the leaks in the wall and roof of the JT-60 rectifier building at the typhoon in June. Hence, the repair work was done for the rectifier building.

1.3.1 Replacement of a New Coil Current Control System in the Toroidal Filed Power Supply

The toroidal field coil power supply (TFPS) is composed of six diode rectifier banks and a motor-generator(MG) with a large flywheel. Four banks of the rectifiers are directly connected to a commercial power grid, and the rest of them are powered from the MG. The toroidal field coil current must be controlled through the output voltage of the generator. Therefore the field control system of the generator is very important for the TFPS. However it became very difficult to maintain the integrity of the original control system, because 15 years have passed since the fabrication. Then we decided to replace the control system including I/Os to the new one which is based on the VME-standard (see Fig.I.1.3-1). The recent microprocessor is so powerful as to make the control system multi-functional. The limit function, coil fault detection, and real-time data display functions are introduced in the new system. This system may greatly enhance the reliability of the toroidal coil current control, and also make it possible to improve the control performance. Several tests using the analog simulator were carried out as a linkage performance test. After the completion of dummy load test, the original control system will be switched to the new one.

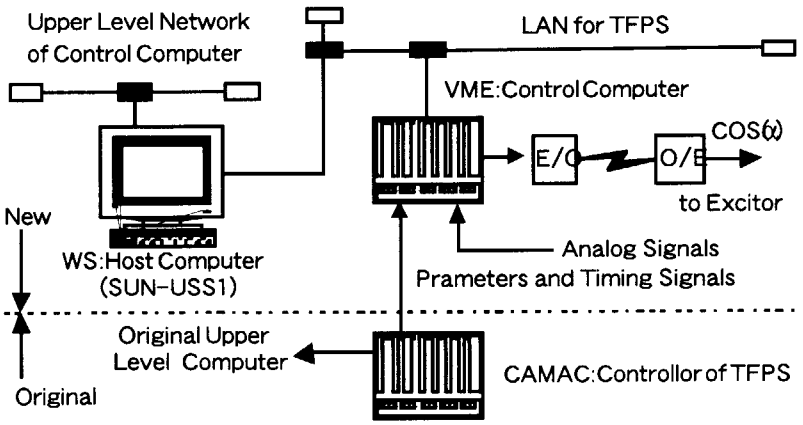

Fig.I.1.3-1. A new control system of the toroidal coil current.

1.3.2 Development of an IGBT Current-Driven PWM Converter

A 100-kW-class current-type PWM (pulse width modulation) converter based IGBTs (insulated-gate bipolar transistors) was developed and the feasibility of its application to a large magnet power supply for nuclear fusion device was investigated. Table I.1.3-1 shows the ratings of developed IGBT converter. Some adjustments for the circuit parameters were needed, but the

target values of the rated performance were successfully achieved. Through the tests of the converter, the following issues to be solved were newly found: transient high voltages of a *LC* filter, distortion of an AC source current for low outputvoltage operation, and decrease in power factor owing to large current operation [1.3-2]. We are planning to optimize the feedback gains in the control of the reactive and output current in order to realize the rapid step response.

Table I.1.3-1 Ratings of the IGBT converter.

capacity	100 kVA
maximum voltage	200 V
maximum current	500 A
IGBT	1S-4P-6Arm
LC filter	2 mH-500 F
load	4mH-17mW

1.3.3 Development of a Water-cooled VCB for a Superconducting Magnet Power Supply

We started to develop a current interrupter which can carry a large current in steady state. The purpose of this development is to offer the key component of a quench protection circuit in superconducting magnet power supplies for fusion devices. As a candidate of the current interrupter, a water-cooled VCB was newly designed and its model test was conducted.

The target values of its performance were determined as follows: (1) continuous current-carrying capacity of 25 kA or more, and (2) current interruption rating of 50 kA or more. Since thermally critical parts of the VCB are contacting surfaces of its electrodes, a key issue of the design is how to remove the heat generated on the surfaces in the electrodes from the vacuum area. For the heat removal with good efficiency, the VCB was designed to possess a short fixed rod with a large coil outside the vacuum area and a fat movable rod where a water-cooling channel can be bored. Thus the new VCB has an up-down asymmetrical structure having the coil that provides co-axial magnetic field for stabilizing the current interruption property (Fig.I.1.3-2). Thermal characteristics of the VCB were analyzed by computer simulation. In addition, a model of the VCB was fabricated and tested to evaluate the characteristics. At the test of the model VCB, it was proved that the water-cooled VCB with a current-carrying capability of about 18 kA is feasible [1.3-3].

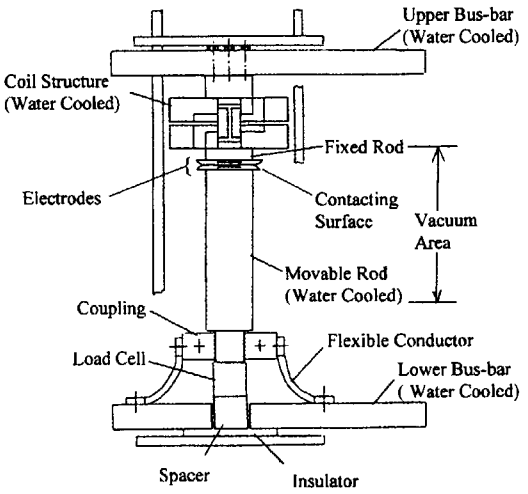

Fig.I.1.3-2. A structure of the newly designed water-cooled VCB.

References

[1.3-1] Mastukawa M, Ohmori Y, Totsuka T, et al., "A New Coil Current Control System of the JT-60 Toroidal Field Coil Power Supply (in Japanese)," to be published in Proc. of JIASC '98, Akita, 1998.

[1.3-2] Miura Y. M., Matsukawa M. and Kimura T., "Development of an IGBT Converter for a Magnet Power Supply," to be published in Proc. of 20th SOFT, Marseille, France, 1998.

[1.3-3] Matsukawa M., Miura Y. M., Kimura T. et al., "Design and Model Test of a Water- cooled VCB for Superconducting Magnet Power Supplies," to be published in Proc. of 13th Topical Meeting on Technology of Fusion Energy, Nashville, 1998.

1.4 Neutral Beam Injection System

1.4.1 Positive-ion Based NBI System

Three beamline units out of fourteen of the positive-ion based NBI system have been modified as an exclusive use of gas pumping for a newly fabricated W-shape diverter in JT-60. The diverter experiments using the beamline cryopumps started in summer 1997. Neutral gas pumping at the diverter region with the cryopumps has been clarified to increase the JT-60 plasma performance. In a simulation experiment of helium ash exhaust, the diverter pumping for a mixed gas of deuterium and helium has been demonstrated with the NBI cryo-sorption pumps which is made through condensing argon gas onto the liquid helium cooled cryo-panels.

The neutral beam injection using the rest of the beamline (11 units) has been conducted with an injection power range of 20-30MW at a beam energy of around 90keV. A total injection power of 203MJ has been obtained in a long pulse beam injection near 10 sec at a moderate injection power of around 22MW, and thus quasi-steady state H-mode plasma near 10 sec has been achieved.

1.4.2 Negative-ion Based NBI System

The beam injection experiment into JT-60 with the negative-ion based NBI system (N-NBI) has been conducted, augmenting the beam power gradually, since the beam operation started in 1996.

Many problems have been experienced in the high voltage beam operation. Most of the problems occurred in the ion source and high voltage power supply were caused by a surge energy at the moment of the ion source breakdown. These have been solved step by step through altering the components of the power supply hardware and remodeling of the control system. Improving the ion source and power supply components, the beam power has increased gradually, and a neutral beam injection power, so far, has reached 5.2 MW at 350 keV with deuterium and 4.2

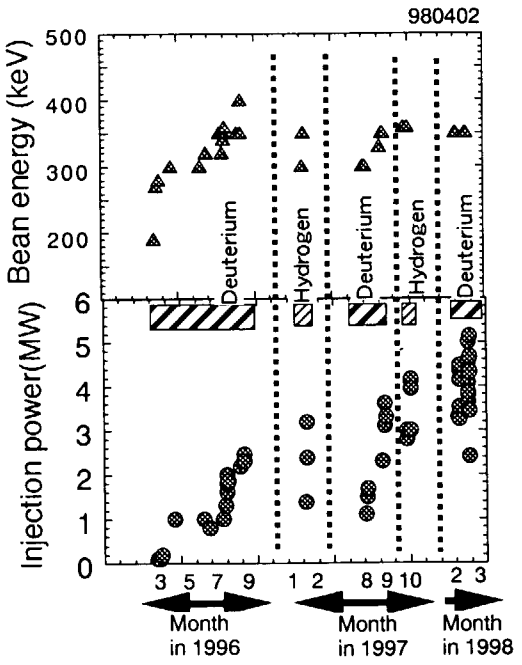

Fig. I.1.4-1 Time evolution of injection power and beam energy.

MW at 360 keV with hydrogen as shown in Fig. I.1.4-1. A negative-ion beam power per one ion source has reached 380 keV, 14.3 A with deuterium and 360 keV, 18.5 A with hydrogen.

The plasma characteristics concerning a NBI current drive efficiency and neutron yield from plasma with the NBI beam injection, so far, have been confirmed to be agreed with a theoretical prediction. The efforts for increasing beam power and energy will be continued aiming at the rated injection power of 10 MW for establishing the technical and physical bases of the ITER.

1.5 Radio-frequency Heating System

1.5.1 ICRF System

The ion cyclotron range of frequencies (ICRF) system for JT-60 was operated well at 102 MHz in FY 1997. Prior to the operation, the stub tuners were modified in April 1997 in order to improve their voltage stand-off capability [1.5-1], because we were afraid that the coupling of the antenna and the plasma would be degraded on the modification from an open divertor to a W-shaped divertor. High power can be coupled to the plasma even with degraded antenna-plasma coupling when the higher voltage stand-off is achieved at the antenna. Then we had to improve the voltage stand-off capability of the coupler system which consists of stub tuners, high power phase shifters, coaxial lines and antennas.

After careful optimization of the plasma shape for the ICRF experiment, we obtained similar antenna-plasma coupling with the W-shaped divertor as one with the open divertor. Plasma shapes for ICRF coupling with open and closed divertor are shown in Fig. I.1.5-1 and Fig. I.1.5-2, respectively. The gap, δ_0, between the antenna and separatrics was tried to kept constant in front of the antenna by means of adjusting a separatrics curvature and a vertical position of the plasma. We paid attention to keep at least 3 cm of the gap at the outer baffle plate of W-shaped divertor in order to reduce the plasma-wall interaction there, by means of adjusting the height of the X-point. Typical parameters for ICRF coupling were the plasma current = 1.7 MA, the toroidal magnetic field on the axis = 3.34 T, the triangularity = 0.28, the plasma volume = 80 m^3 and the gap δ_0 = 6 cm - 15 cm.

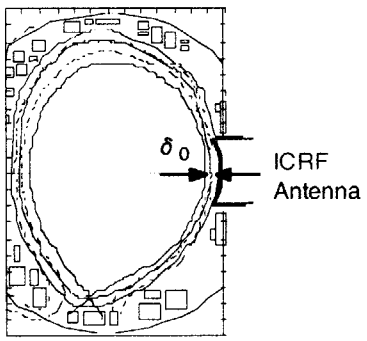

Fig. I.1.5-1 Configuration with open divertor for ICRF coupling.

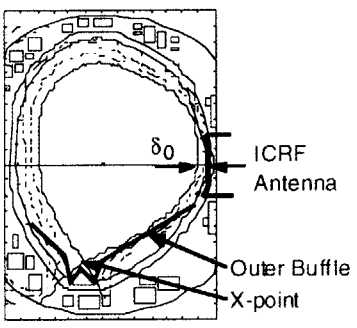

Fig. I.1.5-2 Configuration with W-shaped divertor for ICRF coupling.

To evaluate the antenna - plasma coupling, the coupling resistance (R_C) is often used. R_C is defined as $R_C = 2PZ^2V_{max}^{-2}$, where P is the input power to the antenna, Z the characteristic impedance of the coaxial line in the antenna, and V_{max} the maximum RF voltage of the standing wave on the coaxial line in the antenna. When high R_C is obtained, high power can be coupled to the plasma with low RF voltage at the antenna. About 2.5 W of R_C was obtained with around 10 cm of δ_0. It is consistent to the result of the reciprocating probe measurement [1.5-2, 3] which shows that the gradient of the scrape off plasma density in the W-shaped divertor case is similar to that in the open divertor case. If the breakdown voltage of the antenna is 40 kV which was obtained in the antenna conditioning in vacuum, 6.4 MW will be coupled to the plasma with 10 cm of δ_0.

Coupled power of 1 MW for 1.5 sec and 5.1 MW for 50 ms were obtained after only 5 days' antenna conditioning after divertor modification, as shown in Fig. I.1.5-3. On September 22nd, the 6th's day of the antenna conditioning, 4 MW for 1.5 sec and 4.3 MW for 1 sec were achieved. Energy of 8.6 MJ was coupled to the plasma as a sum of three RF pulses in one plasma shot. After the antenna conditioning, ICRF power of 4 MW was routinely coupled to the plasma for the experiments on ICRF heating of negative magnetic shear plasmas [1.5-4] in September and October.

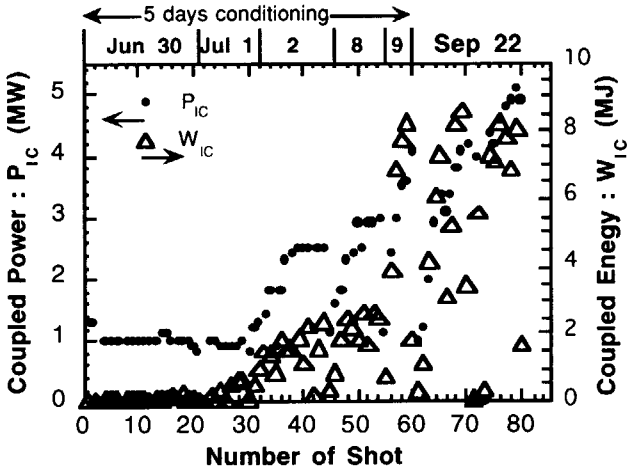

Fig. I.1.5-3 Progress of the coupled ICRF power and energy with W-shaped divertor.

1.5.2 LHRF System

The lower hybrid range of frequencies (LHRF) system in JT-60 was also operated with the W-shaped divertor plasma in FY 1997. At first, coupling properties of LH antennas were investigated. The coupling was good for the LH antenna C located at the upper inclined port of P-11, even with the W-shaped divertor plasma. It is a reason that plasma parameter in the scrape off layer in front of the antenna mouth was not changed after modification from the open divertor to the W-shaped divertor, due to the antenna mouth being far from divertor section. On the other hand, the distance between separatrics and the first wall around the LH antennas A and B located at horizontal port P-18 became shorter as ~8 cm for obtainment of the same low reflection coefficient. The reflection coefficient of the lower-side LH antenna A is plotted as a function of the distance named as δ_{344} in Fig. I.1.5-4. As shown in the figure, the plasma should be closer to the LH antenna for LHRF experiments under good coupling with the W-shaped divertor in

comparison with open divertor. This leads to a limitation of plasma configuration and/or experimental conditions. Then the usage of the lower-side LH antenna system is planned to be utilized for the localized current profile control system. Even though number of LH antennas decreased from three to two, the current profile control and current drive were also available with the W-shaped divertor plasma. Injection of LHRF power highly contributed to reversed magnetic shear experiments, referring to section I.2.4.

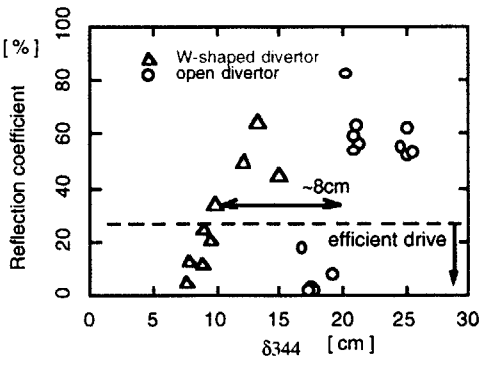

Fig. I.1.5-4 The reflection versus distance δ344.

It is important to establish a conditioning method for the LH antenna with a small number of shots as possible as we can. So, the power injection with pulse modulation was tried in order to avoid serious breakdowns in the LH antenna. This allowed effective conditioning by means of valuable plasma shots, because a small breakdown in the waveguide can not grow up within 1-10 msec and rf injection can continue in the same plasma shot. On the contrary, in the former conditioning shots, the rf power was stopped when a severe breakdown occurred. Moreover the pulse modulated injection can drive plasma current with the same efficiency as shown in Fig. I. 1.5-5, taking into account of the duty for the pulse modulation. This pulse modulated injection will be useful in the next generation tokamak, since the antenna mouth should be healthy without breakdowns.

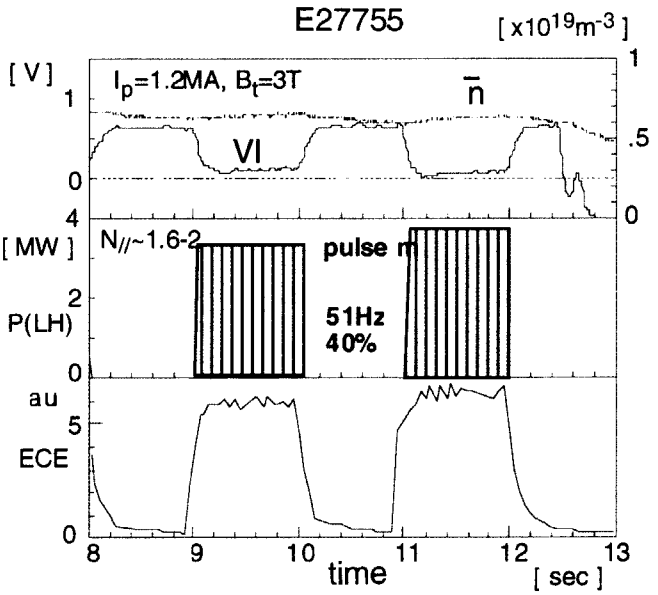

Fig. I.1.5-5 Typical shot in pulse modulation.

References

[1.5-1] Moriyama S., et al, "Annual Report of Naka Fusion Research Establishment From April 1, 1996 to March 31, 1997", JAERI-Review, 97-013, pp.12-14, (1997).

[1.5-2] Moriyama S., and Asakura N., "ICRF coupling in W-shaped divertor configuration", Review of JT-60U experimental results 1997, JAERI-Research 98-039, pp. 74-76 (1998).

[1.5-3] Asakura N., Tsuji-Iio S., Ikeda Y., et al. , "Fast reciprocating probe system for local scrape-off layer measurements in front of the lower hybrid launcher on JT-60U", Rev. Sci. Instrum, 66 (12), pp.5428-5432, (1995).

[1.5-4] Iwase M., et al., "ICRF heating of reversed shear plasma ", Review of JT-60U experimental results 1997, JAERI-Research 98-039, pp. 81-84 (1998).

1.6 Diagnostics System

New installations have been done for the following systems; infrared laser polarimeter, mm-wave Iinterferometer, Mach probe, In-vessel bolometer camera, fast response ionization gauge, core correlation reflectometer and CO_2 laser collective Thomson scattering.

1.6.1 Infrared Laser Polarimeter for Electron Density Measurement

An infrared laser polarimeter has been developed for electron density measurement in large tokamaks [1.6-1]. By using the infrared laser polarimeter, the first measurement of the tangential Faraday rotation of a CO_2 laser wave (wavelength ~10 μm) in a tokamak plasma has been successfully obtained in JT-60U [1.6-2], where the tangential Faraday rotation is approximately proportional to the product of electron density and the toroidal magnetic field.

1.6.2 Mm-wave Iinterferometer in Divertor Region [1.6-3]

A mm-wave interferometer has been developed for divertor diagnostics in JT-60U. Three lines of sight, which pass through the X-point horizontally, the inboard divertor and the outboard divertor were chosen. Two transmitter/receiver units with frequencies of 217 and 183 GHz were employed in order to eliminate the spurious vibration effect using a two color scheme. The two independent units were also arranged to enable two sight lines measurement without the vibration compensation. The measurements performed for several types of discharges indicated the feasibility of the system, and the rapid reduction of the electron density was first measured near the X-point at the transition of the confinement mode.

1.6.3 Mach Probe for the Plasma Flow in SOL

Multi-point measurements of temperature and density distributions in the SOL, i.e. at the midplane, near the x-point and at the divertor plates, were developed in the W-shaped divertor. In particular, Mach probes were installed at the midplane and near the x-point in order to evaluate the plasma flow and its direction. When the single null divertor was operated, it was found that the direction of the ion grad-B drift plays a critical role in determining the SOL flow direction. The plasma flows from the midplane to the x-point for the reversed field (the ion grad-B drift is directed away from the divertor), but it flows from the x-point to the midplane for the normal field direction, suggesting the flow reversal near the midplane. Here the particle source is very small compared to that near the divertor region for both cases. These observations show the existence of parallel ion convection at the SOL of the main plasma.

1.6.4 In-vessel Bolometer Camera for the Divertor Study [1.6-4]

Bolometer cameras were installed inside the W-shaped divertor chamber of the JT-60U. Each camera has a four-channel bolometer head of high temperature version using mica substrate.

Radiation profiles along the separatrix surface from x-point to the divertor tiles were measured with two cameras placed under the divertor dome. Other cameras view an x-point area from horizontal and vertical directions to observe the phenomena such as MARFE. Although the initial operations were successful in obtaining good quality and the time resolution of signals, the detectors were damaged during disruptions. Both thermal and electrical insulation of the camera are planned to be improved.

1.6.5 Fast Response Ionization Gauge for the Neutral Gas Pressure [1.6-5]

Fast response ionization gauges were installed to measure the neutral gas pressure profile at the divertor region, the pumping duct, and the main plasma edge. The gauge and its controller were developed by the ASDEX team. Its dominant advantage is that the sensor head can be applied in strong magnetic fields, so that the sensor head can be located very close to the plasma, which contributes to the fast time response. In front of the sensor head a chevron is placed in order to view the plasma indirectly and to provide thermalization of particles. The time response including the chevron is estimated to be about 3-4 ms, which is two orders of magnitude faster than conventional pressure gauges used in the vacuum vessel of JT-60U.

1.6.6 Core Correlation Reflectometer

A core correlation reflectometer system has been developed under the collaboration between JAERI and PPPL. The polarization of the launched wave is X-mode and the frequencies of the launched waves are 115, 130, $122.5 \pm \Delta f$ GHz. The value of Δf can be changed from 2 to 18 GHz, so that the cut-off layers can be scanned through the region of the internal transport barrier (ITB) for the reversed shear plasma (see Section 2.1). Furthermore the frequencies can be scanned rapidly within a single shot, allowing radial correlation measurements of the fluctuations. The core correlation reflectometer system will help us to understand the physics of ITB plasmas. This system will work from the summer in 1998.

1.6.7 CO_2 Laser Collective Thomson Scattering [1.6-6]

A Collective Thomson Scattering (CTS) is nominated as a candidate in ITER for the measurement of bulk ion temperature and energy distribution of high energy α-particles. The CTS system using a pulsed CO_2 laser with small scattering angle ($\approx 0.5°$) has been developed to measure ion temperature in JT-60U. Estimation of scattered power spectrum shows a reasonable signal to noise ratio for the ion temperature measurement. A pulsed CO_2 laser system (wave length: 10.6 μm, energy: 10 J, pulse length: 1 μs, repetition rate: 0.5 Hz) and a heterodyne receiver system with a hot CO_2 absorber cell as a stray light notch filter, which are developing in Oak Ridge National Laboratory, will be installed in a diagnostic room in 1999.

References

[1.6-1] Kawano Y., Chiba S., Shirai H., et al., "Fast measurement of tangential Faraday rotation of CO_2 laser wave in a tokamak plasma", submitted to Rev. Sci. Instrum (1998).

[1.6-2] Kawano Y. and Nagashima A., Rev. Sci. Instrum. 68, 4035 (1997).

[1.6-3] Takenaga H., Fukuda T., Sakurai S., et. al., "Versatile mm-wave interferometer with two frequencies in divertor region of JT-60U", to be published in Rev. Sci. Instrum.

[1.6-4] Konoshima S., Ishijima T., Tamai H., et al., JAERI-Research 98-039 (1998).

[1.6-5] Tamai H., Takenaga H., Asakura N., et al., "Particle Control and Behaviour of Neutrals in the Pumped W-shaped Divertor of JT-60U", 13th PSI International Conference, San Diego, USA (1998). to be published in J. Nucl. Mater.

[1.6-6] Kondoh T., Nagashima A., Tsukahara Y., et al., "Fast Ion Diagnostics in JT-60U", to be published in Proc. International Conference on Plasma Physics, Prague, Czech (1998).

1.7 Data Analysis System

1.7.1 Data Analysis Tools, Database and Computer System

Developments and improvements have been carried out for data analysis tools of the JT-60 analysis server. A new version of DAISY (DAta Illustration SYstem) has been developed, which has a new graphical user-interface using the X-Window technology. After the divertor modification of JT-60U, the plasma-boundary identification code, FBI, and the MHD equilibrium analysis code, SELENE, have been revised to incorporate the new divertor configuration. The software showing a time slice of experimental data, SLICE, has also been improved to incorporate new diagnostics and has been added as a function of file output. A new statistical analysis tool, SANDER (Statistical ANalysis and Database Exploring Routine), has been developed using the statistical analysis package, SAS. This tool can use both the experimental database on the JT-60 database server and the DARTS (DAtabase ReTrieval System) database on the JT-60 analysis server.

The JT-60 experimental database has enriched the content. Appropriately for the update of diagnostic systems, such as CO_2 polarimeter, heterodyne radiometer, divertor bolometer, and neutral gas pressure diagnostics, these diagnostic data have been added to the experimental database. Plasma equilibrium data by the new FAME, which is described in Sec. 1.7.2, have increased by twice in kinds and 10 times in time points. Calculated data by new RTP (real time processor) and fast sampling ($\geq 5\mu s$) data have also been added to the database.

Some subsystems and programs of JT-60 data processing system have been improved according to the demands of plasma diagnostic systems. Software for the acquisition system of the massive data, FDS (Fast VME Data acquisition System), has been developed to handle the increasing data on ISP (Inter Shot Processor) speedily. New RTP has been utilized to process the increasing amount of input-data and to realize an advanced feedback control. The CPU and the analog-to-digital converter have been improved and are about 10 and 5 times faster than the former

ones, respectively.

ISP has an automatic data storage system of the cartridge tape library, CTL. It contains ~1300 cartridges and stores ~300GB. At present, all JT-60 data of ~4TB are kept in these cartridges. But the CTL does not have sufficient capacity to handle increasing amount of JT-60 data. The amount of data in a cartridge of ~250MB is too small to handle data in the JT-60 data processing system. The reliability of magnetic tape media is also a problem. Therefore, a new data-archiver with another media of more data storage capacity and reliability has been utilized. It is a UNIX file server with ~100GB RAID disks and ~900GB MO (magneto-optical disk) auto-exchangers. This archival capacity corresponds to the data of about one-year JT-60 experiment shots at a present level of data.

1.7.2 FAME System

The original system of FAME (Fast Analyzer for MHD Equilibrium) was developed in 1993 to provide about 130 MHD equilibria in time series which are enough for the non-stationary analysis of the experimental data of JT-60U within a shot interval. The new system, FAME-II, with a high processing speed using IBM RS/6000 SP has been utilized in FY 1997, succeeding the original system. The system is a MIMD type small scaled parallel computers with 7 CPUs and the maximum theoretical speed is 3.42 GFLOPS. The SELENE and FBI codes are tuned up taking the parallel processing into consideration as well as the original system. Consequently, the computational performance of the new FAME system becomes more than 3 times faster than the original system. The new system also has the file server system with the large capacity of the data storage of 50 GB.

Efforts of utility development and update have been concentrated on more effective use of the new FAME system. An equilibrium animating system has been developed on a workstation arranged in the central control room. The system can provide animations of MHD equilibrium analyzed by the FAME, incorporated with SLICE. In order to display typical equilibrium data such as an ellipticity, an internal inductance, and so on, as functions of time with other experimental data, the new FAME system recalculates equilibria at an interval of 10 ms during off-experimental hours in night and transfers the results to JT-60 database server.

1.7.3 Data Link System and Remote Participation in JT-60 Experiments

The remote participation in JT-60 experiments from PPPL was successfully carried out during reverse shear experiments in September, by utilizing the Data Link System and the video conferencing systems. Participants from both JAERI and PPPL jointly analyzed and discussed the JT-60 data together.

In September, the JAERI- DOE overseas line was upgraded from 128 kbps to 768 kbps using state-of-the-art frame-relay technology. It is beneficial to the remote analysis of JT-60 data

from PPPL to use the Data Link System. The Data Link System provides standard JT-60 data analysis tools; DAISY, FBI, EQREAD (MHD equilibrium display code), and SLICE. All tools have been improved to keep the security. Seven projects have been approved as remote collaboration under the Cooperation among the Three Large Tokamak Facilities. These seven projects cover a wide range of research topics and the total number of participants amounts to about one hundred.

Reference

[1.7-1] Aoyagi T., Sato M., Sakata S., et al., "Development of New CICU", JAERI-Tech 97-073 (1998) (in Japanese).

[1.7-2] Hamamatsu K., Matsuda T., Nishitani T., et al., "Remote Laboratory in Fusion Experiments, Present Status and Prospects", J. Plasma Fusion Res., 73, 375 (1996) (in Japanese).

2. Experimental Results and Analyses

2.1 Reversed Shear Experiments

2.1.1 Stability Improvement in Reversed Shear Plasmas with an H-mode Edge

The high performance reversed shear discharges with an internal transport barrier (ITB) encountered a beta collapse when q_{min} decreased to 2, which restricted the fusion performance and the duration of high confinement. The beta limit was β_N~2 (β_N is the normalized beta) at q_{min}~2, and the low-q_{min} region below q_{min} = 1.7 could not be reached [2.1-1]. It was observed that fluctuations of electron temperature grew explosively in the ITB region with a very fast growth time of order ~10 μs just before the collapse [2.1-2]. These observations of the beta limit and instability growth time well agree with calculated values for low-n kink-ballooning modes by using the ERATO-J code [2.1-3, 4]. Since this mode is destabilized by a large pressure gradient in the ITB layer, pressure profile broadening with combining the ITB with the H-mode in the peripheral plasma region was attempted in high triangularity discharges for a toroidal field of 3.5 T. The beam power during the current ramp-up was reduced to prevent the development of a strong ITB (or a steep pressure gradient), because strong ITBs appeared to make the H-mode transition difficult [2.1-1]. Then a high power heating at the current flat-top triggered the H-mode transition and also generated an ITB. The stability in the low-q_{min} region was successfully improved for the H-mode edge discharges, and a high β_N value of 2.3 has been achieved with q_{min} = 1.5.

2.1.2 Sustainment of internal transport barrier

To realize a steady state operation of high confinement reversed shear discharges, simultaneous sustainment of the ITB and the current profile are required. In JT-60U quasi-steady sustainment of ITB with an ELMy H-mode edge was obtained thanks to the enhanced stability in H-mode edge discharges for B_t=3.5 T (see Fig.I.2.1-1 [2.1-5]). Though the current profile was not kept stationary due to the lack of the active non-inductive current drive source, significant advance towards the steady state operation has been obtained as shown in Fig.I.2.1-1. Improved

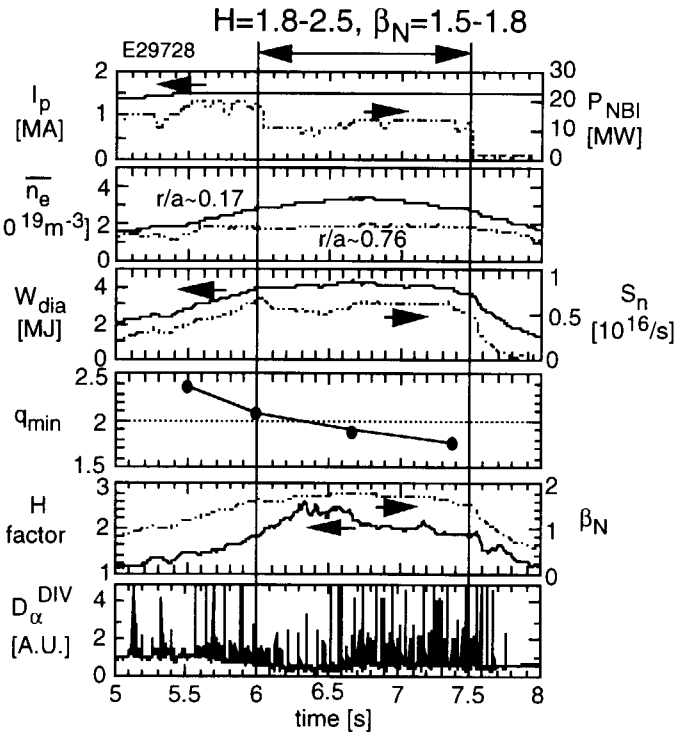

Fig. I.2.1-1. Waveforms of a reversed shear discharge with an ELMy H-mode edge where an ITB was sustained for 1.5 s with an H-factor of 1.8-2.5 and β_N of 1.5-1.8.

confinement with an H-factor of 1.8-2.5 and β_N of 1.5-1.8 is sustained for 1.5 s (or 4-5 times τ_E) in a high triangularity reversed shear discharge (I_p = 1.5 MA, q_{95} = 4.5, δ ~ 0.28). The ITB is established and developed sufficiently by the high power heating before t = 6 s as indicated by the rise of line averaged electron density $\bar{n}_e$ along the central chord (r/a ~ 0.17) , and the beam power is stepped down to avoid a collapse. Though the minimum q, q_{min}, continues to decrease, the reversed shear configuration and the ITB with steep gradients in n_e, T_e and T_i profiles are maintained until the end of neutral beam heating.

Long sustainment, reaching the time duration of 4.3 sec, of the ITB and the reversed shear configuration with an H-factor of ~ 1.7 and β_N of ~ 1.5 was also demonstrated using a feedback control of the beam power to maintain a fixed neutron emission rate.

2.1.3 Formation Condition of Internal Transport Barrier

The ITB, especially with a reduction in electron thermal transport, should be actively controlled in order to obtain steady-state burning plasmas. From this view point, onset conditions of the ITB were investigated by systematic scans of electron density, beam power and magnetic shear. Preliminary results have been obtained as follows.

(1) Under an almost fixed reversed magnetic shear profile, toroidal rotation shear seemed to alleviate the required heating power for the ITB formation.

(2) Even with similar electron density, heating power and toroidal rotation shear, a discharges with a reversed magnetic shear showed an ITB formation, while another discharge with a positive magnetic shear did not. (In different condition, there exists ITB accompanied by a positive magnetic shear.) This difference suggests that reversed magnetic shear mitigates the required conditions for the ITB onset.

References

[2.1-1] Fujita T., Hatae T., Oikawa T., et al., Nucl. Fusion 38, 207 (1998).
[2-1.2] Ishida S., Takeji S., Isayama A., et al., in Controlled Fusion and Plasma Physics (Proc. 24th Eur. Conf. Berchtesgaden, 1997), Vol. 21A, Part II, 489 (1997).
[2.1-3] Ozeki T., Azumi M., Ishii Y., et al., Plasma Phys. Control. Fusion **39**, A371 (1997).
[2.1-4] Ishii Y., Ozeki T., Tokuda S., et al., "Ideal beta limits of negative shear plasma in JT-60U", to be published in Plasma. Phys. Controll. Fusion (1998).
[2.1-5] Shirai H. and JT-60 team, Phys. Plasmas, **5**, 1712 (1998).

2.2 High β_p and High Triangularity Discharges

This section treats recent development of quasi-steady ELMing discharges with enhanced confinement, high-β stability and current drive capabilities, where increase in absolute values of fusion performance and sustainment time are emphasized in addition to the normalized parameters. After modification to the new W-shaped pumped divertor, a long heating time (9sec) of high power NB (20 -25MW) became possible without harmful increase in impurity and particle recycling. The total energy input reached 203MJ. In addition to it, optimization of the plasma

shape, the pressure profile and selection of appropriate electron density enabled us to extend the pulse length with high performances. The new extension of the pulse length accelerates the understanding of roles of parameters with long time constants such as the current profile and particle recycling.

2.2.1 Sustainment of High Integrated Performance and High Fusion Gain

Toward the *simultaneous* achievement of i) high confinement , ii) high β limit, iii) high bootstrap fraction and iv) high efficiency of heat and particle exhaust in the *steady-state*, discharges have been optimized in JT-60U mainly based on the high-βp H-mode with q(0)>1. Up to I_p=1MA, an optimized pressure profile with high triangularity δ (=0.35) enabled the favorable integrated performance with H-factor ($=\tau_E/\tau_E^{ITER89PL}$) ~ 2.5 and β_N~3 under full non-inductive current drive (bootstrap ~60%) sustained for 2s (~$10\tau_E$)[2.2-1,2]. In a 1.5MA/3.6T discharge with δ=0.35, a favorable integrated performance was sustained for ~2.6s (~8 τ_E) with Q_{DT}~0.2, β_N~2.5 and H-factor~2.5, bootstrap current ~50%, beam driven current ~25% (~75% non-inductive). In this discharge regime, a current profile with natural shear reversal close to the steady-state solution was observed because of sustainment of high values of βp. At a higher I_p =1.8MA (B_t=3.6T) with an ITER-like configuration (q_{95}= 3.4, δ= 0.3, κ =1.5), Q_{DT}= 0.27-0.3, β_N= 2.7-2.9, H~2.5, H/q_{95}= 0.74 was sustained for 0.7s (2xτ_E). With the new W-shaped pumped divertor [2.2-3], a long heating time with high power became possible. We obtained an ELMy H-mode with Q_{DT}~0.11, H-factor ~1.7, T_i(0)~10keV and β_N~1.8 sustained for 9 sec (~$40\tau_E$) under a high NB power of 20-25MW (I_p=1.5MA, B_t=3.6T, δ=0.16). Even with the high total energy input up to 203MJ, no increase in impurity (carbon) and particle recycling was observed. Before the divertor modification, increase in carbon and recycling degraded performance at ~3 sec of high power (20-30MW) heating. In case of high δ (=0.3), the better performance with Q_{DT}~0.16, H-factor~2.3, β_N~2 and β_p~1.6 was sustained for 4.5 sec with 60-70% of non-inductive driven current at a relatively high density of ~45% of the Greenwald limit. Duration of the high δ equilibrium is limited (< 5sec) by heat capacity of the shaping coils. Without the divertor pumping, gradual increase in recycling degraded energy confinement.

2.2.2 β-limits in Long Pulses

For maximizing β_N in a long pulse, it is required to keep a sufficient stability margin against the ideal MHD instabilities. Experimentally, these ideal instabilities limit the transiently achievable β_N values. For this purpose, it is essential to control the heating profile to produce the optimum peakedness of pressure profile p(r) [2.2-2]. At a larger peakedness, the β_N-limit is lower due to the β_p-collapse which is consistent with the ideal kink-ballooning limit. At a smaller peakedness, β_N is limited at a low level by giant ELMs which is consistent with the ideal high-n

ballooning limit. Therefore, a medium peakedness of the pressure profile has the highest β_N limit. Since the ELM-limit increases with δ, the β_N limit increases with δ.

However, in a long pulse discharges, another kind of the MHD instability appears and which limits the sustainable β_N much lower than the transiently achievable values. So far, even at the optimum p(r) with the transiently achievable β_N^{max}=3.2, sustainable β_N is ~2.5 for 2.6sec and ~2 for 5-9sec at I_p=1.5MA, B_t=3.6T , q_{95}~4 and l_i~1 with collisionality similar to ITER. This degradation is due to slowly (~100ms) growing resistive instabilities with mode numbers of (m/n)=(3/2), (2/1) etc. The detailed measurement of electron temperature by the heterodyne radiometer with high spatial resolution of 2cm showed growth and saturation of island width (~5cm) [2.2-4]. The neoclassical tearing mode is the candidate of this instability. By appearance of the resistive modes, values of sustainable $H\beta_N$ (H-factor $\times$ β_N) in quasi-steady phase lasting >2sec are smaller than the transiently achievable ones by ~50% (from 13 to 6.5 at δ~0.35). However, even in such long pulse discharges, the stability is also better at higher δ, for example, sustainable values of $H\beta_N$ increases with δ (from ~4 at δ~0.1 to 6.5 at δ~0.35). The threshold β_N for onset of the resistive modes increases with increasing electron density and with broadening of p(r). At a density higher than ~50% of Greenwald limit, β_N decreases because of confinement degradation at high recycling. Therefore, for sustainment of long pulse discharges, we kept the optimum set of δ, density and β_N to avoid both the resistive modes and confinement degradation.

On the other hand, at the edge, the confinement and steadiness of the H-mode are affected by giant ELMs and depth of the edge pedestal Δ_{ped}. The depth Δ_{ped} in the ELMing phase is 2-3 times larger than that in the ELM-free phase and reaches ~10-15cm with a roughly constant pressure gradient. With increasing recycling, the pedestal layer moves inward and the ELM frequency increases, which cause the gradual confinement degradation in a long pulse.

References

[2.2-1] Kamada, Y., et al., Plasma Phys. Cont. Nucl. Fusion Res. Proc.15th Int. Conf. (Seville, 1994) Vol 1, p651.
[2.2-2] Kamada, Y., et al., Fusion Energy Proc. 16th Int. Conf. (Montreal, 1996) Vol 1, p247.
[2.2-3] Hosogane, N., et al., Fusion Energy Proc. 16th Int. Conf. (Montreal, 1996) GP-11.
[2.2-4] Isayama, A., et al., submitted to Plasma Phys. Control. Fusion.

2.3 H-mode Study

2.3.1 Scaling and Neutral Effect of L-H Tansition in the W-shaped Divertor in JT-60U[2.3-1]

The influence of the edge neutrals on the L-H transition condition was investigated in the W-shaped pumped divertor in JT-60U, which is an extension of the previous work published in Ref.[2.3-2]. In the dedicated experiment, the density was scanned in the range of (1.5-4.0) $\times 10^{19} m^{-3}$. It was found, however, that the amount of reduction in the H-mode threshold power in the modified divertor geometry was subtle, in comparison with the open divertor. The

density exponent also remained in the range of 0.5 to 0.75, whilst it was 0.5 for the previous open divertor case. The signs of presumed geometry effect was found in the detailed analysis, where the slight reduction of threshold power was observed as the compression ratio was increased. As for the edge neutrals density, it was found that ν_i^{*95} (ion collisionality at 95% flux surface) stays around unity even under the condition that n_0^{95}/n_e^{95} is considerably large in the modified divertor geometry, although the remarkable reduction of ν_i^{*95} was documented at a high n_0^{95}/n_e^{95} in the open divertor. Here, n_0^{95} is neutral deuterium density averaged in poloidal direction at 95% flux surface. However, it was also found that the consideration of the wall source at the outer buffle plate is necessary, whereas it was negligible in the open divertor geometry. In the basis of DEGAS calculation, the contributions of each source regions, which are divertor and outer buffle plate, can be comparable. This means that the poloidal averaging may possibly produce misleading results, as we have not resolved where in the edge poloidal section of the plasma being the most influential on the L-H transition.

2.3.2 Scaling of H-mode Power Threshold with the Edge Nondimensional Quantities[2.3-3]

We have employed the well established nondimensional treatment, and thereby described the conventional nondimensional quantities in terms of the relevant edge variables. .The nondimensional formulae for the H-mode threshold power P_{th} are also transformed to $P_{th}=[\rho^{*95}]^{\alpha_\rho 95}[\beta^{95}]^{\alpha_\beta 95}[\nu^{*95}]^{\alpha_\nu 95}R^2n_e^{95}[T_i^{95}]^{3/2}$,where $\alpha_\rho 95/2-2\alpha_\nu 95+\alpha_\beta 95+3/2=0$. A postulated hypothesis regarding the significance of the ρ^{*95} dependence, based on the ion orbit loss theory, is that H-mode becomes more accessible and sensitive to the fast ions with ρ^{*95}. The obtained scaling satisfies the constraint written above, with its value being 0.1. In addition, it is quite consistent with our global scaling result of $P_{th}=n_e^{0.5}B^{1.0}R^{1.5}$. As indicated in equation of obtained scaling, ρ^{*95} has a positive contribution to the threshold power against our hypothesis. A speculated reason for the apparent inconsistency on ρ^{*95} is that the above procedure does not separate the bulk plasma transport from the transition physics. Therefore, it would be necessary to take the contribution of nondimensional confinement scaling into account.

References

[2.3-1] Tsuchiya K., Fukuda T., Kamada Y., et al., Plasma Phys. Control. Fusion **40** 713 (1998)
[2.3-2] Fukuda T., Takizuka T., Tsuchiya K., et al., Nucl. Fusion **37** 1199 (1997)
[2.3-3] Fukuda T., Takizuka T., Kamada Y., et al., Plasma Phys. Control. Fusion **40** 827 (1998)

2.4 Current Drive Experiments

Optimization of the operation of Negative-ion-source Neutral Beam Injector (NNBI: designed parameters of 500 keV and 10 MW with two ion sources) progressed and the injection power of 3.2 MW/source at 350 keV was achieved. The maximum injection power increased up to 4.2 MW using two ion sources. Utilizing the NNB and the lower hybrid (LH) waves, following new results were obtained.

The NNB driven current was well identified for the first time by reconstruction of the current density and loop voltage profile using the equilibrium code (EFIT) and the internal magnetic measurements form the motional Stark effect spectroscopy (MSE). A centrally-peaked profile of plasma current driven by the NNB was confirmed. The total driven current and a current density profile are consistent with the predictions with the ACCOME code [2.4-1]. The efficiency of the NNB driven current increased with the central electron temperature as expected from the ACCOME code. The controllability of the plasma current profile was also confirmed by comparing the driven current profiles by the NNB (350 keV) and the PNB (80 keV).

LHCD was applied to a reversed magnetic shear plasma in order to sustain internal transport barriers by keeping a hollow current profile. It was demonstrated in a plasma of I_P = 1 MA, B_T = 3.5 T that internal transport barriers in the electron, ion temperatures and electron density were maintained by applying LHCD. The internal transport barriers have been prolonged for about 2 seconds so far by LHCD. Although the period is not very long, this should be attributed to that an LH driven current profile was not fully optimized for the reversed magnetic shear configuration. A preliminary result of the current profile analysis from the MSE data suggests that some amount of current was driven also in the central region of the plasma, while the contribution of the LH current was dominant to make a hollow current profile outside the internal transport barriers [2.4-2].

References

[2.4-1] Kusama Y., et al., in Proceedings of 24th European Physical Society Conference on Controlled Fusion and Plasma Physics, Berchtesgaden, 9th-13th June 1997, Vol. 21A Part II, p513-p516.
[2.4-2] Ide S., Naito O., Ushigusa K., et al., Proc. 2nd Europhysics Topic. Conf. on Radio Frequency Heating and Current Drive of Fusion Devices, Brussels, 169 (1998).

2.5 W-shaped Divertor and SOL plasmas

The principal goal of experimental campaigns using a new semi-closed W-shaped divertor is the demonstration of a cold-and-dense or detached divertor plasma with the enhanced energy confinement. The divertor was designed to control recycling neutrals [2.5-1] with an exhaust system using cryo-pump units. To increase the neutral density at the strike point, the divertor targets are inclined at angles of 70 and 60 degrees, and joined to baffle plates at the divertor throat. A private dome separates neutral transport between the inner and outer divertors.

2.5.1 Divertor Plasma and Detachment

At relatively high line averaged electron plasma density of a main plasma ($\bar{n}_e$), a large peak in the divertor electron density (n_e^{div}) profile was observed near the strike point on the divertor plate. Comparing to the open divertor case, the local n_e^{div} was a factor of 2 larger at the same $\bar{n}_e$, and divertor temperature (T_e^{div}) was reduced. These results indicate that the inclined divertor target

and the private dome are effective in condensing neutrals near the separatrix. Consequently, onset densities of the divertor detachment and MARFE in the W-shaped divertor were reduced [2.5-2]. The inner private pumping with gas puffing at the plasma top preliminarily demonstrated that the concentration of charged carbon ions (C^{3+}) can be reduced in the divertor region[2.5-3].

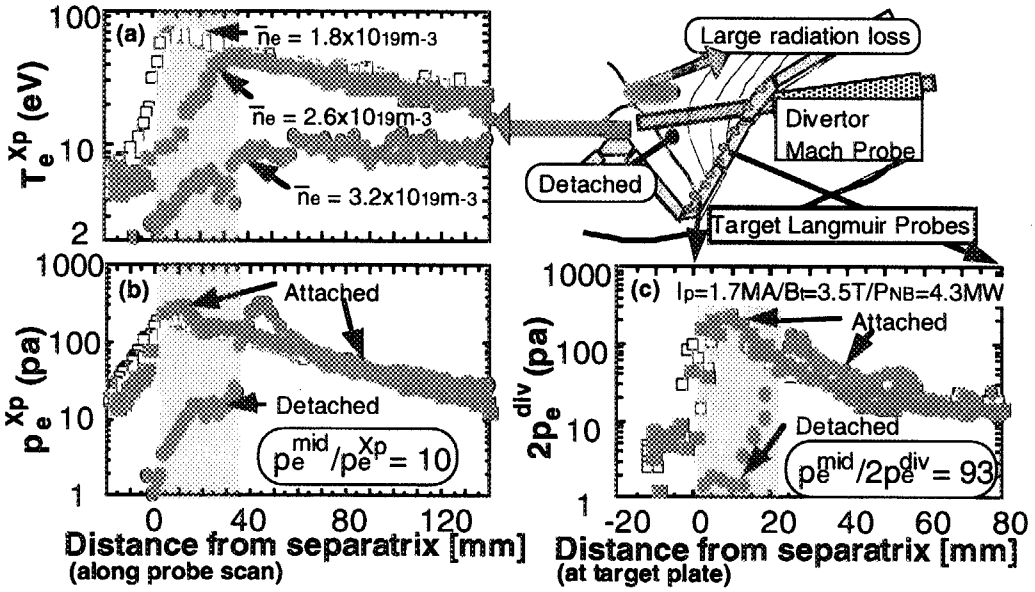

Fig. I.2.5-1 Plasma temperature and pressure profiles for attached and detached divertors.

Divertor plasma detachment simultaneously occurred at all points along the separatrix field line between the x-point and divertor target, which was measured from newly installed divertor Mach probe and target Langmuir probes (see Fig.I.2.5-1). Here the electron temperature profile in the outer flux surfaces becomes flat and density increases. Radial diffusion of particle flux may be enhanced upstream from the x-point. A large pressure loss factor of ~90 at the outer divertor target is obtained, which is larger than < 20 for the open divertor [2.5-2]. Due to the lower T_e^{div} and larger neutral density elastic and charge-exchange collisions may increase near the target.

2.5.2 Control of Recycling Neutrals [2.5-2]

Particle recycling generally does the most important contribution to fueling the main plasma. A change in the divertor geometry affected the distributions of neutral sources and neutral density. Neutral ionization fluxes at the main plasma edge and divertor ($\Phi_{D\alpha}^{main}$ and $\Phi_{D\alpha}^{div}$) were deduced from integrating the D_α signals. For an attached divertor plasma, an increase in $\Phi_{D\alpha}^{div}$ with $\bar{n}_e$ was similar for both W-shaped and open divertors. The value of $\Phi_{D\alpha}^{main}$ also increased with $\bar{n}_e$, but $\Phi_{D\alpha}^{main}$ for the W-shaped divertor was a factor of 2 - 3 smaller than that for the open divertor. The maximum neutral compression ratio, $p_{n0}^{div}/p_{n0}^{main}$, was measured to be 1000 (=1.2Pa/1.2 mPa).

Neutral particle distribution was investigated by a two-dimensional neutral transport code. Above the baffle plates, number of neutrals from the divertor source decreased significantly:

leakage of neutrals from the divertor to the main chamber was small compared to the open divertor. On the other hand, neutral sources, in particular, from the inner and outer baffle plates became dominant. The ionization source inside the separatrix originating from the baffle plates also had a larger contribution for fueling inside the separatrix (40% of the divertor source). As a result, a small reduction in the neutral density at the main plasma edge by the factor of 2 - 3 was obtained. This reduction in the edge neutral density is not as large as was predicted in design calculations.

Two (i.e. first and second) SOL regions with different characteristic lengths were observed in the n_e^{mid} profile measured by a midplane reciprocating probe. The decay length of the second SOL region was 3 - 4 times larger than the *e*-folding length of the first SOL, and was similar before and after the baffle plate installation. Quantitative evaluations of the ion flux to the outer baffle plates and the local recycling flux gave a good agreement, which suggests that the neutral source at the baffle plates is produced due to the interaction with the second SOL plasma.

2.5.3 Core Plasma Confinement of ELMy H-mode Plasmas [2-5-2]

A similar degradation in the H-factor (confinement enhanced over ITER89P-L mode scaling) of the ELMy H-mode plasma was observed at high density for the open and W-shaped divertors. The decrease in the edge neutral density (by a factor of 2-3) had no effect on the energy confinement. The reduction of the H-factor is due to the decrease in the fast ion slowing down time and in the thermal energy with the increase in $\bar{n}_e$. The total plasma pressure at the edge pedestal decreases at higher $\bar{n}_e$, which is caused by a reduction in the width of the pedestal region (from r = 0.95 - 0.99 to 0.97 - 0.99) with almost the same pressure gradient. Here the pressure gradient is not reduced. Effective fueling method inside the separatrix (e.g. a continuous pellet injection) should be implemented for the high density operation.

References

[2.5-1] Hosogane N., Sakurai S., Shimizu K. et al., Proc. 16th Int. Conf., Montreal, IAEA, Vienna, **3**, 555 (1997).
[2.5-2] Asakura N., Hosogane N., Itami K., et al., to be published in J. Nucl. Mater.
[2.5-3] Hosogane N., Sakasai A., Itami K., et al., to be published in J. Nucl. Mater.

2.6 Particle Transport and Exhaust with the W-shaped divertor

2.6.1 Steady-state Helium Exhaust [2.6-1]

When neutral beams of 60 keV helium atoms were injected to ELMy H-mode plasmas for 6 sec, efficient He exhaust was realized with He pumping using Ar frosted cryopumps for the W-shaped pumped divertor (see Fig.I.2.6-1). The He source rate (equivalent to 0.6 Pa·m^3/s) is balanced with its exhaust rate in a steady state, and high He exhaust capability (τ^*_{He}/τ_E=4) is successfully demonstrated, where τ^*_{He} is an effective He exhaust time. The enrichment factor of He is obtained about 1.0, which is 5 times larger than the ITER requirement (0.2). The exhaust rate increased with the electron density in the main plasma. Even without He pumping, an

enrichment factor of 0.5 was obtained thanks to the W-shaped divertor. It seems that the reflection of He neutral particles near the inner strike point is enhanced by the W-shaped divertor. These results strongly support divertor designs in ITER.

In detached ELMy H-mode plasmas, τ^*_{He} is comparable to one in attached plasmas because recycling particle flux is enhanced at the inner strike point in a high density operation. Helium exhaust in detached plasmas is allowable for an ITER divertor operation scenario. The inner leg pumping worked well for He exhaust due to the inboard-enhanced He flux and deuterium flux, when the ion grad-B drift is directed to the target. The in-out asymmetry with He and deuterium flux profiles strongly affects the He exhaust capability.

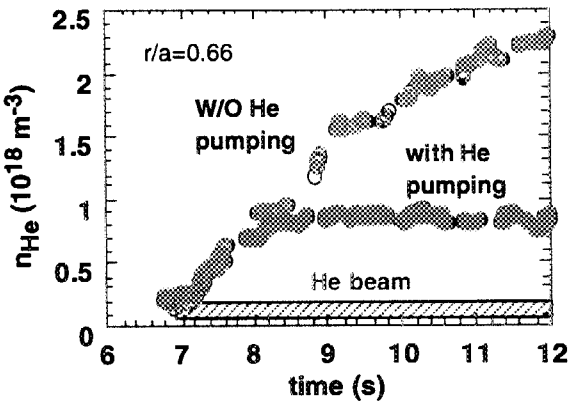

Fig. I.2.6-1 Time evolution of measured He density with and without He pumping. The He density with He pumping reaches a saturation level at 1.2 s after the start of the He beam injection.

2.6.2 Particle Transport in Reversed Shear Plasma [2.6-2]

The particle diffusivity and the convection velocity in the reversed shear plasma were separately evaluated based on the perturbation technique using modulated helium gas-puffing. The particle diffusivity in the region of the internal transport barrier (ITB) was reduced by about a factor of 2 compared with that in the core region surrounded by the ITB. The inward pinch was measured in the region of the ITB, while the outward convection velocity was observed in the core region. These results indicate that both of the particle diffusivity and the convection velocity largely related to the formation of the ITB.

2.6.3 Particle Balance and Neutral Particle Behavior [2.6-3]

The pumping rate of the W-shaped divertor was estimated from the quantitative analyses of the particle balance with and without divertor pumping. Furthermore, in order to understand the divertor pumping characteristics, the neutral particle behavior was analyzed using a neutral particle transport code, DEGAS. The ratio of the divertor pumping rate to the particle flux onto the divertor plates was estimated to be in the range of 0.5-2.5% for the density range of 2-4.3x$10^{19}$$m^{-3}$, and its strong dependence on the distance between the strike point and the pumping duct was observed. In the simulation of neutral particle behavior, a particle source from the outer baffle plates was found to be ~5% of the divertor source. The estimated pumping rate in experiment was a factor of three smaller than the predicted one. This difference might come form the effects of the structure under the baffle plates, which will be investigated in a future work.

2.6.4 Volume Recombination in the Divertor Plasma [2.6-4]

Understanding of the volume recombination for detached plasmas is important in tokamak fusion reactor design, because the detached divertor regime is attractive to reduce the ion flux incident to divertor plates. Balmer-series lines of deuterium atoms were observed and the population distribution for excited levels of the deuterium atoms was investigated. The ratio of the recombination sink to the ionization source was estimated from the ratio of the D_ε line intensity to the D_α line intensity for partially-detached divertor plasmas. While the onset of the recombination was correlated with the plasma detachment, the recombination sink was estimated to be about 1 % of the ionization source. This suggests that the recombination is not a principal cause of the detachment.

2.6.5 Behavior of He Atoms in the Divertor Region [2.6-5]

In JT-60U, it has been found that the Doppler width of He I line emitted from the divertor region increases with the increase in the electron density [2.6-5]. The atom temperature corresponding to the Doppler width is up to 1.7 eV for detached plasmas. Understanding of the He atom behavior is important to establish an effective system for He exhaust. Thus the Doppler broadening has been reproduced by numerical calculations using a neutral particle transport code. The broadening is attributed to elastic collisions with H^+. For an L-mode discharge a probability of penetration of He atoms from the outer divertor tiles into the main plasma was estimated to be 7 %, but this probability drops down to 4.5% in a calculation with neglecting the elastic collisions. Thus the elastic collision is expected to largely affect He contamination in main plasmas.

References

[2.6-1] Sakasai A., Takenaga H., Hosogane N., et al., PSI Conf., San Diego 1997, to be published in Journal of Nuclear Meterials.
[2.6-2] Takenaga H., Nagashima K., Asakura N., et al., Plasma Phys. Control. Fusion 40, 183 (1998).
[2.6-3] JT-60 Team, Review of JT-60U experimental results in1997 JAERI-Research 98-039 (1998).
[2.6-4] Kubo H., Higashijima S., Takenaga H., et al., Proc. 1998 ICCP and 25th EPS, Prague (1998).
[2.6-5] Kubo H., Takenaga H., Sugie T., et al., Proc. 24th EPS, Berchitesgaden, 21A, PartII, 509 (1997).

2.7 Fast Ions and Alfvén Eigenmodes

The Toroidicity-induced Alfvén Eigenmodes (TAEs) and high frequency modes observed in ICRF-heated low-q discharges were analyzed in detail using the NOVA-K code (PPPL). It was shown that TAEs appeared before giant sawtooth crash were excited inside q=1 surface [2.7-1] and high frequency modes observed after the crash were the Ellipticity-induced Alfvén Eigenmodes (EAEs) excited at the q=1 surface [2.7-2]. The interaction between TAEs/EAEs and NNB-injected ions was investigated, and the EAEs were stabilized with the NNB. The stability analysis using the NOVA-K code suggested that the stabilization mechanism was beam ion Landau damping. It was also shown that the q-profile derived from the change in TAE mode frequencies agreed with that obtained from the motional Stark effect spectroscopy [2.7-3]. Chirping modes were observed in ICRF-heated weak magnetic shear plasmas [2.7-4]. The TAEs were excited with

the NNB. Both burst and continuous modes with low toroidal mode numbers were observed in a low β_h regime of $<\beta_h>\leq 0.1$-0.2%, here, β_h is the beta value of energetic ions and $<\beta_h>$ is the volume-averaged one. The amplitude of magnetic fluctuations of the burst modes is about ten times as large as that of the continuous modes. Accompanying these bursting activities were 2-3% drops in the neutron emission rate. This small drop indicates that the loss of the co-injected NNB ions is small.

The ICRF coupling with plasmas in the W-shaped divertor was optimized by adjusting a gap between the first wall and the separatrix. The coupling resistance was similar to that in the open divertor and the ICRF power of ~4 MW was applied to reversed-shear plasmas. By changing the NB power and the ICRF power and by replacing the ICRF power by the NB power, the formation of the ITB was investigated. It was shown that the NB power of 4-5 MW was necessary to sustain the ITB in the electron density profile. The effect of magnetic shear on an increase in electron temperature was also investigated in the ICRF-heated reversed and normal shear plasmas. It was shown that the heating profile was hollow due to an expansion of banana orbits and/or enhanced ripple transport in the reversed shear plasma [2.7-5]. A new scaling including plasma current was obtained for the temperatures of ICRF-driven tail ions, which was based on a diffusion model of fast ion losses. The measured tail temperatures were well described by this scaling.

Enhancement in the ionization cross-section of the NNB was evaluated at 350 keV/amu. Measured shine-through of the NNB was lower than that calculated by assuming the single-step ionization process. This result shows that the multi-step ionization process is needed to be taken into account. The experimentally obtained enhancement factor of the ionization cross-section agrees with that predicted using the enhanced cross-section evaluated by Janev [2.7-6].

References

[2.7-1] Saigusa M., Kimura H., Kusama Y., et al., to be published in Plasma Phys. Control. Fusion.
[2.7-2] Kusama Y., Oikawa T., Nemoto M. et al., in Proceedings of 24th European Physical Society Conference on Controlled Fusion and Plasma Physics, Berchtesgaden, 9th-13th June 1997, Vol. 21A Part II, p513-p516.
[2.7-3] Kramer G. J., Oikawa T., Fujita T. et al., Plasma Phys. Control. Fusion 40 863 (1998).
[2.7-4] Kusama Y., Kimura H., Ozeki T., et al., to be published in Nuclear Fusion.
[2.7-5] Tobita K. and the JT-60 Team, submitted to Plasma Phys. Control. Fusion.
[2.7-6] Nemoto M., Tobita K., Ushigusa K., et al., Journal of Plasma and Fusion Science, 73 1374 (1997).

2.8 Plasma Control and Disruption

2.8.1 Plasma Control

Preparatory work for the equilibrium control of plasmas under the modified divertor geometry started early in this year, including the compilation of over 800 numerical equilibrium data necessary to evaluate the function parametrization coefficients. The discharge procedure was also investigated deliberately with the equilibrium calculation code MEUDAS, considering the

baffle and dome structures. In order to cope with various technical limitations, "startup operation group" was organized, and detailed physics operation procedure was discussed, including the heat load onto the in-vessel components and commissioning program of various divertor diagnostics. Accordingly, the nominal 15 s stable discharge was produced on the 2nd day of the campaign with its discharge waveforms as well as its equilibrium shape and positions exactly as predicted with the calculation code. Subsequently, the dynamic range of physics operation was confirmed, and the halo current experiment was conducted to establish the database to increase the plasma current.

Various real-time feedback schemes were prepared in 1997, in addition to the conventional density, neutron rate and divertor radiation feedback controls. The CO_2 laser interferometer data, which provides the averaged density near the magnetic axis, and neutral pressure signal in the divertor as well as the divertor density information have been made available as feedback tools on ZENKEI-1bR computer. The neutron feedback algorithm was also modified to implement the differential control, which turned out to be an effective method of stability control in the reversed shear high performance experiment.

2.8.2 Disruption Studies

The disruption studies performed in 1997 focused on the investigation of halo current characteristics, which is also an urgent ITER Physics R&D issue. The most dangerous disruption caused by vertical displacement event (VDE) was experimentally simulated, in which a plasma was actively controlled to move downward. Ranges of the measured total halo current normalized by initial plasma current (I_h/I_{p0}) and toroidal peaking factor (TPF) were 0.05 to 0.26 and 1.4 to 3.6, respectively, in the ranges of I_p = 0.7-1.8 MA, B_T = 2.2-3.5 T, κ = 1.3-1.6 and q_{95} = 2.8-7.0. The maximum TPF×(I_h/I_{p0}), corresponding to the maximum local halo current, was 0.52 so far, which was lower than that of the maximum value of the ITER data base of 0.75. The upper boundary of TPF×(I_h/I_{p0}) tended to decrease with the increase in I_{p0}. Other parameter dependencies of TPF×(I_h/I_{p0}) on B_T, κ and q_{95} were not clear. We confirmed that the upper boundary of TPF×(I_h/I_{p0}) decreased with the decrease in the vertical shift velocity ($-dZ_j/dt$). On the other hand, the TPF×(I_h/I_{p0}) clearly decreased with the increase in the stored energy just before the energy quench ($W_{dia}^{eq.}$) and the line integrated electron density at the peak of halo current. These stored energy and density dependencies of the halo current may be explained by a increase of halo resistivity, probably caused by a large amount of impurity generation during disruptions. The magnitude of the halo current decreased by about 40% by applied a strong pulse gas puff (H_2 of 50 Pam^3/s x 0.1s) during VDE. Perfect avoidance of the halo current has been demonstrated by maintaining the plasma vertical position during the current termination [2.8-1].

References

[2.8-1] Neyatani Y., et al., submitted to Nucl. Fusion.

3. Design Progress of the JT-60SU

3.1 Optimization for Steady-state Advanced Operation

The JT-60 Super Upgrade (R_p=4.8 m, B_t=6.25 T, $I_p \leq 10$ MA [3.1-1, 2, 3]) has been designed as a superconducting tokamak for establishing an integrated scientific basis of a steady-state tokamak reactor and for contributing to an advanced steady-state scenario in ITER. Figure 1 shows a schematic drawing of the JT-60SU machine, where the diameter of the cryostat is 22 m and the total weight of the device including the cryostat is ~11000 tons. After 10 years D-D operation and installing the extra shield made of reduced activation ferritic steel, a steady-state D-T operation with Q_{DT}~5 is considered as an optional scenario.

JT-60SU is designed to have a high Greenwald density limit (>1x10^{20}m^{-3}) by selecting B_t/R~1.1-1.3 in order to perform a steady-state operation research at high density regime. At I_p=5-6MA, a fully non-inductive discharge can be expected at $\langle n_e \rangle$~0.88x10^{20} m^{-3} by using 60 MW of CD power, which is much higher than the ITER scaling law for H-mode power threshold (~40 MW). In addition to a 750 keV N-NBI system for core heating and current drive, 150-220 GHz ECH system is adopted to provide flexible current profile control for establishing an advanced steady-state operation scenario with a stable reversed shear configuration in JT-60SU.

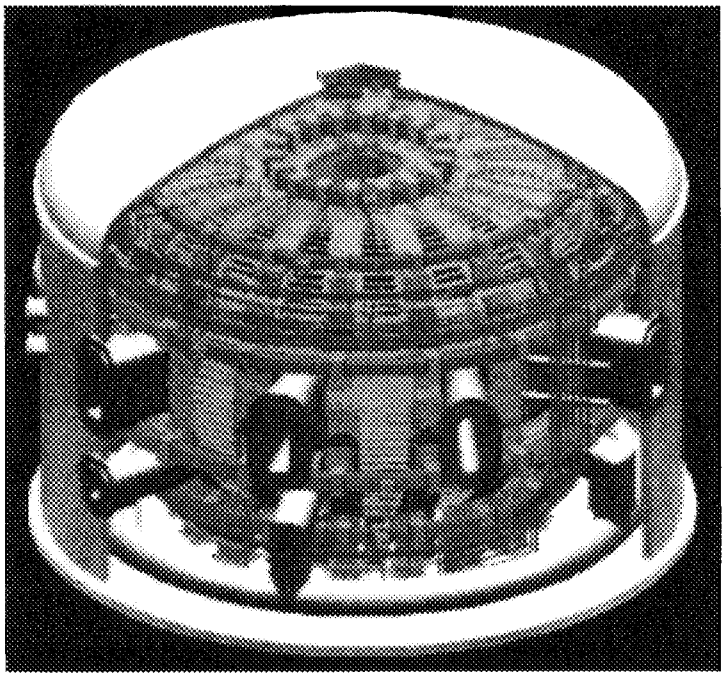

Fig.I.3.1-1 Schematic drawing of JT-60SU

Ten units of independent PF coil system are adopted in JT-60SU to have a capability to produce a wide variety of plasma shaping (elongation κ_X up to 2.0 and triangularity δ_X up to 0.8 for DN divertor) for improving the β-limit in the steady-state operation scenario. Vertical Displacement Event (VDE) in JT-60SU has been also investigated by using Toroidally Symmetric Plasma Simulation (TSPS) code in which the Grad-Shafranov equation and a linearized equations of plasma motion taking into account the effects of eddy current on the vessel and baffle plates are iteratively solved [3.1-4]. Fast vertical position control system composed of two sets of normal conductors (10 turns) located near the vacuum vessel is adopted in JT-60SU for suppressing VDE. TSPS code has indicated that the VDE can be suppressed by fast vertical position control with the

power supply of 200 V when the disturbance is moderate (a rapid change in βp during a minor disruption $\Delta\beta p \leq -0.6$ for 10 ms).

The ideal and resistive stability of the reversed shear scenario on JT-60SU is investigated using the equilibrium assuming a correlation between plasma pressure and magnetic shear scale length observed in JT-60U experiments. Stability analysis has indicated that growth rate of n=2 tearing mode is slightly reduced with increasing β_N, while an n=2 ideal global mode becomes unstable suddenly at around β_N=2.

References

[3.1-1] Kikuchi M., Miya N., Ushigusa K., et al., Proc. 16th Int. Conf. Plasma Physics Contr. Nucl. Fusion Research, IAEA-CN-64/G2-3, Montreal, Canada., 1996.
[3.1-2] Nagashima K., Kikuchi M., Kurita G., et al., Fusion Eng. & Design, 36(1996) 325.
[3.1-3] Ninomiya H., Aoyagi T., Ikeda Y. et al., Proc. 15th Int. Conf. Plasma Physics Contr. Nucl. Fusion Research, Seville 1994, (IAEA, Vienna, 1995) Vol.2, p613.
[3.1-4] Senda I., Shoji T., Nishio S., et al., JAERI-Data/Code 95-010, Internal Report of JAERI, 1995.

3.2 Progress in Engineering Design

Significant progress on the engineering design of JT-60SU has been made. For R&D of Nb3Al superconductor, which is employed for TF coils because of its better mechanical and J_c properties than (NbTi)3Sn superconductor, almost all important engineering techniques for producting Nb3Al strand is thought to be established. It has been demonstrated to make a 11km Nb3Al strand with Jc=650 A/mm^2, RRR=131 without any wire breaking. An Nb3Al strand with a low AC loss (a filament diameter of 31μm) with Jc=701A/mm^2 is also developed. Fe-Cr-Mn steels (C:0.02-0.2wt%, Mn:15wt%, Cr:15-16wt%, N:0.2wt%) with a lower induced-radio-activity than 316SS has been developed as a material of structure components for JT-60SU[3.2-1]. It has been confirmed that the developed high manganese steels have excellent mechanical properties and high resistance within standard temperature of JT-60SU vacuum vessel. By using this steel as the vacuum vessel, a rapid decay of the radioactivity of the machine than 316SS can be realized after two years DT operation. A fine modification of TF coil design was made for reducing a local stress on radial disk. By increasing the length of the wedge part of coil case, the maximum local stress

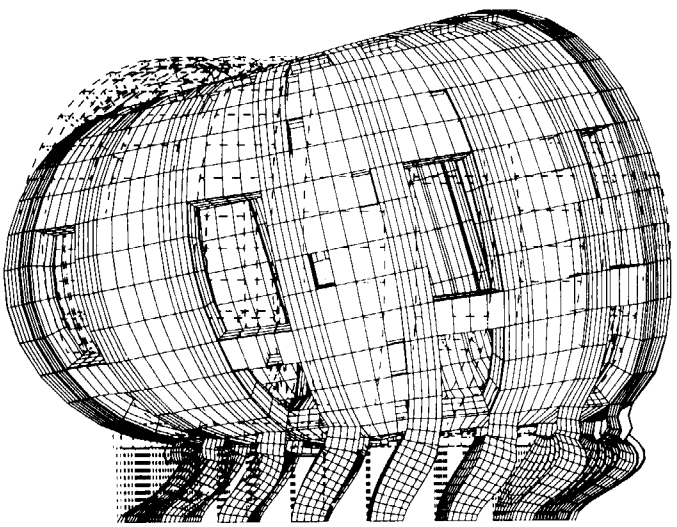

Fig.I.3.2-1 Model of superconducting coils for vibration analysis in JT-60SU; n=1 vibration with 16.2Hz

is reduced to 643 MPa.

In addition to a safety design of a low tritium inventory (<100 g) in the DT optional operation scenario, a dynamic analysis of JT-60SU machine at emergency events such as earthquake and short circuit of TF coil is also performed. With respect to the safety of a fusion reactor; confinement of tritium, the eigen mode frequency on vibrations of the machine should be 10-20 Hz to reducing displacement of each component. JT-60SU superconducting coil systems (TF:2340 tons, EF:520tons, shear panels:660 tons and CS is not included) are modeled to analyzing their dynamic behaviors during an earthquake as shown in Fig.3.2-1. Fundamental frequency of vibration in JT-60SU coil systems is around 10 Hz, which is larger than ~1.5 Hz in ITER [3.2-2]. It is found that a weight reduced design of TF coils, shear panel connection and favorable design of supporting system contribute to realize a higher fundamental frequency for vibration. Preliminary analysis applying EL Centro wave form with 0.326 gal on the basement of machine room has indicated that the maximum displacement of the TF coil is within 2 mm.

References

[3.2-1] Ishiyama S., Tanaka H., et al., to be published in J. of Nuclear Materials.
[3.2-2] Draft of Technical Basis of the ITER Final Design Report (1997), Chapter IV, p.46.

II. JFT-2M PROGRAM

Objectives of the JFT-2M program are (1) advanced and basic researches for the development of high-performance plasmas for nuclear fusion and (2) contribution to the physics R&D for ITER, with a merit of flexibility of a medium-size device. In the closed divertor experiments, effects of reduction of gas back-flow from a divertor region have been investigated by progressively changing a degree of closure at the divertor throat. It was found that more closed divertor geometry can further extend a coexistent regime of the high confinement and a dense & cold divertor plasma. It was also found that divertor biasing which produces $E_r \times B$ flow in the SOL from the inside to the outside, enhances the divertor function significantly with baffle plates. A compact toroid (CT) injection system has been installed in collaboration with the Himeji Institute of Technology (Prof. T. Uyama) for the development of the advanced fuelling for a fusion reactor, such as ITER. Encouraging results were obtained with initial CT injection experiments, such that reduction of radiation loss power was observed after the CT injection into OH plasmas. In JFT-2M H-mode, H-factors are different according to the beam injection angle, i.e. H(CO)>H(CO+CTR). It was found that larger H-factors with co-NBI is due to the increased E_r sheared region. A heavy ion beam probe system, which was developed by the National Institute for Fusion Science (Prof. Y. Hamada), has been installed for clarifying mechanism of improved confinement more definitely through fast measurements of the electric field. Preionization experiment using the FWCD combline antenna was attempted, showing that the loop voltage at the plasma current start-up decreased from 22 V to 14 V by the FW preionization. Test of newly installed EC antenna for current drive and MHD control was carried out in the vacuum. For the development of structure material for a DEMO reactor, such as low-activation ferritic steel for SSTR, design studies of the Advanced Material Tokamak Experiment (AMTEX) program have progressed, where toroidal field ripple reduction by ferritic inserts and high performance plasma production in a ferritic vacuum vessel will be tested.

JFT-2M was operated in accordance with the experimental plan of FY 1997. Periodical check-ups of the tokamak, heating and power supply system were done in January and February, 1998. Operation was restarted in March. The JFT-2M operations were carried out smoothly on schedule in FY 1997, counting 2369 experimental shots.

1. Experimental Results and Analyses

1.1 Closed Divertor

The neutral gas pressure or particle recycling level around the core plasma should be low for a good confinement. On the other hand, a high recycling condition and high gas pressure in the divertor chamber are required in order to form a cold divertor plasma for the reduction of heat load

onto a divertor plate and to pump the fuel or diverted impurities as well. Divertor configuration of many tokamak machines have been modified to a closed configuration with baffle plate in order to decouple main and divertor chambers, but the decoupling is still insufficient.

We proposed a measure of tdegree of divertor closure, δ/λ, where δ is a distance from the separatrix to the baffle plate and λ is a scale length of the particle flux.[1.1-1]. For a quantitative comparison of the results obtained with various divertors, this measure is better to put together with each data set because even if the data obtained with the same machine or the same divertor configuration, the degree of closure can be varied according to the various plasma configurations, and the data set could vary with this.

In the JFT-2M tokamak, the degree of divertor closure has been modified step by step, i.e. $\delta/\lambda \gg 1$ (open divertor) $\rightarrow$ $\delta/\lambda=1.3$ (closed divertor: CD1) $\rightarrow$ $\delta/\lambda=0.8$ (closed divertor: CD2) as shown in Fig.II.1-1. (The degree of divertor closure of other machines are grater than unity in general.) In the extremely closed case, CD2, the decoupling of divertor and midplane pressures has been much improved (Fig.II.1-2). With an open divertor configuration, the main chamber pressure measured by a penning gauge at outer midplane, P_{mid}, as well as the recycling light is increased with increasing divertor pressure, P_{div} (the correlation factor is almost unity), but there is much less correlation with a closed divertor as shown in Fig.II.1-2.

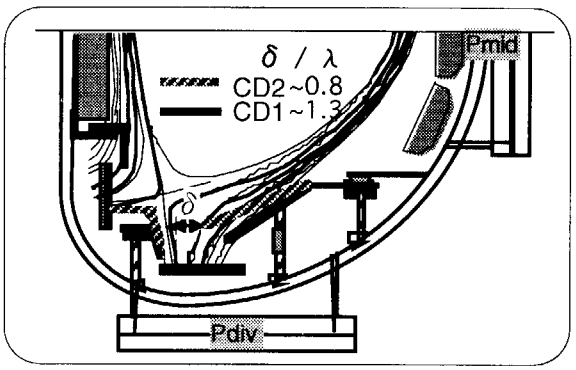

Fig. II.1-1 Variation of divertor closure on JFT-2M

This enabled extension of a coexistent regime of H-mode and a dense and cold divertor plasma with a strong gas puff in the divertor region. Typically, H factor of 1.6 was obtained at $\bar{n}_e/n_e^{GW}\sim0.6$ with $n_e=3\times10^{19}m^{-3}$, $T_e=5$ eV in the divertor. Furthermore, a new quasi-steady-state improved confinement mode compatible with dense (3×10^{19} m^{-3}) and cold (4 eV) divertor appeared when a strong gas puff was applied to high density H-mode plasma.

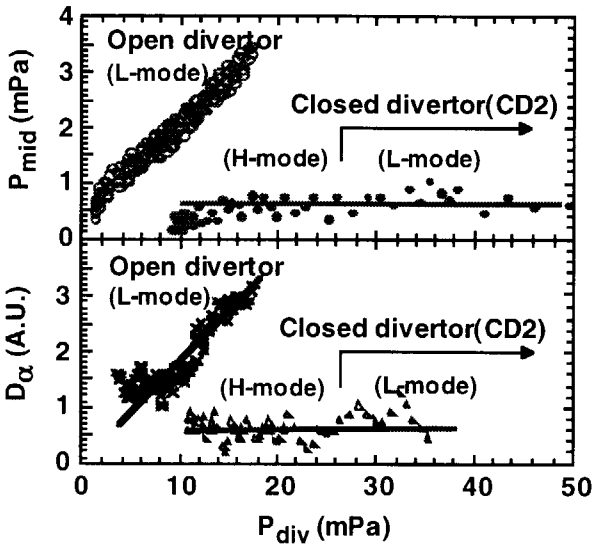

Fig. II.1-2 Correlation between midplane pressure, P_{mid}, and divertor pressure, P_{div}, with open and closed divertor (The recycling light from outer edge of the main plasma, D_α, also shows similar trend as P_{mid})

References

[1.1-1] Sengoku S. and the JFT-2M group, Bull. Amer. Phys. Soc., **42** (1997) 1962.

1.2 Compact Toroid Injection

A dense and fast compact toroid (CT) injection is considered to be a core fueling method for a fusion reactor. The CT experiments on the JFT-2M tokamak started in November 1997 for the purpose of realizing a high confinement H-mode at high density using the CT injector (HIT-CT1) developed by the Himeji Institute of Technology. The penetration depth of the CT into the tokamak magnetic field is determined by the balance between the kinetic energy of the CT and the toroidal magnetic field (B_T) pressure. A fast framing camera is used to observe the extent of CT penetration into the JFT-2M vacuum toroidal field. Figure II.1-3 shows pictures of CT at different B_T; (a) B_T =0, (b) B_T =1 T with the counter clock-wise (CCW) direction and (c) B_T =1 T with clock-wise (CW) direction. The CT travels straight and crashes into the inside wall at B_T =0. At B_T =1 T, the CT is able to go to the extent of plasma region ($r/a \geqq 0.7$) and moves up or down on the poloidal plane, according to the direction of B_T. Initial plasma injection experiments were performed at B_T =0.9 - 1.3 T with a single null plasma configuration. The stored energy W_{MHD} increased after the CT injection accompanied decreases in the radiation loss P_{RAD} and the loop voltage V_L. In an ELM-free H-mode plasma, Giant ELMs occurred 5 ms after the CT injection. The ELM free H-mode did not disappear just after the CT injection, because the life time of the CT is in the order of 50 μs in tokamak magnetic field, which was confirmed from observation by the fast framing camera.

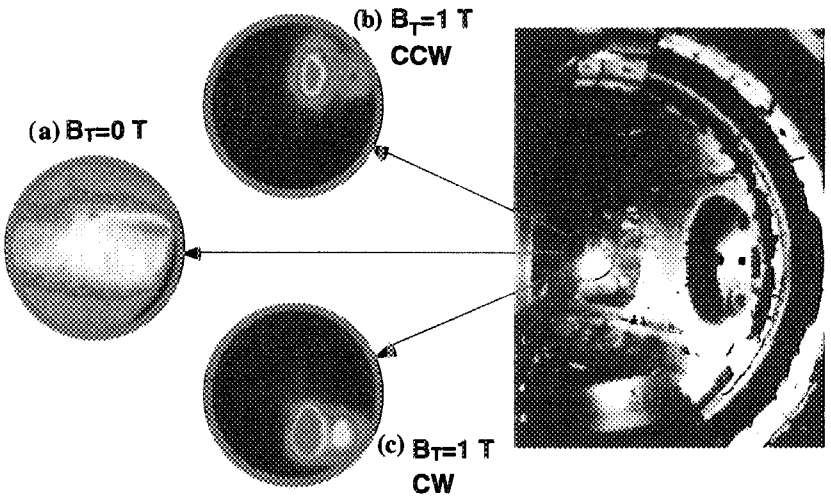

Fig.II.1-3 Pictures of the CT inside the JFT-2M vacuum vessel taken by a fast framing camera. (exposure time: 50ms)

1.3 H-mode Study and Development of Heavy Ion Beam Probe System

The improvement of the H-mode confinement in the JFT-2M tokamak shows the difference between CO- and CTR-NB heating. The improvement in CO is larger than that in CO+CTR or

CTR H-mode. The reason of τ(CO)> τ(CO+CTR) is considered to be not the effect of the sheared toroidal rotation, dv_ϕ/dr in the core. The v_ϕ at the last closed flux surface shows a finite value (about 20-40 km/s and the direction is depending on the beam injection angle) in a divertor H-mode. The finite toroidal rotation at edge is playing a role for the observed τ(CO)> τ(CO+CTR). Since the radial electric field formed by the poloidal rotation is negative, then the electric field shear at edge is increased by the positive electric field of $v_\phi(CO)\times B_\theta$. On the contrary, the electric field by $v_\phi(CTR)\times B_\theta$ is negative, then it reduces the electric field shear. Figure II.1-4 shows the difference of the radial electric field and its shear between the case of CO and CO+CTR H-mode. In the case of CO H-mode, the sheared region of the radial electric field is increased by the finite toroidal rotation just inside separatrix. Therefore, the difference of the improvement between CO- and CO+CTR H-mode, which comes from the difference of the pedestal height, is related to the electric field shear at edge[1.3-1].

The time resolution of the radial electric field measurement is 16.67msec. It is impossible to know the causality between the formation of a radial electric field and that of a transport barrier. Then we are preparing the Heavy Ion Beam Probe (HIBP) diagnostic system collaborating with National Institute for Fusion Science. Now we are doing the calibration of the system.

References

[1.3-1] Miura Y., Shinohara K., Suzuki N. and Ida K., Plasma Phys. Control. Fusion, **40** (1998) 799-803.

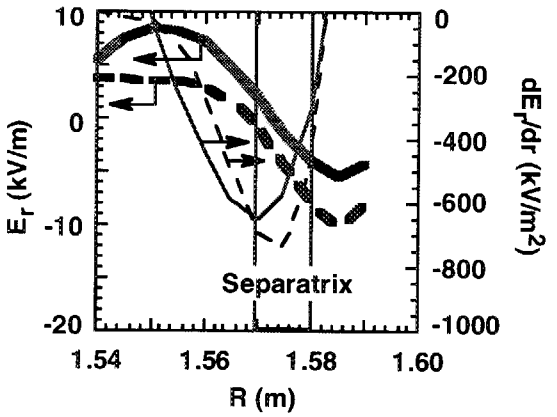

Fig.II.1-4 Thick solid and broken lines show E_r in the case of CO and CO+CTR H-mode, respectively. Thin solid and broken lines show dE_r/dr in those cases.

1.4 Radio-frequency Experiments

1.4.1 Pre-ionization by fast waves

Fast wave start-up assist is one of the high priority issues of the ITER physics R&D. Experiments of pre-ionization and start-up assist by 200 MHz fast waves were carried out using a travelling-wave-type antenna (combline antenna, developed by General Atomics). This antenna is well suited for this objective because of its load insensitivity. Plasma production was observed over a wide range of the toroidal field, 0.5 - 2.2 T. Figure II.1-5 shows reduction of the peak loop voltage from 22 V to 14 V using

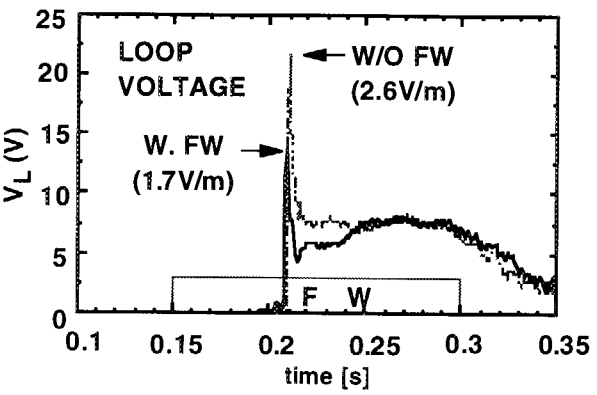

Fig.II.1-5 Time evolution of loop voltage with and without fast wave start-up assist.

fast wave pre-ionization at B_T=1.3 T.

1.4.2 Testing of new electron cyclotron wave antenna for current drive

A new antenna for ECCD installed in the JFT-2M tokamak can launch the wave in the HE_{11} mode with variable injection angle (toroidal/poloidal: ±25/20 degrees from perpendicular injection, respectively). The direction of the beam and beam divergence were measured using the three horn reflector antennas newly settled on the wall in the opposite side. The measured full half width of the rf beam (160 kW, 3 ms from one gyrotron) was 12 degrees in the toroidal direction and 10 degrees in the poloidal direction as expected.

1.5 Advanced Material Tokamak Experiment (AMTEX) Program

1.5.1 Ripple reduction by ferritic inserts and ferritic vacuum vessel [1.5-1]

There are some advantages using a ferritic steel as a material for a DEMO fusion reactor. The reason is a possibility to reduce radioactive waste, good thermal properties and high swelling resistance. Therefore, the ferritic steel is proposed for blankets in SSTR. However, its magnetism is worried about because of an error field in a magnetic fusion device. At the same time, its magnetism is considered to be used to reduce toroidal field (TF) ripple. If the ferritic steel is positioned appropriately, such that it strengthens the magnetic field between the toroidal field coils (TFC), where the toroidal magnetic field is weaker than that just inside the TFC, the TF ripple can be reduced. In ITER, it is indeed planned to use a ferritic steel to reduce the toroidal field ripple (to reduce fast ion losses). In order to examine the effects of ferritic steel on ripple reduction and plasma properties, AMTEX will be carried out in JFT-2M. In the first phase of AMTEX, in order to test TF ripple reduction, the ferritic boards are added between the nonmagnetic material vacuum vessel (VV) and the TFC. The equi-ripple-amplitude region in the cases of the nonmagnetic VV without (present VV) and with ferritic board are shown in Fig.II.1-6.

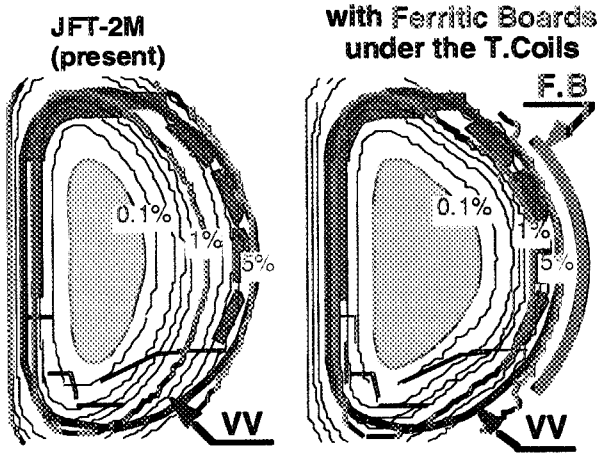

Fig.II.1-6 Equi-ripple-amplitude region in the cases of the nonmagnetic VV without (present VV) and with ferritic board.

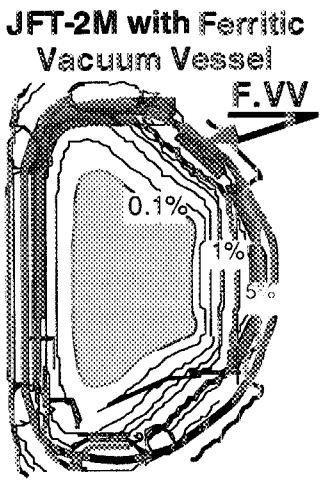

Fig.II.1-7 Equi-ripple-amplitude region in the case of the ferritic VV.

Computational results show that the ripple is reduced in the whole plasma region of low field side by the appropriate setting of the ferritic board near the VV. The ripple amplitude can be reduced by a factor of 3: ripple amplitude is reduced from 1.8 % to 0.6 % on the plasma boundary. In the second phase of AMTEX, plasma properties with the ferritic steel VV will be tested after replacing the present VV with the ferritic steel VV. The equi-ripple-amplitude region in the case of the ferritic VV with realistic horizontal port is shown in Fig.II.1-7. The ripple in the case of ferritic VV with realistic horizontal port is comparable with that in the case of nonmagnetic VV with the ferritic board.

1.5.2 Preliminary experiment with ferritic inserts

Preliminary experiments with ferritic board insertion ($0.5m^{H}$ x $0.15m^{W}$ x $24\sim48mm^{D}$) just inside only two TFCs (ripple reduction) and at only one toroidal section between a pair of TFCs (ripple enhancement) were carried out. In those experiment, we could not find any effect of the FB insertion on the global plasma parameter. The error field in the order of several ten Gauss may be below a limit of the allowable error field.

1.5.4 Irradiation of vanadium alloy in tokamak

The vanadium alloy is one of the candidate material for a DEMO reactor. Since its brittle fracture by hydrogen and oxygen absorption is worried about, the Vanadium alloy was exposed in JFT-2M in collaboration with GA, MIT and Hokkaido University. Initial results show that the hydrogen absorption and the brittle fracture of the Vanadium alloy are smaller than those of pure vanadium and titanium alloy.

References

[1.5-1] Sato M., Miura Y., et al., Proc. of 8th Int. Conf on Fusion Reactor Materials (Sendai, 1997) P2-C060 to be published in J.Nucl. Material.

2. Operation and Maintenance

2.1 Tokamak Machine

The operation and management of the tokamak device went very smoothly. After all joints of the toroidal coil coolant were replaced last fiscal year, no water leak was observed and there was no problem in insulators of magnets. An anomalous waveform of the Q poloidal coil power supply appeared possibly due to a noise. It was solved by fixing the potential of the control output signal. Damaged divertor probes and MI cables were replaced. Old equipments were renewed, and check and maintenance works were carried out in the gas fueling, the vacuum pumping, the cylister cooling system of the poloidal power supply, and the coil secondary cooling system.

In collaboration with the Experimental Plasma Physics Laboratory, installation of the CT injection device, the power supply, and the vacuum pumping system was completed in October. The CT injection device was developed by the Himeji Institute of Technology. The power supply and the vacuum pumping system were designed and fabricated by JAERI. After tests of the power supply with dummy loads and standalone tests of the CT injector, the injector system was connected to the JFT-2M device. After optimization of the CT plasma production, CT plasma injection experiments were started.

As a part of the Advanced Materials Tokamak Experiment (AMTEX) program, the toroidal field ripple reduction by ferritic inserts is being planned. Investigation was done for the installation of ferritic steel boards between the vacuum vessel and the toroidal coils. Technical assessments were made on the mounting structure and shape of the ferritic steel boards.

2.2 Neutral Beam Injection System and Radio-frequency Heating System

The systems of Neutral Beam Injection (NBI) heating, Electron Cyclotron Heating (ECH) and Fast Wave (FW) current drive were operated without a major problem. These systems were efficiently used for the experiments. A turbomolecular pump of a magnetic levitation type was damaged due to vibrations of the gate valve in a shut-down operation. To prevent such a vibration problem, the exhaust manifold support was reinforced and a bellows was installed to absorb vibrations. Old equipments of the acceleration-power-supply control system were replaced and check and maintenance works were carried out. Inspection, maintenance and aging of the ECH system were carried out in order to increase injection power and pulse duration. A power combiner was installed for the traveling wave antenna (combline antenna) of the FW current drive system, and it was used in the experiments.

2.3 Power Supply System

The toroidal coil power supply (MG) ran smoothly and contributed to the experiments. Furthermore, following works and improvements were done for increasing the efficiency of operations; inspection and maintenance of commutators, improvements of interlocks of the main circuit switch and reduction of time for stopping the MG.

III. THEORY AND ANALYSIS

The principal objective of theoretical and analytical studies is to improve the understanding of physics of tokamak plasmas. Remarkable progress was made on the physical understanding of the reduced transport and the stabilities not only of ideal MHD modes but also of kinetic ballooning mode in reversed shear plasmas. Progress was also made on the neoclassical transport calculation by the Matrix Inversion method and on the scaling law of an offset nonlinear form for the ELMy H-mode confinement. A five point model for the scrape-off layer and divertor plasmas was developed and the inside/outside divertor asymmetry was investigated.

The main purposes of the NEXT (Numerical EXperiment of Tokamak) project, which began in 1996, are researches on complex physical processes in core plasmas, such as transport and MHD, and in divertor plasmas by using recently-advanced computer resources. The Next project also includes the development of simulation models suitable for a large, high temperature tokamak with reactor parameters, and the development of simulation technology on massively parallel computers.

1. Confinement and Transport

Recent experimental and analytic progress in the JT-60U was reported in [1-1]. Especially the confinement and transport in reversed shear (RS) plasmas were investigated. Ion and electron thermal diffusivities in a quasi-steady-state RS plasma were obtained, which become very small inside the thin ITB (internal transport barrier) layer and are the same level or smaller than the neoclassical ion thermal diffusivity in the core region enclosed by ITB. This transport feature is similar to that in the transient phase. The stability of high-n toroidal drift modes was analyzed. The ExB shearing rate becomes of the same order of magnitude as the linear growth of the dominant mode around the ITB. It was found that the anomalous transport cannot be enhanced by the steep pressure gradient of the ITB.

In the improved confinement plasmas, such as RS plasmas, the ion thermal diffusivity is reduced to the neoclassical level. The accurate estimation of the neoclassical transport coefficients is required. A Matrix Inversion (MI) method for calculating the bootstrap current was modified to calculate the

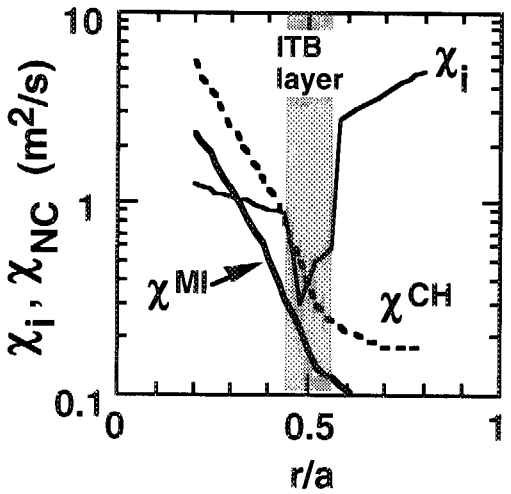

Fig.III.1-1 Profiles of ion thermal diffusivity, χ_i, and neoclassical diffusivity, χ_{NC}, evaluated by MI method and by Chang-Hinton's formula in the reversed shear plasma with internal transport barrier (ref. [1-1]).

neoclassical ion thermal diffusivity including the effect of impurity [1-2]. It was found that the ion thermal diffusivity calculated by the MI method is about half of that calculated from the Chang-Hinton formula for a typical hot-ion H-mode in JT-60U.

The role of convective heat losses in tokamak plasmas was studied analytically and numerically [1-3]. A the natural forms for the energy confinement scaling law was suggested. An analytical formula of the ion temperature limit in the steady-state neutral beam injection discharges caused by convective heat losses was obtained. A new technique for the determination of convective heat losses from experimental measurements was applied to the analysis of a JT-60U NBI discharge. The particle source and convective heat losses calculated directly from the experimental data were in good agreement with ASTRA calculations. The convective heat loss obtained from the data was about 50% of the absorbed NB power in the core region.

An offset nonlinear scaling was developed for the ELMy H-mode confinement by analyzing the ITER H-mode database ITERH.DB2 combined with JT-60U data [1-4]. The offset part of the stored energy is determined by the MHD stability of the ELM, and the incremental confinement time of a nonlinear function of heating power is determined by gyro-Bohm-like transport in the core plasma. This scaling predicts a lower confinement time for ITER than that predicted by general power-law scaling.

A non-linear Fokker-Planck code was applied to the study of a JT-60U hot ion plasma in which the experimentally measured carbon impurity temperature T_C reached up to 45 keV with 90 keV deuterium beam injection [1-5]. A non-Maxwellian deuteron distribution function is obtained numerically and the deuteron bulk temperature T_D, which has not been determined experimentally, is evaluated from the slope of the energy spectrum. It was found that T_D can exceed T_C, indicating that the T_C measurement does not lead to overestimation of the ion temperature. The deuteron effective temperature based on the average energy was found to be almost the same as T_C. The DD fusion reactivity is also around a value given by the Maxwellian distribution with its temperature equal to T_C. Consequently, the T_C may possibly be regarded as an equivalent ion temperature.

References

[1-1] Shirai H, JT-60 Team, "Recent Experimental and Analytic Progress in the Japan Atomic Energy Research Institute Tokamak-60 Upgrade with W-shaped Divertor Configuration", Phys. Plasmas **5** (1998) 1712.

[1-2] Kikuchi M., Shirai H., Itakura H. Azumi M., "Effect of Impurity on Neoclassical Ion Thermal Diffusivity", in "Review of JT-60U Experimental Results in 1997" JAERI-Research 98-039 (1998) . 3.6.

[1-3] Polevoi A., Neudatchin S., Shirai H., Takizuka T., "Analysis of Convective Losses in JT-60U Neutral Beam Injection Experiments", Jpn. J. Appl. Phys. **37** (1998) 671.

[1-4] Takizuka T., "An Offset Nonlinear Scaling for ELMy H-mode Confinement", Plasma Phys. Control. Fusion **40** (1998) 851.

[1-5] Yamagiwa M., Koga J., Ishida S., "Non-linear Fokker-Planck Code Study of High Ion Temperature Plasma in JT-60U", Nuclear Fusion **37** (1997) 1735.

2. Stability

Ideal MHD stabilities were studied for the negative shear plasmas with steep pressure gradient observed in JT-60U [2-1]. In order to improve the ideal β-limit, effects of the location of a minimum value of the safety factor, q_{min}, and of the location of the maximum pressure gradient on ideal MHD stability were investigated. When the maximum pressure gradient is inside the $q = q_{min}$ surface, the ideal β-limit is determined by the n = 1 kink-ballooning mode. When the maximum pressure gradient is on or outside the $q = q_{min}$ surface, the infernal and high n ballooning modes become more unstable than the n = 1 mode. It is found that the ideal β-limit is improved when the maximum pressure gradient is inside the $q = q_{min}$ surface and the edge pressure gradient is high. The experimentally observed β-limit in negative shear plasmas in JT-60U is consistent with the numerically obtained β-limit determined by the n = 1 mode.

The Mercier criterion in a reversed shear plasma of a tokamak was studied numerically [2-2]. A reversed shear plasma has negative magnetic shear and negative pressure gradient in the inner region of a plasma. In the negative shear region, stabilizing terms due to the parallel current and the magnetic well produced by the poloidal current change to destabilizing ones. As the value of $(q_0-q_{min})/q_{min}$ increases, the destabilizing effects increase and the Mercier criterion can be violated. Here, q_0 and q_{min} are the safety factor on the plasma axis and the minimum value along the minor radius, respectively. In JT-60U reversed shear plasmas, the value of $(q_0-q_{min})/qmin$ becomes large. The violation of the Mercier criterion seems to be consistent with the observation of MHD activity localized near the internal transport barrier.

Research on the asymptotic matching analysis of resistive MHD stability has been performed. A new code MARG1D for solving the Newcomb equation in the ideal MHD region and computing the matching data was developed [2-3]. The Newcomb equation is solved as a boundary value/eigenvalue problem to which the finite element method can be applied. The extension of the MARG1D to the two dimensional toroidal problem is now under development.

The kinetic ballooning mode (KBM) at the internal transport barrier (ITB) with negative magnetic shear in a tokamak was analyzed numerically by using a kinetic shooting code. The eigenvalues (growth rates and real frequencies) of a KBM equation were calculated by carefully checking the convergence of solutions at large shooting distances. The second stability regime for negative magnetic shear, predicted by Hirose et al. [Hirose A., Elia M., Phys. Rev. Lett. **76** (1996) 628], was shown to disappear. The mode with comparatively low toroidal mode number and the real frequency ~100 kHz was found to be destabilized only around the ITB for the JT-60U parameters. These characteristics are consistent with the experimental observations of the mode inducing the mini β collapse in the vicinity of the ITB. The KBM is considered to be a possible candidate for the experimentally observed MHD activities, whereas lower frequency drift type modes might be responsible for the thermal transport [2-4].

References
[2-1] Ishii Y., Ozeki T., Tokuda S., et al., "Ideal Beta Limits of Negative Shear Plasma in JT-60U", to be published in Plasma Physics and Controlled Fusion.
[2-2] Ozeki T., Azumi M., Ishida S. Fujita T., "Violation of the Mercier Criterion in Reversed Shear Confinement Configurations in Tokamaks", Plasma Phys. Control. Fusion, **40** (1998) 871.
[2-3] Tokuda S., Watanabe T., "Eigenvalue Method for the Outer-Region Matching Data in Resistive MHD Stability Analysis", J. Plasma and Fusion Res. **73** (1997) 1141.
[2-4] Yamagiwa M., Hirose A., Elia M., " Kinetic Ballooning Modes at the Tokamak Transport Barrier with Negative Shear", Phys. Plasmas **4** (1997) 4031.

3. Divertor

A five-point model for the scrape-off layer (SOL) and divertor plasmas was developed to study the inside/outside divertor asymmetry induced by the divertor biasing [3-1]. Effects of divertor biasing on the asymmetry were studied for low and high recycling states. In the low recycling state, the biasing has a little influence on the asymmetry. On the other hand, in the high recycling state, the biasing substantially controls the asymmetry. The energy loss due to the ionization and impurity radiation plays an important role to cause the heat flux asymmetry. The divertor plasma has higher density, lower temperature and lower heat flux at the anode-side plate compared with those at the cathode-side plate.

This five-point model was used to study the characteristics of JT-60U divertor plasmas [3-2]. A high-recycling divertor is formed when the particle flux from the main plasma exceeds $(1\sim2)\times10^{22}$ s^{-1} for the safety factor of ~5 and the heating power of (1~20) MW. At the onset of the high recycling, the density at the SOL mid-plane is $n_{mid} \approx 0.5\times10^{19}$ m^{-3}.

References
[3-1] Hayashi N., Takizuka T., et al., "Analysis of Biasing Induced Divertor Asymmetry Using a Five-Point Model", J. Phys. Soc. Japan **66** (1997) 3815.
[3-2] Hayashi N., Takizuka T., et al., "Analysis of JT-60U Divertor Plasma Using a Five-Point Model", in "Review of JT-60U Experimental Results in 1997" JAERI-Research 98-039 (1998), 6.5.

4. Numerical Experiment of Tokamak (NEXT)

4.1 Development of Computational Algorithm

One of the main obstacles for the global particle simulation such as kinetic MHD instabilities in a tokamak is the large discrepancy between the characteristic time scale of the mode and the transit time of the electron motion parallel to the magnetic fields. To resolve such difficulties, a particle-fluid hybrid model for the simulation of the kinetic MHD instabilities was developed [4-1], which treats electrons as a fluid and retains the electron inertia effect. The model was applied to the nonlinear simulation of the m/n = 1/1 internal kink mode and was confirmed to agree well with the previously performed gyro-kinetic particle simulation, while only consuming 1/8 to 1/4 of the CPU time.

The above approach was extended to the electrostatic drift wave problem in a slab geometry

and a new system of gyrokinetic Vlasov-Maxwell equations was derived [4-2]. In the formulation, the motion of the high energy transit electron is averaged over the periodic unperturbed orbit. The resultant equations for the high energy electrons involve only the EIB nonlinearity, and the adiabatic response to the low frequency fluctuation is renormalized in the field equation. The numerical experiments verified the efficiency of this simulation model.

4.2 Transport and MHD Simulation

In order to study the transport in a tokamak, a particle based global simulation code which has a full toroidal geometry was developed. To treat the delicate toroidal coupling problem under the weak/reversed magnetic shear configuration, the toroidal metric (r, θ, ϕ) with a nonuniform grid for the radial direction is employed and the electrostatic potential is solved via Fourier mode expansion both for poloidal/toroidal directions [4-3]. Recently, the code was developed so that the effect of the self-generated radial electric field, i.e. the (0,0) mode, which will be nonlinearly derived through the Reynolds stress, can be simulated. The (0,0) mode driven by semi-global "radial mode" of ITG instability which also shows the semi-global radial extent is excited. Such a (0,0) mode induces a fluctuating "zonal flow". The flow disintegrates the semi-global ITG vortices into small species and reduces the fluctuation level and transport [4-4].

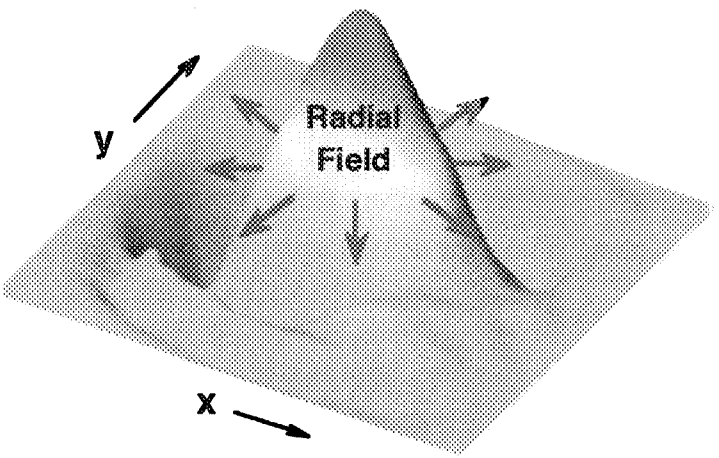

Fig.III.4.2-1 The electrostatic potential profile on a toroidal cross-section. m/n=0/0 mode (radial electric field) induced by the nonlinear interaction grows to the same level as the 1/1 mode.

We have been developing the non-linear MHD code using a full set of resistive MHD equations. To this end, we compared the linear results obtained by a linear version of the code to those obtained by the FAR code developed by Oak Ridge National Laboratory in USA. The eigenvalues and eigenfunctions calculated by both codes were in close agreement and showed that the finite beta effect is stabilizing on the toroidal tearing mode, while compressibility has little effect [4-5].

The effects of the density gradients on the kinetic m/n = 1/1 internal kink mode were investigated by the electromagnetic gyrokinetic-particle code. The first reconnection process was confirmed to be similar to that for the uniform density case. However, after the first reconnection, it was found that self-generated radial electric fields are induced by the nonlinear interaction, and the combination of the growth of 0/0 mode and the attenuation of 1/1 mode produces a vortex structure in the density profile [4-6].

4.3 Divertor Simulation

Simulation codes have been developed for the purpose of understanding physical processes in the divertor plasma. PARASOL is a particle code to verify the physical model for SOL plasmas, such as sheath conditions and heat transport. SOLDOR is a fluid code to predict the plasma parameter accounting for interactions with the neutral particles. IMPMC is a 2D Impurity Monte-Carlo code to analyze the impurity behavior in the divertor plasma. The assumptions widely used in impurity fluid codes, (i.e. instantaneous thermalization of impurity ions and simplified evaluation of self-sputtering outflux) was examined with the IMPMC code. It was found that they could not be applied for impurity ions with low charge states near the plates, and they lead to overestimation of the impurity influx into the main plasma [4-7].

4.4 Massively Parallel Computing

In the particle-fluid hybrid simulation, the computational cost for the electron fluid and electromagnetic fields is comparable to the cost of ion particle-pushing. High performance of the vector computation is required for the fluid equations and Maxwell's equations, while a large amount of memory is necessary for the ion particles [4-1]. Therefore, heterogeneous computing is an effective parallel computing technique for the hybrid simulation. We have demonstrated the efficiency of heterogeneous computing using the Hybrid3D code by connecting a vector parallel computer (VPP300) with a scalar parallel computer (SR2201); the fluid equations and Maxwell's equations are solved on the VPP300 and the equations of motion for ions are solved on the SR2201. The necessary performance of network between two computers was estimated, and it was shown that 10 parallel network system of 800 Mbytes HIPPI is sufficient for the present hybrid simulation. This research was performed in collaboration with the Center for Promotion of Computational Science and Engineering, JAERI.

References

[4-1] Tokuda S., Naitou H., Lee W.W., "A Particle-Fluid Hybrid Simulation Model Based on Nonlinear Gyrokinetics", J. Plasma and Fusion Res. 74 (1998) 44.

[4-2] Idomura Y., Tokuda S., Wakatani M., "Gyrokinetic Particle Simulation Using the Orbit Averaged Electron Drift-kinetic Equation", submitted to Phys. Plasmas.

[4-3] Kishimoto Y., T.Tajima T., et. al., "Theory of Self-organized Critical Transport in Tokamak Plasmas", Phys. Plasmas 3, (1996) 1289.

[4-4] Kishimoto Y. et. al., "Discontinuity Mode for Internal Transport Barrier in Reversed Magnetic Shear Plasma", 1998 International Sherwood Fusion Theory Conference, Mar 25, 1998, Atlanta, Georgia.

[4-5] Leboeuf J.N.G., Kurita G., " Finite Beta and Compressibility Effects on Stability of Resistive Modes in Toroidal Geometry", JAERI-Research 98-010 (1998).

[4-6] Matsumoto T., Tokuda S., Naitou H., "Density Gradient Effect for m = 1 Kinetic Internal Kink Mode", in Proc. of 1997 Workshop on MHD Computations - Numerical Methods and Optimization Techniques in Controlled Thermonuclear Fusion Research - (Institute of Statistical Mathematics, Tokyo, 1998) p.88.

[4-7] Shimizu K., Takizuka T., Sakasai A., "A Review on Impurity Transport in Divertors", J. Nucl. Mater. 241-243 (1977) 167.

IV. TECHNOLOGY DEVELOPMENT

Research and Development of nuclear fusion reactor technology has been focused on the ITER/EDA-related areas: blankets, superconducting magnets, Neutral Beam Injection (NBI) heating system, Radio-Frequency (RF) heating system, tritium, fueling and pumping system, plasma facing components, reactor structures, and remote maintenance. Major highlights of Research and Development (R&D) in FY 1997 are as follows:

In the area of superconducting magnet (1) successful completion of all eight layers of winding and heat treatment of Nb_3Sn conductor for the outer module of the ITER CS model coil, (2) development of the assembling (transfer) technology for the outer module, and (3) successful completion of the 1-ton mass-production of the Nb_3Al strand and 46-kA cable of 1152 Nb_3Al strands for the insert coil.

The fabrication of the full-scale sector models of the ITER vacuum vessel with a D-shaped cross section of approximately 9 m wide and 15 m high was continued and completed at the end of September 1997. Although the different fabrication procedures and welding techniques were employed for the fabrication, both sectors have satisfied the dimensional accuracy of within ± 3 mm of the total height, total width and total wall thickness.

A prototype mock-up (~1.6 m wide x 0.9 m height x 0.3 m thickness) of the ITER shielding blanket module has been successfully fabricated. Also design-oriented engineering data on the breeding blanket pebble bed have been obtained, and elementary R&D's on the breeding blankets fabrication technology have been continued.

Regarding the development of ITER plasma facing components for full-scale divertor mock-ups, vertical target mock-ups and wing mock-ups, thermal cycling experiment was performed successfully to demonstrate durability of all the mock-ups at a stationary heat load of 5 MW/m^2 for 30 sec for a repetition of 10^3 cycles.

The full-scaled rail mounted ITER vehicle system, which includes rail transporter, vehicle manipulator/end-effector, and rail support structures have been assembled and performance test was initiated for the demonstration of remote replacement of 4-ton blanket module with a handling accuracy of ± 2 mm.

Stable negative hydrogen ion beam H^- at 1 MeV of 25 mA has been successfully produced with the five-staged accelerator. It is also confirmed that the extraction voltage with the good beam optics in the experiment is in good agreement with that obtained from the beam trajectory calculation. As for the gyrotron development for ITER the maximum energy of 520 kW x 5 sec was demonstrated at 170 GHz with the Chemical Vapor Deposition diamond disk window.

To investigate tritium behavior released into confinement system and environment, a large caisson of 12 m^3 was designed, manufactured and installed in a room of TPL in FY 1997.

1. Blanket Technology

1.1 Development of ITER Shielding Blanket

For fabrication technology development of the ITER shielding blanket, R&D activities within the framework of ITER/EDA have proceeded to successful fabrication of a prototype shielding blanket mock-up, and small-scale Be-HIPed first wall (FW) and baffle FW mock-ups.

1.1.1 HIP Conditions for DSCu/SS and Properties of the HIPed Joints

To investigate the joint integrity of alumina dispersion strengthened copper (DSCu)/stainless steel (SS) HIPed at three different temperatures of 980 ℃, 1030 ℃ and 1050 ℃, mechanical tests and metallurgical observations have been performed. As a result of the mechanical tests, the joint HIPed at 1050 ℃ showed the highest ductility, impact values and fatigue strength [1.1-1]. Results of metallurgical observations also confirmed good bondability at the HIPed interface, i.e., no harmful voids [1.1-2]. From these results, it was concluded that temperature of 1050 ℃, pressure of 150 MPa and holding time of 2 hours were optimal HIP conditions. For the DSCu/SS joints HIPed in these conditions, mechanical properties including fracture toughness and crack propagation behavior were additionally investigated [1.1-3].

References

[1.1-1] Sato S., et al., "Optimization of HIP Bonding Conditions for ITER Shielding Blanket/First Wall made from Austenitic Stainless Steel and Dispersion Strengthened Copper Alloy", to be published in Proc. 8th Int. Confer. Fusion Reactor Mater., J. Nucl. Mater., Elservier, (1998).

[1.1-2] Kanari M., et al., "Characterization of HIP Bonded DS-Cu/SS316L Joints for Fusion Experimental Reactors", JAERI-Research 98-004, (1998) (in Japanese).

[1.1-3] Hatano T., et al., "Fracture Strengths of HIPed DS-Cu/SS Joints for ITER Shielding Blanket/First Wall", to be published in Proc. 8th Int. Confer. Fusion Reactor Mater., J. Nucl. Mater., Elservier, (1998).

1.1.2 Fabrication of a Prototype Blanket Mock-up [1.1-4]

A prototype mock-up (1570 mm^W x 930 mm^H x 344 mm^T) of the ITER shielding blanket module has been successfully fabricated, which was composed of FW DSCu heat sink, SS circular tubes built-in DSCu, and SS shield block. This mock-up incorporates the major design features, i.e., toroidally curved FW, poloidally oriented FW coolant tubes, toroidally oriented coolant channels in the shield block, and 30-mm-diameter front access holes. The

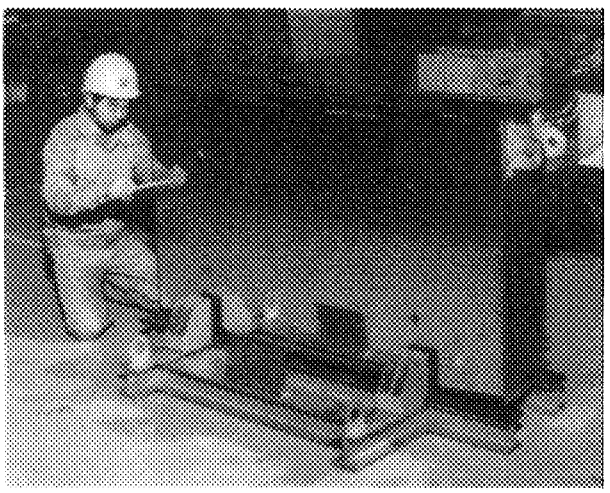

Fig. IV.1.1-1 Fabricated prototype mock-up

FW coolant tubes are routed to avoid the interference with the front access holes. Simultaneous HIPing of DSCu/SS, DSCu/DSCu and SS/SS was adopted to minimize thermal effects on the material properties and reduce fabrication steps. The HIP conditions applied were 1050 ℃, 150 MPa and holding time of 2 hours based on the previous studies [1.1-5, 1.1-6]. Before the HIP process, a deep drilling was performed for the coolant channels of the forged SS shield block from both sides, then the shield block was bent by 10,000 ton press to provide the specified curvature. A series of measurements and inspections were performed in the course of this fabrication including dimensional accuracy and integrity of pressure boundaries. A destructive inspection was also performed with a cut specimen from the edge of the fabricated module to examine the bondability of HIPed interfaces. A final appearance of the fabricated prototype mock-up is shown in Fig. IV.1.1-1.

References

[1.1-4] Sato S., et al., "Fabrication of ITER Shielding Blanket Prototype", to be published in Proc. 13th Topical Meeting on the Technol. of Fus. Energy, Nashville (1998).

[1.1-5] Sato S., et al., "Optimization of HIP Bonding Conditions for ITER Shielding Blanket/First Wall made from Austenitic Stainless Steel and Dispersion Strengthened Copper Alloy", to be published in Proc. 8th Int. Conf. Fusion Reactor Mater., J. Nucl. Mater., Elservier, (1998).

[1.1-6] Hatano T., et al., "Fracture Strengths of HIPed DS-Cu/SS Joints for ITER Shielding Blanket/First Wall", to be published in Proc. 8th Int. Conf. Fusion Reactor Mater., J. Nucl. Mater., Elservier, (1998).

1.1.3 Fabrication of Small-scale Mock-ups for First Wall Structure

To bonding of Be armor on the DSCu heat sink of the shielding blanket FW, HIP technology has also been applied. After screening tests, HIP conditions of 550-580 ℃, 140 MPa and 2-hour-holding time with Ti/Cu or Al/Ti/Cu interlayer were preliminarily selected [1.1-7, 8]. A small-scale FW mock-up was successfully fabricated as shown in Fig. IV.1.1-2 [1.1-8]. The mock-up consists of DSCu heat sink, built-in SS coolant tube, SS backing plate simulating the shield block, and Be armor tiles, which is relevant to the ITER shielding blanket design. Four Be armor tiles, two with Ti/Cu interlayer and two with Al/Ti/Cu interlayer, were HIP bonded under the above-selected conditions.

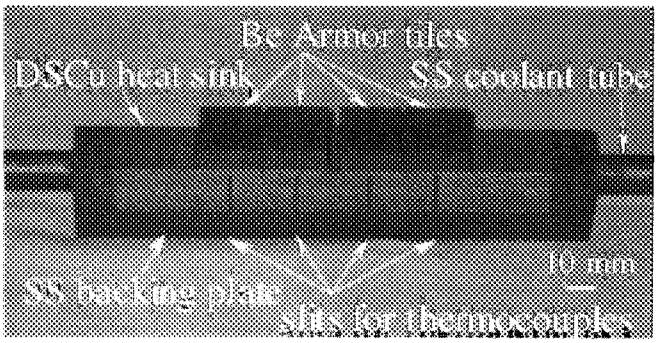

Fig. IV.1.1.-2 Fabricated small scale first wall mock-up with Be armor tiles HIP bonded to DSCu/SS structure

Another small-scale mock-up of the baffle FW has been fabricated aiming at developing armor bonding techniques for Ag-free brazing. DSCu and carbon fiber composite (CFC) were used as the heat sink and armour materials, respectively. The new bonding technique was based

on two-step brazing : CFC armour tiles were brazed to an oxygen free copper (OFCu) plate in the first step and the OFCu plate was brazed, in turn, to the DSCu heat sink in the second step. After screening tests a brazing material and conditions of Cu-Mn and 960 ℃ x 15 min., respectively, were selected for the first step and Al and 675 ℃ x 15 min., respectively, were selected for the second step. The fabricated baffle FW mock-up is 400 mm in length, 50 mm in width and 50 mm in thickness [1.1-9]. A final appearance of the fabricated mock-up is shown in Fig. IV.1.1-3. To estimate thermo-mechanical propertities of the mock-up, high heat flux testing will be performed on the electron beam facility, JEBIS, at JAERI, Naka.

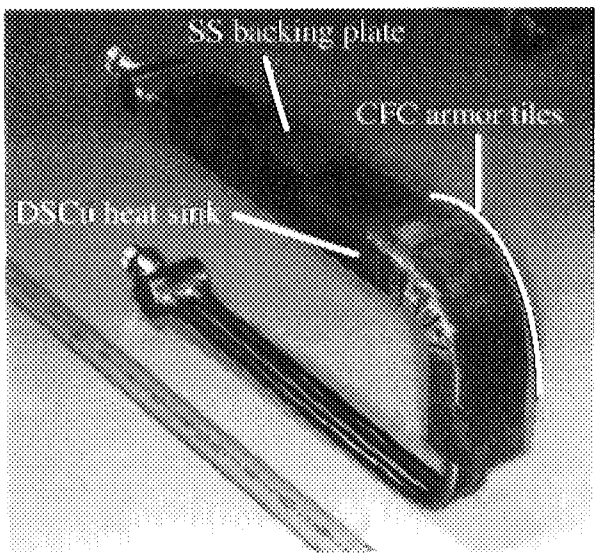

Fig. IV.1.1-3 Fabricated small scale baffle first wall mock-up with CFC armor tiles

References

[1.1-7] Kuroda T., et al., "Development of Be/Cu-Alloy and Be/SS Joining Technology by HIP", to be published in Proc. 8th Int. Confer. Fusion Reactor Mater., J. Nucl. Mater., Elservier, (1998).

[1.1-8] Hatano T., et al., "Fabrication of a small-scaled first wall mock-up with beryllium armor HIP bonded to DSCu/SS structure", to appear in 20th Symp. of Fusion Technol., Marseilles (1998).

[1.1-9] Hatano T., et al., "High Heat Flux Testing of HIP Bonded DS-Cu/316SS First Wall Panel for Fusion Experimental Reactors", to be published in Proc. 13th Topical Meeting on the Technol. of Fusion Energy, Nashville (1998).

1.2 Development of Breeding Blanket

Fabrication method and procedure of the breeding blanket focusing on the interaction of thermal and mechanical behaviors have been preliminarily established. Design-oriented engineering data on a pebble bed has been obtained, and elementary R&D's for fabrication of the breeding blanket have been continued. Additionally, the measurement of effective thermal conductivity of ceramic breeder pebble bed by Hot Wire Method was initiated as one of subtasks in the Solid Breeder Subtask Group of IEA implementing agreement on Nuclear Technology of Fusion Reactors.

1.2.1 Thermo-mechanical Analysis of ITER Breeding Blanket

The ITER breeding blanket has been designed to use two binary pebble beds, Be pebble bed as neutron multiplier and Li_2ZrO_3 pebble bed as tritium breeding material. Thermo-

mechanical analyses of the breeding blanket have been conducted taking into account the interaction between the thermal and mechanical behaviors of the pebble bed. The Coupled Temperature-Displacement procedure of the ABAQUS code was applied so that the spatially varying thermal conductivity of the pebble bed was automatically calculated depending on the local compressive stresses in the pebble bed. The modified Drucker-Prager/Cap plasticity model was applied to simulate mechanical features of pebble bed such as shear failure flow and plastic consolidation. As the result, it was shown that the temperature distribution is strongly affected by the mechanical stress distribution in the Be pebble bed region. The analysis clarified that it is necessary to evaluate detailed experimental data on the relationship between the pebble bed thermal conductivity and mechanical stress.

1.2.2 Heat Transfer Test of Packed Pebble Bed [1.2-1]

Heat transfer tests have been conducted using cylindrically packed pebble beds to evaluate effective thermal conductivity and heat transfer coefficient between the packed bed and the container wall for ceramic breeding blanket. The test mock-up consists of layered pebble beds and an internal heater equipped at its center as shown in Fig. IV.1.2-1. Heat transfer tests have been conducted with a cylindrically layered pebble bed mockup to demonstrate the thermal performance of pebble layered concept for breeding blanket. Prior to the heat transfer tests with Li_2O (Li_2TiO_3 and Li_2ZrO_3)/Be pebbles, the tests with Al_2O_3/Al and Be/Al pebbles have been conducted. As the result, the observed temperature profile and heat flux are transformed to the measured effective thermal conductivities of Al_2O_3 and Be packed beds are consistency with the correlation proposed by Schlünder et al. The effective thermal conductivity of Be (1 mm in diameter) packed bed with 61.1 % packing fraction were 2 to 3.6 W/mK at average Be temperatures from 150 to 430 ℃. The evaluated heat transfer coefficient between the Be packed bed and the wall were 500 to 1200 W/m^2K at Be temperatures near the wall of 160 to 510 ℃.

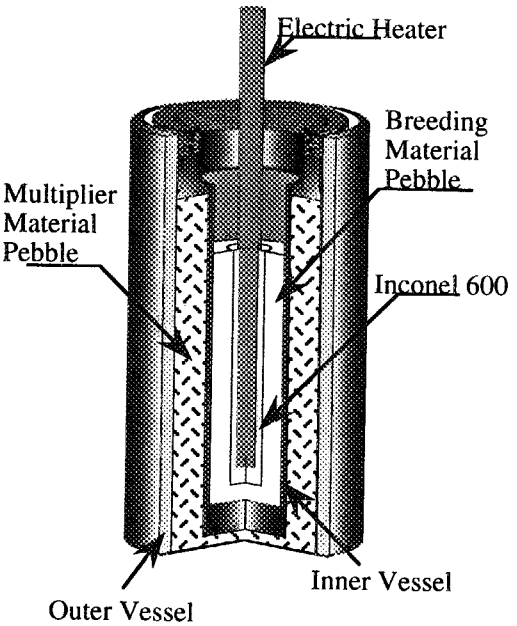

Fig. IV.1.2-1 Set-up of layered pebble bed test mock-up

References

[1.2-1] Sato S., et al., "Heat Transfer Tests of Packed Pebble Bed for Ceramic Breeder Blanket", to appear in 20th Symp. of Fusion Technol., Marseilles (1998).

2. Superconducting Magnet Development

JAERI has been developing superconducting magnet technology under the Engineering Design Activities of the ITER Program. In FY 1997, the followings were achieved:
(a) Successful completion of winding and heat treatment of Nb_3Sn conductor consisting of 2.7-km in total length and 46-kA capability for the outer module of the Central Solenoid (CS) model coil,
(b) Development of the assembling (transfer) technology for the outer module,
(c) Development of the winding technology for the CS insert coil,
(d) Successful completion of the 1-ton mass-production of the Nb_3Al strand and 46-kA cable having 1152 Nb_3Al strands for the insert coil,
(e) Development of the large capacity supercritical-helium pump, which achieved large mass flow rate of 800 g/s with a pump head of 0.25 MPa and high adiabatic efficiency of more than 70% for the fusion experimental reactor such as ITER.

2.1 Development of CS Model Coil

The CS model coil program is going on to demonstrate the justification of the central solenoid design for the ITER. The model coil, which can generate the maximum field of 13T, consists of two modules; inner and outer modules, as shown in Fig. IV.2.1-1. The outer module, which is fabricated in Japan, is composed of 8 layers with two conductors-in-hand per a layer. All sixteen conductors for the outer module were delivered from Italy to Japan in September 1997. The coil fabrication process [2.1-1] using their conductors are as follow: (1) Winding with two conductors for each layer, (2) Heat treatment at 650℃ for 240 hr to produce Nb_3Sn every two layers, (3) Turn insulation of the conductors for each layer, (4) Assembly of eight layers with layer insulation on the same axis (Transfer), (5) Installation of the joints, (6) Epoxy impregnation of the coil with vacuum and pressure technique. In this fiscal year, all the winding, bending processing and the heat treatment have been completed. Turn insulation of four layers and transfer of two layers have been completed.

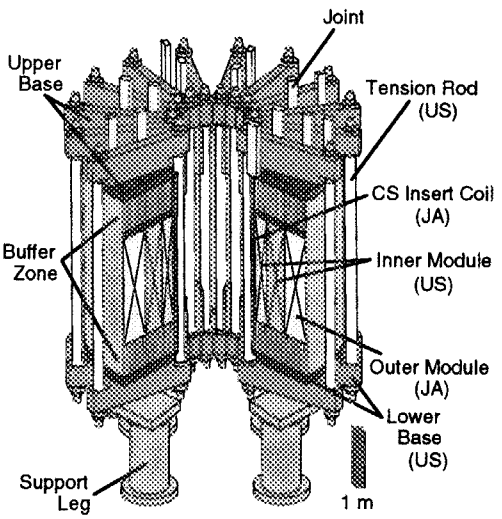

Fig.IV.2.1-1 Cutaway view of CS Model Coil

Reference

[2.1-1] Nakajima H., et al., Proc. of the 15th Intern. Conf. on Magnet Technology (1997).

2.1.1 Winding Technique

The development of winding technique for the CS model coil with layer structure, is one of key issues, because final tolerance in a radius of the coil is within ±1.5 mm. A free winding radius of the layer and a variation of curvature before transfer operation are determined to be +10/-50 mm and ±2 mm, respectively. A conductor is wound with a speed of 1 m/min. Figure IV.2.1-2 shows the winding system, which consists of an uncoiler, a straighten bender, a forming bender and a mandrel, with the first conductor as a part of two conductors in hand structure. The second conductor is wound into a gap of 49 mm between the first helical conductor. The winding operation was started in December 1996 and completed in September 1997, successfully.

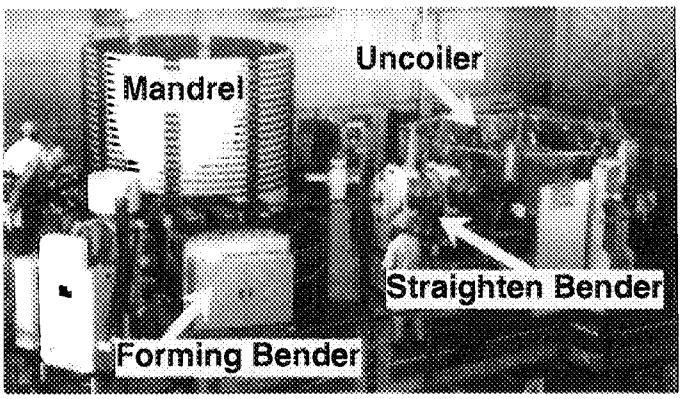

Fig.IV.2.1-2 Winding system for Outer Module of CS Model Coil

2.1.2 Heat Treatment Technique

Heat treatment is an inevitable process of the coil fabrication, generating superconductor by reacting the specified superconductor composites. The Nb_3Sn cable and its jacket are simultaneously heat-treated. Incoloy 908 has been selected as the jacket material for the conductor, because it has a low coefficient of thermal expansion that is similar to that of the Nb_3Sn composite, expecting to minimize a critical current degradation due to differential contraction after the reaction heat treatment. However, Incoloy 908 exhibits a characteristic problem that is oxygen embrittlement along grain boundaries as a result of heating in an oxygen atmosphere in the presence of tensile surface stress, causing intergranular cracking during heat treatment from oxidation along grain boundaries (SAGBO: Stress Accelerated Grain Boundary Oxidation). It was found that the SAGBO avoidance technique is only to attain a SAGBO-free oxygen atmosphere such as 0.1 ppm through R&D, for both outer and inner surfaces of the conductor jacket. A baking process and desorption technique of impurity gases were successfully developed to accomplish such oxygen atmosphere. Every two layer was heat-treated for one month. Accordingly, all eight layers for the outer module, that amount to the total length of 2.7 km, had successfully heat-treated without any SAGBO occurrence and their critical current performances had also been verified to satisfy their criteria by testing their samples that were simultaneously heat-treated as shown in the section 2.1.4.

Reference

[2.1-1] Kato, T. et al., Advances in Cryogenic Engineering - Materials Vol.44, (1998).

2.1.3 Transfer Technique

Transfer technique to fabricate the outer module is totally new technique because it is the first large coil using layer-winding technique in the world. An average radius of a winding after transfer has to be controlled within ±1.5 mm to assemble all layers. Therefore, a circumference of the winding is measured turn by turn and the radius is adjusted by insertion of thin GFRP shims based on the measurement. A scribed mark, which should be lined if the average radius is the same as a design, is also used to monitor the average radius during the transfer. Figure IV.2.1-3 shows the first layer winding after the transfer operation. The average radius of 1426.4 mm within the tolerance of ±1.5 mm was successfully achieved in the first transfer operation. The second transfer operation was also completed in March and the final transfer operation will be completed by the end of May, 1998.

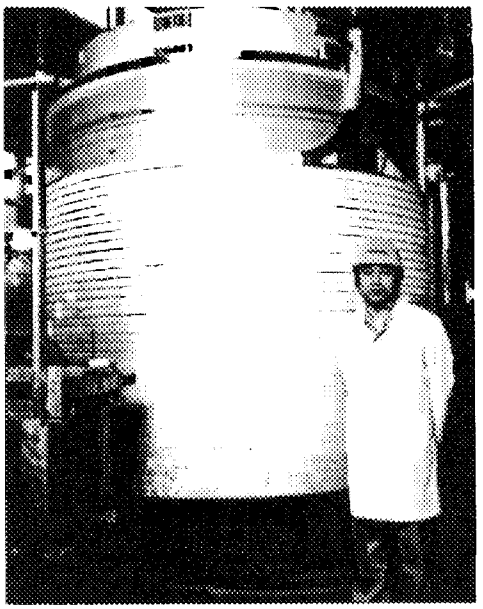

Fig.IV.2.1-3 The first layer after successful transfer operation

2.1.4 46-kA Nb_3Sn Conductor Test

In order to confirm the conductor performance and the proper heat treatment procedure, a full-size conductor sample which had the same conductor as the first and the second layers of the outer module and was heat-treated simultaneously with the module. The sample was composed of two parallel conductors whose ends were connected electrically each other. The sample was tested in the Conductor Test Facility at JAERI, whose maximum field and current were 11T and 60 kA, respectively. The test results are shown in Fig. IV.2.1-4. The estimated critical current at 11T and 4.5K is 74±6 kA and around 160% of the designed operating one. It was confirmed by this test that these conductor have enough superconducting performance as

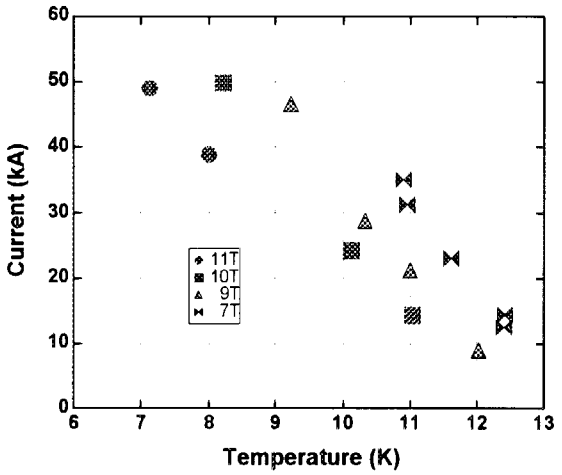

Fig.IV.2.1-4 Measured critical current as a function of conductor temperature at various magnetic field.

expected.

2.2 Development of CS Insert Coil

The winding trial was carried out to demonstrate the fabrication procedure of CS insert coil by using a 100m-long dummy conductor. The dummy conductor was wound into 24 turns in helix with the target radius of 712.5 mm by the winding machine, as shown in Fig. IV.2.2-1. The supply conductor is assembled on the supporting structure on the machine. The conductor is wound by a three point bender without the mandrel. The deviation of the average radius from the target is 0.7 mm. After winding the conductor, the conductor at the top and the bottom of the winding was bent with the radius of 500 mm for the current terminals. The deviation of the average radius during the bending for the terminals is also 0.7 mm. According to the results of the winding trial, it was confirmed that the winding machine could wind the conductor with the acceptable tolerance.

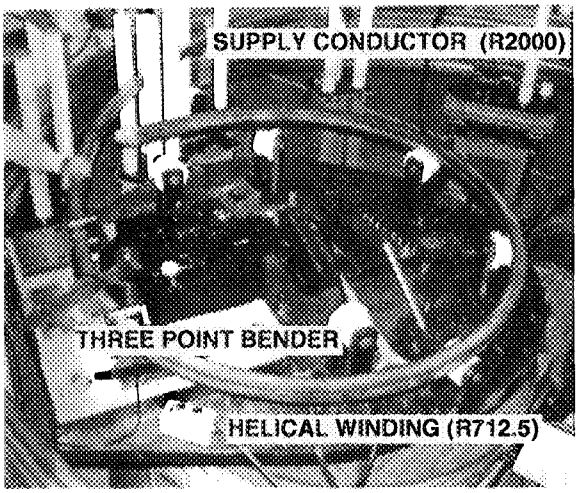

Fig.IV.2.2-1 The winding machine of the helical winding of the CS insert coil

2.3 Production of Nb_3Al Conductor

The Nb_3Al Insert Coil project has been started under ITER-EDA to demonstrate applicability of a Nb_3Al conductor to the ITER-TF coil with react-and-wind method [2.3-1, 2.3-2] since Nb_3Al has excellent superconducting performance against strain in comparison with Nb_3Sn.

In FY 1996, JAERI has developed the technique to fabricate the strand having high critical current density with high drawing ability, 3700 m at the maximum unit length, because not only high critical current performance but also high drawing ability are required for the strands to be used for the fusion machine. One ton of Nb_3Al strands, whose diameter and critical current density are 0.81 mm and 620 A/mm^2 at 12T, was fabricated by using this technique for the Insert Coil in this FY 1997. The cross-sectional view of the strands is shown in Fig. IV.2.3-1. This strand is coated by 2-μm of Cr plating, in order to reduce AC losses. The Nb_3Al cable of 150 m in length has been fabricated already by using the strands. Figure IV.2.3-2 shows the cross sectional view of the fabricated cable. The cable has 1152 (3x4x4x4x6) strands, a center channel in the center of cable

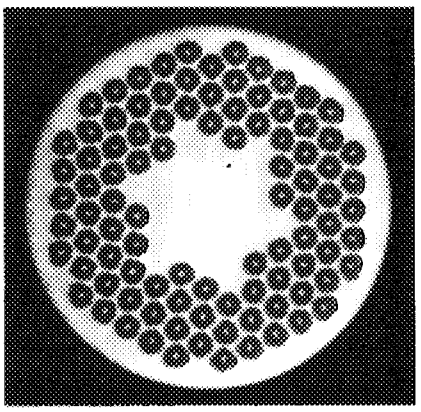

Fig.IV.2.3-1 Cross sectional view of Nb_3Al stramd

to reduce the pressure drop and the Inconel tapes outside of sub-cables to reduce AC losses. The Nb_3Al cable will be inserted into a circular jacket. The material of jacket is the austenitic stainless steel (JN1HR) which has enough ductility after the heat treatment for Nb_3Al fabrication. Jacketing is carried out by the roll-forming and continuous welding method. The 150m-length jacketing trial by using a Cu dummy cable had been performed successfully and the jacketing technique was established.

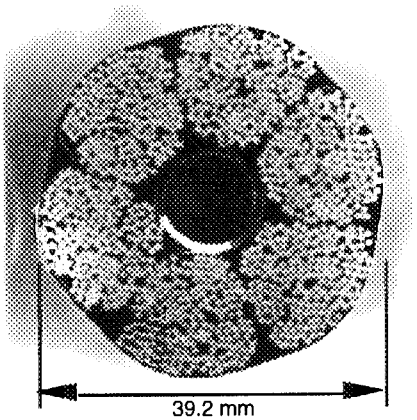

Fig.IV.2.3-2 Cross sectional view of Nb_3Al cable

References

[2.3-1] Koizumi N., et al., IEEE Trans. on MAG-32, pp.2236 (1996).
[2.3-2] Koizumi N., et al., to be published in Proc. of ISFNT-4 (1997).

2.4 Cryogenic Technique

A large capacity supercritical-helium (SHe) pump has been successfully developed for the use of a fusion experimental reactor such as ITER. The pump adopts one-stage centrifugal type and have a designed mass flow of 0.8 kg/s and a pump head of 0.25 MPa, respectively. The adiabatic efficiency is expected to be more than 70 % at the design point. The performance test has been carried out by using the 5-kW helium refrigerator. As a result, high pump performance was obtained as shown in Fig. IV.2.4-1. Measured mass flow range is 0.3 to 1.1 kg/s with the head of 0.05 to 0.27 MPa. Obtained adiabatic efficiency performance has also more than the designed value of 70 % for the flow range of 0.4 to 1.0 kg/s [2.4-1] . It was verified that the developed pump had a largest capacity in the world.

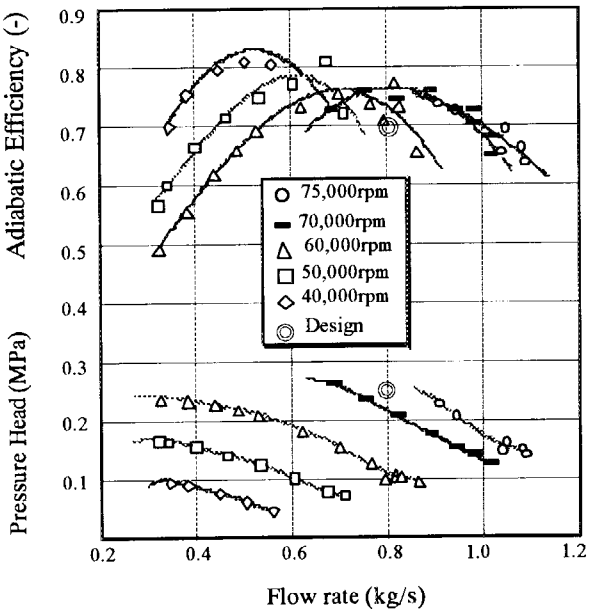

Fig.IV.2.4-1 Obtained pump performance

Reference

[2.4-1] Kawano, K., et. al., to be published in Proc. of ICEC-17 (1998).

3. Beam Technology

3.1 Development of Negative Ion Beam Technologies

Neutral beam (NB) injection has capabilities of heating a plasma, driving a plasma current for steady state operation, and controlling a plasma rotation for stable plasma operation simultaneously. Presently two major programs for negative-ion-based NB (N-NB) system are progressed at JAERI. One is the development of a 1 MeV accelerator for ITER, and the other is the development of high current negative ion sources for JT-60 and ITER. In the development of the high energy accelerator, a 1 MeV, 25 mA H^- beam has been successfully produced stably. This was the first production of the high energy negative ion beam required for ITER. High current negative ion beams of more than 18 A also have been produced in the JT-60 negative ion source, which is described section I.1.4.2.

3.1.1 Demonstration of Negative Ion Beam Acceleration

An intense ion beam source producing a 40 A, 1 MeV D^- beam is required for N-NB system for ITER. To realize such a high power and high energy beam source, it is essential to demonstrate a high current negative ion beam acceleration up to the energy of 1 MeV. For this

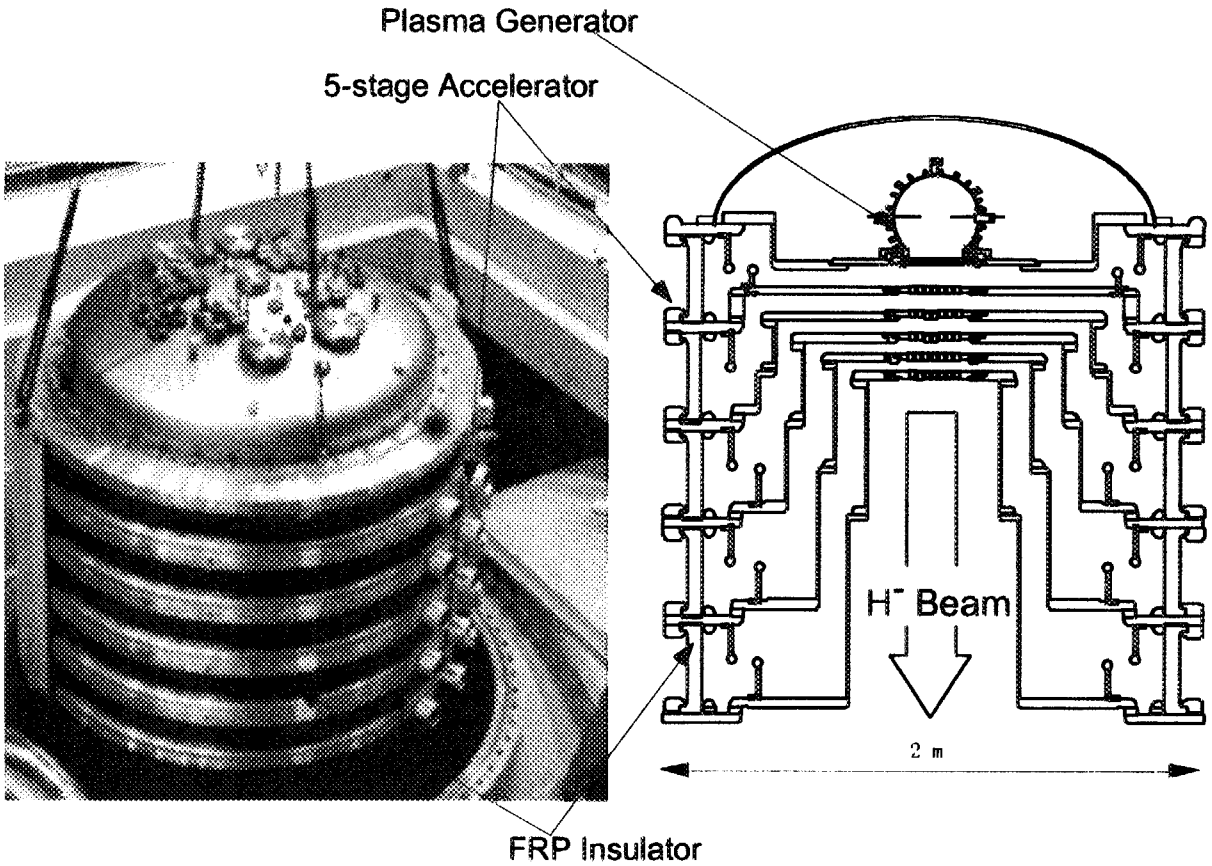

Fig.IV.3.1-1 A 1 MeV negative ion source and accelerator

purpose, a prototype accelerator of the ITER-NBI system has been developed and tested at the MeV Test Facility (MTF). The acceleration power supply of the MTF is a Cockcroft-Walton type, whose capacity is 1 MV, 1 A for 60 s. Figure IV.3.1-1 shows the negative ion source and the accelerator. The ion source (the KAMABOKO type) is a Cs-seeded volume type with semi-cylindrical geometry that can be operated at a low gas pressure of less than 0.3 Pa to reduce the stripping loss of negative ions in the accelerator. The accelerator is the same type as the reference design for ITER, i.e., a multi-aperture, multi-grid (MAMuG) type, which has a three-grid extractor and a five-stage accelerator.

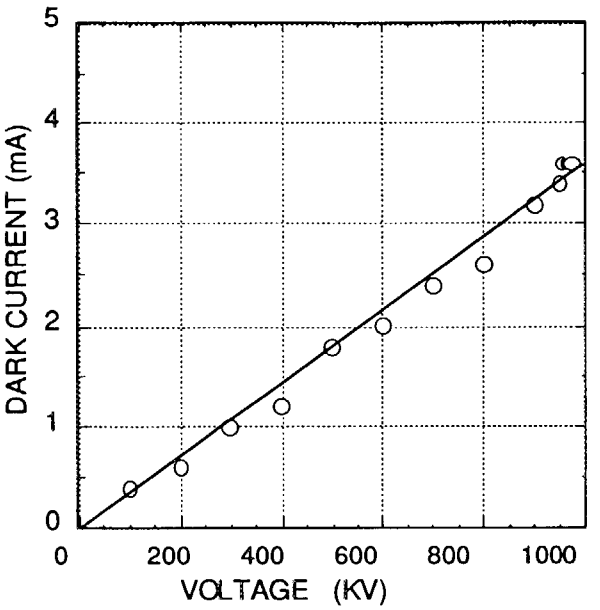

Fig.IV.3.1-2 The dark current in the accelerator as a function of the acceleration voltage

At the beginning of the operation, a significant degradation of the voltage holding was observed in the accelerator. Glow-like discharges occurred on the surface of the insulators and degraded the voltage holding capability. It was found that the discharge was initiated by micro-discharge at the triple junction, i.e., at a triple point of FRP insulator, vacuum region and metal electrode. To solve the problem, protection resistors for intermediate acceleration stages were

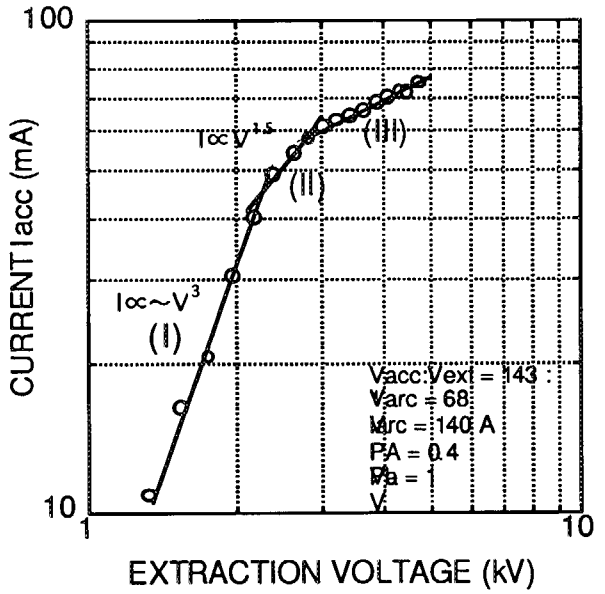

Fig.IV.3.1-3 Beam current as a function of the extraction voltage

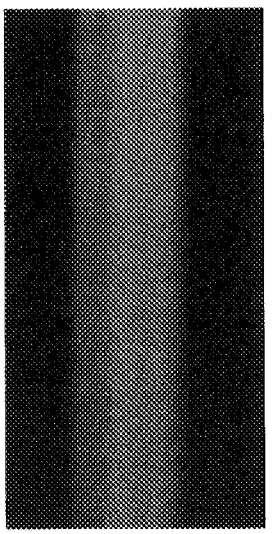

Fig. IV.3.1-4 Beamlets produced from 3x3 apertures

increased to reduce the surge currents. In addition, each acceleration stage was individually conditioned up to 200 kV by a 300 kV, 10 mA high impedance power supply with a capacitance of 8000 pF. Then the accelerator was installed in the MTF vessel to condition the accelerator at 1 MV. After 12-hour conditioning, the accelerator has successfully sustained the 1 MeV voltage. A dark current including the current flowing cooling water was as low as 3.7 mA at 1 MV as shown in Fig. IV.3.1-2. Followed by the conditioning, a 25 mA, 1 MeV H^- beam was stably produced for 1 s from 9 apertures [3.1-1, 2, 3].

The beam optics of the five-stage accelerator was studied experimentally. The dependence of the beam current on the extraction voltage (Vext) is shown in Fig. IV.3.1-3. It increases in proportion to $Vext^3$ in the region of the low extraction voltage, where some of the negative ions were intercepted directly by the extraction grid and the electron suppression grid (region I). It also increases in proportion to $Vext^{1.5}$ at higher extraction voltages, where the ion extraction sheath was formed properly in the source, so that all the extracted negative ions passed through the grids in the extractor and accelerated in the following five acceleration gaps (region II). In this region, it was limited by space charge, i.e., the Child-Langmuir law. Then it tends to saturate (region III). In the region III, it was limited by the emission of the negative ions in the negative ion source. Good beam optics was obtained at the inflection point from the region II to the region III, as shown in Fig.IV.3.1-4. It was found that the extraction voltage of the good beam optics obtained in the experiment was in good agreement with that obtained from the beam trajectory calculation.

3.1.2 Long Pulse Operation of a Negative Ion Source

A long pulse operation of the negative ion source has been demonstrated in a joint experiment between JAERI and CEA-Cadarache in France. The negative ion source used in the experiment was a Cs-seeded source with semi-cylindrical shape (the KAMABOKO source), which was the same type of the source designed for the ITER-NBI system. The long pulse operation of the Cs-seeded source requires the control of a plasma grid temperature to continue a Cs-effect, i.e., high negative ion production, low source pressure and low extracted electron. Since the Cs effect are enhanced by the plasma grid temperature and maximized at the temperature of 200-300 ℃, the temperature of the plasma grid should be controlled within this high temperature range. To control the plasma grid temperature, two types of the plasma grid, i.e., a frame cooling grid and an active cooling grid were designed. The frame cooling grid has a water cooling channel only on the frame at the edge of the grid, and there is a thermal bridge between the grid and the frame. The active cooling grid has small cooling channels between the apertures. The cooling channels are connected via small disks made of stainless steel with the grid. Taking 15 W/cm^2 of heat flux as the design value, both of the grids were designed to

keep the temperature at 250℃ in the long pulse operation [3.1-4].

Using the frame cooling grid, a 20 mA /cm^2 D^- beam has been produced continuously for 1000 seconds by seeding a 650 mg cesium. The beam current density and the pulse length satisfy the ITER requirements. The temperature of the plasma grid was kept to be constant at higher than 200 ℃ after about 100 seconds from the onset of the arc discharge as predicted by a three-dimensional thermal calculation code. No significant degradation of the Cs effect was observed during the pulse. It was also observed that the voltage holding of the accelerator due to the cesium flow from the source to the accelerator was not degraded during and after the 1000 second pulse [3.1-5].

3.1.3 Engineering Design and the Other R&D for the ITER NBI System

The beam ion source, which is one of the key components for the ITER-NBI system, has been designed at JAERI. It is designed to produce a 1 MeV, 40 A D^- beam with a beam divergence of < 5 mrad. Two types of the beam sources have been designed. One is a gas insulated beam source (GIBS), and the other is a vacuum insulated beam source (VIBS). The GIBS is the present reference design for ITER, and composed of the KAMABOKO source and a multi-aperture, multi-grid accelerator insulated by a large ceramic insulator. The VIBS is designed to reduce the manufacturing cost and to avoid the problem of the ionization of the insulation gas due to neutron irradiation. Although the VIBS is composed of the same ion source and accelerator as those in GIBS, small post insulators are used instead of the large ceramic insulator in the GIBS.

A 1 MV transmission line for supplying intermediate acceleration voltages is the other key component in realizing the ITER-NBI system. In the present ITER design, the transmission line is filled with a pressurized insulation gas, and connected with HV deck and the ion source via large multi-connector bushings at the edges of the line. The feedthroughs for source power supplies such as filaments and arc are installed in a inner central cylindrical tube, around which four pairs of the feedthroughs for supplying intermediate acceleration voltages of -200 kV, -400 kV, -600 kV and -800 kV are positioned. To clarify the allowable electric and mechanical stresses, a 1 MV bushing has been designed and fabricated for testing. The outer diameter of the epoxy bushing is about 2 m.

References

[3.1-1] Watanebe K., Fujiwata Y., Hanada M., et al., "Multi-stage, multi-aperture electrostatic accelerator for H- beam", Proc. of the joint meeting of the 8th Int. Symp. on the production and neutralization of negative ions and beams and 7th European workshop on the production and application of light negative ions, Giens, France, Dec.15, (1997).

[3.1-2] Watanabe K., Fujiwara Y., Hanada M., et al., "Development of a multiaperture, multistage electrostatic accelerator for hydrogen negative ion beams", Rev. Sci. Instrum., 69 (2), pp. 986-988 (1997).

[3.1-3] Watanabe K., et al., "Recent Progress of High-Power Negative Ion Beam Development for Fusion Plasma, Heating", Radiat. Phys. Chem., 49, No. 6, pp. 631-639 (1997).
[3.1-4] Fujiwara Y, Miyamoto N., Okumura Y., et al., "Temperature control of plasma grid for continuous operation in cesium-seeded volume negative ion source", Rev. Sci. Instrum., 69 (2), pp. 1173-1175 (1997).
[3.1-5] Trainham R., Jacquat C., Miyamoto K., et.al., "Negative ion source for neutral beam injection into fusion machines", Rev. Sci. Instrum., 69 (2), pp. 926-928 (1997).

3.2 Application of High Intensity Ion Beam Technologies

3.2.1 Development of the Ion Source for High Energy Accelerator

A high brightness negative ion source has been developed for high energy accelerator applications. A Cs-seeded volume source with semi-cylindrical shape (the KAMABOKO source) has been applied to suppress the stripping losses of negative ions. The accelerator is composed of an extractor with three multi-aperture grids and a grounded grid with a single hole. All the grids on the extractor are curved and oriented geometrically at 15 cm downstream from a plasma grid to merge the extracted beamlets into a single beam. In the experiment, the negative ions were extracted from the nine apertures of 10 mm in diameter.

The source was operated by seeding a small amount of Cs (about 1 g) while the temperature of a plasma grid was controlled to be higher than 200 ℃ to enhance the Cs effect. By optimizing the beam optics, a 165 mA, 45 keV merged H^- beam has been successfully produced. The current density, defined as the beam current divided by the total area of 9 apertures on the plasma grid, reached 30 mA/cm^2 [3.2-1].

3.2.2 Development of a Super Low Energy Ion Source

The beam technology developed for NBI has been applied also to the development of a super low energy ion source for the material study. So far, a 0.5 A, 250 eV hydrogen and helium ion beams have been produced and used in the sputtering experiment on plasma surface interaction. The feature of the source is that the electrodes are composed of small tungsten wires. By using the tungsten wires, the slit width, gap length between the electrodes and thickness of the electrodes are reduced, so that the sufficiently strong electrical field for the ion extraction is created. The tungsten wires of a 0.5 mm diameter are strung at every 1mm to make the slit of a 0.5 mm width [3.2-2, 3].

References

[3.2-1] Miyamoto K., Okumura Y., Watanabe K., et al., to be submitted for publication.
[3.2-2] Nakamura K., Dairaku M., Akiba M., "Sputtering experiments on B_4C doped CFC under high particle flux with low energy", J. Nucl. Materials, 241-243, pp. 1180-1184 (1997).
[3.2-3] Jimbou R., Nakamura K., Akiba M., "High Heat Flux Experiments on a Saddle-shaped Divertor Mock-up", Proc. of the 16th Int. Conf. on Fusion Energy, 7-11 Oct. 1996, pp. 565-570, IAEA, Vienna, 1997.

4. RF Heating Technology

Radio-frequency (RF) wave is a key tool for heating and current drive of the tokamak fusion reactor. Developments of high efficiency RF source and tritium barrier window for electron cyclotron heating (ECH at 100-300 GHz), and high performance launching systems for ECH, lower hybrid current drive (LHCD at 2-8 GHz) and ion cyclotron range of frequency (ICRF at 40-200 MHz) are the main efforts of JAERI RF heating technology. The most outstanding point in FY 1997 is the progress of the ITER gyrotron for ECH, which resulted in the world record of 520 kW x 5 sec. operation at 170 GHz with the Chemical Vapor Deposition (CVD) diamond disk window.

4.1 Gyrotron Development

The gyrotron is a high power millimeter wave source which is a key component of the ECH system. Under the task agreement of ITER/EDA, the 170 GHz gyrotron development has been conducting since 1995. We obtained a pulse duration of 10 sec at 180 kW and 0.75 sec at 520 kW in 1996 [4.1-1]. However, both pulse duration and power were limited by temperature increase of a silicon nitride output window as shown in Fig. IV4.1-1. To overcome the window problem, we developed a novel diamond window. Detail of the diamond window is described in section 4.2. The output window was replaced by the diamond window. The baking of the gyrotron was performed for degassing at 450° C. No vacuum leakage was recognized after the baking. Figure IV.4.1-2 shows the picture of the diamond window gyrotron, installed on the test stand.

The gyrotron experiment was done using the JAERI gyrotron test stand. The pulse duration was extended at the output power P_{rf}~520 kW. Here, beam voltage V_b, beam current I_b and depressed collector voltage V_d were 84 kV, 31 A and 32 kV, respectively. The window temperature was monitored with an infrared camera. The loss tangent of the diamond disk was relatively high, $\tan\delta \sim 1.3\times10^{-4}$ and the temperature increased up to ~150° C. However, the temperature almost saturated after 5 sec, which agrees well with the simulation. If the high quality diamond disk such as $\tan\delta \sim 2\times10^{-5}$, which is already developed, is used, the temperature increase would be 30° C even when the Gaussian beam of 1 MW is transmitted. As the diamond disk is proved to be operational up to at least 150° C, the diamond window has a potential for the multi-megawatt power transmission. Total shot number of operation longer than 1 sec was about 1000. After the experiment, the surface of the diamond disk was inspected and no damage and no trouble was found.

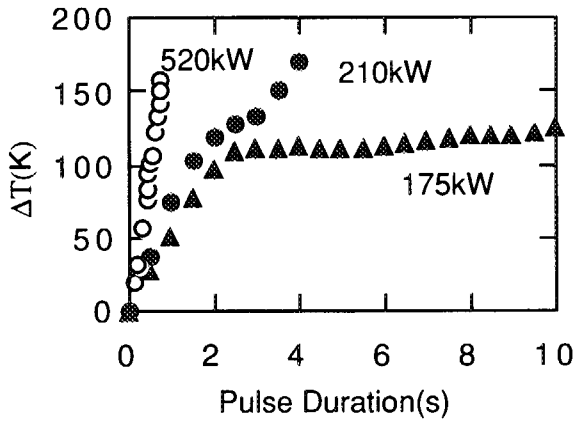

Fig. IV.4.1-1 Temperature rise of silicon nitride double disk window vs. pulse duration.

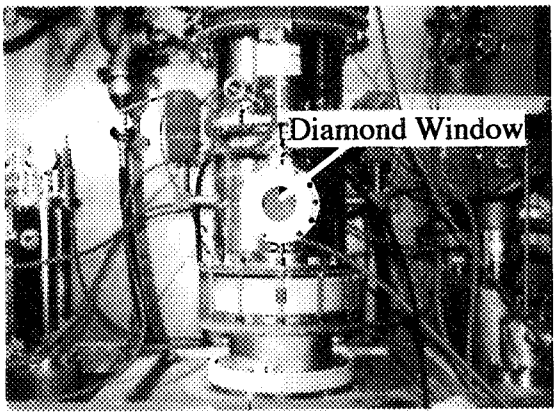

Fig. IV.4.1-2 Picture of 170 GHz gyrotron installed on the test stand. Center of the picture is the diamond window.

It is concluded that the synthetic diamond disk is useful and reliable for the gyrotron output window. It should be pointed out that the diamond window has a potential for multi-megawatt and CW power transmission of millimeter wave when the disk of lower loss tangent of 2×10^{-5} is used.

References

[4.1-1] Sakamoto K., Kasugai A., Tsuneoka M., et al., "Development of 170 GHz/500 kW Gyrotron", J. Infrared and Millimeter waves, 18, No.9, pp. 1637 (1997).

4.2 Development of Transmission Line and Launcher

4.2.1 ECH Window, Transmission Line and Antenna

The diamond disk is an ideal material for the ECH window of 1MW/CW RF transmission at 170 GHz since it has extremely high thermal conductivity and low dielectric loss [4.2-1], temperature increase of the window due to absorption of high power millimeter wave could be minimized by simple water edge cooling at room temperature. The diamond disk was produced from CVD and is 96 mm in diameter and 2.23 mm thick. The disk was built into an window assembly with water cooling channel, leaving an effective window aperture of 83 mm. The diamond window is shown in Fig. IV.4.2-1. During transmission of a focused Gaussian beam of 170 GHz, 110 kW, 10 sec, temperature increase at the center of the window saturated at value of 40° C, in good agreement with calculated value as shown in Fig. IV.4.2-2 [4.2-2]. Water-edge-cooled diamond window promises to provide a technical solution for continuous millimeter wave transmission in excess of 1 MW for the ECH window.

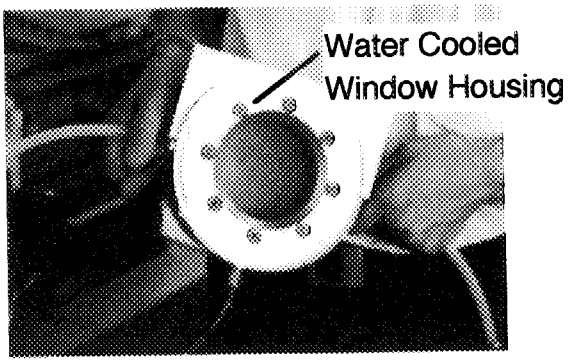

Fig. IV.4.2-1 Picture of the diamond window

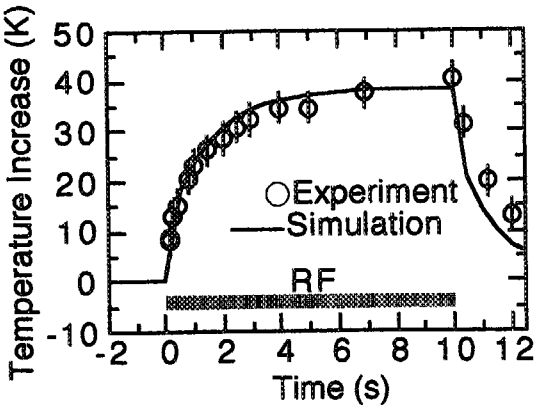

Fig. IV.4.2-2 Temperature increase of the window center (Circle : measured, solid line : calculation)

The steerable antenna for electron cyclotron heating/current drive (ECH/ECCD) was designed and installed in the JFT-2M/60 GHz system. The antenna, shown in Fig. IV.4.2-3, consists of the fixed focus mirror and the movable flat one. The movable mirror is located 20° lower from the equatorial plane and the injection angle of rf beam can be changed by the mirror. The range of toroidal and poloidal injection angle are ±25° and ±20°, respectively. The high power, short pulse injection test of 160 kW, 1 -2 msec using the antenna was carried out and the e-folding beam width at the inboard wall of the vacuum vessel was measured as 220~230 mm, which quite agreed with simulation. The maximum injection power and the pulse were 180 kW and 30 msec, which is limited by power source. The corresponding power density at the mirror surface is 2.3 kW/cm^2, which is more than the design value of the ITER. No damage or breakdown was observed on the antenna.

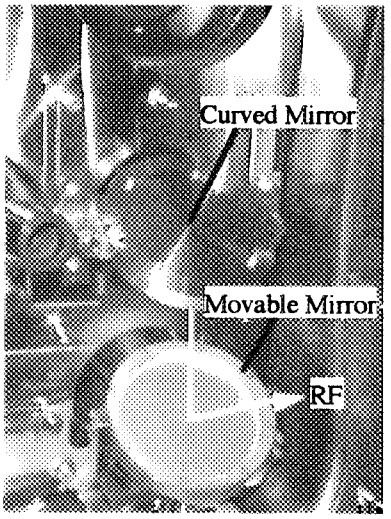

Fig. IV.4.2-3 Picture of ECH Antenna

References

[4.2-1] Braz O., Kasugai A., Sakamoto K., et al., "High Power 170 GHz Test of CVD Diamond for ECH Window", Int. J. Infrared and Millim. Waves 18, pp. 1495 (1997).

[4.2-2] Kasugai. A, Sakamoto K., Takahashi K., et al., "Chemical Vapor Deposition Diamond Window for High Power and Long Pulse Millimeter Wave Transmission", Rev. Sci. Instruments 69, pp. 2160 (1998).

4.2.2 LH Antenna

A mock-up of a 3.7 GHz Lower Hybrid Current Drive (LHCD) antenna module was fabricated from Carbon Fiber Composite (CFC) for the development of heat resistive low Z

module facing the plasma. This four-divided waveguide module with a water-cooled channel is made from CFC plates and rods which are Cu-plated to reduce the RF losses. The RF properties and the outgassing rates for long pulses and high RF power were tested at the Lower Hybrid test bed facility of Cadarache in the collaborative work between JAERI and CEA, France. It was concluded that the outgassing rate of CFC is about seven times the outgassing of a reference DSC module which was built with the same geometry. Stationary conditions of temperature and pressure were obtained at rather high power density (45 MW/m^2) with a RF injection time of 1,200 sec. It is assessed that a CFC module is an attractive candidate for LHCD antenna tip.

4.2.3 ICRF Antenna

An all metal antenna support (AMS) is a key element of the ICRF all metal antenna. The full size mock-up of AMS for ITER ICRF antenna was designed and fabricated for high power RF tests, as an R&D task in the ITER/EDA. The RF characteristic of the pair of mock-up connected by the coaxial line was measured with the network analyzer for various coaxial line lengths. The optimum coaxial line length between the AMSs was 1925 mm. In this case, VSWR < 2.3 which satisfies the Vacuum Transmission Line (VTL) specification (VSWR ≤ 3.0) is obtained in the full band width of 40-85 MHz. The voltage stand-off capability of the AMS was confirmed at 60 MHz, the main ICRH frequency of ITER. The achieved RF voltage stand-off at the AMS was 55 kV for 1 msec, 45.5 kV for 0.1 sec, and 42.5 kV for 1 sec. The voltage was limited not by the AMS mock-up but by an arcing probably near the ceramic feed through and by the RF generator capability. This result satisfies the target of the ITER R&D task.

4.3 Millimeter Wave Free Electron Laser

Induction linac driven mm-wave FEL is one of most promising methods for GW level high power mm-wave source by employing a high current beam of kA level. To establish basic study of the GW class mm-wave FEL, joint work is in process at JAERI. The JAERI Large current Accelerator (JLA) of an induction linac was assembled with KEK (National Laboratory of High Energy Physics) induction modules. The KEK modules of 1.6 MeV are used for the injector unit, the existing modules of 2.5 MeV are operated for the post accelerator unit. The beam parameters are expected to be beam energy of 4 MeV, current of 3 kA and pulse duration of 50 nsec. On the other hand, Backward Wave Oscillator (BWO) experiment using 1 MeV induction linac (LAX-1) have been also done for seed power of FEL. The output power of 1.2 MW was obtained with the BWO at a frequency of 7.8 GHz. This is the first demonstration of the induction linac-BWO system.

5. Tritium Technology

To establish tritium technology, research and development work on tritium safety technology and tritium processing technology was progressed and remarkable achievements were obtained. Experiments using tritium were performed without any unsafe trouble in the Tritium Process Laboratory (TPL). Safe operation of the TPL tritium facility, itself, is a valuable on-site experience that demonstrates the capability of tritium safe handling in Japan.

5.1 Development of Tritium Safety Technology

To establish safety technology for handling a large amount of tritium in fusion reactor, research and development at TPL in this fiscal year was focused on (1) advanced tritium removal system, (2) tritium accountancy, (3) tritium-material interactions, and (4) tritium behavior in confinement systems and environment.

For development of tritium removal technology applied to the ITER Atmosphere Detritiation System, test of a system using a gas separation membrane module made by polyimide hollow fibers was continued for recovery of hydrogen isotopes and moisture from atmosphere in various confinement systems. An acceleration test was carried out to confirm its performance after a long period exposure to tritium relevant to the worst condition assumed for the design basis accidents of ITER. As a result, no degradation was observed on its performance even after the severest test.

In regard to tritium accountancy, two new techniques were developed and tested. A remote on-line real-time process gas analysis system using optical fibers, with an application of laser Raman spectroscopy, was developed and upgraded to a system able to carry out multi-location analysis, which was enabled by dividing spectral images from different analytical points on the CCD detector of very high sensitivity [5.1-1]. The current system can analyze four different analytical points simultaneously. Figure VI.5.1-1 presents successful result obtained with remote and multi-location analytical system applied on process line of hydrogen isotope separation system during test of fusion fuel simulation loop described in section 5.2 [5.1-2].

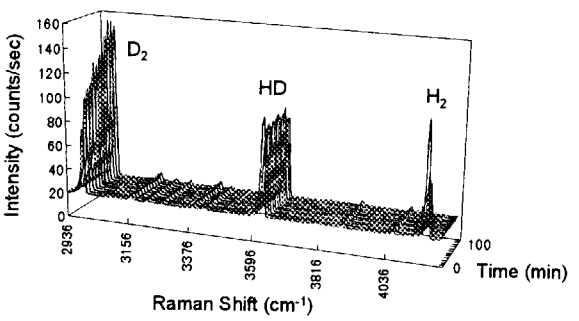

Fig. IV.5.1-1 Trend of hydrogen isotope composition on the line of isotope separation system successfully achieved with newly developed laser Raman analytical system.

To establish an "in-bed" tritium accounting technology for the ITER-scale tritium storage system, a scaled Zr-Co bed with an application of gas flowing calorimetry was developed and tested. Its principle is to know the amount of tritium stored in bed by measuring temperature rise of helium gas

flowing in a pipe installed in bed under an equilibrated condition as shown in figure IV.5.1-2 [5.1-3]. Demonstration tests were successfully carried out not only with pure tritium gas (up to 22 g) but also with tritium and deuterium gas mixture. This technique enables easy and safe tritium accountancy without moving tritium out from the storage bed. Target tritium accounting accuracy of the ITER storage bed, ±1 g for 100 g storage, was successfully demonstrated with this bed.

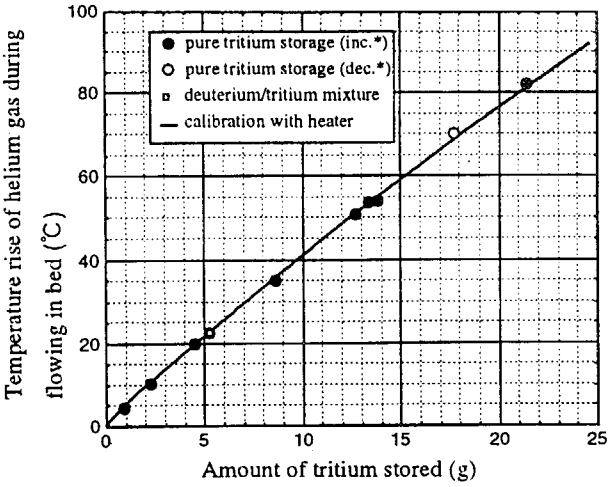

Fig. IV.5.1-2. Relation between amount of tritium stored and temperature rise of He gas flowing in bed.
* inc: measured after introduction of additional tritium; dec: measured after removal of some tritium from bed.

In a study of tritium-material interactions related to tritium inventory investigation, tritium distribution in 2-dimensional CFC (CX-2002U) exposed to deuterium / tritium RF plasma was observed using a method of micro-auto-radiography. Obtained tritium depth profile showed that tritium migrated into not only near surface area but also in deep bulk possibly by diffusion of tritium atom through pore of CFC. The amount of tritium diffused into deep bulk was almost equivalent to one trapped at near surface [5.1-4].

For study of tritium behavior in confinement systems and environment, a large caisson was designed, made and installed in a room of TPL. Some demonstration tests are scheduled in the next fiscal year.

References

[5.1-1] O'hira S. and Okuno K., Fusion Technol., 30, pp. 869 (1996).
[5.1-2] Yamanishi T., Konishi S., Kawamura Y., et al., 13th Topical Meeting on Technology of Fusion Energy, June 1998, Nashville USA.
[5.1-3] Hayashi T., Suzuki T., Yamada M., et al., 13th Topical Meeting on Technology of Fusion Energy, June 1998, Nashville USA.
[5.1-4] Tadokoro T., O'hira S., Nishi M., et al., to be published in J. Nucl. Materials.

5.2 Development of Tritium Processing Technology

Fusion fuel simulation loop system was constructed and integrated fusion fuel processing system test was successfully started with it. Figure IV.5.2-1 shows a configuration of the fusion fuel simulation loop system [5.2-1]. The loop system is composed of a front-end palladium diffuser, a fuel cleanup system (FCU) and an isotope separation system (ISS) with a torus mockup tank. The FCU system is composed of an electrolytic reactor and a palladium diffuser [5.2-2].

Plasma exhaust simulation gas stream is made by adding impurity gas such as helium and methane to hydrogen gas before it reaches the front-end diffuser. A pure hydrogen isotope stream obtained by passing through the front-end diffuser is sent to the ISS. The rest impurity stream (helium and methane) with some hydrogen isotopes is sent to the electrolytic reactor of the FCU, where methane is reduced to hydrogen and CO_2. Produced hydrogen isotope gas is sent to the ISS by passing through the palladium diffuser. The gas which does not permeates the diffuser, He and CO_2, is exhausted from the system. The ISS separates protium (H), deuterium (D) and tritium (T), and H is exhausted. In this system, to make plasma exhaust simulation gas, hydrogen isotope gas containing H is supplied to the torus mockup tank from the ISS. Table IV.5.2-1 shows the present experimental conditions. Gas flow rate of this loop system was about 1/8 of the averaged rate of the ITER fusion fuel loop. The helium and methane gas added to the hydrogen isotope stream was 0.1~0.3 mol/h. Under these conditions, the ISS and the FCU were successfully operated, and the impurity gases were exhausted. As described in section 5.1, four laser Raman cells were installed on lines of the ISS, and a set of real-time (1 minute interval), remote analysis results for all the molecular species of hydrogen isotopes could be achieved, which suggested to enable the system control. A series of preliminary demonstration test of the fusion fuel simulation loop system was thus successfully carried out in this fiscal year.

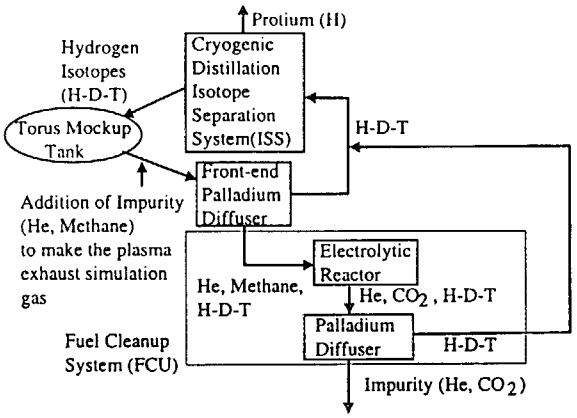

Fig. IV.5.2-1. Configuration of fusion fuel simulation loop system constructed in TPL.

Table IV.5.2-1 Conditions of integrated experiments

Amount of tritium used : 1 g
Concentration of tritium : ~1%
Inventory of hydrogen isotopes within integrated system : 20 mol
Flow rate of integrated system : 10 mol/h
Flow rate of H_2 exhausted from the integrated system : 0.27 mol/h

For the design of the control system of cryogenic distillation column used in the ISS of ITER, simulation study was continued [5.2-3].

A series of experiments on thermal diffusion column, attractive ISS for small amounts of hydrogen isotopes, was carried out with the H-T system, and its separation factor was found to be increased greatly by cooling the column wall with liquid nitrogen and by increasing the diameter of its inner heater [5.2-4].

A combination system of water distillation and Vapor Phase Catalytic Exchange (VPCE) columns was designed as the ITER tritiated water processing system. A basic study on the VPCE column was carried out.

Development of Cryogenic Molecular Sieve Bed (CMSB) for breeding blanket interface system was continued. CMSB was adopted also as the ITER recovery system of tritium from the He discharge cleaning exhaust gas. Figure IV.5.2-2 shows the CMSB prototype developed in this year. Molecular Sieve 5A was charged in it, pellet size of which was 1.6 mm in diameter and 3.2 mm in length. Tests of this CMSB prototype was just started.

As the basic study for the solid breeder blanket development, preparation of experimental apparatus was started [5.2-5].

Figure IV.5.2-2 Aspect of prototype CMSB (left) and its inner main body separated from outer LN2 bath (right).

References

[5.2-1] Konishi S., Maruyama T., Okuno K., et al., "Development of Electrolytic Reactor for Processing of Gaseous Tritiated Compounds", to be published in Fusion Eng. and Design.

[5.2-2] Konishi S., Yamanishi T., Enoeda M., et al., "Integrated Fusion Fuel Cycle Development at the Tritium Process Laboratory of the Japan Atomic Energy Research Institute", to be published in Fusion Eng. and Design.

[5.2-3] Yamanishi T. and Okuno K., "Control Characteristics of Cryogenic Distillation Column with a Feedback Stream for Fusion Reactor", J. Nucl. Sci. and Technol., 34, pp. 375 (1997).

[5.2-4] Arita T., Yamanishi T., Okuno K., et al., "Experimental Study for Separation Characteristics of Cryogenic-Wall Thermal Diffusion Column with H-D and H-T Systems, to be published in Fusion Eng. and Design.

[5.2-5] Kawamura Y., Enoeda M. and Okuno K., " Isotope exchange reaction in Li2ZrO3 packed bed", to be published in Fusion Eng. and Design.

5.3 Operation of Tritium Safety System in TPL

The tritium safety system at TPL has been in service day and night to support tritium engineering research activities since 1988. During this fiscal year, the Glovebox Gas Purification System (GPS) was operated for about 6,300 hr to remove tritium and to control the pressure and oxygen concentration in nitrogen atmosphere gloveboxes. The Air Cleanup System (ACS) was operated for cleaning about 177,000 m^3 of air in a glovebox for handling tritium waste water and about 53,000 m^3 of spot ventilated gas during maintenance of gloveboxes and hoods and during disposal of solid waste. The Effluent Tritium Removal System (ERS) removed 5.0×10^{13} Bq of tritium from 3,060 m^3 of exhaust gas of experimental apparatus. The Dryer Regeneration System (DRS) recovered 800 liters of tritiated water from the dryers of GPS and ACS. Regular checkup was made for all the devices and apparatus of the tritium safety system. "Year of 2000" problem in the program of Central Control System (CCS) was resolved, and a new Central Monitor System (CMS) was installed to monitor the operation rooms. ACS, ERS and CCS were modified to connect the new Caisson experimental apparatus. A plan of tritium transportation using a BU-type package was approved by the authorized offices of Canada and USA, and the tritium absorbed in a zirconium-cobalt bed will be shipped from Canada in FY 1998. Fig. IV.5.3-1 shows the monthly environmental tritium release from the stack of TPL for this fiscal year. The total tritium release was less than 2.0×10^{10} Bq, which is three orders of magnitude smaller than the target value of the Tokai Research Establishment of JAERI. Safe tritium handling operation at TPL has thus been demonstrated since 1988.

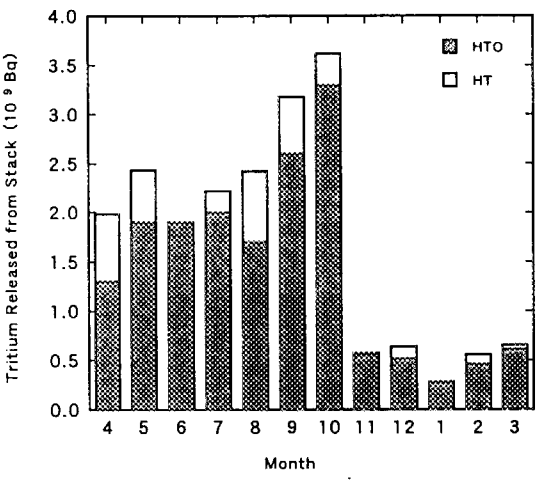

Fig. IV.5.3-1. Monthly release of tritium from TPL in FY1997.

6. Fueling/Pumping and Vacuum Technology

6.1 Improvement of First Stage Injector for Railgun

An electromagnetic railgun type injector has been studied to develop a repetitive and a speed-controllable pellet accelerator for fueling the reactor-relevant plasmas. This injector consists of two parts, a pneumatic gun for the first stage acceleration and the railgun accelerator for the second stage acceleration. Since the performance of the first stage accelerator is a very important factor to achieve good reliability of the electromagnetic railgun, a freezing system of the first stage accelerator has been improved to obtain a stable freezing temperature. The new system uses a refrigerator machine, instead of a liquid helium. In freezing and producing/injection tests, stable freezing temperature of 8 ± 1 K for hydrogen was established and pellets with about 3 mm in diameter were ejected at a speed of 1 km/s with good reproducibility of about 90 %.

6.2 Development of Helical Grooved Pump

The ITER torus mechanical pumping system for cryopump regeneration comprises a 3-stage roots blowers pump and a 4 stage dry piston pump rated at 180 m^3/h as the final stage. An alternative configuration of the mechanical pumping system is the use of helical grooved pumping system.

A Helical Grooved Pump (HGP) characterized by a rotor with grooved shape can compress and exhaust H_2 molecules efficiently in the transient flow range (several hundred Pa range) that is approximately 1000 times higher than the working pressure of a conventional turbo-molecular pump.

In order to get a high outlet pressure (>150 Pa for H_2 : minimum crossover inlet pressure of an ITER dry piston pump) and a high H_2 throughput (>2 Pa m^3/s), two types of HGPs (GX30M and GX150M) which are used in series have been developed (Fig.IV.6.2-1) as an ITER R&D task. These pumps are suspended by active 5-axis control magnetic bearing, and have the characteristics of which are a high pumping speed (0.13 m^3/s : design specification) for

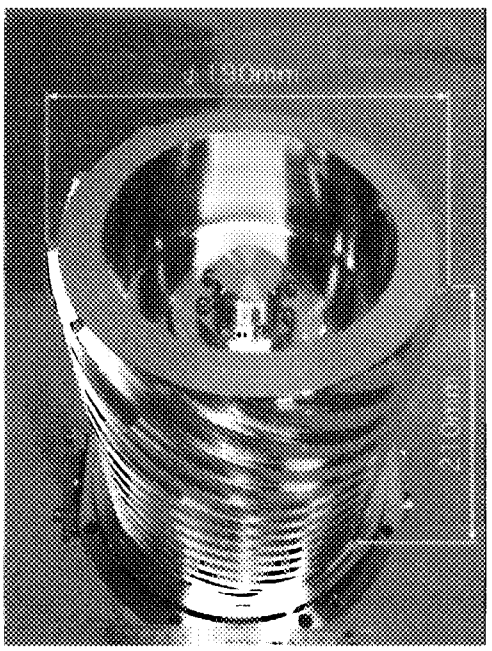

Fig.IV.6.2-1 Appearance of rotor of helical grooved pump (GX30M, Rotation speed : 27,000 rpm)

GX150M and a high compression ratio (1×10^3 : design specification) for GX30M.

The measurements of compression ratio on each pump, and pumping speed on GX30M and the 2-stage HGP system have been performed for N_2,He, D_2 and H_2. The results show that the maximum outlet pressure for H_2 is approximately 1000 Pa and the H_2 throughput is approximately 4 Pa m^3/s, which satisfy the requirement of ITER.

6.3 Vacuum Technology

6.3.1 Development of Ceramic Film Coating Technique

Plasma spray coating method of alumina film on stainless steel substrate with a Ni-Cr intermediate layer has been developed for the electric insulation of the in-vessel components like the blanket module. Durability of dielectric voltage stand-off (>2,000 MΩ, 1kV-DC) of the film (alumina film thickness : 228 μm) has been examined. Alumina coated specimens with flat ended surfaces were impacted repeatedly with a stress of 638 MPa which corresponds to two times of the yield strength of stainless steel substrate. As the result, the alumina film has shown high durability on the electric insulation against the repeated impact load of over 70,000 cycles (Fig.IV.6.3-1).

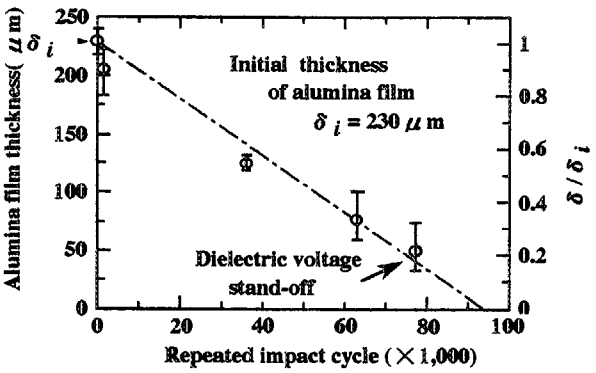

Fig. IV.6.3-1 Variation of alumina film thickness against repeated impact load

This alumina coating film has been used on the actual divertor of JT-60 for the reduction of the eddy current, and it has shown the electric insulation characteristics as expected.

6.3.2 Research Activity for SAGBO Avoidance

As for the preparation of the manual on thermal treatment in order to decrease oxygen contents and to avoid the crack generation due to Stress Accelerated Grain Boundary Oxidation (SAGBO) on the superconductor conduit material of Incoloy, the quantitative analysis of oxygen absorption on to Incoloy has been performed by the measurement with the vacuum thermobalance. As a result of heat treatment according to this manual, SAGBO cracking has been avoidable in the conductor heat-treatment process during Central Solenoid (CS) model coil fabrication as an ITER R&D task.

7. Development of Plasma Facing Components

Plasma Facing Components (PFCs) of next fusion devices, such as ITER, are mainly composed of two high heat flux parts. One is the first wall and the other is the divertor plate. In particular, the divertor plate is exposed to severe thermal load because the divertor plate is located across the magnetic field line. In the ITER design, the divertor is exposed to a steady state heat flux of 5 MW/m^2 in normal operation, and also exposed to a heat flux of more than 20 MW/m^2 in transient operation of about 10 s. In addition, the incident energy to the divertor plate exceeds 100 MJ/m^2 during plasma disruptions of several ms. Figure IV.7-1 shows a schematic of the ITER divertor plate. In the present design of the ITER divertor, the upper half of the divertor plate is covered with tungsten materials to minimize the sputtering erosion due to high ion flux from plasma. On the other hand, the lower half of the divertor plate is covered with Carbon-Fiber-reinforced Carbon composites (CFC) to remove high heat loads during transient operation. To investigate the thermal performance and the durability, mock-ups of the ITER divertor plate have been fabricated and tested.

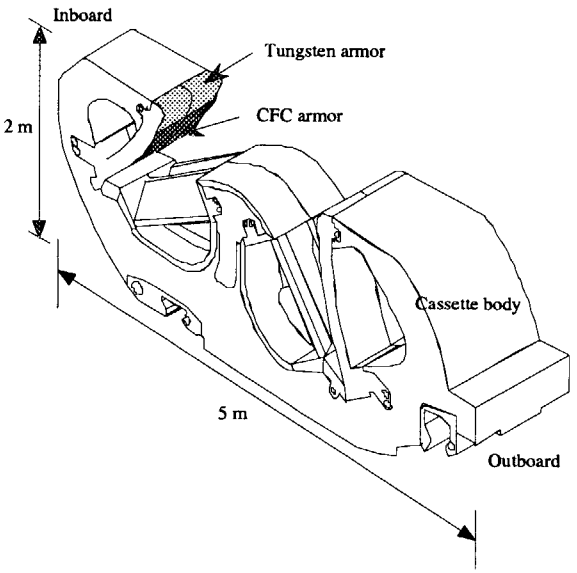

Fig. IV.7-1 ITER divertor plate (cassette structure)

In FY 1997, a large scale divertor mock-up having a dimension of 1.3 m long was fabricated and tested in an ion beam test facility. It was demonstrated that the divertor mock-up withstood a heat load of 5 MW/m^2, 30 s for a repetition of 1,000 cycles. The sputtering yield was also measured to estimate the life time of armor materials.

7.1 High Heat Flux Experiments of Large Scale Divertor Mock-up

A large ion source was developed to perform the high heat flux experiments of the large scale divertor mock-ups. A sufficient irradiation area for the large scale mock-ups was obtained in the Particle Beam Engineering Facility (PBEF) using the ion source. The ion source consists of a plasma generator and a positive ion accelerator. The dimension of the semi-cylindrical plasma generator is 34 cm in inner diameter and 129 cm in length. The positive ion accelerator, which consists of three grids, can accelerate hydrogen ions up to 50 keV. Each grid is actively cooled to produce an intense ion beam continuously. The source produces ion beams with a heating area of 900 mm long x 80 mm wide with heat fluxes of 4 ~ 7 MW/m^2.

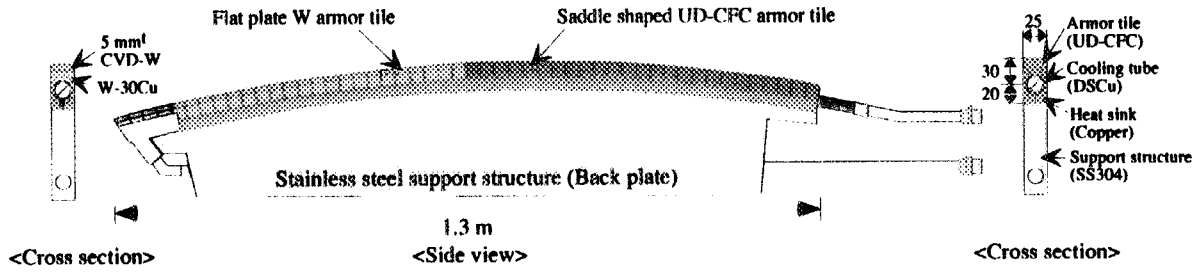

Fig. IV.7.1-1 Large scale divertor mock-up

Based on the ITER divertor design, a large scale divertor mock-up consisting of 8 modules was developed. Figure IV.7.1-1 shows a schematic of one module. The dimension of the module is 1300 mm long x 30 mm wide x 240 mm high (max.). The upper half of the mock-up is covered with flat plate tungsten armor tiles, which are made of 5 mm thick chemical vapor deposited-tungsten (CVD-W) layer with W-Cu (30wt% Cu infiltrated W) heat sink. JAERI has proposed CVD-W [7.1-1,2], because disruption erosion of CVD-W is about 50 % lower than other tungsten materials such as sintered tungsten [7.1-3]. The dimension of CVD-W armor tile is 25 mm long x 30 mm wide x 5 mm thick. These CVD-W armor tiles were directly coated onto the W-Cu heat sink, since the thermal expansion of W-Cu is close to that of CVD-W. The lower half of the mock-up is covered with unidirectional CFCs. The UD-CFC armor was brazed directly onto the pure copper heat sink with Ti-Cu-Ag braze material. The heat sink was also directly brazed onto the stainless steel back plate.

In the thermal cycling experiment, a surface heat flux of 5 MW/m^2 was cyclically loaded on the mock-up to evaluate the thermal fatigue behavior as shown in Fig. IV.7.1-2. The pulse duration was selected 30 s, which is long enough to reach thermal steady state of the mock-up. The coolant temperature, the pressure, and the flow velocity were 25 ℃, 2 MPa and 10 m/s, respectively. The large scale mock-up successfully withstood a heat load of 5 MW/m^2, 30 s for 1,000 thermal cycles without failure.

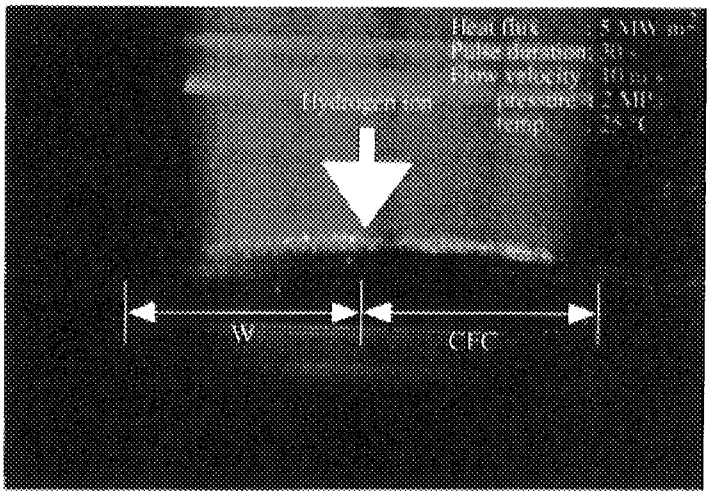

Fig. IV.7.1-2 Large scale divertor mock-up under 5 MW/m^2 for 30 s

References

[7.1-1] Nakamura, K., Akiba, M., Dairaku, et al., "Disruption erosions of various kinds of tungsten at low and high temperature", Proc. International Workshop on Interaction Effects in Quantum Engineering System (IEQES-96), Mito, Japan, Aug. 21-23, (1996).

[7.1-2] Tanabe T., Philipps V., Nakamura K., et al., J. Nuclear. Materials, 241-243, pp. 1164-1168 (1997).
[7.1-3] Akiba M., Madarame H., J. Nuclear Materials, 212-215, pp. 90-96 (1994).

7.2 Erosion of Plasma Facing Materials

Erosion of plasma facing materials(PFMs) is one of the key issues for the prediction of the lifetime of PFCs, and sputtering is one of the most dominant erosion processes of PFMs.

Sputtering yields of UD, 2D and 3D CFCs, which are the reference or alternative materials of the divertor armor tiles in ITER, were measured with the Super Low Energy particle Irradiation System (SLEIS). In addition, sputtering yields of 10 % SiC or 5 % B_4C doped UD CFCs were also measured because doping of SiC or B_4C was proposed to reduce the chemical sputtering of carbon materials. Typical experimental conditions were as follows; a particle flux of 1~2 x 10^{20} ion/m^2/s, an incoming D_3^+ energy of 200 eV, which corresponds to a particle energy of 67 eV, an incident particle angle of 30°~60° and temperature range from 200 ℃ to 700 ℃. The measured sputtering yields of these CFCs are shown in Fig. 7.2-1. It was found that a peak of the sputtering yields of CFCs in this energy range is broad, which is consistent with previous works [7.2-1]. The sputtering yields of doped CFCs were ~20% smaller than those of non-doped CFCs.

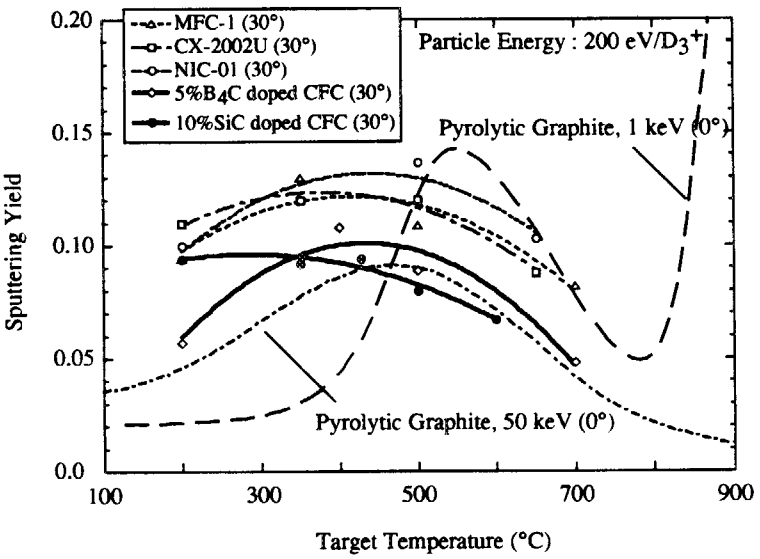

Fig. IV.7.2-1 Temperature dependence of sputtering yields for several CFCs with D_3^+ ions of 200 eV at 30 °C

Self-sputtering yields of CVD-W and powder sintered tungsten (P-W) , which are also the reference materials of the divertor armor tiles in ITER, were measured in the self-sputtering test facility (SSP), it was confirmed that the present results agree well with the results calculated by TRIM code [7.2-2].

References

[7.2-1] Roth J., J. Nuclear Materials, 87, pp. 145-147 (1987).
[7.2-2] Moller W., Eckstein W., Nucl. Instr. and Meth. B2 pp. 814, (1984).

8 Reactor Structure Development

The major factors driving the development here in this area are the manufacturing technology of large components and remote assembly/disassembly technology. In this fiscal year, R&D efforts have been focused on the development of a full-scale vacuum vessel sector, a full-scale manipulator for blanket module handling, a divertor transportation system and radiation-hard components.

8.1 Reactor Structure Development

In ITER, the vacuum vessel is designed to be a large torus structure made of 316L+N stainless steel with a D-shaped cross section approximately 9 m wide and 15 m high. The vacuum vessel is divided toroidally into 20 sectors which are joined by field welding at the central plane of the ports during initial assembly [8.1-1]. Its large size, tight manufacturing tolerances required for assembly, large thermal and mechanical loads necessitate the fabrication and testing of a prototype vacuum vessel to demonstrate the fabrication technologies of the double-walled ITER Vacuum vessel prior to ITER construction. For this purpose, the fabrication of a full-scaled sector was initiated in 1995 as one of the Large Seven ITER R&D Projects [8.1-2]. The full-scale sector model corresponds to an 18° toroidal sector. The model is composed of two 9° sectors, Sector-A and B, which are spliced at the port center according to the current ITER segmentation. In order to satisfy tight manufacturing tolerances of ±5 mm and to assure the structural integrity of double-walled structure, a combination of TIG/EB welding and TIG/MIG welding were adopted for Sector-A and B, respectively. In this year, the fabrication of both sectors was continued on schedule and completed at the end of September 1997, as shown in Fig. IV.8.1-1. Although the different fabrication procedures and welding techniques were employed for the fabrication, both sectors have satisfied the dimensional accuracy of within ±3 mm to the total height, total width and total wall thickness. Through the fabrication of full-scale models, the feasibility of fabrication procedures adopted has been successfully demonstrated and sufficient technical data base on fabrication has been accumulated to finalize the current ITER design. After the completion of fabrication, both sectors were installed in the test stand and final assembly test was begun in November 1997. This assembly test corresponds to the first demonstration of initial assembly using automatic narrow gap TIG welding for the field joints between sectors. The assembly test is continuing to complete 18° sector in June 1998.

References

[8.1-1] Koizumi K. et al., "Design and Development of the ITER Vacuum Vessel", 4th International Symposium on Fusion Nuclear Technology, Apr. 6, Tokyo (1997).

[8.1-2] Koizumi K. et al., "Development of Double-walled Vacuum Vessel for ITER", 16th IAEA Fusion Energy Conference, Montreal, IAEA-CN-64/FP-8 (1996).

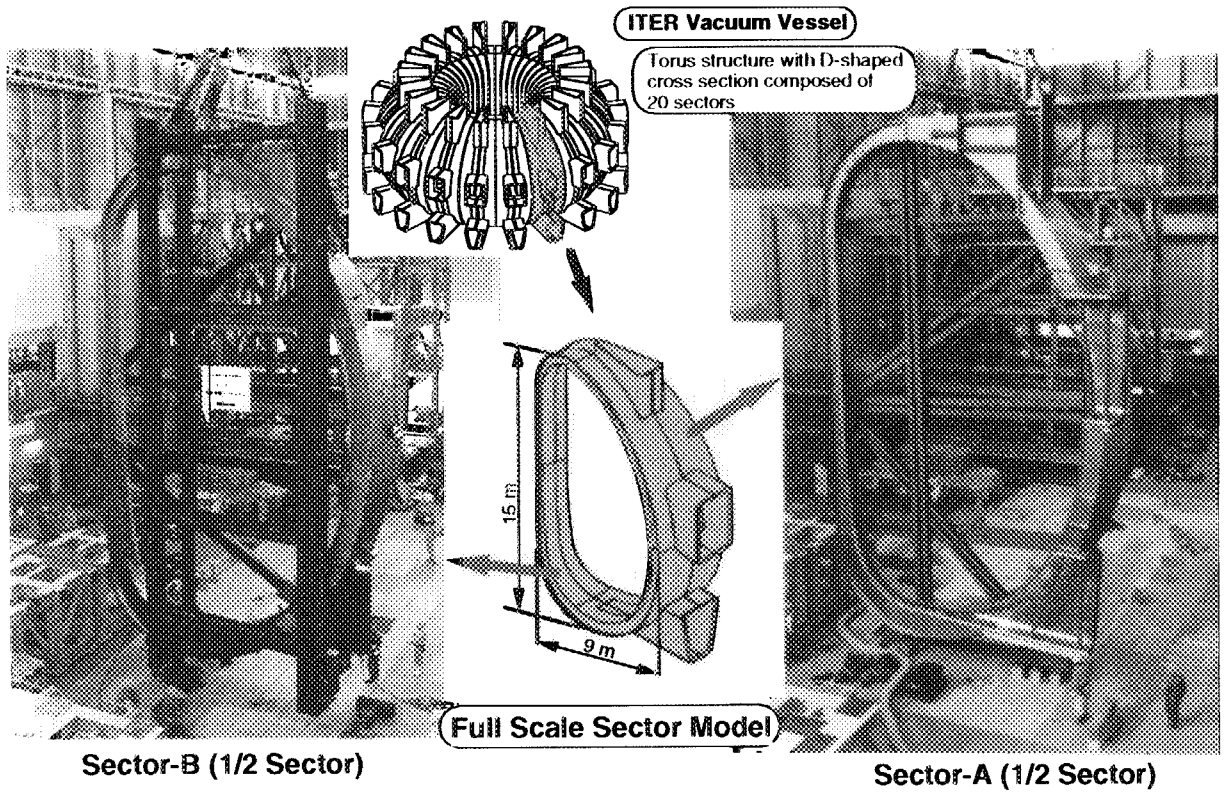

Fig. IV.8.1-1 Full-scale sector model of ITER vacuum vessel completed in September 1997 with dimensional accuracy of ± 3 mm

8.2 Remote Maintenance Development

Since the reactor core of the ITER will be highly activated due to D-T operation, the assembly and maintenance of the tokamak components will have to be conducted by remote handling technology. In particular, the blanket and divertor are categorized into the schedule maintenance component. Thus, development of blanket and divertor remote maintenance is essential and full-scale mock-up tests are continued under the ITER Large R&D Project to demonstrate their maintainability.

8.2.1 Blanket Module Maintenance System

Blanket module replacement requires advanced technologies that include heavy component handling of more than 4 ton and welding/cutting in restricted space under intense gamma radiation and high temperature conditions. The replacement of shield blankets with breeding blankets is an important milestone in the ITER operation for the transition from the Basic Performance Phase (BPP) to the Enhanced Performance Phase (EPP). The required installation accuracy is specified to be 2 mm as a step gap between modules. A rail-mounted vehicle maintenance system was developed to meet these requirements. In this year, the full-scale rail mounted vehicle system, which includes rail transporter, vehicle manipulator/ end-effector, and rail support structures have been assembled as shown in Fig. IV.8.2-1, and performance test was initiated [8.2-1]. The

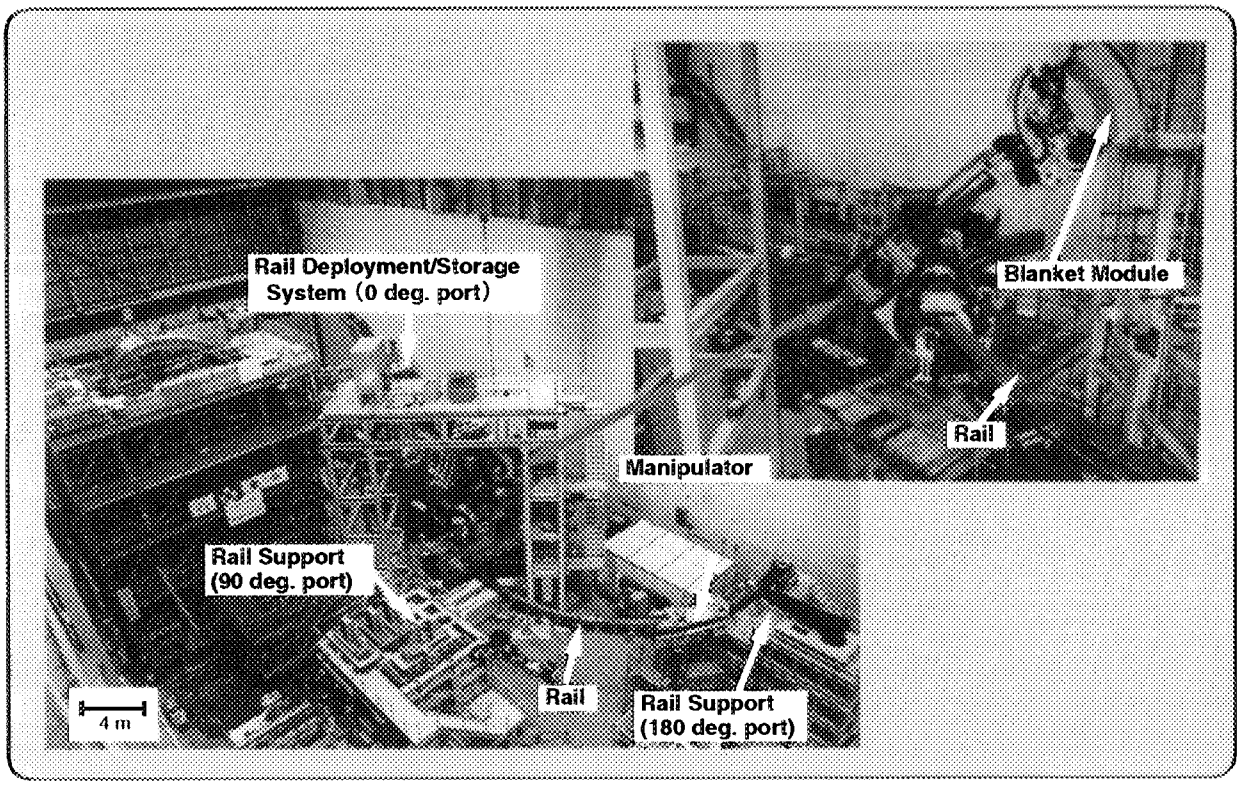

Fig. IV.8.2-1 Full-scale vehicle manipulator system for blanket maintenance (Payload: ~ 4 ton, Arm length: ~ 6 m)

performance tests on rail deployment/storage, mechanical characteristics of vehicle manipulator/end-effector, and blanket module handling are continued for the demonstration of remote replacement of 4-ton blanket module with a handling accuracy of ±2 mm.

8.2.2 Divertor Cassette Remote Maintenance System

The divertor of ITER is classified into scheduled maintenance component because of the exposure of high heat and particle flux. It is divided into 60 cassettes in the toroidal direction and its weight is about 25 ton. The remote maintenance system for divertor is required to install the cassette with a tolerance of ±2 mm and to replace all the cassettes in six months period and replace one cassette in an eight weeks period. To meet these requirements, a skid-type maintenance system, as shown in Fig. IV.8.2-2, was developed. In this fiscal year, the fabrication of full-scale prototype skids, which are named central cassette carrier (CCC) and second cassette carrier (SCC), have been completed [8.2-2]. After the performance test, the CCC was shipped to Europe in January 1998 for the integrated cassette replacement test at the Divertor Test Platform (DTP). For the transfer cask system, the double-seal door for preventing dispersion of activated dust during maintenance and transportation, has been fabricated and assembled to the full-scale mock-up of transfer cask. The performance test of docking and open/close operation showed the sufficient position alignment and leak tightness capability required for the ITER divertor maintenance.

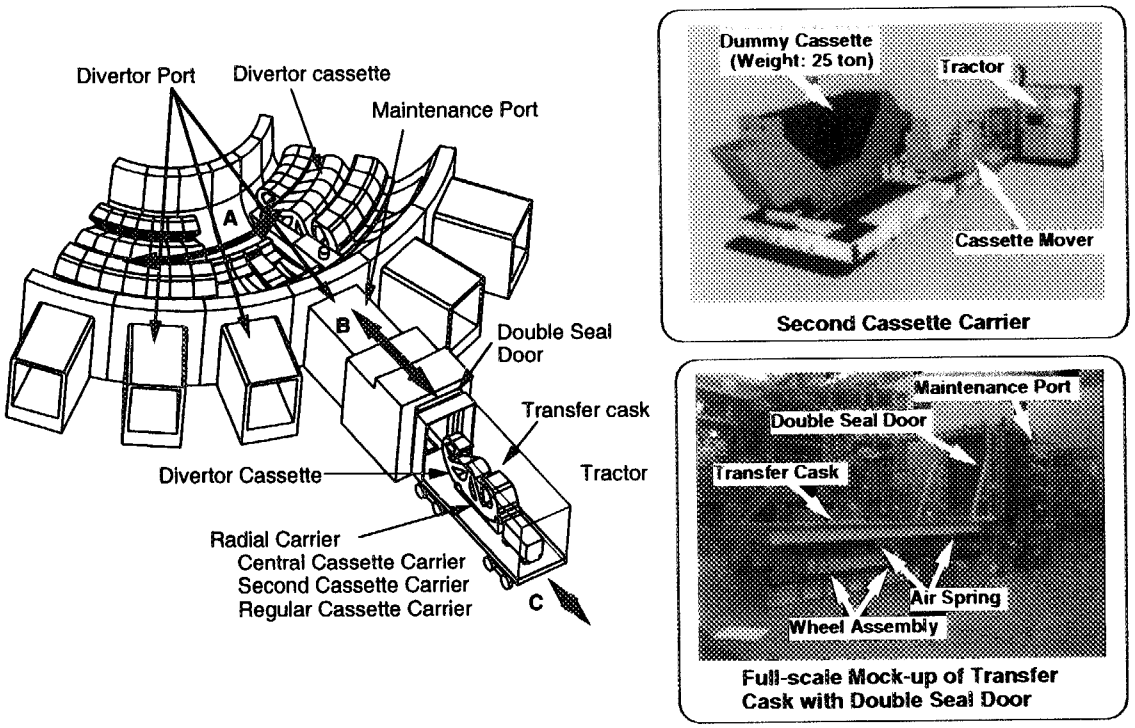

Fig. IV.8.2-2 Concept of remote maintenance of divertor cassette

8.2.3 Development of Radiation Hardened Components for the ITER Remote Handling System

Gamma irradiation tests on a number of critical components for the ITER remote handling system have been extensively conducted under ITER in-vessel radiation conditions. As a result, testing of more than 70 types of critical component has been successfully completed. Typical results of the radiation-hard components are presented in Table IV.8.2-1. As a whole, many of critical components which satisfy the minimum requirement of 10 MGy or reach to the final target of 100 MGy have been successfully developed.

Table IV.8.2-1 Typical results of radiation-hard components

Component	Radiation-hardness
AC servo motor	10~50 MGy
Induction motor with polyimide insulation	> 10 MGy
Grease lubricant	50 MGy
Reduction gears	30 MGy
Position sensor	10~30 MGy
Strain gauge	10~80 MGy
Proximity sensor	> 26 MGy
Electric insulation material	100 MGy
Electric cable	10~100 MGy
CCD camera with improved camera control unit	> 3 kGy
Periscope	> 160 MGy
Reflecting mirror, lens	300 MGy
Polymer insulated electric connector	100 MGy

References

[8.2-1] Nakahira M. et al., "Remote Handling Test and Full Scale Equipment Development for ITER Blanket Maintenance", 17th Symposium on Fusion Engineering, Oct. 8, San Diego, USA (1997).

[8.2-2] Takeda N. et al., "Development of Divertor Cassette Transporters in ITER", 17th Symposium on Fusion Engineering, Oct. 8, San Diego, USA (1997).

V. INTERNATIONAL THERMONUCLEAR EXPERIMENTAL REACTOR (ITER)

1. Progress of ITER Engineering Design Activities (EDA)

The Final Design Report (FDR), which is the last technical milestone of the six year period since the start of the EDA in July 1992, has been delivered to the ITER Council in February 1998 as planned, after a review by the Technical Advisory Committee (TAC). The FDR was then reviewed by each Party and the report was evaluated as an appropriate one in the reviews of the all four Parties. Based on those review results, the FDR was formally accepted by the ITER Council in June 1998.

The Japanese Home Team has contributed to the progress of the ITER design in various fields through design tasks it shared by a number of task agreements with the Director of ITER EDA. The Home Team conducted its tasks in close collaboration with the Joint Central Team (JCT). The number of the JCT members has grown to 161 including 46 from Japan as of December 1997.

The cut-away view and the machine parameters of the ITER tokamak are shown in Fig.V.1-1 and Table V.1-1. The design has been judged as an appropriate one as the engineering design, and also a judgement has been made by all four Parties that the designed machine has a reasonable margin to accomplish the technical objectives of ITER.

The original plan was to start construction of ITER right after the end of the six year period of ITER EDA, and an informal investigation and preparation of legal and administrative sides of ITER joint construction had been made since 1995, and an informal, non-committal Exploration among the four Parties had also been started in 1996. However, due to economic difficulties of the four Parties, it became impossible to get decisions on ITER construction and the construction site. The four Parties started preparations to extend the ITER EDA Agreement for three years to conduct more designs and to conduct operation tests using models made in the six years in the technology research and development (R&D) activities under ITER EDA. It is also planned to conduct a design work of a reduced cost ITER with a little less technical objectives but expected to be more fit to the economic situation. It is expected that due to recent progresses of tokamak research, the reduced cost ITER would have a good chance to accomplish enough data for the next step, a DEMO.

The activities and current status of the ITER Technology R&D are summarized in Table V.1-3. Japan takes responsibilities in the construction of a CS model coil test facility,

development of a outer module of CS model coil , manufacturing and testing of a full-scale 1/20 sector of the double-walled vacuum vessel, and the demonstration of a full-scale vehicle-type remote maintenance system for blanket module replacement. The details of the R&D progress in FY 1997 are described in Chapter IV.

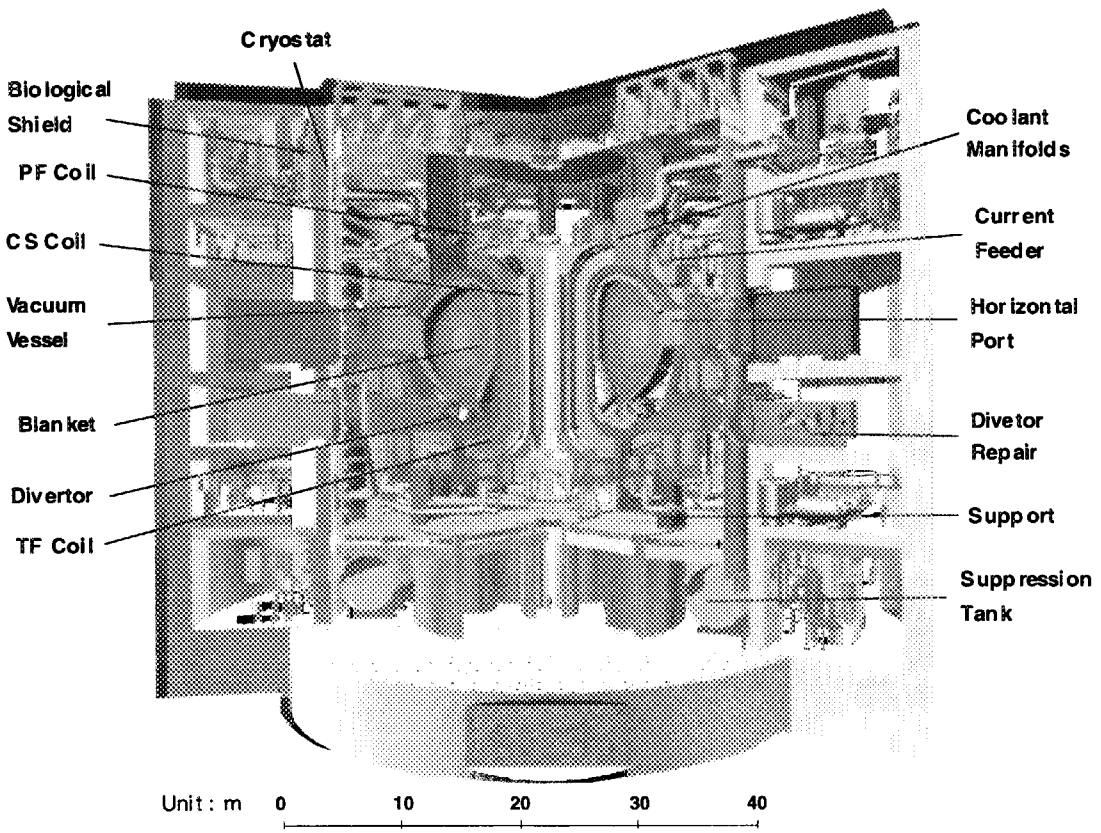

Fig. V.1-1 Cut-Away View of ITER (FDR)

Major Radius	8.14 m
Minor Radius	2.8 m
Plasma Current	21 MA
Toroidal Magnetic Field at major radius at superconductor	5.7 T
Fusion Power	1.5 GW
Burn Time (Inductive)	1000 s
Neutron Wall Loading (Nominal)	1.0 MW/m^2
Total Neutron Fluence (BPP)	0.3 MWa/m^2
Plasma Heating Power	100 MW

Table V.1-1 ITER Major Parameters (FDR)

Table V.1-2 Main features of the ITER Tokamak system (FDR)

Component	Features
Toroidal field coils (20 coils) - Superconductor - Structure	 Nb3Sn in circular Incoloy jacket in grooved radial plate Pancake wound , steel encased "wind, react and transfer" technology
Poloidal field coils (CS, PF1-PF9) - Superconductor - Structure	 CS : Nb3Sn, PF1 - PF9: NbTi Square Incoloy jacket, layer wound for CS, pancake wound for all others CS : "wind, react and transfer" technology
Vacuum Vessel - Structure - Material	 Double-wall welded ribbed shell structure Stainless Steel 316LN ($0.06 \leq N \leq 0.08$ wt%)
First Wall/Blanket (Basic Performance Phase) - Structure - Material	 Armor-faced modules on toroidal backplate Be armor Copper alloy heat sink Stainless Steel 316LN ($0.06 \leq N \leq 0.08$ wt%)
Divertor - Configuration - Structure	 Single-null 60 solid replaceable cassettes W alloy and C plasma facing components Copper alloy heat sink Stainless Steel 316LN ($0.06 \leq N \leq 0.08$ wt%)
Cryostat - Structure - Material	 Single-wall welded ribbed cylinder with flat end 36 m diameter, 30 m height Stainless Steel 304L
Heat Transfer System (water-cooled) - Heat released in the Tokamak during nominal pulsed operation	 2200 MW at ~4 MPa water pressure, 150°C
Cryoplant - Nominal average He refrigeration/liquefaction rate for magnets and Divertor cryopump (4.5K) - Nominal cooling capacity at 80 K	 100 kW/ 0.27kg/s 440 kW
Additional Heating and Current Drive - Total injected power - Candidate Additional Heating and Current Drive (H&CD) systems	 100 MW Electron Cyclotron, Ion Cyclotron, Neutral Beam from 1 MeV negative ions, Lower Hybrid
Electrical Power Supply - Pulsed power supply from grid Total active/reactive power demand - Steady-state Power Supply from grid Total active/reactive power demand	 650 MW / 500 Mvar 230 MW

Table V.1-3 Activities and Current Status of Technology R&D

Field/Subjects	Activity and Current Status
Superconducting Coil	- Completion of the winding and thermal treatment of the CS model coil (13T) This coil has an outer diameter of 3.6m and the winding of 8 layers. Thermal treatments were done at 650°C for 240 hours. These treatments successfully prevent the Incoloy pipes covering super conducting material from SAGBO cracking. The reacted conductors were confirmed to become super conducting state.
Test Facility for the Model Coil	- Development of a high performance supercritical helium circulation pump The high performance pump was developed successfully to circulate supercritical helium at 4°K in the coils. This pump circulates supercritical helium at a rate of 800 g/s, which is the highest helium flow-rate in the world.
Vacuum Vessel	- Completion of a full-scale 1/20 sector of the Vacuum Vessel Key technology to fabricate the full-scale sector has been established with an accuracy of 3 mm. The technology of connecting and assembling the sectors in the field has been established.
Remote Handling System for Blanket	- Fabrication and assembly of full-scale vehicle-type remote maintenance system The system shows the capability to handle the 4 ton blanket module with an accuracy of 2 mm.
Remote Handling System for Divertor	- Fabrication and assembly of full-scale cassette movers The movers demonstrated the repeatable performance to move and install the cassette of 25 ton with accuracy of 1 mm in the basic performance test. - Fabrication and basic performance test of a full-scale cask The accessibility of the cask to the maintenance port was confirmed. - Fabrication and basic performance test of double sealed door The sealing, opening and closing performance of the door was confirmed.
Development of Remote Welding and Cutting Tools	- Development of welding/cutting tools of in-pipe access The tools can move inside a pipe with an internal diameter of 100 mm and bends with a radius of 400 mm. The tools also demonstrate the performance of welding and cutting pipes with an internal diameter of 50 mm and 100 mm by YAG laser. - Development of an inspection tool for pipe welding parts Its accessibility in the bends and characteristic data of crack detection were acquired. - Acquisition of characteristic data of leak detection head at pipe welding part
Development of Radiation-Resistant Components for Remote Maintenance	- Development of motors, bearings, detectors, insulation wires, optical components and standard components that withstand radiation fluence of 10 - 100 MGy - Manufacturing of a full-scale radiation resistant periscope The length is 15 m and radiation resistant lens are used. The optical performance was demonstrated in the heating conditions up to 250°C.
Shield Blanket	- Optimization of HIP condition for joining Cu alloy and stainless steel - Manufacturing of a prototype blanket module integrated with first wall - Soundness of HIP joints demonstrated by thermal load tests - Acquisition of the data on the mechanical properties of HIP joints
Divertor	- Development of high heat flux components composed of carbon and copper cooling tube The components withstood the following heat load tests: 1)heat flux: 5 MW/m2, heating time: 15 sec, thermal cycle: 10,000 cycles 2)heat flux: 20 MW/m2, heating time 10 sec, thermal cycle: 1,000 cycles - Fabrication of a full-scale divertor having a length of 1.3m and a width of 30 cm - Development of high heat flux components composed of tungsten and copper cooling tube The components withstood the following heat load tests: 1)heat flux: 5 MW/m2, heating time: 30 sec, thermal cycle: 10,000 cycles
Neutral Beam Injector	- Development of a MeV ion source test facility (1 MeV, 1A) - Development of a high current negative ion source (18 A, 360 keV, D^- ion) - Generating high-density negative ion in the low pressure gas (H^-, >30 mA/cm^2, 0.2Pa) - Development of a high energy negative ion accelerator (1 MeV, 0.02A)
Electron Cyclotron Heating Facility	- Development of Gyrotron (170 GHz, 500 kW, 6.2 sec, 450 kW, 8 sec) - Development of artificial diamond windows
Development of Tritium System	- Development of 1/5 scale fuel circulation system for ITER - Development of a 1/8 scale fuel circulation system including fossil purification system - Development of a high performance air purification system using separation membrane - Demonstration of safety tritium handling for 10 years - Development of a Laser-Raman remote multi-point analyzer
Development of Fuel Injection and Pumping	- Measurement of pumping speed and compression rate of an ITER helical-groove type pump for H_2 ,D_2, He and N_2 gases - Manufacturing and performance test of the motor using ceramic coated wires
Safety Analysis and Assessment	- Acquisition of preliminary test data on the accidents of coolant ingress into Vacuum Vessel and on the accidents of Vacuum Vessel fracture - Characteristic analysis of radioactive dust and development of its removal system - Development of SAFALY to analyze interaction of plasma with in-vessel component materials - Measurement of decay heat of in-vessel component materials - Proposal of Be waste processing method

VI. FUSION REACTOR DESIGN AND SAFETY RELATED RESEARCH

In FY 1997, the DREAM(DRastically EAsy Maintenance) tokamak conceptual design activity was focused on the prototype reactor whose major mission is a demonstration of the electricity generation.

In the area of safety research, safety evaluation code development, basic experiments of LOVA (Loss Of VAcuum event) and ICE (Ingress of Coolant Event), and study of Tokamak dust removal method were carried out. A numerical simulation of LOVA has started, which aims at the quantitative evaluation of the behavior of radioactive dust inside the vacuum vessel.

1. Fusion Reactor Design

The conceptual design study on the commercial type DREAM reactor with very high aspect ratio configuration and SiC/SiC composite as the structural material has been continued for several years. The SiC/SiC composite material is suitable for fusion reactor because no electromagnetic loads are introduced because of its high resitivity and radioactivity produced is so low to enable easy maintenance. The very high aspect ratio configuration enables easier accessibility of maintenance apparatus as it makes the large space for coolant pipe arrangement in central region of tokamak. The steady state operation can be easily realized because of relatively low plasma current and high fraction of bootstrap current. We have shown the intermediate step between the experimental reactor such as ITER and the commercial reactor, which is called a prototype reactor. Because of the COE (cost of electricity) competitiveness requirement, material properties and fabrication technology needed for the commercial type DREAM reactor are inevitably assumed to be at the higher level. On the other hand, the prototype DREAM

Table VI.1-1 Major Specifications of DREAM tokamaks for both Prototype and Commercial types

Parameter	Prototype	Commercial type
Assembling scheme (number of assembling units)	Sector & cassette (14)	Sector & cassette (16)
Structural material	SiC/SiC Composite	SiC/SiC Composite
Thermal conductivity (W/m/K)	15	60
Design stress (MPa)	200	200
Coolant (Pressure, MPa)	Helium(3.0)	Helium(10.0)
Plasma major radius (m)	12	16
Plasma minor radius (m)	1.5	2
Plasma elongation	1.3	1.3
Burn time	∞	∞
Maximum toroidal field (T)	18	20
Neutron wall loading (MW/m^2)	1.2	3.0
Fusion power (GW)	1.5	5.5
Fusion gain	20	>50
Plasma current (MA)	6.0	9.2
Bootstrap current fraction	0.87	0.87
Current driving power (MW)	75	50
Thermal power (GW)	1.8	6.4
Coolant temperature (°C)	500/800	600/900
Thermal eff.(gross/net) (%)	42/40	50/47
Availability (%)	50	75

reactor is based on the material properties and the fabrication technology which are more feasible in the near future [1-1]. The major specifications of both the prototype and commercial types are listed in Table VI.1-1.

References

[1-1] Nishio S., Ueda S., Kurihara R., et al., "Prototype Tokamak Fusion Power Reactor Based on SiC/SiC Composite Material, Focusing on Easy Maintenance", 6th IAEA Technical Committee Meeting on Fusion Power Plant Design, Fusion Engineering and Design, March, 1998.

2. Fusion Safety

2.1 Study of In-vessel Abnormal Events

In LOVA experiments, the stirring behavior of the dust at the vacuum rupture was investigated by inserting the dust in the vacuum vessel. The ICE experiments in the vacuum vessel were carried out by varying temperature of the vacuum vessel wall and the injection water, with switching the valve to the vapor condensation tank open or close. These experiments were made to be a part of the ITER task including the verification of safety evaluation codes [2-1].

As one of those codes, the TRAC-BF1 code was modified to be applicable to the ICE analysis, for example, by adding an option of the changeable gravity direction [2-2]. By modeling the ICE experimental system using the modified TRAC-BF1, simulation of an ICE experiments were carried out and compared with the experimental results. Figure VI.2-1 shows the comparison of the ICE experimental results and the TRAC-BF1 calculation results on the internal pressure in the vacuum vessel [2-1]. The pressure increase rate of the calculation result is a little slower than that of the experimental result. A pretty good agreement was obtained between calculated and experimental results.

The comprehensive safety analysis code, SAFALY, which had been developed to analyze events caused by plasma transient, was updated regarding the plasma physical model in collaboration with the ITER Joint Central Team.

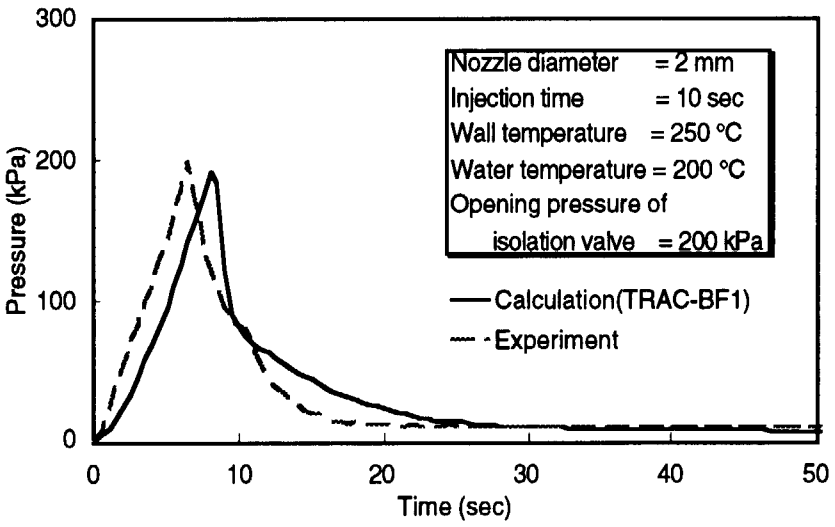

Fig. VI.2-1 Comparison of ICE experiments and TRAC-BF1 calculations on the internal pressure in the vacuum vessel

Especially, the transition model of plasma detached and attached conditions to the divertor was adopted in the code. This code was used in the ITER safety analysis concerning the plasma transition behavior [2-3].

2.2 Study of Tokamak Dust Removal Method

A conceptual design of dust removal system for ITER was performed. Activated and tritiated dust on surface of the first wall, the divertor target plate and the divertor port should be removed to keep within allowable limit. The major progresses in the study are as follows:

(1) To remove the dust efficiently without any bad influence on plasma experiments under vacuum condition, a remote handling mechanism with end effectors under vacuum condition could be applied. The access method by remote handling is based on the in-vessel maintenance tools for the blanket module maintenance developed by JAERI. Figure VI.2-2 shows a concept of the electrostatic dust removal system [2-4] using the vehicle manipulator system with changing end effector as applied to ITER.

(2) A conveyer-belt type electrostatic dust removal system operating under vacuum condition was designed to remove the main part of generated dust of ITER. It is estimated to be able to remove 44 kg of dust per month.

(3) Test of dust transport by gas puffing under vacuum condition was carried out. The results show that local gas puffing will be able to blow down the dust into the conveyer-belt under vacuum condition with only little deleterious effect on vacuum.

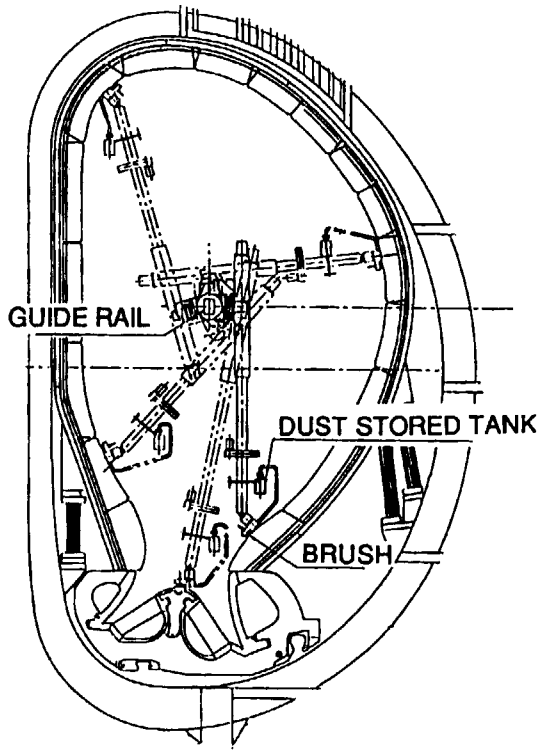

Fig. VI.2-2 Concept of dust removal system using the vehicle manipulator system

References

[2-1] Topilski L.N., et al., "Validation and Verification of ITER safety computer codes", Proceedings of the SOFE '97, San Diego (1997).

[2-2] Kurihara R., Ajima T., Kunugi T., et al., "Analysis and Experimental Results on Ingress of Coolant Event in Vacuum Vessel", to be published in Fusion Enging. Des., (1998).

[2-3] Honda T., Bartels H-W., Uckan N.A., Okazaki K., Seki Y. "Development of Safety Assessment Method for Plasma Abnormaly Events in Fusion Reactors", J. Fusion Energy, Vol.16, No.1/2, pp.175-179 (1997).

[2-4] Onozuka M., Ueda Y., Oda Y., Takahashi K., Seki Y., et al., "Development of Dust Removal System using Static Electricity for Fusion Experimental Reactors", J. Nuclear Science and Technology, Vol.34, No.11, pp.1031-1038 (1997).

VII. FUSION INTERNATIONAL COOPERATIONS

In the area of fusion research and development, Japan is recognized as one of the leading nations of the world together with Europe, USA and Russian Federation. Fusion reactor development is a long-term project which requires large resources both in man-power and in fund. It covers also broad area of science and technology. International cooperation has been recognized quite efficient in avoiding unnecessary duplication and in enhancing world's fusion program. JAERI is carrying out various international cooperation in fusion through multilateral cooperation under International Energy Agency (IEA) in Organization for Economics Cooperation and Development (OECD), International Atomic Energy Agency (IAEA), and bilateral cooperation such as Japan-US cooperation. The multilateral and bilateral cooperation carried out in JAERI are summarized in Table VII. 1-1 and VII. 1-2.

1. Multilateral Cooperations

1.1 IAEA

Under the coordination of International Fusion Research Council, IAEA holds various conferences such as the International Fusion Energy Conference and Technical Committee Meeting (TCM). IAEA also undertakes the Engineering Design Activity (EDA) in the ITER program.

1.2 IEA

Fusion Power Coordinating Committee (FPCC), which is organized under IEA, coordinates the research and development programs for member nations, selects the important areas and reviews the cooperation activities.

Cooperation under the IEA Implementing Agreement among the Three Large Tokamak Facilities pursues personal exchange, holding expert meetings and information exchange among JT-60, JET in EU, and TFTR in USA. Currently six tasks, namely "High-βp Plasma Research", "Disruption Studies", "Divertor Plate Technology", "Neutral Beam Current Drive Research", "Remote Participation in Experiments" and "impurity Content of Radiative Discharges", have been successfully continued. In connection with the Remote Participation in Experiments, Provisional Guidelines for Remote Research on the JT-60 under Co-operation among the Three Large Tokamak Facilities were approved by the Committee. The collaboration among the Three Large Tokamak Facilities has made remarkable achievements and significant contributions to improving tokamak plasma performance and to providing sufficient basis for fusion energy development including ITER.

In the Implementing Agreement on Plasma Wall Interaction in TEXTOR, a plasma-wall interaction research cooperation is carried out utilizing the facility of the TEXTOR tokamak built in

Forschungszentrum Julich, Germany.

The agreement for cooperation on fusion materials research is investigate the irradiation damages by applying neutrons from a fission rector to fusion materials. In order to develop fusion materials after a prototype reactor, a conceptual design of a 14 MeV intense neutron source (Fusion Materials and Irradiation Test Facility : IFMIF) is carried out by for parties of Japan, USA, EU and Russia.

The agreement for cooperation on environments, safety and economics is to carry out their evaluation researches which are ongoing with particular emphasis upon environments and safety.

The agreement for cooperation on fusion reactor engineering is to carry out research cooperation and information exchange in terms of neutron engineering, tritium breeding blanket and so on.

Multilateral Cooperation	
IAEA	· ITER (International Thermonuclear Experimental Reactor) /EDA Project [Japan, USA, EC, Russia] · Information Exchange on Large Tokamaks · Information Exchange on Atomic and Molecular Data · International Conferences
IEA	· Three Large Tokamak Cooperation [JT-60(J), TFTR(US), JET(EU)] · Plasma Wall Surface Interaction Program [Japan, USA, EU, Canada] · Program of Research and Development on Radiation Damage in Fusion Reactor Materials [Japan, EU, Canada, Switzerland, USA] · Joint Program for Environmental, Safety and Economic Performance of Nuclear Fusion Technology [Japan, USA, EU, Canada] · Cooperative Program on Nuclear Technology of Fusion Reactors [Japan, USA, EU, Canada]

Table VII.1-1. Multilateral cooperation in fusion international cooperation at JAERI

2. Bilateral Cooperations

On Japan-US cooperation, Coordinating Committee of Fusion Energy (CCFE) is formed to synthetically coordinate the cooperation activities under Agreement between the government of Japan and the government of the United States on cooperation in Research and Development in Energy and Related Fields. The Japan-US cooperation consists of four frameworks of exchange program, joint program, joint project and plasma physics. In particular, broad joint projects based on agreements and annexes have produced fruit results, playing a leading role in world's fusion research and development.

On Japan-EU cooperation, Agreement for Cooperation between the Government of Japan and the European Atomic Energy Community in the field of controlled thermonuclear fusion was concluded February 1988. Based on this agreement, a joint experiment is carried out in which lower hybrid (LH) wave launcher module built at JAERI are installed into the LH test facility in Cadarache Institute.

With Canada, JAERI carries out information exchange and expert meeting on tritium technology and tokamak research through Atomic Energy Canada Ltd. (AECL). With Australia, information exchange and expert meeting are carried out by holding workshops mainly in the area of diagnostics, experiment and theory for toroidal plasmas. With Russia, information exchange and expert meeting on plasma and fusion are planned under Agreement between the government of Japan and the government of Russia in Research and Development in Science and Technology.

Bilateral Cooperation	
Japan-US	· Doublet III Project · HFIR Joint Irradiation Experiment Program · Fusion Fuel Processing Technology Development Program · Cooperation in Fusion Research and Development · Data Link Program
Japan-EU	· Cooperative Activities Concerning a lower Hybrid Antenna Module
Japan-Canada	· Cooperation in the Field of Controlled Nuclear Fusion
Japan-Australia	· Cooperation on Diagnostics, Experiments and Theory
Japan-Russia	· Cooperation in Fusion Research and Development

Table VII.1-2. Bilateral cooperation in fusion international cooperation at JAERI

3. Cooperative Program on DIII-D (Doublet III) Experiment

3.1 Highlights of FY 1997 Research Results

Integration of the advanced tokamak concept, which encompasses to acquire the improved confinement in a steady-state with high normalized-beta and a large non-inductive current fraction, and the highly-evolved divertor functions was emphasized in the 1997 experimental campaign at DIII-D. Accordingly, the H-factor of 2 was sustained for 2 seconds in a reversed shear plasma with ELMs under the divertor pumping, by means of the effective modification of edge pressure gradient, mainly in terms of the shaping and edge density control . Furthermore, based on the highest performance discharge in 1996, which recorded the equivalent QDT of 0.32, the product of normalized beta and H-factor was sustained at 7 over 1 s. Intensive studies on the physics of internal transport barrier were also pushed forward.

As to the development of advanced divertor, the geometry and pumping capabilities are modified in multiple steps i.e., the baffle plates and pumps will be installed both at upper and lower divertor in 1999. In the baffled upper pump experiment performed in 1997, high density H-mode plasmas at a density of 1.5 times the Greenwald limit was obtained with the low-field side pellet injection as shown in Fig. VII.3.1-1, which made direct contribution to the ITER Physics R&D. In addition, RI-mode operation was first undertaken, and normalized beta of 4 and H-factor of 3 to 4 were simultaneously obtained at 60% of the Greenwald density.

On the other hand, studies of ECCD experiment was remarkably progressed in 1997. The effective heating and central current drive was demonstrated with 2 MW of 110 GHz EC waves.

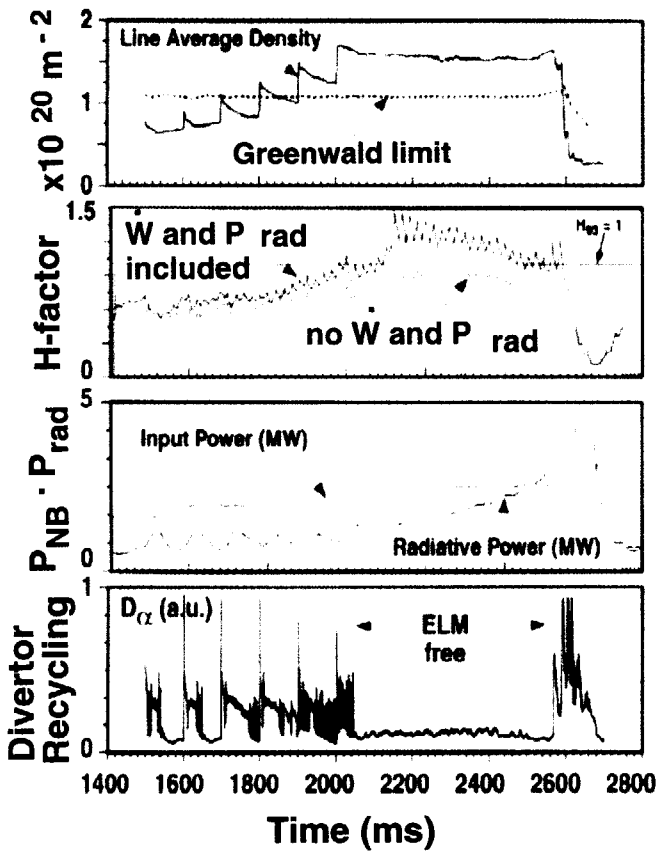

Fig. VII.3.1-1 Discharge waveforms of RI-mode

4. Collaborative Activities Concerning Fusion Technologies

4.1 Collaborative Activities on Environmental, Safety, and Economics Aspects of Fusion Power

Designated by the Government of Japan, JAERI has been participating in the IEA Implementing Agreement on a Cooperative Programme on the Environmental, Safety and Economic (ESE) Aspects of Fusion Power. This collaborative activity is carried out by Canada, EURATOM, JAERI, MINATOM and USA since 1992 and extended for another five years in 1997. JAERI is coordinating the tasks on Transient Thermofluid Modeling and Validation Tests and Safety System Study Methodology. Two new tasks on "Socio-Economics Aspects of Fusion Power" and on "Radioactive Waste from Fusion Power" are being considered for collaboration.

4.2 Collaborative Activities on Research and Development of Plasma Wall Interaction in TEXTOR

An IEA implementation for a collaboration program of research and development on plasma wall interaction in TEXTOR is expected up to December 2002. TEXTOR management is under KFA (Forschungszentrum Juelich GmbH), ERM/KMS (Ecole Royale Militaire) Brussels and FOM (Stichting voor Fundamenteel Onderzok der Materie) Nieuwegein under the TEC (Trilateral Euregio Cluster). Japan is a member of the executive committee and NIFS organizing Japanese programs as a cooperation center of Japan. JAERI has been joined the program as a Japanese technical committee member. In this fiscal year, four staff members visited TEXTOR to exchange informations on the design of dynamic ergodic divertor and on plasma edge diagnostics and discuss experimental results.

4.3 Collaborative Activities on Technology for Fusion-Fuel Processing between US-DOE and JAERI

Research and development of technology for Fusion Safety has been carried out at the Tritium Systems Test Assembly (TSTA) of Los Alamos National Laboratory since 1995.

Following the first experiment carried out in FY 1996, the second and third tritium release experiments, which were associated with a 1 Ci tritium release, were carried out to obtain data such as, 1) diffusion process of tritium in a room, 2) conversion rate of tritium gas to tritiated water, 3) tritium behavior when the ventilation system runs for tritium removal from room, and 4) adsorption of tritium on wall materials, etc. The experiments were successfully carried out on December 16, 1997 and March 3, 1998 [4.3-1].

Beta Scintillation Detector (BSD) is a newly proposed technique for measuring total tritium concentration in gases. A new BSD was installed at TSTA to explore this technique. As a result of a series of experiments using various kinds of tritium gas mixture with other hydrogen isotopes,

helium and nitrogen, the response of the BSD to tritium was found to be almost unaffected by presence of other gases. This shows that the BSD is a particularly promising technique for tritium accountancy in fusion fuel processing.

For decontamination study, measurement of adsorption isotherms of hydrogen isotopes, particularly pure tritium on Molecular Sieve 5A (MS5A), Molecular Sieve 4A (MS4A) and Activated Carbon (AC) at liquid nitrogen temperature (77 K) was carried out using the constant volume method, in which a measured amount of tritium was adsorbed on the sample stepwise and equilibrium pressure was measured as a function of adsorbed amount. Obtained result with MS5A is shown in Figure VII.4.3-1. The adsorption isotherms of pure tritium on MS5A, MS4A and AC at 77 K can be expressed with the two sites Langmuir equation, and the Langmuir coefficients were obtained as the functions of the reduced mass. These data will be utilized effectively in development of the blanket tritium recovery system and the helium glow discharge exhaust gas cleanup system.

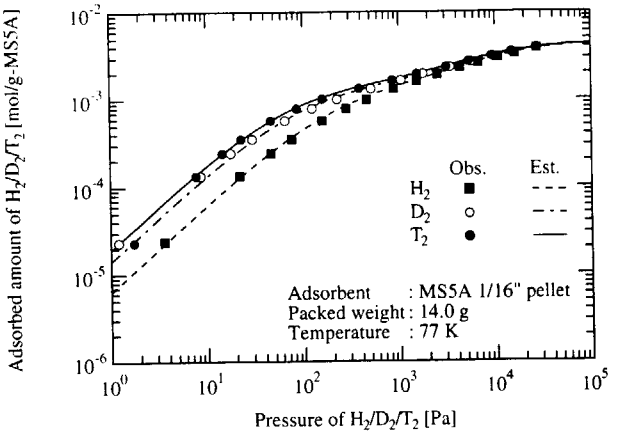

Fig. VII.4.3-1 The adsorption isotherms of H_2, D_2 and T_2 on MS5A at 77 K.

References

[4.3-1] Hayashi T., Kobayashi K., Carlson R.V., et al., 13th Topical Meeting on Technology of Fusion Energy, June 1998, Nashville USA.

4.4 Collaborative Activities on Research and Development of Plasma Facing Components between US and Japan

The JAERI-SNL collaborative activities on the divertor mock-ups have been carried out under the US-Japan Fusion Cooperation Program. In FY 1997, a critical heat flux (CHF) experiment and a thermal cycling test of a Be divertor mock-up were performed in Sandia National Laboratory (SNL). The objective of the experiment is to clarify heat transfer behavior of a cooling tube for the divertor plate over CHF region (post-CHF regime). It was found that the post-CHF regime was clearly appeared in lower flow velocity (~ 1 m/s). The Be divertor mock-up was developed at JAERI. Be armor tiles were bonded onto a Cu heat sink with a HIP method. In the thermal cycling test, a surface heat flux of 3 MW/m^2 was cyclically loaded on the mock-up to evaluate the thermal fatigue behavior. The mock-up successfully withstood a heat load of 3 MW/m^2, 10 s for 1,000 thermal cycles without failure.

4.5 Collaboration between JAERI and CEA-Cadarache for Lower-Hybrid

Antenna Modules

Cooperative activities have been started to obtain a detail outgassing database during a high power and a long pulse RF operation for a launcher design in a future LHCD system from 1993. RF power test was performed at CEA-Cadarache RF Test Facility which allowed high power injection up to 500 kW, under quasi-continuous operation at a frequency of 3.7 GHz. In the first step, the outgassing rate of Dispersion Strengthened Copper waveguide module during RF injection was identified. In the second step of the collaboration from 1995, outgassing rate with mouth modules made of Carbon Fiber Composite (CFC) has been measured to develop heat resistant LH antenna front and the aimed data base was obtained. It was concluded that no external pumping for the antenna is necessary with the appropriate antenna design.

4.6 Collaborative Activities on Research and Development of Plasma Facing Components between EU and Japan

Under the Japan-EURATOM Fusion Agreement, two collaborative activities have been performed. One is the JAERI-CEA collaboration and the other is the JAERI-KFA collaboration. The critical heat flux (CHF) benchmark experiment was performed at CEA. To investigate the influence of the heat flux profile upon CHF, the experiments were carried out with a flat profile and a peak profile which simulates the real heat flux on the ITER divertor plate. It was turned out that the incident CHF with the ITER modified profile is 20 ~ 40 % higher than that with flat profile.

High heat flux experiments on mock-ups developed by KFA were performed at JAERI. In the high heat flux tests of CFC/Cu and B_4C/TZM mock-ups, the surface heat flux was stepwise increased to evaluate critical performance. Both mock-ups successfully withstood up to heat loads of 12 ~ 15 MW/m^2, 15 s.

4.7 Collaborative Activities on Technology for Tritium Transfer between AECL and JAERI

The objectives of cooperation in the field of controlled nuclear fusion between JAERI and Atomic Energy of Canada Limited (AECL) are to conduct information and personnel exchanges to develop fusion technologies on tritium handling, breeding blanket, and plasma physics. In 1997, a technical meeting was held at the Tritium Process Laboratory, JAERI to discuss the technical items for loading and shipping of tritium from Chalk River Laboratory of AECL. Procedures for accountancy and calibration were discussed and general information was exchanged for mutual understanding of this program. The third shipment of tritium is planned in 1998 based on the contract for purchasing tritium for research and development of tritium handling technology for fusion, which was renewed in March 1998.

5. Other Activities

The mutual information and personal exchanges between JAERI and fusion research institutes in Asian area are rapidly increasing during this several years under significant development on fusion research in this area, especially in China and Korea. These exchanges are performed under STA scientist exchange program (in 1997, three scientists from China for one year and three JAERI scientists to China for two weeks), the scientist invitation program (in 1997, on senior scientist from China for one month), STA and JAERI fellowships and so on. A new framework to make more fruitful cooperation between JAERI and these countries on fusion research filed should be prepared under Science and Technology Cooperation Agreement between Japan and these countries.

Appendix A 1 Publication List (April 1997-March 1998)

A.1.1 List of JAERI reports

1) Ajima T., Kurihara R., Seki Y., et al., JAERI-Data/Code 97-034, "Improvement of TRAC-BF1 Code to Analyze the Ingress of Coolant Event (ICE)", (1997) (in Japanese).

2) Aoki I., Seki Y., Sasaki M., JAERI-Data/Code 97-042, "Development of Dynamic Simulation Code for Fuel Cycle of Fusion Reactor (1. Single Pulse Operation Simulation)", 1997) (in Japanese).

3) Aoyagi T., Sato M., Sakata S., et al., "Development of New CICU", JAERI Tech 97-073 (1997).

4) Furuya K., Sato S., Hatano T., et al., JAERI-Tech 97-022, "Design of ITER Shielding Blanket", (1997).

5) HatanoT., Sato S., Fukaya K., et al., JAERI-Research 97-017, "High Heat Flux Testing of HIP bonded DS-Cu/316SS First Wall Panel for Fusion Experimental Reactors", (1997).

6) Hayashi T., Miya N., Kikuchi M., et al., JAERI-Research 97-007, "The Design Study of the JT-60U Device (No. 9) - Fuel Handing, Confinement and Clean Up System for JT-60U", (1997) (in Japanese).

7) Hiranai S., Yokokura K., Moriyama S., et al., "development of Temperature Measuring System of ICRF Antenna for JT-60", JAERI-Tech 98-006 (1998).

8) Ikeda Y., Ushikusa K., Seki M., et al., "ECR Discharge Cleaning on JT-60U", JAERI-Research 97-075 (1997).

9) Ishii Y., "Ideal MHD Stability in Negative Shear Plasma", JAERI-Research 97-047, Review of JT-60U Experimental Results from February to November,1996 , p.14-17.

10) Kanari M, Hatano T., Sato S., et al., JAERI-Research 98-004, "Characterization of HIP Bonded DS-Cu/SS316L Joints for Fusion Experimental Reactors", (1998).

11) Kurihara K. and JT-60 Control Group, "Improvement of Equilibrium Control Algorithm", in "Review of JT-60U Experimental Results (Feb. to Nov.," JAERI-Research 97-047(1997) pp.129-132.

12) Kurihara K., Kawamata Y., Akiba K., et al., " Development of the Real-time Plasma Shape Visualization System in JT-60," JAERI-Research 97-055 (1997) (in Japanese).

13) Kurihara K., "A Study on Current Density Distribution Reproduction by Bounded-Eigenfunction Expansion for a Tokamak Plasma," JAERI-Research 97-084 (1997) (in Japanese).

14) Kurihara K. and Kawamata Y., "Development of a Precise Long-time Digital Integrator for Magnetic Measurements in a Tokamak," JAERI-Research 97-072 (1997) (in Japanese).

15) Maki K., Sato S., Kawasaki H., JAERI-DATA/Code 97-002, "Development of Displacement Cross Section Set for Evaluating Radiation Damage by Neutron Irradiation in Materials Used for Fusion Reactors", (1997).

16) Matsukawa M., Aoyagi T. and Miura Y. M., "General Tokamak Circuit Simulation Program GTCSP," JAERI-DATA/Code 97-017 (1997) (in Japanese).

17) Miura H., Sato S., Enoeda M., et al., JAERI-Tech 97-051, "Design of Test Blanket System for ITER Module Testing", (1997).

18) Miura Y. M., Matsukawa M., Miyachi K., et al., "Development of a Current-type PWM Converter with High Power Factor - I," JAERI-Tech 98-001 (1998) (in Japanese).

19) Miya N., Kikuchi M., Ushigusa K., et al., "The Design Study of the JT-60SU Device (No. 8) -Nuclear Shielding and Safety design-", JAERI-Research 98-012 (1998).

20) Nagaya S., Onizawa M., Kawai I., et al., "Assessment and counterplan for JT-60U spectroscopic system", JAERI-Tech 97-062(1997).

21) Neudatchin S.V., Takizuka T., Shirai H., et al., "Analysis of Space-time Structure of Internal Tansport Barrier in JT-60U", JAERI-Research 97-052 (1997) .

22) Oda M., Kurasawa T., Kuroda T., et al., JAERI-Tech. 97-013, "Development of HIP Bonding Procedure and Mechanical Properties of HIP Bonded Joints for Reduced Activation Ferritic Steel F-82H", (1997).

23) Ohmori S. and Kusaka M., "Degradation in Dielectric Strength of FRP Insulators and Its Measures in a Static Scherbius System Speed Controller of the JT-60 Motor Generator," JAERI-Tech 97-025 (1997) (in Japanese).

24) Oohara H. and Kuriyama M., "Evaluation of re-ionization loss in the drift duct of the negative ion based NBI for JT-60", Japan Atomic Energy Research Institute Report, JAERI-Tech 97-031(1997)

25) Polevoi A., Shirai H., Takizuka T., "Benchmarking of the NBI Block in ASTRA CodeVersus the OFMC Calculation", JAERI-Data/Code 97-014 (1997).

26) Sato M., Isei N., Isayama A., et al., "Position determination of electron temperature measurement with electron cycrotron radiation (scaling for radial displacement)", JAERI-Research 97-011(1997).

27) Sato M., Isei N., Isayama A., et al., "Determination of Position on the Measurement of Electron Temperature Radial Profile fom Electron Cyclotron Emission (Scaling of the Apparent Radial Shift)", JAERI-Research 97-011 (1997) (In Japanese).

28) Sato S., Hatano T., Furuya K., et al., JAERI-Research 97-092, "DSCu/SUS Joining Techniques Development and Testing", (1997).

29) Shinohara K., "Study of Density Fluctuation in L-mode and H-mode Plasmas on JFT-2M by Microwave Reflectometer", JAERI-Research 97-045 (1997).

30) Shinohara K., "Study of Density Fluctuation in L-Mode and H-Mode Plasmas on JFT-2M by Microwave Reflectometer", K., JAERI-Research 97-045 (1997).

31) Tabara T., Yamano N., Seki Y., et al., JAERI-Tech 97-054 (in Japanese), "Radioactive Waste Management and Disposal Scenario for Fusion Power Reactors", (1997).

32) Tchernychev F.V., Afanassiev V.I., Kusama Y., et al., "Experimental Scaling for Fast Ion Temperature during Ion Cyclotron Heating in JT-60U", Report to the Review of JT-60U Experimental Results 1997.

33) The JT-60 Team, "Review of JT-60U Experimental Results from February to November, 1996", JAERI-Research 97-047.

34) Tokuda S., Watanabe T., "MARG2D Code (1) : Eigenvalue Problem for Two Dimensional Newcomb Equation ", JAERI-Data/Code 97-040 (1997).

35) Tokuda S.,Watanebe T., "Theory of Asymptotic Matching for Resistive Magnetohydrodynamic Stability in a Negative Magnetic Shear Configuration(II) - Global Solution of the Newcomb Equation - ", JAERI-Research 97-034.

36) Totsuka T. and Kurihara K., "Development of a New Database System for JT-60 Experiments Utilizing UNIX Workstations," JAERI-Tech 97-026 (1997) (in Japanese).

37) Tsukahara Y., Neyatani Y., Sunaoshi H., et al., "Report of the transformation measurement of O-ring for large measurement window of the vacuum vessel", JAERI-Tech 98-004(1997).

38) Watanabe K., Higa O., Ohara Y., et al, JAERI-TECH 97-34, "Design of ITER NBI Power Supply System" ,(1997).

39) Yamagiwa M., Nemoto T., Hirose A., Elia M., "Parallelization of Kinetic Ballooning Shooting Code KBSHOOT", JAERI-Data/Code 97-032.

40) Yokokura K., Moriyama S., Terakado M., "Development of Diagnostic System for JT-60 ICRF Heating system", JAERI-Tech 97-044 (1997).

A.1.2 List of papers published in journals

1) Afanassiev V.I., Kusama Y., Nemoto M., et al., "Neutral Particle Analysis in MeV-Energy Range and Relative Role of He+ and C5+ Ions in Fast Proton Neutralization in ICRF and Combined ICRF/NBI Heated JT-60U Plasmas", Plasma Phys. Control. Fusion 39, 1509 (1997).

2) Akiba M., Araki M., Suzuki S., et al., "ITER design report", J. Plasma Fusion Research, 73 supplement (1997).

3) Akiba M., et al., Research committee on plasma surface interactions under burning plasma state, "Plasma surface interactions under burning plasma state in a fusion reactor", J. Atomic Energy Society of Japan, 39, 854-862 (1997).

4) Ando T., et al., "Development of Nb3Al coil for the ITER TF magnet", Fusion Technology 1996, 1083-1086 (1997).

5) Ando T., et al., "Dependence of Temperature and Magnetic Field on Critical Current Density in Multifilamentary Nb3Al Strands made with the Jerry Roll Process", IEEE Transactions on Applied Superconductivity, 7, 1568-1571 (1997).

6) Arita M., Hayashi T., Okuno K., et al , "Permeation behavior of deuterium implanted into Ti-6Al-4V alloy", Journal of Nuclear Materials, 248, 60-63 (1997).

7) Arita T., Yamanishi T., Okuno K., et al., "Experimental Study for Separation Characteristics of Cryogenic-Wall Thermal Diffusion Column with H-D and H-T Systems", to be published in Fusion Eng. and Design (1997).

8) Asakura N., Shimizu K., Shirai H., et al., "Degradation of Energy and Particle Confinement in High-density ELMy H-mode Plasmas on JT-60U", Plasma Phys. Control. Fusion 39 (1997) 1295-1314.

9) Asakura N., Shimizu K., Shirai H., et al.,"Degradation of energy and particle confinement in high density ELMy H-mode plasmas on JT-60U", Plasma Phys. Control. Fusion 39, 1295 (1997).

10) Baba A., Nishikawa M., Kawamura Y., et al., "Isotope Exchange Capacity of Solid Breeder Materials", Journal of Nuclear Materials, 248, 106 (1997).

11) Connor J.W., (Shirai H., Takizuka T.) et al., "Validation of 1-D Transport and Sawtooth Models for ITER", Fusion Energy 1996 (proc. 16th Int. Conf., Montreal, 1996), Vol. 2 (IAEA, Vienna, 1997) 935-944.

12) Fujita T. and the JT-60 Team,"High-performance experiments towards steady-state operation in JT-60U", Plasma Phys. Control. Fusion 39, B75 (1997).

13) Fujita T., Ide S., Kimura H., et al., "Enhanced Core Confinement in JT-60U Reversed shear Discharges", Nucl. Fusion Supplement (Proc. of the 16th Int. Conf. on Fusion Energy, Montreal, 1996) 1, 227 (IAEA, Vienna, 1997).

14) Fujita T., Hatae T., Oikawa T., et al., "High performance reversed shear plasmas with a large radius transport barrier in JT-60U", Nucl. Fusion 38, 208 (1998).

15) Fujita T., Hatae T., Oikawa T., et al., "High Performance Reversed Shear Plasmas with a Large Radius Transport Barrier in JT-60U", Nucl. Fusion 38, 207 (1998).

16) Fujita T., Ide S., Kimura H., JT-60 Team, "Enhanced core confinement in JT-60U reversed shear discharges", Proc. 16th IAEA Fusion Energy Conference Vol. 1(1997) p227.

17) Fujita T. and JT-60 Team, "High-performance experiments towards steady-state operation in JT-60U", Plasma Phys. Control. Fusion 39, B75 (1997).

18) Fujita T., Ide S., Shirai H., et al., "Internal Transport Barrier for Electrons in JT-60U Reversed Shear Discharges", Phys. Rev. Lett., 78, 2377 (1997).

19) Fujita T., Ide S., Kimura H., and JT-60 Team, "Enhanced core confinement in JT-60U reversed shear discharges", Fusion Energy (IAEA, 1997) Vol. 1 p. 227.

20) Fujita T. and JT-60 Team, "High-performance experiments towards steady-state operation in JT-60U", Plasma Phys. Control. Fusion 39 (1997) p.75.

21) Fujiwara Y, Miyamoto N., Okumura Y., et al., "Temperature control of plasma grid for continuous operation in cesium-seeded volume negative ion source", Rev. Sci. Instrum. 69(2), 1173-1175 (1997).

22) Fukuda T., Sato M., Takizuka T., and JT-60 Team, "H-mode Transition and Power Threshold in JT-60U", Fusion Energy (IAEA, 1997) Vol. 1, p. 857.

23) Fukuda T., Sato M., Takizuka T., et al., "H Mode Transition and Power Threshold in JT-60U", Fusion Energy 1996 (proc. 16th Int. Conf., Montreal, 1996), Vol. 1 (IAEA, Vienna, 1997) 857-866.

24) Fukuda T., Sato M., Takizuka T., JT-60 Team, "H-mode Transition and Power Threshold in JT-60U", Proc. 16th IAEA Fusion Energy Conference Vol. 1 (1997) 857.

25) Fukuda T., Takizuka T., Tsuchiya K., et al., "H Mode Transition Threshold Power Scaling and Its Relation to the Edge Neutrals in JT-60U", Nucl. Fusion 37 (1997) 1199-1213.

26) Fukuda T., Takizuka T., Tsuchiya, K., et al., "H-mode Transition Power Threshold and its Relation to the Edge Neutrals in JT-60U", Nucl. Fusion 37, 1199 (1997).

27) Furuya K., Takatsu H., Hatano T., et al., "Trial Fabrication of Small-Scaled First Wall Panels with Embedded Cooling Channels Made of Reduced Activation Ferritic Steel F82H by Hot Isostatic Pressing Method", to be published in J. Nucl. Materi., Elservier, (1998).

28) Hamamatsu K., Chang C.S, Takizuka T., et al., "Removal of Helium Ash and Impurities by Using ICRH Driven Ripple Transport", Fusion Energy 1996 (proc. 16th Int. Conf., Montreal, 1996), Vol. 2 (IAEA, Vienna, 1997) 683-691.

29) Hamamatsu K., Chang C.S., Takizuka T., et al., "Numerical Analysis of Helium Ash Removal by Using ICRF-driven Ripple Transport", Plasma Phys. Control. Fusion 40 (1998) 225-270.

30) Hamamatsu K., Matsuda T., Nishitani T., et al., "Remote Laboratory in Fusion Experiments, Present Status and Prospects", J. Plasma and Fusion Research 73 (1997) 369-394 (in Japanese).

31) Hanada M., Fujiwara Y., Miyamoto K., et al., "Grid power loading in multi-aperture multi-stage negative ion accelerator", Rev. Sci. Instrum. 69 (2), 947-949 (1997).

32) Hara S., Abe T., Takatsu H., "Hydrogen Absorption and Mechanical Strength Properties of Low Activation Ferritic Steel F82H", to be published in J. Nucl. Materi., Elservier, (1998).

33) Hatano T., Sato S., Gotoh M., et al., "Fracture Strengths of HIPed DS-Cu/SS Joints for ITER Shielding Blanket/First Wall", to be published in J. Nucl. Mater., Elservier, (1998).

34) Hatano T., Sato S., Hashimoto T., et al., "Low Cycle Fatigue Lifetime of HIP Bonded Bi-Metallic First Wall Panels of Fusion Reactors under Cycling Mechanical Loads", to be published in J. Nucl. Sci. Tecnol., (1998).

35) Hatano T., Sato S., Sato K., et al., "High Heat Flux Testing of HIP Bonded DS-Cu/316SS First Wall Panel for Fusion Experimental Reactors", Fusion Technol., 30, 752 (1997).

36) Hatano T., Suzuki T., Yokoyama K., et al., "High Heat Flux Testing of a HIP Bonded First Wall Panel with Built-in Circular Cooling Tubes", to be published in Fusion Eng. Design, Elsevier, (1998).

37) Hayashi N., Takizuka T., Hatayama A., et al., "Analysis of Biasing Induced Divertor Asymmetry Using a Five-Point Model", J. Phys. Soc. Japan 66 (1997) 3815-3825.

38) Hayashi T., "Tritium Behavior in Confinement Room", Journal of Plasma and Fusion Research, 73, 1341 (1997) (in Japanese).

39) Hayashi T., Okuno K., Ishida T., et al., "Effective Tritium Processing Using Polyimide Films", to be published in Fusion Eng. and Design (1997).

40) Hirose A., Yamagiwa M., "Effects of radical gradient of the Shafranov shift on the Kinetic balooning and drift-type modes in high-performance tokamcs", Can.J.Phys.,75 (1997) 599-604.

41) Hiwatari R., (Takizuka T., Shirai H.) et al., "Transport Simulation of JT-60U L-mode Discharges", J. Phys. Soc. Jpn., 67 (1998) 147-157.

42) Honda T., Bartels H-W., Seki Y., et al., "Safety Analyses for Transient Behavior of Plasma and In-vessel Components during Plasma Abnormal Events in Fusion Reactor", J. Nuclear Science and Technology, 34, No.7, pp.628-638 (1997).

43) Honda T., Bartels H-W., Seki Y., et al., "Analyses of Passive Plasma Shutdown during Ex-vessel Loss of Coolant Accident in the First Wall/Shield Blanket of Fusion Reactor", J. Nuclear Science and Technology, 34, No.6, pp.538-543 (1997).

44) Honda T., Bartels H-W., Seki Y., et al., "Development of Safety Assessment Method for Plasma Abnormal Events in Fusion Reactors", J. Fusion Energy, 16, No.1/2, pp.175-179 (1997).

45) Horton W., Tajima T., Dong J.Q., Kim J-Y., and Kishimoto Y., "Ion Transport Analysis of a High-Beta Poloidal JT-60U Discharge", Plasma Phys. Control. Fusion 39, 83-104 (1997)

46) Horton W., (Kishimoto Y.), et al., "Coherent Drift-wave Structure in Toroidal Plasma", J. Plasma Phys. 56 (1996) 605-613.

47) Hosogane N., Sakurai S., Shimizu K., et al., "A compact W-shaped pumped divertor concept for JT-60U," Nucl. Fusion Supplement (Proc. of the 16th Int. Conf. on Fusion Energy, Montreal, 1996) 3, 555 (IAEA, Vienna, 1997).

48) Hosogane N., Sakurai S., Shimizu K., et al., "A Compact W-shaped Pumped Divertor Concept for JT-60U", Fusion Energy 1996 (proc. 16th Int. Conf., Montreal, 1996), Vol. 3 (IAEA, Vienna, 1997) 555-563.

49) Ide S., Naito O., Fujita T., et al., "Application of LHCD for Sustainment and Control of a Reversed Magnetic Shear Plasma in JT-60U", Nucl. Fusion Supplement (Proc. of the 16th Int. Conf. on Fusion Energy, Montreal, 1996) 3, 253 (IAEA, Vienna, 1997).

50) Inabe T., " Safety design requirement on nuclear fusion facility". Journal of Plasma and Fusion Research, vol.73-08 (1997)

51) Ishida S., Neyatani Y., Kamada Y., JT-60 Team, "High performance experiments in JT-60U high current divertor discharges", Proc. 16th IAEA Fusion Energy Conference, Vol.1(1997)315.

52) Ishida S., Fujita T., Akasaka H., et al.,"Achievement of High Fusion Performance in JT-60U Reversed Shear Discharges", Phys. Rev. Lett. 79 (1997) 3917.

53) Ishida S., Neyatani Y., Kamada Y., and JT-60 Team, "High performance experiments in JT-60U high current divertor discharges", Fusion Energy (IAEA, 1997) , Vol.1, p. 315.

54) Ishida S., Neyatani Y, Kamada Y., et al., "High Performance Experiments in JT-60U High Current Divertor Discharges", Fusion Energy (IAEA, 1997) , Vol.1, 315.

55) Ishida S., Fujita T., Akasaka H. et al., "Achievement of high fusion performance in JT-60U reversed shear discharges", Phys. Rev. Lett. 79, 3917 (1997).

56) Ishida S., Fujita T., et al., "Achivement of High Fusion Performance in JT-60U Reversed Shear Discharges", Phys. Rev. Lett. 79 (1997) 3917- 3921.

57) Ishida S., Itoh T., et al., "Achievement of High Fusion Performance in JT-60U Reversed Shear Discharges", Phys. Rev. letters.Vol.79 (20) (1997) p. 3917-3921.

58) Ishii T., Eto M., Akiba M., et al., "Study on the visual detection of defects in divertor structures for the fusion reactor by means of infrared radiometer", J. Visualization Society of Japan, 18, 272-278 (1997).

59) Ishizawa A. and Hattori Y., "Wavelet Analysis of Two-dimensional MHD Turbulence", Journal of the Physical Society of Japan, 67 (1998) 441-450.

60) Ishizawa A. and Takahashi T., "Vorticity distribution caused by three-dimensional disturbance in two-dimensional shear flow", Fluid Dynamics Research, 21 (1997) 29-46.

61) Ishizuka H., Kawasaki S., Kubo H., et al., "Emittance diagram of electron beam generated by a field-emitter array", Japanese J. of Applied Phys. 35, Part1,5471 (1996).

62) Isobe K., Hatano Y., Sugisaki M., et al., "Observation of Spatial Distribution of Tritium in Zirconium Alloy with Microautoradiography", to be published in J. Nucl. Materials (1997).

63) Isobe M., Tobita K., Nishitani T., et al., "Effect of up-down asymmetric toroidal field ripple on fast ion loss in JT-60U", Nucl. Fusion 37, 437 (1997).

64) Itami K., Hosogane N., Asakura N., et al., "Radiative divortor with improved core plasma confinement in JT-60U", Nucl. Fusion Supplement (Proc. of the 16th Int. Conf. on Fusion Energy, Montreal, 1996) 1, 385 (IAEA, Vienna, 1997).

65) Itami K., Yoshino R., Asakura N., et al., "Isolation of the improved core confinement from high reaycling and radiative boundary in reversed magnegic shear plasmas of JT-60U", Phys. Rev. Lett. 78, 1267 (1997).

66) Itoh T., Hayashi T., Okuno K., "Studies on Self Radiolysis Decomposition Behavior of High Level Tritiated Water", to be published in Fusion Eng. and Design (1997).

67) Iwai Y., Yamanishi T., Nishi M., "A Steady-State Simulation Model of Gas Separation System by Hollow Filament Type Membrane Module", to be published in J. Nucl. Sci. and Technol. (1998).

68) Jimbou R., Saido M., Nakamura K., et al., "Development of B4C-Carbon Fiber Composite Ceramics as Plasma Facing Materials in Nuclear Fusion Reactor", J. Ceramic Society of Japan, 105, 1091-1098 (1997).

69) Jimbou R., Kodama K., Saidoh M., et. al., "Thermal conductivity and retention characteristics of composites made of boron carbide and fibers with extremely high thermal conductivity for first wall armour", J. Nucl. Mater. 241-243 (1997) p. p. 1175-1179.

70) Kamada Y., Yoshino R., Ushigusa K., JT-60 Team, "High Triangularity Discharges with Improved Stability and Confinement in JT-60U", Proc. 16th IAEA Fusion Energy Conference Vol.1 (1997) 247.

71) Kamada Y., Yoshino R., Ushigusa K., et al., "High Triangularity Discharges with Improved Stability and Confinement in JT-60U", Fusion Energy 1996 (proc. 16th Int. Conf., Montreal, 1996), Vol. 1 (IAEA, Vienna, 1997) 247-258.

72) Kamada Y., Yoshino R., Ushigusa K., and JT-60 Team, "High Triangularity Discharges with Improved Stability and Confinement in JT-60U", Fusion Energy (IAEA, 1997) Vol.1, p. 247.

73) Kanari M., Tanaka K., Nakamura K., et al., "Nanoindentation test on electron beam-irradiated boride layer of carbon-carbon composite for plasma facing component of large Tokamak device", J. Nucl. Materials, 244, 166-172 (1997).

74) Kasugai A., Sakamoto K., Tsuneoka M., et al., "Development of 170GHz long pulse Gyrotron with Deprressed Collector", Fusion Technology, 549 (1996).

75) Katsuta T., Takiyama K., Oda T., et al., "Supersonic Helium beam for Measurement of Electric Field in Torus Plasma Edges", Fusion Engineering and Design, 34-35 (1997) 769-772.

76) Kawamura Y., Enoeda M., Okuno K., "Isotope exchange reaction in Li2ZrO3 packed bed", to be published in Fusion Eng. and Design (1997).

77) Kawano Y., Yoshino R., Neyatani Y., and JT-60 team, "Fast current shutdown scenario for major disruption softening in JT-60U", Fusion Energy (IAEA, 1997) Vol. 1, p. 345.

78) Kawano Y., Nagashima A., Tsuchiya K., et al., "Tangential CO2 Laser Interferometer for Large Tokamaks", J. Plasma and Fusion Research 73, 870 (1997).

79) Kawano Y., Yoshino R., Neyatani Y., JT-60 team, "Fast current shutdown scenario for major disruption softening in JT-60U", Proc. 16th IAEA Fusion Energy Conference, Vol. 1(1997) 345.

80) Kawano Y., Nagashima A., Tsuchiya K., et al., "Improvement of the dual CO2 laser interferometer", Fusion Engineering and Design Vol. 34-35, 375 (1997).

81) Kawano Y., Nagashima A., et al "Two-color polarimeter for electron density measurement on large tokamaks", Rev. of Sci. Instrum. Vol. 68, 4035 (1997).

82) Kaye S.M., ITER Confinement Database Working Group (Takizuka T., JT-60 Team, Miura Y., JFT-2M Group et al.), "ITER L Mode Confinement Database", Nucl. Fusion 37 (1997) 1303-1328.

83) Kaye S.M., ITER Confinement Database Working Group, "ITER L-mode Confinement Database", Nuclear Fusion, 37 (1997) 1303-1328.

84) Kikuchi M., Miya N., Ushigusa K., et al., "Design Progress of JT-60SU", Fusion Energy (IAEA, 1997). Vol.3, p.451.

85) Kimura H., JT-60 team, "ICRF heating and TAE modes in reactor relevant JT-60U discharges", Proc. 16th IAEA Fusion Energy Conference, Vol. 2 (1997) 295.

86) Kimura T., Kurihara K., Kawamata Y., et al., "JT-60U Plasma Control System", Fusion Technology 32, No.11 (1997) pp.404-415.

87) Kishimoto K., Tani T., "Contorol characteristics of DC generator-motors with flywheels for toroidal field power source", DENKIGAKKAI RONBUNSHI May, (1997), p.579 (in Japanese).

88) Kishimoto Y. and Fujita T., "Formulation of Internal Transport Barrier and Associated Confinement Improvement in Tokamaks", Butsuri, Vol. 52, No.11, 854-857 (1997)

89) Kishimoto Y., Koga J.K., Tajima T. and Fisher D., "Phase space control and consequences for cooling by using a laser-undulator beat wave", Phys. Rev. E, 55, 5948-5963 (1997)

90) Koide Y., Burrell K.H., Rice B.W. and Fujita T., "Comparison of Internal Transport Barriers in JT-60U and DIII-D NCS Discharges", Plasma Phys. Control. Fusion 40 (1998) 97.

91) Koide Y. and JT-60 Team, "Progress in confinement and stability with plasma shape and profile control for steady-state operation in the JT-60U", Phys. Plasmas 4 (1997) p. 1623.

92) Koide Y. and JT-60 Team "Progress in confinement and stability with plasma shape and profile control for steady-state operation in the JT-60U", Phys. Plasmas 4, 1623 (1997)

93) Koizumi N., et al., "Stability Simulation of a cable-in-conduit Conductor on Non-uniform Mesh, IEEE Transactions on Applied Superconductivity, 7, 219-222 (1997).

94) Koizumi N., et al., "Ramp-rate limitation due to current imbalance in a large cable-in-conduit conductor consisting of chrome-plated strands", Cryogenics, 37, 441-452 (1997).

95) Koizumi N., et al., "Stability and heat removal characteristics of a cable-in-conduit superconductor for short length and short period perturbation", Cryogenics, 37, 487-495 (1997).

96) Kondo T., Kusama Y., Kimura H., et al., "Investigation of Interaction between MeV-Ions and First Wall from Neutron and Ei-ray Measurements in JT-60U", J. Nucl. Mater. 241-243 (1997) p. 564.

97) Konishi S., Maruyama T., K. Okuno, et al., "Development of Electrolytic Reactor for Processing of Gaseous Tritiated Compounds", to be published in Fusion Eng. and Design (1997).

98) Konishi S., Yamanishi T., Enoeda M., et al., "Integrated Fusion Fuel Cycle Development at the Tritium Process Laboratory of the Japan Atomic Energy Research Institute", to be published in Fusion Eng. and Design (1997).

99) Kramer G.J., Saigusa M., et al."Noncircular Triangularity and Ellipticity-induced Alfven Eigenmodes Observed in JT-60U", Phys. Rev. Lett. 80, 2594 (1998).

100) Krasilnikov A.V., Kaneko J., Isobe M., et al., "Fusion Neutronic Source deuterium-tritium neutron spectrum measurements using natural diamond detectors", Rev. Sci. Instrum. 68, 1720 (1997).

101) Kubo H., Takenaga H., Sugie T., et al.,"Spectral profile of Da line emitted from the divertor region of JT-60U," Plasma Phys. Control. Fusion, 40, 1 (1998).

102) Kumagai A., Asakura N., Itami K., et al.,"Parallel currents in the scrape-off layer of high-density JT-60U discharges", Plasma Phys. Control. Fusion 39, 1189 (1997).

103) Kurihara K., "Power System for Tokamak Fusion Experiments, Control System and Protection Procedures for Tokamak Power Supplies," J. Plasma and Fusion Research 73, No.5 (1997) p. 486-495 (in Japanese).

104) Kurita G., Nagashima K., Ushigusa K., et al., "Vertical Positional Instability in JT-60SU", Fusion Engng. and Des., 38 (1998) 417.

105) Kuroda T., Hatano T., Enoeda M., et al., "Development of Be/Cu-Alloy and Be/SS Joining Technology by HIP", to be published in J. Nucl. Materi., Elservier, (1998).

106) Linke J., Akiba M., Bolt H., et al., "Performance of beryllium, carbon and tungsten under intense thermal fluxes", J. Nucl. Materials, 241-243, 1210-1214 (1997).

107) Liu C.G., Yamagiwa M., Qian S J., "Production of Sheared Flow duaring Ion Cyclotron Resonance Heating in Tokamak Plasmas", Physics of Plasmas, 4, 2788 (1997).

108) Maebara S., Seki M., Suganuma K., et al., "Development of a new lower hybrid antenna module using a poloidal power divider", Fusion Technology, 637 (1996).

109) Maeda M., Uehara K., and Amemiya H., "Simultaneous Measurement of Plasma Flow and Ion Temperature Using the Asymmetric Double Probe", Jpn. J. Appl. Phys. part 1, 36 (1997) 6992-6993

110) Miura Y., Asahi Y., Hoshino K., et al., "Divertor Biasing Effects to Reduce L/H Power Threshold in the JFT-2M Tokamak", Fusion Energy (IAEA, 1997), Vol. 1, 167-175.

111) Miyachi K., "Power System for Tokamak Fusion Experiments, Motor Generator with Flywheel Effect," J. Plasma and Fusion Research 73, No.5 (1997) p. 427-433 (in Japanese).

112) Miyamoto K. and Asakura N., "An improved two points model of scrape-off-layer plasma of tokamaks with divertor", J. Plasma and Fusion Res. 74, 266 (1998).

113) Miya N., Hayashi T., Suzuki Y., et al., "Design Study of Nuclear Shielding and Fuel Cycle for Steady-State Tokamak Device JT-60SU", Fusion Eng. and Design, 36, 309-324 (1997).

114) Miya N., "Safety Problems of DT Experiments on Large Plasma Experimental Devices", J. Plasma and Fusion Res., 73 (1997) 805.

115) Nagatsu M., Takada N., Akiba M., et al., "Effect of ion-beam irradiation on power reflectivity of boron-doped CFC materials", J. Nucl. Materials, 241-243, 1180-1184 (1997).

116) Nakamura H., Hayashi T., O'hira S., et al., "Implantation Driven Permeation Behavior of Deuterium through Stainless Steel type 316L", to be published in J. Nucl. Materials (1997).

117) Nakamura K., Akiba M., "Erosion characteristics on plasma facing materials", J. Plasma and Fusion Research, 73, 594-599 (1997).

118) Nakamura K., Dairaku M., Akiba M., et al., "Sputtering experiments on B4C doped CFC under high particle flux with low energy", J. Nucl. Materials, 241-243, 1142-1146 (1997).

119) Nakanishi Y., Tani T., et al., "Development of the largest DC generator", SANGYOU TO DENKI April, (1997) p.1 (in Japanese).

120) Nakanishi Y., Tani T., et al., "The largest DC generator with a capacity of 51300kW", DEKIGAKKAISHI, Februaly, (1997) p.108 (in Japanese).

121) Nakayama T., Abe M., Tadokoro T., et al., "Evaluation of Magnetic Field due to Ferromagnetic Vacuum Vessel in Tokamak" J. Plasma and Fusion Research, 74 (1998) 274-283 (In Japanese).

122) Nemoto M., Tobita K., Ushigusa K., et al., "Enhancement in the Ionization Cross-Section of a 350 keV Hydrogen Beam on JT-60U plasmas", J. Plasma Fusion Research, 73, 1374 (1997).

123) Nemoto M., Kusama Y., Afanassiev V. I., "Ion heating up to 1 MeV-range with higher harmonic ICRF wave on JT-60U", Plasma Phys. Control. Fusion 39, 1599 (1997).

124) Neyatani N., Kawamata Y., Kimura T., et. al., "Feedback control of neutron emission rate in JT-60U", Fusion Engineering Design 36 (1997) pp. 429-443.

125) Neyatani Y., Fukuda T., Nishitani T. et al, "Feedback Control of Neutron Emission Rate in JT-60U", Fusion Engineering and Design 36, 429(1997).

126) Nishikawa M., Baba A., Kawamura Y., "Tritium Inventory Estimation in Solid Blanket System", to be published in Fusion Eng. and Design (1997).

127) Nishitani K., Harano H., Wurden G.A., "Directional neutron detector using scincilation fiber", Hoshasen, Vol.24, No1, 67(1998).

128) Nishitani T., Kasai S., et.al., " Design of radial neutron spectrometer array for the International Thermonuclear Experimental Reactor " , Rev. Sci. Instrum. 68(1), P.565 (1997)

129) Nishitani T., Ebisawa K., et.al., Design of ITER neutron yield monitor using microfission chamber, Fusion Engineering and Design,vol.34-35 P.567 (1997)

130) O'hira S., Steiner A., Nakamura H., et al., "Tritium Retention Study of Tungsten using Various Hydrogen Isotope Irradiation Sources", to be published in J. Nucl. Materials (1997).

131) O'hira S., Hayashi T., Okuno K., "Tritium Safety Related Studies at TPL of JAERI", Journal of Fusion Technology, 16 (3), 219 (1997).

132) O'hira S., "Procurement of Tritium for Fusion Reactor (2): Transportation of Large Amounts of Tritium for Fusion Reactors", Journal of Plasma and Fusion Research, 73, 764 (1997) (in Japanese).

133) O'hira S., Hayashi T., "Radiation Effects and Safety Control of Tritium" (V-1 and V-2), J. Atomic Energy Soc. Japan, 39, 933 (1997) (in Japanese).

134) Ohdachi S., Shoji T., Nagashima K., and JFT-2M group, "Flow profile measurement with a rotating Mach probe in the scrape-off layer of the JFT-2M tokamak", Fusion Engineering and Design 34-35 (1997) 725.

135) Ohdachi S., Shoji T., Nagashima K., and JFT-2M group, "Flow Profile Measurement with a Rotating Mach Probe in the Scrape-off Layer of the JFT-2M Tokamak", Fusion Engineering and Design, 34-35 (1997) 725.

136) Ono M., et al., "Electrical Circuit Models among Superconducting Strands in Real-scale CICCs", IEEE Transactions on Applied Superconductivity, 7, 215-218 (1997).

137) Onozuka M., Ueda Y., Seki Y., et al., "Development of Dust Removal System using Static Electricity for Fusion Experimental Reactors", J. Nuclear Science and Technology, 34, No.11, pp.1031-1038 (1997).

138) Ozeki T., Azumi M., Ishii Y., Kishimoto Y., Fu G.F., "Physics issues of high bootstrap current tokamaks", Plasma Physic and Controlled Fusion 39, A371-A380 (1997).

139) Polevoi A., Neudatchin S., Shirai H., "Analysis of Convective Heat Losses in JT-60U Neutral Beam Injection Experiments", Jpn. J. Appl. Phys. 37 (1998) 671-677.

140) Putvinski S., (Shimada M., Takizuka T., Yoshino R.) et al., "ITER Physics", Fusion Energy 1996 (proc. 16th Int. Conf., Montreal, 1996), Vol. 2 (IAEA, Vienna, 1997) 737-753.

141) Saigusa M., Kusama Y., Ozeki T., et al., "Effect of Shear in Toriodal Rotation on Toroidicity Induced Alfven Eigenmode", Nucl. Fusion 37, 1559 (1997).

142) Saigusa M., Kusama Y., Ozeki T., et al., "Effect of Shear in Toroidal Rotation on Toroidicity Induced Alfven Eigenmodes", Nuclear Fusion, 37, No.11 (1997) p. 1559.

143) Saigusa M., Moriyama S., H Kimura,. et al., "Effect of Non-Linear Wave Absorption on the Radiation Loss Fraction during Second Harmonic Minority Ion Cyclotron Resonance Heating Experiments in JT-60U" , Jpn. J. Appl. Phys. 36 (1997) p. 345.

144) Saigusa M., Moriyama S., Kimura H., et al., "Effect of Non-Linear Wave Absorption on the Radiation Loss Fraction during Second Harmonic Minority Ion Cyclotron Resonance Heating Experiments in JT-60U", Japanese J. of Applied Phys. 36, Part1, 345 (1997).

145) Saji G., Oikawa T., The ITER Safety Approach for External Events, Journal of Fusion Energy, Vol.16, No.1/2 (1997)

146) Saji G., Iida H., et.al., Safety and Environmental Activities for ITER, ibid. No.3 (1997)

147) Sakamoto K., Kasugai A., Takahashi K., et al., "Stable, Single-Mode Oscillation with High-Order Volume mode at 1MW, 170GHz gyrotron", J. Physical Soc. of Japan, 65, no.7, 1888 (1996).

148) Sakasai A. and JT-60 Team, "Divertor diagnostics and physics in the JT-60U tokamak", Fusion Engineering and Design 34-35 (1997) p. 45.

149) Sakasai A. and the JT-60 Team, "Divertor diagnostics and physics in the JT-60U tokamak," Fusion Engineering and Design 34-35, 45(1997) .

150) Sakasai A., Kubo H., Shimizu K. et al., "Active Control of Helium Ash Exhaust and Transport Characteristics in JT-60U", Nucl. Fusion Supplement (Proc. of the 16th Int. Conf. on Fusion Energy, Montreal, 1996) 1, 789 (IAEA, Vienna, 1997).

151) Sato M., Ishida S., Isei N., et al., "Measurements and Analysis of Electron Cyclotron Emission in JT-60U", Fusion Engineering and Design 34-35 (1997) 477-481.

152) Sato M., Ishida S., Isei N., et al., "Measurements and Analysis of Electron Cyclotron Emission in JT-60U", Fusion Engineering and Design, 34-35 (1997).

153) Sato M., Ishida S., Isei N. et al., " Measurements and Analysis of Electron Cyclotron Emission in JT-60U" , Fusion Engineering and Design, 34-35 (1997).

154) Sato S., Kuroda T., Hatano T., et al., "Development of First Wall/Blanket Structure by HIP in JAERI", to be published in Fusion Eng. Design, Elsevier, (1998).

155) Sato S., Takatsu H., Seki Y., et al., "Streaming Analysis of Gap between Blanket Modules for Fusion Experimental Reactor", Fusion Technol., 30, 1129 (1997).

156) Sato S., Hatano T., Kuroda T., et al., "Optimization of HIP Bonding Conditions for ITER Shielding Blanket/First Wall made from Austenitic Stainless Steel and Dispersion Strengthened Copper Alloy", to be published in J. Nucl. Mater., Elservier, (1998).

157) Sato S., Takatsu H., Utsumi T., et al., "Streaming Analysis for Radiation through ITER Mid-Plane Port", to be published in Fusion Eng. Design, Elsevier, (1998).

158) Sato S., Maki K., Takathu H., et al., "Shielding Analysis for Toroidal Field Coils around Exhaust Duct in Fusion Experimental Reactors", Fusion Technol., 30, 1076 (1997).

159) Seki M., Maebara S., Fukuda H., et. al., "Development of a Power Divider in the H Plane Using Posts in a Rectangular Waveguide for the Next Generation Lower Hybrid Current Drive Antenna", Fusion Eng. Design 36 (2-3) (1997) p. 281.

160) Senda I., A model of ions interacting with neutrals in high electric field and application to sheath formation, Physics of plasmas Vol.4, No.5, P.1308 (1997)

161) Senda I., Shoji T., et.al., " Approximation of eddy currents in three-dimentional structures by toroidally symmetric modes and plasma control issues ". Nuclear Fusion Vol.38, No.8, P1129(1997)

162) Sengoku S. and JFT-2M Group, "Extension of coexistent regime of H-mode with a dense and cold divertor plasma on JFT-2M", Bull. Amer. Phys. Soc. 42 (1997) p. 1934.

163) Sengoku S., Kawashima H. and JFT-2M Group, "Extension of Coexistent Regime of H-mode with a Dense and Cold Divertor Plasma on JFT-2M", Bull. Amer. Phys. Soc. 42 (1997) p. 1962.

164) Shiho M., Ogawa M. , Horioka K., et al., "Lightning control system using high power microwave FEL", Nuclear Inst. & Methods in Phys. Res. Section A, 375, 396 (1996).

165) Shimizu K., Takizuka T., Sakasai A., "A review on Impurity transport in divertors", J. Nucl. Mater. 241-243 (1997) 167-181.

166) Shimomura Y., Matsuda S. et al., " ITER Design Report ". Journal of Plasma and Fusion Research, vol.73 Supplement P.1-294 (1997)

167) Shinohara K., Shiraiwa S., Hoshino K., Miura Y., Hanada K., Toyama H., JFT-2M Group, "A new method to analyze density fluctuation by microwave reflectometry", Jpn. J. Appl. Phys. 36, 7367 (1997).

168) Shinohara K., Hoshino K., Shiraiwa S., et al., "Measurement of density fluctuations by JFT-2M reflectometer", Fusion Engineering and Design, 34-35 (1997) 433-436.

169) Shinohara K., Shiroiwa S., Hoshino K., and JFT-2M Groupe, "A New method to analyze density fluctuation by microwave reflectometry", Jpn. J. Appl. Phys. , 36 (1997) p. 7367-7374.

170) Shinohara K., Shiraiwa S., Hoshino K., et al., "A New Method to Analyse Density Fluctuation by Microwave Reflectometry", Jpn. J. Appl. Phys., 36 (1997) 7367-7374.

171) Shirai H., and JT-60 Team, "Recent experimental and analytic progress in the Japan Atomic Energy Research Institute Tokamak-60 Upgrade with W-shaped divertor configuration", Phys. Plasmas 5 (1998) p. 1712-1720.

172) Suzuki A., Takizuka T., Shimizu K., et al., "An Implicit Monte Carlo Method for Simulation of Impurity Transport in Divertor Plasma", J. Comput. Phys. 131 (1997) 193-198.

173) Suzuki S., Akiba M., "High heat flux component of ITER", J. Plasma Fusion Research, 73, 581-587 (1997).

174) Suzuki S., Araki M., Sato K., et al., "High Heat Flux Experiments on a Saddle-shaped Divertor Mock-up", Fusion Energy 1996, Vol. 3, pp.565-570, IAEA, Vienna, 1997.

175) Tadokoro T., O'hira S., Nishi M., et al., "Tritium Retention in CX-2002U and Methods to Reduce Tritium Inventory", to be published in J. Nucl. Materials.

176) Takahashi K., Kasugai A., Sakamoto K., et al., "Measurement of Temperature dependence of Dielectric Permittivity of Sapphire Window for High Power Gyrotron", Japanese J. of Applied Phys. 35, Part1, no.8, 4413 (1996).

177) Takatsu H., Kawamura H., Tanaka S., "Development of Ceramic Breeder Blanket in Japan", to be published in Fusion Eng. Design, Elsevier, (1998).

178) Takeji S., Kamada Y., Ozeki T. et al., "Ideal magnetohydrodynamic instabilities with low toroidal mode numbers localized near an internal transport barrier in high-bp mode plasmas in

the Japan Atomic Energy Research Institute Tokamak-60 Upgrade", Phys. Plasmas Vol.4, No.12, 4283 (1997).

179) Takeji S., Kamada Y., Ozeki T., et al., "Ideal Magnetohydrodynamic Instabilities with Low Toroidal Mode Numbers Localized near an Internal Transport Barrier in High bp Mode Plasmas in the Japan Atomic Energy Research Institute Tokamak-60 Upgrade", Phys. Plasmas 4 (1997) 4283-4291.

180) Takenaga H. , Nagashima K. , Sakasai A., et. al.,"Determination of particle transport coefficients in reversed shear plasma of JT-60U", Plasma Pysics and Controlled Fusion, 40, 183 (1998).

181) Takenaga H., Nagashima K., Asakura N., et al., "Effect of source distribution and edge density on particle confinement in JT-60U", Nucl. Fusion 37, 1295 (1997) .

182) Takiyama K., Katsuta T., Watanabe M., et al., "Spectroscopic Method to Directly Measure Electric Field Distribution in Tokamak Plasma Edge", Review of Scientific Instruments, 68, No.1 Part II (1997) 1028-1031.

183) Takiyama K., Katsuta T., Toyota H., et al., "Low-Energetic He-Atom Beam as a Diagnostic Probe for Electric Field Measurement in the Plasma Edges" J.Nucl. Mater. 241-243 (1997) 1222-1227.

184) Takizuka T., ITER Confinement Database and Modelling Expert Group (Miura Y., JT-60 Team, JFT-2M Team et al.), "Threshold Power and Energy Confinement for ITER", Fusion Energy 1996 (proc. 16th Int. Conf., Montreal, 1996), Vol. 2 (IAEA, Vienna, 1997) 795-806.

185) Takizuka T., ITER Confinement Database and Modelling Expert Group (Takizuka T., Miura Y., Fukuda T., and JT-60 Team, "Threshold Power and Energy Confinement for ITER", Fusion Energy (IAEA, 1997) , Vol. 2 p. 795-806.

186) Tamai H., Konoshima S., Hosogane N., et al., "Feedback Control of Radiative Divertor on JT-60U Tokamak", Fusion Engineering and Design 39-40, 163 (1998).

187) Tamai H., Kikuchi M., Arai T., et al., "Stress analysis for the crack observation in cooling channels of the toroidal field coils in JT-60U", Fusion Engineering and Design 38, 429 (1998).

188) Tanabe T., Philipps V., Nakamura K., et al., "Examination of material performance of W exposed to high heat load", J. Nucl. Materials, 241-243, 1164-1168 (1997).

189) Tobita K., Harano H., Nishitani T., et al., "Loss of fast tritons in JT-60U reversed magnetic shear discharges", Nucl. Fusion 37, 1583 (1997).

190) Tobita K., JT-60 team, "Transport and loss of energetic ions in JT-60U", Proc. 16th IAEA Fusion Energy Conference, Vol. 1 (1997) 497.

191) Toda S., Itoh S-I., Yagi M. et al., "A Theoretical Model of H-Mode TransitionTriggered by Condensed Neutrals Near X-Point", Plasma Phys. Control. Fusion, 39 (1997) 301-312.

192) Tokami I., Nakahira M., Sato S., et al., "Welding and Cutting Methods for Blanket Support Legs of Fusion Experimental Reactor", Fusion Technol., 30, 574 (1997).

193) Tokuda S., Naito H., Lee W.W., "A Particle-Fluid Hybrid Simulation Model Based on Nonlinear Gyrokinetics", J. Plasma and Fusion Research ,74 (1998) 44-53.

194) Tokuda S., "Bilinear Formulation of the Frieman-Rotenberg Equation", J. Plasma and Fusion Research 74 (1998) 503-511.

195) Tokuda S., Watanabe T., "Eigenvalue Method for the Outer-Region Matching Data for Resistive MHD Stability Analysis", J. Plasma and Fusion Research, 73 (1997) 1141-1154.

196) Trainham R., Jacquat C., Miyamoto K., et.at., "Negative ion source for neutral beam injection into fusion machines", Rev. Sci. Instrum. 69 (2), 926-928 (1997).

197) Tsuneoka M., Fujita H., Imai T., et al., " Development of DC100kV, 100A, 360A Break IGBT Switch", Trans. IEE of Japan, 116-D, No.4, April, 1996.

198) Uehara K., Tsushima A. and Amemiya H., "Direct Measurement of Ion behaviour Using Modified Ion Sensitive Probe in Tokamak Boundary Plasma", J. Phys. Soc. Jpn. 66 (1997) 921-924 .

199) Uehara K., "Toothbrush Probe for Instantaneous Measurement of Radial Profile in Tokamak Boundary Plasma", Jpn. J. Appl.Phys, Vol. 36, Part 1, No. 4A, 2351(1997).

200) Uehara K., Sengoku S. and Amemiya H., "Toothbrush Probe for Instantaneous Measurement of Radial Profile in Tokamak Boundary Plasma", Jpn. J. Appl. Phys. 36 (1997) 2351-2355.

201) Uehara K., and JFT-2M Group, "Toothbrush probe for instantaneous measurement of radial profile in tokamak boundary plasma", Jpn. J. Appl. Phys. 36 (1997) pp.2351-2355.

202) Uehara K., and JFT-2M Group, "Direct measurement of ion behavior using modified ion sensitive prove in tokamak boundary plasma", J. Phys. Soc. Jpn. , 66 (4).

203) Ushigusa K., "Conceptual Design of JT-60SU", J. Plasma and Fusion Res., 74 (1998) 117.

204) Ushigusa K., and the JT-60 Team, "Steady State Operation Research", Nuclear Fusion Supplement (Proc. 16th Int. Conf. on Plasma Phy. & Controlled Nucl. Fusion Res., Seville, 1996), 1 (IAEA, Vienna, 1997) p. 37.

205) Ushigusa K. and the JT-60 Team, "Steady-State Operation Research in JT-60U", Fusion Energy, (IAEA, Vienna, 1997) Vol. 1, p. 37.

206) Ushigusa K. and JT-60 Team, "Steady-State Operation Research in JT-60U", Fusion Energy (IAEA, 1997) Vol. 1, p. 37.

207) Ushigusa K. and JT-60 Team, "Steady-state in JT-60U Reversed shear Discharges", Fusion Energy (IAEA, 1997) , Vol. 1 p. 37.

208) Watanabe K., Akino N., N, Aoyagi T., et al., "Recent Progress of High-Power Negative Ion Beam Development for Fusion Plasma Heating", Radiat. Phys. Chem. Vol. 49, No.6 (1997) pp. 631-639.

209) Watanabe K., Fujiwara Y., Hanada M., et al., "Development of a multiaperture, multistage electrostatic accelerator for hydrogen negative ion beams", Rev. Sci. Instrum. 69 (2), 986-988 (1997).

210) Watanebe K., Akino N, Aoyagi T., et al., "Recent progress of high-power negative ion beam development for fusion plasma heating", Radia. Phys. Chem. 49, No.6, pp.631-639, (1997).

211) Wong F., "Selection of jacket materials for Nb3Sn supercondoctor", Fusion Technology 1996, 1115-1118 (1997).

212) Yagyu J., Ogiwara N., Saidoh M., et. al., "Properties of thin boron coatings formed during deuterated-boronization in JT-60", J. Nucl. Mater. 241-243 (1997) p. 579-584.

213) Yamagiwa M., Hirose A. and Elia M., "Kinetic Ballooning Modes at the Tokamak Transport Barrier with Negative Magnetic Shear", Phys. Plasmas 4 (1997) 4031-4034.

214) Yamagiwa M., Koga J. and Ishida S. ,"Non-Linear Fokker-Planck Code Study of High Ion Temperature Plasma in JT-60U", Nuclear Fusion, 37 (1997) 1735-1739.

215) Yamai H., Konishi S., Yamanishi T., et al., "Design of Tritiated Water Processing System Using the LPCE and Solid Oxide Electrolyte for Next Stage Fusion Reactor", Accept for publication in Fusion Eng. and Design.

216) Yamanishi T., Okuno K., "Control Characteristics of Cryogenic Distillation Column with a Feedback Stream for Fusion Reactor", J. Nucl. Sci. and Technol., 34, 375 (1997).

217) Yamanishi T., Nishikawa M., Nakashio N., "Tritium Behavior in Fusion Fuel Systems", Journal of Plasma and Fusion Research, 73, 1326 (1997) (in Japanese).

218) Yamauchi T., Dimock D., "A large aperture laser triggered intensified charge coupled device using second-harmonic laser light triggering", Rev. Sci. Instrum. 68 (1997) 2384-2386.

219) Yoshino R., Nakamura Y., Neyatani Y., "Plasma Equilibrium Control during Slow Plasma Current Quench with Avoiding of Plasma-Wall Interaction in JT-60U", Nucl. Fusion 37, 1161 (1997).

A.1.3 List of papers published in conference proceedings

1) Akiba M., Suzuki S., "Overview of the Japanese Mock-up Tests for ITER High Heat Flux Components", Proc. 4th Int. Symp. on Fusion Nuclear Technology, Tokyo, Japan, April 6-11, (1997).

2) Ando T., et al., "Design and testing of 10kA current lead using high temperature superconductors for fusion magnets", 15th Int. Conf. on Magnet Technology (MT-15), China, 1997.

3) Arai T., Honda M., Koike T., et al., "Inspection techniques for JT-60 toroidal field coil cooling pipes", FUSION TECHNOLOGY 1996 (1997) p.1099-1102.

4) Araki M., Kitamura K., et.al., Analyses of divertor high-heat flux components on thermal and electromagnetic loads, ibid.

5) Araki M., Kude Y., Sohda Y., Nakamura K., Satoh S., Suzuki S., Akiba M., " Development of 3D-based CFC with high thermal conductivity for fusion application " . Proc. of Symp. on Fusion Technol., Lisbon (1997) p359-362

6) Araki M., Kitamura K., Suzuki S., "Analyses of divertor high-heat-flux components on thermal and electromagnetic loads", Proc. 4th Int. Symp. on Fusion Nuclear Technology, Tokyo, Japan, April 6-11, (1997).

7) Azuma K., et al., "Dependence of CICC's stability on coolant flow rate", 15th Int. Conf. on Magnet Technology (MT-15), China, 1997.

8) Bandourko V., Jimbou R., Nakamura K., et al., "Tungsten selfsputtering yield with different incidence angles and target temperatures", Proc. 8th Int. Conf. on Fusion Reactor Materials, P1-A057, Sendai, Japan, Oct. 26-31, (1997).

9) Barabash V., Akiba M., Bonal J.P., et al., "Carbon fiber composites application in ITER plasma facing materials", Proc. 8th Int. Conf. on Fusion Reactor Materials, OI-04, Sendai, Japan, Oct. 26-31, (1997).

10) Boscary J., Suzuki S., Nakamura K., et al., "Thermal fatigue tests on CVD-W/Cu divertor mock-ups", Proc. 4th Int. Symp. on Fusion Nuclear Technology, Tokyo, Japan, April 6-11, (1997).

11) Chiocchio S., Ioki K., Araki M. et al., "Loads on the ITER in-vessel components from electromagnetic transients ". Proc. of Symp. on Fusion Technol., Lisbon (1997) p719-

12) Ezato K., Kunugi T., "Molecular dynamics simulation of energetic cluster impact to metallic thin film", Proc. 8th Int. Conf. on Fusion Reactor Materials, P1-A005, Sendai, Japan, Oct. 26-31, (1997).

13) Fujiwata Y., "Radiation induced conductivity and voltage holding characteristics of insulation gas for the ITER-NBI", Proc. of the joint meeting of the 8th Int. Symp. on the production and neutralization of negative ions and beams and 7th European workshop on the production and application of light negative ions, Giens, France, Dep.15, (1997).

14) Gotoh Y., Okamura H., Akiba M., et al., "Development and material testing of OF-Cu/DS-Cu duplex tube and trial fabrication of vertical target mock-ups for ITER divertor", Proc. 8th Int. Conf. on Fusion Reactor Materials, P3-A006, Sendai, Japan, Oct. 26-31, (1997).

15) Gribov Y., Fujieda H., Shoji T., Shinya K., Senda I. et al., "ITER poloidal field scenario, error fields and correction coils ". 24th European Conference on Controlled Fusion and Plasma Physics (1997)

16) Hamada K., et al., "Development of winding technique for ITER CS model coil", 15th Int. Conf. on Magnet Technology (MT-15), China, 1997.

17) Hanada M., "Stripping loss and grid power loading in an electrostatic negative ion accelerator", Proc. of the joint meeting of the 8th Int. Symp. on the production and neutralization of negative ions and beams and 7th European workshop on the production and application of light negative ions, Giens, France, Dep.15, (1997).

18) Hashimoto M., Tsunematsu T., et.al., Pipe support across iolated and seismic structure in ITER, bid.

19) Hatae T., Fujita T., Kamada Y., et al., "Condition for Formation of ITB in JT-60U Reversed Shear Plasmas", presented at 39th APS-DPP in Pittsburgh (1997)

20) Hatano T., Suzuki S., Yokoyama., et al., "High heat flux testing of a HIP bonded first wall panel with built-in circular cooling tubes", Proc. 4th Int. Symp. on Fusion Nuclear Technology, Tokyo, Japan, April 6-11, (1997).

21) Hatayama A., Schneider R., (Hayashi N., Sugihara M., Shimizu K.) et al., "Analysis of JT-60U Divertor Plasma Using "B2-Eirene" Code", Proc. 24th EPS Conf.

22) Hayashi M., Shibata K., Matsumoto R., "Flares and MHD Jets in Protostar", International Astronomical Union Symposium No. 188 The Hot Universe, Kyoto, August 25-29, 1997.

23) Hiratsuka H., Sasajima T., Kodama K., et al., "Effects of plasma behavior on in-vessel components in JT-60 operation", FUSION TECHNOLOGY 1996 (1997) p.763-766.

24) Hirose A., Elia M. and Yamagiwa M., "Stability of Kinetic Ballooning and Drift Type Mode in Tokamks with Negative Shear", Proceedings of the 16th international conference on fusion energy, Montreal, 7-11 Oct. 1996 (IAEA, Vienna, 1997), Vol.2 703-709.

25) Hiwatari R., Amano T., Ogawa Y., Takizuka T., ITER Combined Workshop of Confinement and Transport Expert Group and Confinement Databaseand Modeling Expert Group, "Model Validation - Analytic Benchmark on TTCNT code -", April 14-18, 1997, San Diego.

26) Hosokai I., Ikeda T., Koizumi K., et al., "Thermal and Hydraulic Assessments of the Cooling System for ITER Vacuum Vessel", 17th Symp. on Fusion Engineering, Oct. 8, San Diego, USA (1997).

27) Iida H., Plentedar R. et al., " Three-dimensional analysis of nuclear heating in the superconductiong magnet system in ITER due to n-16 gamma-rays in the ITER shielding blanket water cooling system". 17th Symposium on Fusion Eng. (San Diego) 1997

28) Iiida F., Yoshida K., et al., " International thermonuclear experimental reactor (ITER) magnet interface system". 15th Int. Conf. on Magnet Tech. (MT-15), (Beijiing) 1997

29) Inabe T., Seki M., et.al, Fusion Reactor Safety -Issues and Perspective, ibid.

30) Ioki K., ITER First Wall/Shield Blanket, ibid.

31) Ise H., Satoh S., Akiba M., et al., "Development of fabrication technologies for the ITER divertor", Proc. 4th Int. Symp. on Fusion Nuclear Technology, Tokyo, Japan, April 6-11, (1997).

32) Ishida S., Takeji S., Isayama A., et al., "Disruptive Beta Limits for High Performance Discharges in JT-60U", Proc. 24th European Conference on Controlled Fusion and Plasma Physics, Berchtesgaden, 1997, Part II-489.

33) Ishida S. and JT-60 Team, "Recent Results from High Performance Regimes in JT-60U", Proc. 24th Plasma Physics and Controlled Nuclear Fusion Conference, Zvenigorod, Russia, 1997, p.3.

34) Ishida S., Takeji S., Isayama A., et al., "Disruptive beta limits for high performance discharges in JT-60U", Proc. 24th European Conference on Controlled Fusion and Plasma Physics, Berchtesgaden, Vol. 21A, Part II, 489 (1997).

35) Ishida S. and JT-60 Team, "Recent Results from High Performance Regimes in JT-60U", Proc. 24th Plasma Physics and Controlled Nuclear Fusion Conference, Zvenigorod, Russia, p.3 (1997).

36) Ishio K., et al., "Mechanical properties of 110mmt hot rolled plates of JJ1 and JK2 for ITER TF coil", 15th Int. Conf. on Magnet Technology (MT-15), China, 1997.

37) Ishizawa A., Tokuda S., "Linear Analysis of Forced Mabnetic Reconnection ", The Institute of Statistical Mathematics Cooperative Research Report 110, Proceedings of 1997-Workshop on MHD Computations-Numerical methods and optimization techniques in controlled thermonuclear fusion research- March, 1998, p.36-45.

38) Itami K. and JT-60 Team, "Divertor plasma characteristics in the W-shaped pumped divertor of JT-60U", 39th American Physical Society Meeting, Pittsburgh (1997).

39) Itoh T., Akino N., Aoyagi T., et al., "Beamline performance of 500 keV negative ion based NBI system for JT-60U, Proc. of the 4th International Symp. on Fusion Nuclear Technology, Tokyo, Japan, April 6-11, (1997).

40) Itou A., Oka K., Kakudate S., et al., "Development of Bore Tools for Blanket Cooling Pipe Connection in ITER", 17th Symp. on Fusion Engineering, Oct. 8, San Diego, USA (1997).

41) Jayakumar R., et al., "The ITER CS Model Coil Project", 16th IAEA Fusion Energy Conference, Montreal, Canada, CN-64 / FP-12 (1996).

42) Jayakumar R., Okuno K. et al., " Design and fabrication of ITER CS model coil inner module and support structure". 15th Int. Conf. on Magnet Tech. (MT-15), (Beijiing) 1997

43) Jimbou R., Nakamura K., Bandourko V., et al., "Temperature dependence of sputtering yield of carbon fiber-reinforced carbon composites with low energy and high flux deuterium ions", Proc. 8th Int. Conf. on Fusion Reactor Materials, P1-A032, Sendai, Japan, Oct. 26-31, (1997).

44) Johnson L.C., Barnes Cris W., Ebisawa K., Krasilnikov A.V., Mrcus F.B., Nishitani T., et al., "Overview of fusion product diagnostics for ITER", Workshop on Diagnostics for ITER, Varenna Italy (1997), Proc. "Diagnostics for Experimental Thermonuclear Reactor II" (to be published in Prenum Press,1998Åj

45) Kamada Y., JT-60 Team, " High Performance Discharges in JT-60U with Transport Barriers ", Proc. International Symposium on Plasma Dynamics in Complex Electromagnetic Fields, IAE-PR-98 054 (Mar. 1998)

46) Kawamura Y., Enoeda M., Nishikawa M., "Tritium Recovery from Helium Purge Stream of Solid Breeder Blanket by Cryogenic Molecular Sieve Bed (II)", The 6th international workshop on Ceramic Breeder Blanket Interactions, Oct. 22-24 (1997), Mito, Japan.

47) Kawano Y., Yoshino R., Neyatani Y., and JT-60 team, "Suppression of Runaway-Electrons Generation during Disruptive Discharge-Terminations in JT-60U", Proceedings of 24th European Physical Society Conference on Controlled Fusion and Plasma Physics, Berchtesgaden, 9-13 June (1997), Vol. 21A, Part II (1997) p. 501.

48) Kawano Y., Yoshino R., Neyatani Y., JT-60 team, "Suppression of Runaway-Electrons Generation during Disruptive Discharge-Terminations in JT-60U", Proc. 24th European Conference on Controlled Fusion and Plasma Physics, Berchtesgaden,Vol. 21A, Part II, 501 (1997).

49) Kawashima H., Sengoku S., and JFT-2M Group, "Study of dense and cold divertor with H-mode in the JFT-2M", in Controlled Fusion and Plasma Physics (Proc.of 24th European Conf. , 1997) Vol 21A, part2, (1997) p705-708.

50) Kawashima H., Sengoku S., Ogawa T. et al., "Study of dense and cold divertor with H-mode in the JFT-2M", in Controlled Fusion Plasma Physics (Proc. of 24th European Conf., 1997) Vol. 21A, part 2, (1997) 705-708.

51) Kikuchi M., Seki Y., Nakagawa K., "The Advanced SSTR", 6th IAEA TCM on Fusion Power Plant Design and Technology (to be published in Fusion Engineering and Design).

52) Kikuchi M., Johnson M., "Technical Break-throughs with Construction of ITER", Panel Discussion, ISFNT-4, April 6-11, 1997, Tokyo, Japan.

53) Kikuchi M., Kuriyama M., et al., "Design Progress of JT-60SU", 16th International Conference on Fusion Energy, Montreal, Oct. (1997).

54) Kikuchi M., "Japanese Reactor Design Activity(SSTR)", IEA Workshop on Reduced Activation Ferrtic / Martensitic Steels, Nov 3-4,1997.

55) Kikuchi M., "Design and Materials for SSTR and A-SSTR", Discussion session in ICFRM-8, Sendai, Oct 28, 1997.

56) Kimura S., Tada E., Oka K., et al., "Laser technology for maintenance of nuclear piping", European Symposium on Lasers and Optics in Manufacturing, June 16, Munchen (1997).

57) Kishimoto H., Nagami M., Kikuchi M., "Recent Results and Engineering Experiences from JT-60", ISFNT-4 (4th International Symposium on Fusion Nuclear Technology), 1997.

58) Kishimoto H., Nagami M., Kikuchi M., "Recent Results and Engineering Experiences from JT-60", ISFNT-4 (4th International Symposium on Fusion Nuclear Technology), April 6-11, 1997, Tokyo, Japan.

59) Kishimoto Y., "Toroidal Mode Structure and Related Transport in Reversed Magnetic Shear Plasma", Invited talk in Asia Pacific Plasma Theory Conf. 1997, Sep 24, 1997, National Institute for Fusion Science, Toki.

60) Kishimoto Y., Tajima T., Downer M., "Cluster Plasma and its Linear and Nonlinear Properties, The Thirty Ninth Annual Meeting of the Division of Plasma Physics (17-21 Nov. 1997 Pittsburgh, Pennsylvania), APS Bulletin, 39th DPP, Vol.42, No.10 (1997) kWeaP3 16, p1967.

61) Kishimoto Y., Koide Y., Horton W., et al., "Discontinuity mode for Internal Transport Barrier in Reversed Magnetic Shear Plasma", 1998 International Sherwood Fusion Theory Conference, Mar 25, 1998, Atranta, Georgia.

62) Kishimoto Y., Koide Y., Horton W., Tajima T., Kim J.Y., "Discontinuity mode for Internal Transport Barrier in Reversed Magnetic Shear Plasma", 1998 International Sherwood Fusion Theory Conference, Mar 25, 1998, Atranta, Georgia.

63) Kishimoto Y., Kim J-Y., Fukuda T., Ishida S., Fujita T., et. al., "Effect of Weak/Negative Magnetic Shear and Plasma Shear Rotation on Self-organized Critical Gradient Transportin Toroidal Plasmas: Formation of Internal Transport Barrier", Proceedings of the 16th international conference on fusion energy, Montreal, 7-11 Oct. 1996 (IAEA, Vienna, 1997), Vol.2, 581-591, 1997

64) Kishimoto Y., "Global Gyrokinetic Particle Simulations of Transport Barriers Produced by Er and Low Magnetic Shear", Invited talk in Eleventh Transport Task Force Workshop, Mar 18, 1998, Atranta, Georgia.

65) Koizumi K., Nakahira M., Itou Y., et al., "Design and Development of the ITER Vacuum Vessel", Inter. Symp. on Fusion Nuclear Technology - 4, Apr. 6, Tokyo (1997).

66) Koizumi K., Nakahira M., Itou Y., et al., "Fabrication of Full-scale Sector Model for ITER Vacuum Vessel", 17th Symp. on Fusion Engineering, Oct. 8, San Diego, USA (1997).

67) Koizumi K., Nakahira M., Itou Y. et al., " Fabrication of full-scale sector model for ITER vacuum vessel ". 17th Symposium on Fusion Eng. (San Diego) 1997

68) Koizumi N., et al., "Analysis of current imbalance in a large CICC consisting of chrome plated strand", N.Koizumi, et. al. , 15th Int. Conf. on Magnet Technology (MT-15), China, 1997.

69) Koizumi N., et al., "Effect of heating zone length on the stability of a cable-in-conduit conductor", 15th Int. Conf. on Magnet Technology (MT-15), China, 1997.

70) Koizumi N., et al., "Stability simulation of 46-kA-13T Nb3Al insert coil", 15th Int. Conf. on Magnet Technology (MT-15), China, 1997.

71) Kubo H., Takenaga H., Sugie T., et al., "Behavior of Neutral Deuterium and Helium Atoms in the Divertor Region of JT-60U", Proc. of 24th EPS Conf. on Cotrolled Fusion and Plasma Physics, Berchtesgaden, Part II, 509 (1997).

72) Kurihara K. and Kawamata Y., "Development of a Precise Long-time Digital Integrator for Magnetic Measurements in a Tokamak", in Proc. of 19th Symposium on Fusion Technology, (Losbon, Portugal,1996) Elsevier Science (1997) pp.795-798.

73) Kurita G., Ushigusa K., Kikuchi M., et al., "Present Status of JT-60SU Design", 17th IEEE/NPSS Symposium on Fusion Engineering, SanDiego USA (1997).

74) Kuriyama M., Akino N., Aoyagi T., et al., "Operation of the negative-ion-based NBI for JT-60U, Proc. of the 4th International Symp. on Fusion Nuclear Technology, Tokyo, Japan, April 6-11, (1997).

75) Kuriyama M., et al., "Initial Beam Operation of 500keV Negative-ion based NBI system for JT-60U," 9th Symp. on Fusion Technology, (Lisbon 1996),vol.1,693-696 (1997).

76) Kusama Y., Kimura H., Saigusa M., et al., "Confinement of ICRF-Driven Energetic Protons and TAE Modes in JT-60U Negative Shear Plasmas", IEA Tripartite Workshop on TAE and Energetic Particle Physics, Naka Fusion Research Establishment, JAERI, February 25-27, 1997.

77) Kusama Y., Oikawa T., Nemoto M., JT-60 Team, "Heating and Current Drive Experiments with Negative-ion-based Neutral Beam on JT-60U", Proc. 24th European Conference on Controlled Fusion and Plasma Physics, Berchtesgaden,Vol. 21A, Part II, 513(1997).

78) Kusama Y., Oikawa T., Nemoto M., and JT-60 Team, "Heating and Current Drive Experiments with Negative-ion-based Neutral Beam on JT-60U", 24th European Physical Society Conference on Controlled Fusion and Plasma Physics, Berchtesgaden, 9th-13th June 1997, Vol. 21A Part II (1997) p. 513.

79) Maeda M, Uehara K. and Amemiya H., "Measurement of the Plasma Flow Using the Asymmetric Double Probe in the JFT-2M Tokamak", in Controlled Fusion Plasma Physics (Proc. of 24th European Conf., 1997) Vol. 21A, part 2, (1997) 709-712.

80) Matsuda S., Status of ITER Technology R&D in Japan, to appear in Fusion Eng. and Design Special issue (1998)

81) Matsuda T., et al., "Recent Developments in JT-60 Data Processing System", IAEA TCM on Data Acquisition and Management for Fusion Research (Garching, July 1997).

82) Matsukawa M., Aoyagi T. and Miura Y., "Development of a General Tokamak Circuit Simulation Program and Some Application Results to the JT-60 Power Supply System", in Proceedings of the Power Conversion Conference-Nagaoka (1997) pp.457-462.

83) Matsumoto T., Naitou H. and Tokuda S., "Gyrokinetic and gyro-fluid simulation of kinetic m = 1 mode instability", Proceedings of the International Workshop on Nonlinear MHD and Extended-MHD, Madison, April 30-May 2, 1997.

84) Matsumoto T., "Density Gradient Effects of m=1 Kinetic Internal Kink Mode", The Institute of Statistical Mathematics Cooperative Research Report 110, Proceedings of 1997-Workshop on MHD Computations-Numerical methods and optimization techniques in controlled thermonuclear fusion research- March, 1998, p.88-99.

85) Mitchell N., Bessette D., Okuno K. et al., " Conductor developpment for the ITER magnets". 15th Int. Conf. on Magnet Tech. (MT-15), (Beijiing) 1997

86) Miyamoto K., Akino N., et al., "Production of Multi-MW deuterium negative ion beams for Neutral beam injectors," 16th IAEA Fusion Energy conference,(Montreal 1996) IAEA-CN-64/GP-10, pp.547-554 (1997).

87) Miyamoto K., Fujiwara Y., Hanada M., et al., "Development of high power negative ion source/accelerator", Proc. of the joint meeting of the 8th Int. Symp. on the production and neutralization of negative ions and beams and 7th European workshop on the production and application of light negative ions, Giens, France, Dep.15, (1997).

88) Mori M., "Progress of fusion research with tokamak", Global Nuclear Symposium.

89) Nagashima A., Fujisawa T., Sugie T., et al., "Development of New Vacuum Window Seal for ITER Optical Diagnostics", Proc. of the Int. School of Plasma Physics "Piero Caldirola" Workshop on Diagnostics for Experimental Fusion Reactors (Varenna, 1997), Plenum Press, New York, 257 (1998).

90) Nakahira M., Kakudate S., Oka K., et al., "Remote Handling Test and Full Scale Equipment Development for ITER Blanket Maintenance", 17th Symp. on Fusion Engineering, Oct. 8, San Diego, USA (1997).

91) Nakajima H., et al., "4K mechanical properties of aged jacket materials for Superconducting coils, 15th Int. Conf. on Magnet Technology (MT-15), China, 1997.

92) Nakamura H., .Ladd P, et.al., ITER Fuelling, Pumping, Wall Conditioning System and Fuel Dynamics Analysis ibid.

93) Nakamura K., Suzuki S., Dairaku M., et al., "Disruption and sputtering erosions on SiC doped CFC", Proc. 8th Int. Conf. on Fusion Reactor Materials, P1-B039, Sendai, Japan, Oct. 26-31, (1997).

94) Nakamura K., Suzuki S., Tanabe T., et al., "Disruption erosions of various kinds of tungsten", Proc. 4th Int. Symp. on Fusion Nuclear Technology, Tokyo, Japan, April 6-11, (1997).

95) Nemoto M., Kusama Y., Afanassiev V.I., et al., "Beam Acceleration up to 1 MeV with 2-4wcH ICRF Waves and NBI", IEA Tripartite Workshop on TAE and Energetic Particle Physics, Naka Fusion Research Establishment, JAERI, February 25-27, 1997.

96) Neudatchin S.V., Shirai H., Takizuka T., et al., "Analysis of Transient Transport Processes on JT-60U Tokamak", 24th EPS Conf. on Controlled Fusion and Plasma Physics, Berchtesgaden, June 1997.

97) Nishikawa M., Baba A., Kawamura Y., et al., "Isotope Exchange Reactions on Ceramic Breeder Materials and Their Effect on Tritium Inventory", The 6th international workshop on Ceramic Breeder Blanket Interactions, Oct. 22-24 (1997), Mito, Japan.

98) Nishitani T., Ebisawa K., Johnson L.C., et al., "In-vessel neutron monitor using micro fission chambers for ITER", Workshop on Diagnostics for ITER, Varenna Italy (1997), Proc. "Diagnostics for Experimental Thermonuclear Reactor II" (to be published in Prenum PressÅj.

99) Nishitani T., Ishitsuka E., Kakuta T., et al., "Japanese contribution to ITER task of irradiation tests on diagnostics", ISFNT-4, Tokyo (1997), to be published in FED.

100) Obara K., Itou A., Kakudate S., et al., "Development of 15-m Long Radiation Hard Periscope for ITER In-vessel Viewing", International Symposium on Fusion Nuclear Technology - 4, Apr. 10, Tokyo (1997).

101) Obara K., Kakudate S., Oka K., et al., "Development of Radiation Hard CCD Camera and Camera Control Unit", 4th European Conference, Sept. 15, Cannes, France (1997).

102) Okumra Y., "Overview on R&D programme at JAERI", Proc. of the joint meeting of the 8th Int. Symp. on the production and neutralization of negative ions and beams and 7th European workshop on the production and application of light negative ions, Giens, France, Dep.15, (1997).

103) Okuno K., Vieira R. et al., " ITER model coil test program ". 15th Int. Conf. on Magnet Tech. (MT-15), (Beijiing) 1997

104) Onozuka M. Johnson G., Ioki K. et al, "Design progress of the vacuum vessel for ITER ". 17th Symposium on Fusion Eng. (San Diego) 1997

105) Putvinski S., Fujisawa N. et al., " Halo Current, runaway electrons, and disruption mitigation in ITER". 24th European Conference on Controlled Fusion and Plasma Physics (1997)

106) Sakamoto N., Nakagawa T., Nakamura K., et al., "Modifications of electron beam facility(OHBIS) for irradiated divertor element with cooling water channel", Proc. 4th Int. Symp. on Fusion Nuclear Technology, Tokyo, Japan, April 6-11, (1997).

107) Sakasai A. and JT-60 Team, "High Performance and Steady-state Experiments on JT-60U", Proc. of 17th Symposium on Fusion Engineering, San Diego, Vol. 1, 18 (1998).

108) Sakurai S., Hosogane N., Kodama K., et al., "Design of a compact W-shaped pumped divertor in JT-60U", FUSION TECHNOLOGY 1996 (1997) p.471-474.

109) Santoro R., Iida H. et al., " Status of radiation shielding analyses for ITER". 17th Symposium on Fusion Eng. (San Diego) 1997

110) Santoro R., Khripunov V., Iida H. et al., " Raionuclide production in th ITER water coolant". 17th Symposium on Fusion Eng. (San Diego) 1997

111) Sasaki T., Obara K., Itou A., et al., "Gamma Irradiation Test of Ultrasonic Transducer for High and Low Temperature Use", 4th European Conference, Sept. 14, Cannes, France (1997).

112) Seki M., "Material for ITER and Beyond" . 8th Int. Conference on Fusion Reactor Material (Sendai) 1997

113) Senda I., Shoji T., et.al., Optimization of plasma initiation in ITER tokamak, ibid.

114) Sengoku S., Kawashima H. and JFT-2M Group, "Extension of Coexistent Regime of H-mode with a Dense and Cold Divertor Plasma on JFT-2M", Bull. Amer. Phys. Soc. 42 (1997) 1962.

115) Sherman R.H., Taylor D.J., Honnell K.G., et al., "Radio-chemical Reactions between Tritium and Air", Proceedings of the Symposium on Fusion Engineering, San Diego, USA, 1997.

116) Shikazono N., Seki M., Current Status of Japanese ITER Activities, ibid.

117) Shimomura Y., Saji G., ITER Safety and Operational Scenario, ibid.

118) Shirai H., "Confinement and Transport Properties in JT-60U Improved Mode", US-Japan JIFT Workshop on "Turbulence and Transport in Toroidal Plasmas", February 23-25, 1998, JAERI Naka.

119) Smid I., Akiba M., Vieider G., et al., "Development of bonding, tungsten armor and copper alloys for plasma-interactive components", Proc. 8th Int. Conf. on Fusion Reactor Materials, OI-07, Sendai, Japan, Oct. 26-31, (1997).

120) Sugihara M., Federici G., et al., " Modelling of wall pumping, fuelling and associated density behaviour in tokamaks". 24th European Conference on Controlled Fusion and Plasma Physics (1997)

121) Sugimoto M., et al., "Development of CS insert coil", 15th Int. Conf. on Magnet Technology (MT-15), China, 1997.

122) Suzuki S., T. Suzuki T., Araki M., et al., "Development of divertor plate with CFCs bonded onto DSCu cooling tube for fusion reactor application", Proc. 8th Int. Conf. on Fusion Reactor Materials, P3-A014, Sendai, Japan, Oct. 26-31, (1997).

123) Tada E., Kakudate S., Oka K., et al., "Development of Remote Maintenance Equipment for ITER Blankets", International Symposium on Fusion Nuclear Technology - 4, Apr. 10, Tokyo (1997).

124) Tado S., Kitamura K., et.al., Dynamic Analysis of Tokamak support system in ITER, ibid.

125) Takeda N., Akou K., Kakudate S., et al., "Development of Divertor Cassette Transporters in ITER", 17th Symp. on Fusion Engineering, Oct. 8, San Diego, USA (1997).

126) Takeuchi K., et al., "Quench analysis of 46kA-13T Nb3Al insert coil, 15th Int. Conf. on Magnet Technology (MT-15), China, 1997.6) Tsuji H., et al., "ITER central solenoid model coil outer module; Design and fabrication", 15th Int. Conf. on Magnet Technology (MT-15), China, 1997.

127) Takizuka T., "Confinement Scaling and Edge Barrier", US-Japan JIFT Workshop on "Turbulence and Transport in Toroidal Plasmas", February 23-25, 1998, JAERI Naka.

128) Takizuka T., "Offset Log-linear Law Scaling for ELMy H-mode Confinement", ITER Combined Workshop of Confinement and Transport Expert Group and Confinement Databaseand Modeling Expert Group, April 14-18, 1997, San Diego.

129) Takizuka T., "Reduction of the Uncertainty in the Threshold Power Scaling", ITER Combined Workshop of Confinement and Transport Expert Group and Confinement Database and Modeling Expert Group, April 14-18, 1997, San Diego.

130) Tamai H., Konoshima S., Asakura N., et al., "Behaviour of Radiation Power Loss from Radiative Divertor with Reversed Shear Plasmas in JT-60U", 24th European Physical Society Conference on Controlled Fusion and Plasma Physics 21A II, 493 (1997).

131) Tanabe T., Akiba M., Ueda Y., et al., "On the utilization of high Z materials as plasma facing component", Proc. 4th Int. Symp. on Fusion Nuclear Technology, Tokyo, Japan, April 6-11, (1997).

132) Tanaka S., Matera R. et al., " ITER materials R&D data bank". 8th Int. Conference on Fusion Reactor Material (Sendai) 1997

133) Taneda M., et al., "Design of Superconducting coil interface for ITER magnet system, 15th Int. Conf. on Magnet Technology (MT-15), China, 1997.

134) Tobita K., Harano H., Hamamatsu K., et al., "Transport and Losses of Energetic Tritons and Beam Ions in JT-60U", IEA Tripartite Workshop on TAE and Energetic Particle Physics, Naka Fusion Research Establishment, JAERI, February 25-27, 1997.

135) Tobita K., Hamamatsu K., Harano H., et al., "Ripple losses of fast particles from reversed magnetic shear plasmas", Proc. 24th European Conference on Controlled Fusion and Plasma Physics, Berchtesgaden,Vol. 21A, Part II, 717(1997).

136) Tobita K., Hamamatsu K., Harano H., et al., "Fast Ion Confinement in JT-60U and Implication for ITER", IAEA TCM on Alpha Particles.

137) Tobita K., Hamamatsu K., Harano H., et al., "Ripple Losses of Fast Particles from Reversed Magnetic Shear Plasmas", 24th EPS Conf. on Controlled Fusion and Plasma Physics, Berchtesgaden, June 1997.

138) Tokuda S., Naitou H. and Lee W W., "A Particle-Fluid Hybrid Simulation Model Based on Nonlinear Gyrokinetics", Proceedings of the International Workshop on Nonlinear MHD and Extended-MHD , Madison, April 30-May 2, 1997.

139) Topilski L., Inabe T. et al., " Validation and verification of ITER safety computer codes ". 7th Symposium on Fusion Eng. (San Diego) 1997

140) Topilski L.N., Seki Y., Kurihara R., et al., "Validation and Verification of ITER safety computer codes", Proc. of Symposium on Fusion Engineering (SOFE'97), San Diego (1997).

141) Trainham R., Jacquot C., Riz D, et al., "Long pulse operation of the Kamaboko negative ion source on the Mantis test bed", Proc. of the joint meeting of the 8th Int. Symp. on the production and neutralization of negative ions and beams and 7th European workshop on the production and application of light negative ions, Giens, France, Dep.15, (1997).

142) Tsunematsu T., Namba H., et.al., Effect of seismic isolation on Tokamak in ITER, ibid.

143) Ulrickson M., Tivey R., Akiba M., et al., "The status of development and testing of mock-ups of the ITER high-heat-flux components", Proc. 4th Int. Symp. on Fusion Nuclear Technology, Tokyo, Japan, April 6-11, (1997).

144) Watanabe K., Akino N., Aoyagi T., et al.,"Recent progress of high power negative ion beam development for fusion plasma heating", Proc. of the 7th International Symp. on Advanced Nuclear Energy Research, Takasaki, March 18 - 20 (1997).

145) Watanebe K., Fujiwata Y., Hanada M., et al., "Multi-stage, multi-aperture electrostatic accelerator for H-beam", Proc. of the joint meeting of the 8th Int. Symp. on the production and neutralization of negative ions and beams and 7th European workshop on the production and application of light negative ions, Giens, France, Dec.15, (1997).

146) Yamagiwa M., Koga J., Ishida S., "Nonlinear Fokker-Planck Analysis of Ion Temperature in JT-60U Hot Ion Plasma", 24th Europian Physical Society Conf. on Controlled Fusion and Plasma Physics (EPS, Berchtesgaden, 1997)

147) Yokomine T., Shimizu A., Akiba M., et al., "Numerical simulation of erosion of gas-solid suspension flow in a pipe with a twisted-tape insert", Proc. 1997 ASME Fluids Engineering Division Summer Meeting, pp.1-8, Bancouver, Canada, June 22-26, 1997.

148) Yoshida K., Iida F., et.al., Protection Measures for Selected ITER Magnet System Off-Normal Conditions, ibid.

149) Yoshino R. and JT-60 Team, "Plasma Control Experiments in JT-60U", Proc. of 36th IEEE Conf. on Design and Control, San Diego, 4, 3709 (1997)

A.1.4 List of other papers

1) Araki M., "Analyses of divertor HHFCs under ITER conditions ", ITER/EDA Working Meeting on L-5 R&D

2) Araya T., Koizumi K., " Current status and preliminary results of full scale model sector-A ", ITER/EDA Working Meeting on Vacuum Vessel

3) Barabash V., Tanaka S. et al., " Beryllium Assessment and Recommendation for Application in ITER Plasma Facing Components ", 3rd IEA Int. Workshop on Beryllium Technology for Fusion

4) Costley A., Ebisawa K. et al., " Measurements of plasma parameters". ITER/EDA FDR Document: ITER Phys. Base, Chap. 7 (1997)

5) DiPietro E., Inoue T. et al, "The design of the High Heat Flux Components of ITER Neutral Beam Injection System ", 6th Conf. on Engineering Problems of Thermonuclear Reactors

6) Ebisawa K., "Stationary Dust Monitoring System ", ITER/EDA Working Meeting on Dust Task

7) Ebisawa K., " VUV Divertor Impurity Monitor for ITER ", Workshop on Diagnostics for Experimental Fusion Reactors

8) Ebisawa K., "Dust Survey Fiber Scope ", ITER/EDA Working Meeting on Dust Task

9) Fujita, T., "Effect of negative shear on plasma confinement (1) -Experimental investigation -" J. Plasma and Fusion Research Vol 73, No.6, 549(1997).

10) Fujisawa N., " Capabilities of the ITER NBI systems ", ITER/EDA Phys. Expert Meeting on Heating and Current Drive (Naka)

11) Fujiwara Y., Miyamoto N. etal., "Temperature Control of Plasma Grid for Continuous Operation in Cesium-Seeded Volume Negative Ion Source ", 7th Int. Conf. on Ion Sources

12) Hashimoto M., "Safety Analysis on ITER test blanket Modules ", ITER/EDA Technical Meeting on Safety and Environment

13) Hirose A., Yamagiwa M., "Effects of Radial Gradient of the Shafronov Shift on the Kinetic Balooning and Drift Type Modes in High Performance Tokamaks", University of Suskatchewan Plasma Physics Laboratory Report, PPL-166 (1997).

14) Honda T., Inabe T., " Analysis of loss of vacuum and estimation of dust release ", ITER/EDA Design Task Report (D328-JA-2)

15) Honda T., Inabe T., " Analysis of loss of vacuum and radiation release ", ITER/EDA Design Task Report (D328-JA-3)

16) Hoshi Y., Matsumoto H., Maruyama S. Ito K. et al., " Water cooling system". ITER/EDA FDR Document: DDD Sec 4.3 (1997)

17) Ide S., Naito O., Ushigusa K., et al., "RF Experiments on JT-60U", Second Europhysics Topical Conference on RF Heating and Current Drive of Fusion Devices, Brussels, BELGIUM (1997).

18) Ide S. and the JT-60 Team, "Progress in Physics R&D withLHCD", Tripatite Large Tokamak Workshop (W39) on "Optimization of Heating and Current Drive for Improved Tokamak Performance", Naka, JAPAN (1997).

19) Ide S., Naito O., Ushigusa K., et al., "LHCD Current Profile Optimization in Reversed Shear in JT-60U", Tripatite Large Tokamak Workshop on "Optimization of Heating and Current Drive for Improved Tokamak Performance", Naka, JAPAN (1997).

20) Inabe T., Hashimoto M., Mitsui J., Okazaki T., " Task report for assissting JCT in preparation for NSSR-1 Volume II - Safety Design- ", ITER/EDA Design Task Report (D328-JA-2)

21) Inoue T., " The vacuum insulated beam source ", ITER/EDA Working Meeting on Review of NBI

22) Inoue T., " Status of neutronic calculations ", ITER/EDA Working Meeting on Review of NBI

23) Inoue T., " The Design of electrostatic stress shields and triple point protection ", ITER/EDA Working Meeting on Review of NBI

24) Ioki K., " ITER Vacuum Vessel Issues ", ITER/EDA Working Meeting on Vacuum Vessel

25) Ioki K., " Shielding blanket design overview ", ITER/EDA Working Meeting on Blanket (Garching)

26) Ishida S., Takeji S., Isayama A., et al., "Termination of High Performance High-bp H-mode and Reversed Shear Discharges in JT-60U", Trilateral Workshop on High Performance Regimes, JET (1997).

27) Johnson L., Ebisawa K. et al., "Plasma Management Capability of ITER Diagnostic System ", APS Meeting of the Division of Plasma Physics

28) Kajiura S., Araya T., Koizumi K., "Structural design of horizontal and lower port ", ITER/EDA Working Meeting on Vacuum Vessel

29) Kamada Y., Ishida S., Ozeki T., et al., "Achievement of break-even condition in JT-60 and prospect for fusion reactor development", J. Atomic Energy Society of Japan, Vol39, 31 (1997).

30) Kikuchi M., Seki Y., Nakagawa K., "The Advanced SSTR", 6th IAEA-TCM on Fusion Power Plant Design and Technology.

31) Kodama T., " Back plate structural analysis ", ITER/EDA Working Meeting on Blanket (Garching)

32) Koizumi K. , " Fabrication of full-scale sector model". ITER/EDA Design Task Report (T204-209/ Subtask-1)

33 Koizumi K., Usami S., Shibui M., " Weld joint analysis between outer skin and poloidal rib -TW-EB weld joint -Insert TIG weld joint ", ITER/EDA Working Meeting on Vacuum Vessel

34) Koizumi K., " Overview of the progress in full-scale sector model -Design , fabrication and test plan-", ITER/EDA Working Meeting on Vacuum Vessel

35) Koizumi K., Obara K., "Activity on T204-9 Subtask-2 ", ITER/EDA Working Meeting on Vacuum Vessel

36) Koizumi K., Itou Y., "Assessment of fabrication and assembly procedure ", ITER/EDA Working Meeting on Vacuum Vessel

37) Koizumi K. , " Design and analysis of the ITER vacuum vessel". ITER/EDA Design Task Report (D201)

38) Koizumi K., Abe M., " Seismic analysis of ITER vacuum vessel using simplified coil and VV 360 degree model ", ITER/EDA Working Meeting on Vacuum Vessel

39) Koizumi K. , " Vacuum vessel design : Subtask 1, 3, 5". ITER/EDA Design Task Report (D306)

40) Koizumi K., " L-3 Vacuum Vessel Sector ", ITER/EDA TAC-12 Meeting

41) Krylov A., Hanada M. et al., " Beam transmission in the ITER neutral beam injection ", 8th Int. Symp. on the production and neutralization of negative ions and beams

42) Kubo H. and Sawada K., "Volume recombination in Divertor Plasmas", J. Plasma and Fusion Research, 74, 562 (1998).

43) Kunugi T., Takase K., Shibata M., et al., "Thermofluid Tests for Fusion Reactor Safety Part 3, Test Results of the ICE Experiment at Vacuum Conditions and the LOVA experiment at Various Breach Combinations", JAERI-memo 09-052 (1997).

44) Kurihara R., Ajima T., "TRAC-BF1 Pre- and Post-test Calculation Results", ICE/LOVA and Code Validation Meeting, San Diego, February 17, 1998.

45) Kurihara R., Ajima T., Kunugi T., et al., "Analysis and Experimental Results on Ingress of Coolant Event in Vacuum Vessel", 4th Int. Symp. on Fusion Nuclear Technology, April 1997.

46) Maki K., Inabe T., " Analysis of ITER skyshine dose ", ITER/EDA Design Task Report (D328-JA-2)

47) Maruo T., Inabe T., Mitsui J., " Safety design guideline for confinement ", ITER/EDA Design Task Report (D328-JA-2)

48) Maruo T., Mitsui J., Inabe T., Honda T., Nakayama T., Okazaki T., " Task report for assissting JCT for NSSR-2 Volume II - Safety Design- ", ITER/EDA Design Task Report (D328-JA-3)

49) Matsuda T., "Remote Laboratory in JT-60, Present Status and Future Plan", RIST NEWS No.24 (1997).

50) Miki M., " Comments on ISDC ", ITER/EDA Working Meeting on MPH and ISDC

51) Miki N., " EM anlysis on blanket ", ITER/EDA Working Meeting on Blanket (Garching)

52) Moriyama T., Okawa Y. et al., " Concept and technical issues of electromagnetic-insulated buildings ", 3rd Int. Symp. on Non-metallic Reinforcement for Concrete Structure

53) Murano Y., Okawa Y. et al., " Insulation breakdown and radiation resistance of primary construction materials for electromagnetic insulated buildings ", 3rd Int. Symp. on Non-metallic Reinforcement for Concrete Structure

54) Neyatani Y., Yoshino R., "Halo Current Measurement in JT-60U", 7th Workshop of ITER Disruption, Plasma Control and MHD Expert Group, Lausanne (1997).

55) Nishio S., Ueda S., Aoki I., et al., "Improved Tokamak Concept Focusing on Easy Maintenance", 4th Int. Symp. on Fusion Nuclear Technology, April 1997.

56) Nishio S., Ueda S., Kurihara R., et al., "Prototype Tokamak Fusion Power Reactor Based on SiC/SiC Composite Material, Focusing on Easy Maintenance", 6th IAEA Technical Committee Meeting on Fusion Power Plant Design, Fusion Engineering and Design, March, 1998.

57) Ohkawa Y., " Supervisory control system design support ". ITER/EDA Design Task Report (D325/JA-P3)

58) Ohkawa Y., " Preliminary study on fire protection". ITER/EDA Design Task Report (D325/JA-B7)

59) Ohkawa Y., Yagenji A., " Structual study on the tokamak buildings". ITER/EDA Design Task Report (S62TD11FJ, D325/JA-B8)

60) Ohkawa Y., " Structual study of HTS vault". ITER/EDA Design Task Report (D325/JA-B6)

61) Ohkawa Y., " Detail design of the divertor heat transfer system". ITER/EDA Design Task Report (D312)

62) Ohkawa Y., " Hot cell and waste treatment processes". ITER/EDA Design Task Report (D326/JA)

63) Ohkawa Y., " Structual study on penetration". ITER/EDA Design Task Report (D325/JA-B4)

64) Ohkawa Y., Hashimoto M., Ohno I., " Detail design of the divertor heat transfer systems". ITER/EDA Design Task Report (D313)

65) Ohkawa Y., " Heat rejection system design support ". ITER/EDA Design Task Report (D325/JA-P2)

66) Ohkawa Y., " Waste treatment and storage". ITER/EDA Design Task Report (D232)

67) Okazaki T., Maruo T., Inabe T., " Safety design guideline for reliability ", ITER/EDA Design Task Report (D328-JA-2)

68) Okazaki T., Mitsui J., Hashimoto M., Inabe T., " Safety design guideline for maintenance ", ITER/EDA Design Task Report (D328-JA-2)

69) Okuno K., " CS Model Coil Schedule Summary ", ITER/EDA Working Meeting of CS Model Coil Coordination

70) Okuno K., " Implementation Plan for the Test Programme for the CS Model Coil and Inserts ", ITER/EDA Working Meeting on CS Model Coil Test Programme

71) Okuno K., " CS Model Coil Schedule Summary ", ITER/EDA Working Meeting on CS Model Coil Coordination (San Diego)

72) Okuno K., " CS model coil status ", ITER/EDA Working Meeting on TF Model Coil Project Review (Belfort)

73) Okuno K., " Schedule summary ", ITER/EDA Working Meeting on CS Model Coordination (Karlsruhe)

74) Okuno K., " Future plan for test program group, testing group and test description document ", ITER/EDA Working Meeting on CS Model Coordination (Karlsruhe)

75) Omomo J., Okawa Y. et al., " Electric insulation, dielectric properties and electromagnetic shielding properties of primary construction materials of electromagnetic insulated buildings ", 3rd Int. Symp. on Non-metallic Reinforcement for Concrete Structure

76) Onozuka M., "Main Vessel Design ", ITER/EDA Working Meeting on Vacuum Vessel

77) Ozaki F., " Blanket RH status and issues ", ITER/EDA Working Meeting on Blanket (Garching)

78) Ozawa Y., " Introductory presentation on 4th QA meeting from the JAHT ", ITER/EDA Technical Meeting on Quality Assurance

79) Ozawa Y., " JAHT Review on QA documents ", ITER/EDA Technical Meeting on QA

80) Ozawa Y., " Cost estimation for FDR". ITER/EDA Design Task Report (S93TD05FJ)

81) Seki Y., Tabara T., Aoki I., et al., "Composition Adjustment of Low Activation Material for Shallow Land Disposal", 6th IAEA Technical Committee Meeting on Fusion Power Plant Design, Fusion Engineering and Design, March, 19.

82) Seki Y., Ueda S., Nishio S., "Impact of Low Activation Materials to Fusion Reactor Design", ICFRM-8, International Conference of Fusion Materials, October, 1997.

83) Seki Y., "Overview of the Japanese Fusion Reactor Studies Programme", 6th IAEA Technical Committee Meeting on Fusion Power Plant Design, March, 1998.

84) Senda I., Takase H., Yaguchi E., Sugimoto M., Shoji T., Tsunematsu T. , " Eddy current analyses", ITER/EDA Design Task Report (MD-10 subtask)

85) Senda I., Shoji T., Nishio T., " Dynamical analysis of the plasma control for FDR ", ITER/EDA Working Meeting on Poloidal Field Scenario & Control

86) Shibui M., Koizumi K., "Thermo-hydraulic analyses of vacuum vessel ", ITER/EDA Working Meeting on Vacuum Vessel

87) Shibui M., Koizumi K., "Current status of sector-B fabrication ", ITER/EDA Working Meeting on Vacuum Vessel

88) Shoji T., " Outline of the JA design task D318J ", ITER/EDA Working Meeting on Coil Power Supply and Distribution System Design

89) Shoji T., Senda I., Fujieda H. et al, " PF Configuration and scenario study for FDR ", ITER/EDA Working Meeting on Poloidal Field Scenario & Control

90) Sugie T., Ogawa H., Katsunuma J., et al., "Divertor Impurity Monitor for ITER", Proc. of the Int. School of Plasma Physics "Piero Caldirola" Workshop on Diagnostics for Experimental Fusion Reactors (Varenna, 1997), Plenum Press, New York, 327 (1998) .

91) Sugihara M., "Present status of ITER edge divertor database ", ITER/EDA Phys. Expert Meeting on Divertor Physics and Divertor Modeling & Database

92) Tado S., " VV/TF coil removal procedure and issues ", ITER/EDA Working Meeting on VV/Backplate Maintenance

93) Tado S., Koizumi K., " Dynamic analysis of ITER Tokamak ", ITER/EDA Working Meeting on Vacuum Vessel

94) Tado S., Koizumi K., " Manufacturing and assembly tolerance of ITER Tokamak components ", ITER/EDA Working Meeting on Vacuum Vessel

95) Takahashi K., "T301 task overview ", ITER/EDA Working Meeting on VV/Backplate Maintenance

96) Takahashi K., " VV maintenance procedure and issues ", ITER/EDA Working Meeting on VV/Backplate Maintenance

97) Takahashi K., " Welding / Cutting plan for VV ", ITER/EDA Working Meeting on VV/Backplate Maintenance

98) Takahashi K., " Current status of blanket backplate design ", ITER/EDA Working Meeting on VV/Backplate Maintenance

99) Takahashi K., " Current status of VV top port design ", ITER/EDA Working Meeting on VV/Backplate Maintenance

100) Takase H., Senda I., Shoji T., Tsunematsu T. et al., " Design Task D324-2 ; Dynamical analysis of the plasma control ", ITER/EDA Working Meeting on Poloidal Field Scenario & Control

101) Takigami H., " Validation of the thermohydraulic simulation with extra cooling circuit ", ITER/EDA Working Meeting on Conductor Analysis

102) Takigami H., " Validation of the thermohydraulic simulation ", ITER/EDA Working Meeting on CS Model Coil Test Programme

103) Takigami H., " Estimation of CSMC cable performance ", ITER/EDA Working Meeting on CSMC Test Program (Naka)

104) Takigami H., " Processing of CSMC data to assess cable performance ", ITER/EDA Working Meeting on SC Design Criteria (Cadarache)

105) Takizuka T., Shimizu K., "Transport Simulation of Neutral Particles", in "Synthetical Study on Physical and Chemical Processes of High-heat-flux Plasma Flame", edited by Takamura S. (Nagoya Univ., 1997) pp.335-343.

106) Tanaka S., " Status of Experimental Data Related to Be in ITER Materials R&D Data Bank ", 3rd IEA Int. Workshop on Beryllium Technology for Fusion

107) Tokuda S., "Effect of Magnetic Perturbations on Runway Electrons Generation", 7th Workshop of ITER Disruption, Plasma Control and MHD Expert Group, Lausanne (1997).

108) Tsunematsu T., " Cost and schedule control". ITER/EDA Design Task Report (D329, G16TD78FJ)

109) Ueda S., Nishio S., Seki Y., et al., "A Fusion Power Reactor Concept Using SiC/SiC Composites", ICFRM-8, International Conference of Fusion Materials, October, 1997.

110) Ueda S., Nishio S., Yamada R., et al., "Maintenance and Material Aspects of DREAM Reactor", 6th IAEA Technical Committee Meeting on Fusion Power Plant Design, Fusion Engineering and Design, March, 1998.

111) Ushigusa K., "Present Status of JT-60SU Design", The first Japan-China Workshop on Improved Performance in Toroidal Plasmas, ASIPP, Hefei Anhui P.R.China (1997).

112) Ushigusa K., "Steady-state Improved Performance in JT-60U", The first Japan-China Workshop on Improved Performance in Toroidal Plasmas, ASIPP, Hefei Anhui P.R.China (1997).

113) Watanabe K., Fujiwara Y. et al., " Development of a multiaperture, fivestage electrostatic accelerator for hydrogen negative ion beams ", 7th Int. Conf. on Ion Sources

114) Yamagiwa M., Hirose A., Elia M., "Kinetic Ballooning Modes at the Tokamak Transport Barrier with Negative Magnetic Shear", University of Saskatchewan, Plasma Physics Laboratory Report, PPL-167 (1997).

115) Yamamoto S., " Overview of the T246 irradiation task ", ITER/EDA T246 Related Working Meeting

116) Yamamoto S., " Radiation effects". ITER/EDA FDR Document: DDD Sec 5.5 (1997)

117) Yamamoto S., " Irradiation Tests on ITER Diagnostic Components ", Workshop on Diagnostics for Experimental Fusion Reactors

118) Yamamoto S., " Present Status of ITER Diagnostics Development and Specification of Problems of Radiation Effects in Ceramics ", IEA Workshop on Radiation Effects in Ceramic Insulators

119) Yamamoto S., " Status of R&D on magnetics ", ITER/EDA Phys. Expert Meeting on Diagonostics (San Diego)

120) Yamamoto S., " Report on ceramics R&D program and ICFRM Meeting ", ITER/EDA Phys. Expert Meeting on Diagonostics (San Diego)

121) Yonekawa I., " Data Acquisition and Management Requirement for ITER ", IAEA TCM on Data Acquisition and Management for Fusion Research

122) Yoshino R., "Runaway Termination in JT-60U", 7th Workshop of ITER Disruption, Plasma Control and MHD Expert Group, Lausanne (1997).

Appendix

A.2 Personnel and Financial Data

A.2.1 Change in number of personnel and annual budget (FY 1988-1997)

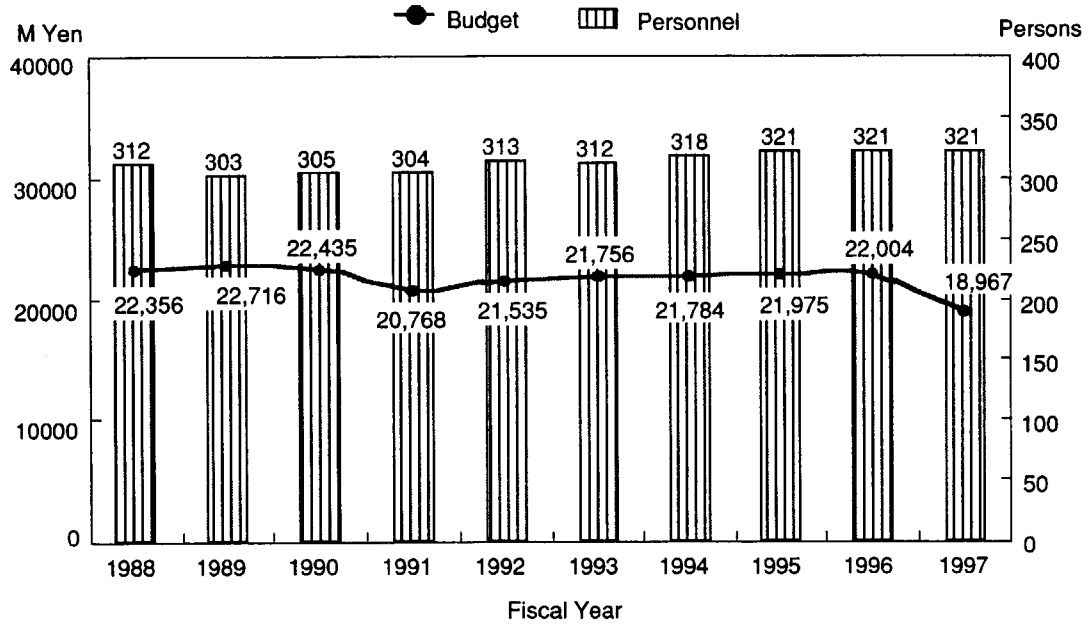

A.2.2 Organization Chart(Mar. 31, 1998)

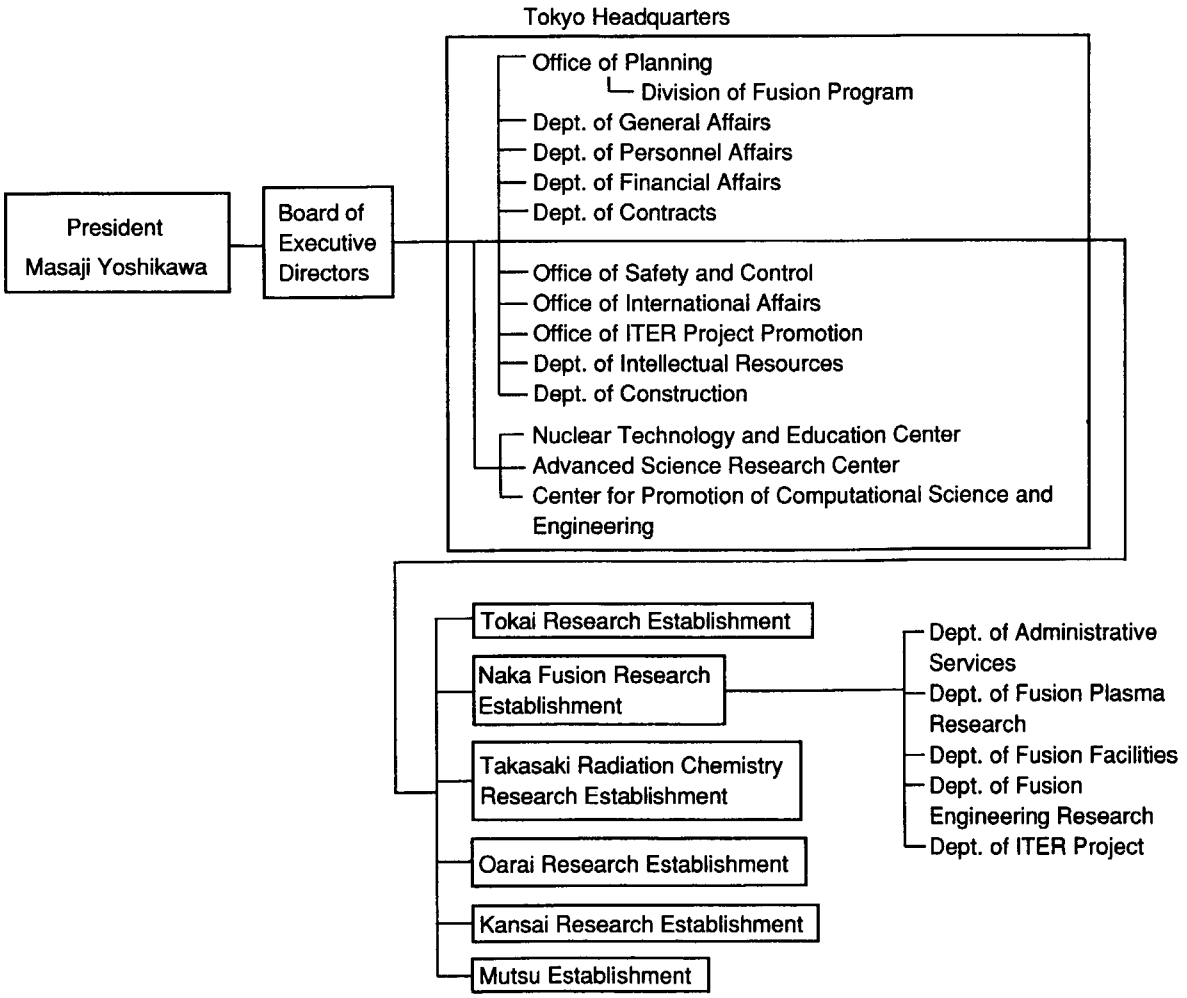

A.2.3 Scientific Staffs in the Naka Fusion Research Establishment (April, 1997 - March, 1998)

Naka Fusion Research Establishment

KISHIMOTO Hiroshi	(Director General)
OHKAWA Tihiro	(Scientific Consultant)
SEKIGUCHI Tadashi	(Scientific Consultant)
TANAKA Yuji	(Scientific Consultant)
MIYAMOTO Kenro	(Invited Researcher)
KAWASAKI Sunao	(Invited Researcher)
SHIMAMOTO Susumu	(Invited Researcher)
TOMABECHI Ken	(Invited Researcher)

Department of Administrative Services

KOMAKI Akira	(Director)

Department of Fusion Plasma Research

AZUMI Masafumi	(Director)
NAGAMI Masayuki	(Deputy Director)
TAKAHASHI Ichiro	(Administrative Manager)

Tokamak Program Division

NAGAMI Masayuki	(General Manager)	
IDE Shunsuke	ISHIDA Shinichi	KITAI Tatsuya (*15)
KURITA Gen-ichi	MORI Katsuharu (*15)	NAGASHIMA Keisuke
NAKAGAWA Shouji (*15)	OGURI Shigeru (*15)	TOYOSHIMA Noboru
USHIGUSA Kenkichi		

Plasma Analysis Division

KIKUCHI Mitsuru	(General Manager)	
HAMAMATSU Kiyotaka	HASEGAWA Yukihiro	KISHIMOTO Yasuaki
KOIWA Motonao (*31)	MATSUDA Toshiaki	NAITO Osamu
NAKAMURA Yukiharu	NEUDATCHIN Sergei V. (*23)	
OHSHIMA Takayuki	POLEVOI Alexei (*11)	SAITO Naoyuki
SAKATA Shinya	SATO Minoru	SHIMIZU Katsuhiro
SHIRAI Hiroshi	SUZUKI Mitsuhiro (*33)	TAKIZUKA Tomonori
TSUGITA Tomonori		

Large Tokamak Experiment Division I

MORI Masahiro	(General Manager)	
CHIBA Shinichi	FUKUDA Takeshi	HAMANO Takashi
ISAYAMA Akihiko	ISEI Nobuyuki	INOUE Akira
IWASE Makoto (*36)	KAMADA Yutaka	KASHIWABARA Tsuneo
KAWANO Yasunori	KITAMURA Shigeru	KOKUSEN Shigeharu
KRAMER Gerrit Jakob (*41)	KUSAMA Yoshinori	MENG Yuedong (*8)
MORIOKA Atsuhiko	NAGAYA Susumu	NEMOTO Hirofumi
NEMOTO Masahiro	NEYATANI Yuzuru	NISHITANI Takeo
OIKAWA Toshihiro	SAKUMA Takeshi	SHITOMI Morimasa
SUNAOSHI Hidenori	TAKEJI Satoru	
TCHERNYCHEV Fedor Vsevodovich (*9)		TOBITA Kenji
TSUCHIYA Katsuhiko	TSUKAHARA Yoshimitsu	UEHARA Kazuya
URAMOTO Yasuyuki	YOSHIDA Hidetoshi	ZHAO Junyu (*8)

Large Tokamak Experiment Division II
YOSHINO Ryuji (General Manager)
ASAKURA Nobuyuki, DaCOSTA Olivier (*2), FUJITA Takaaki
HATAE Takaki, HIGASHIJIMA Satoru, HOSOGANE Nobuyuki
ITAMI Kiyoshi, KONDOH Takashi, KONOSHMA Shigeru
KOOG Joong San (*36), KUBO Hirotaka, NAGASHIMA Akira
SAKASAI Akira, SAKURAI Shinji, SHINOHARA Kouji
SUGIE Tatsuo, SUZUKI Shingo (*36), TAKENAGA Hidenobu

Plasma Theory Laboratory
HIRAYAMA Toshio (Head)
DETTRICK Sean (*41), HUDSON Stuart (*41), HAYASHI Mitsuru (*36)
ISHII Yasutomo, ISHIZAWA Akihiro (*36), OZEKI Takahisa
MATSUMOTO Taro, SUGAHARA Akihiro (*31), TOKUDA Shinji
TUDA Takashi, YAMAGIWA Mitsuru

Experimental Plasma Physics Laboratory
KIMURA Haruyuki (Head)
HOSHINO Katsumichi, KAWAKAMI Tomohide, KAWASHIMA Hisato
LIU Wandong (*49), MAEDA Mitsuru (*14), MAENO Masaki
MIURA Yukitoshi, OGAWA Hiroaki, OGAWA Toshihide
OASA Kazumi, SATO Masayasu, SENGOKU Seio
SHIINA Tomio, YAMAUCHI Toshihiko

Department of Fusion Facility
FUNAHASHI Akimasa (Director)
SHIMIZU Masatsugu (Deputy Director)

Fusion Facility Administration Division
TAKAHASHI Ichiro (General Manager)

JT-60 Facility Division I
KIMURA Toyoaki (General Manager)
ADACHI Hironori (*25), AKASAKA Hiromi, ARAKAWA Kiyotsugu
FUKUDA Hiroyuki (*15), FURUKAWA Hiroshi (*32), KAWAMATA Youichi
KURIHARA Kenichi, MATSUKAWA Makoto, MIURA M. Yushi
NOBUSAKA Hiromichi (*15), OKANO Jun, OMORI Shunzo
OMORI Yoshikazu, OOBA Toshio (*32), SEIMIYA Munetaka
SHIMONO Mitsuru, TAKANO Shoji (*33), TERAKADO Tsunehisa
TOTSUKA Toshiyuki

JT-60 Facility Division II
SAIDOH Masahiro (General Manager)
ARAI Takashi, HIRATSUKA Hajime, HONDA Masao
ICHIGE Hisashi, KAMINAGA Atsushi, KODAMA Kozo
KOMURO Ken-ichi (*28), MASAKI Kei, MIYATA Hiroshi (*6)
MIYO Yasuhiko, MORIMOTO Masaaki (*27), OKABE Tomokazu
SANO Junya (*12), SANTO Masahide (*6), SASAJIMA Tadayuki
SASAKI Noboru (*6), TAKAHASHI Shoryu (*6), YAGYU Jun-ichi

RF Facility Division
YAMAMOTO Takumi (General Manager)
ANNOU Katsuto, IKEDA Yoshitaka, ISAKA Masayoshi
ISHII Kazuhiro (*32), HIRANAI Shinichi, HIROI Toshikazu (*42)

KAJIYAMA Eiichi (*28) KIYONO Kimihiro MORIYAMA Shinichi
SEKI Masami SHINOZAKI Shin-ichi TERAKADO Masayuki
YOKOKURA Kenji

NBI Facility Division
KURIYAMA Masaaki (General Manager)
AKINO Noboru EBISAWA Noboru HONDA Atsushi
ITOH Takao KAWAI Mikito KAZAWA Minoru
MOGAKI Kazuhiko OHGA Tokumichi OHSHIMA Katsumi (*28)
OHMORI Ken-ichiou OOHARA Hiroshi SEKI Hiroshi (*32)
TAKENOUCHI Tadashi (*47) TANAI Yutaka (*32)
TOYOKAWA Ryoji(*28) USUI Katsutomi YAMAZAKI Haruyuki (*6)
ZHOU Capin(*40) GRISHAM Larry (*37) HU Liquen (*8)

JFT-2M Facility Division
KOIKE Tsuneyuki (General Manager)
YAMAMOTO Masahiro (Deputy General Manager)
HASEGAWA Koichi KASHIWA Yoshitoshi KIKUCHI Kazuo
KOMATA Masao OKANO Fuminori SAWAHATA Masayuki
SHIBATA Takatoshi SUZUKI Sadaaki TANI Takashi
UMINO Kazumi (*32)

Department of Fusion Engineering Research
OHTA Mitsuru (Director)
NAGASHIMA Takashi (Deputy Director)
MURASAWA Michihiko (Administrative Manager)

Blanket Engineering Laboratory
TAKATSU Hideyuki (Head)
ABE Tetsuya ENOEDA Mikio FURUYA Kazuyuki
HARA Shigemitsu (*6) HATANO Toshihisa KASAI Satoshi
KANARI Moriyasu (*36) KIKUCHI Shigeto (*48) KURODA Toshimasa (*19)
NAKAMURA Jyun-ichi (*35) SATO Satoshi YANO Atsushi (*35)

Superconducting Magnet Laboratory
TSUJI Hiroshi (Head)
ANDO Toshinari AZUMA Katsunori (*6) HAMADA Kazuya
HANAWA Hiromi (*32) HIYAMA Tadao ISONO Takaaki
ISHIO Koutarou (*13) KATO Takashi KAWANO Katsumi
KOIZUMI Norikiyo MATSUI Kunihiro NAKAJIMA Hideo
NUNOYA Yoshihiko OSHIKIRI Masayuki (*32) SAWADA Kenji (*26)
SEKI Syuichi (*32) SHIMBA Toru (*10) SUGIMOTO Makoto
TAKAHASHI Yoshikazu TAKANO Katsutoshi (*32) TANEDA Masanobu (*20)
WAKABAYASHI Hiroshi (*32) YAMAMOTO Kazutaka (*48)

NBI Heating Laboratory
OKUMURA Yoshikazu (Head)
AKIBA Masao BANDOURKO Vassi (*11) BOSCARY Jean (*41)
DAIRAKU Masayuki EZATO Koichiro (*36) FUJIWARA Yukio
GILANYI Attila (*36) HANADA Masaya JIMBOU Ryutaro (*6)
MIYAMOTO Naoki (*30) MIYAMOTO Kenji NAKAMURA Kazuyuki
SAWAHATA Osamu (*32) SUZUKI Satoshi SUZUKI Takayuki (*6)
WATANABE Kazuhiro YOKOYAMA Kenji

RF Heating Laboratory

IMAI Tsuyoshi	(Head)	
IKEDA Yukiharu	KASUGAI Atsushi	KATO Yasushi (*32)
KOARAI Tohru (*32)	MAEBARA Sunao	NUMATA Hideyuki (*29)
SAKAMOTO Keishi	SHIHO Makoto	TAKAHASHI Koji
TSUNEOKA Masaki	WATANABE Akihiko (*29)	ZHENG Xaodong (*36)

Tritium Engineering Laboratory

NISHI Masataka	(Head)	
ARITA Tadaaki (*42)	HAYASHI Takumi	ISHIDA Toshikatsu (*19)
ISOBE Kanetsugu (*24)	ITO Takeshi (*17)	IWAI Yasunori
KAKUTA Toshiya (*19)	KAWAMURA Yoshinori	KOBAYASHI Kazuhiro
MARUYAMA Tomoyoshi (*27)		NAKAMURA Hideki (*48)
NAKAMURA Hirofumi	O'HIRA Shigeru	SHU Weimin
SUZUKI Takumi	TADOKORO Takahiro (*6)	YAMADA Masayuki
YAMANISHI Toshihiko		

Reactor System Laboratory

SEKI Yasushi	(Head)	
AOKI Isao	AJIMA Toshio (*6)	KURIHARA Ryoichi
NISHIO Satoshi	UEDA Shuzo	

Reactor Structure Laboratory

TADA Eisuke	(Head)	
AKOU Kentaro (*19)	ITOU Akira (*10)	KAKUDATE Satoshi
NAKAHIRA Masataka	OBARA Kenjiro	OKA Kiyoshi
TAGUCHI Kou (*32)	TAKAHASHI Hiroyuki (*6)	
TAKIGUCHI Yuji (*48)	TAKEDA Nobukazu	

Department of ITER Project

MATSUDA Shinzaburo	(Director)
SEKI Masahiro	(Prime Scientist)
SHIMOMURA Yasuo	(Prime Scientist)
FUJISAWA Noboru	

Administration Group

SHOJI Kuniaki	(Leader)

Project Management Group

SEKI Shogo	(Leader)

Joint Central Team Group

SEKI Shogo	(Leader)	
ANDO Toshiro	EBISAWA Katsuyuki (*48)	HATTORI Yukiya (*6)
HIROKI Seiji	HORIKIRI Hitoshi (*39)	HOSHI Yuichi (*10)
IIDA Fumio (*6)	IIDA Hiromasa	IIZUKA Takayuki
IOKI Kimihiro (*27)	INOUE Takashi	ITOH Kazuyoshi (*42)
ITOH Mitsuyoshi (*10)	KATAOKA Yoshiyuki (*6)	KAWAI Shigetaka (*26)
KOBAYASHI Noriyuki (*48)	KODAMA Tetsuhiko (*27)	MARUYAMA So
MATSUMOTO Hiroshi	MIZOGUCHI Tadanori (*6)	MOHRI Kensuke (*19)
MORIYAMA Kenichi (*43)	MITA Yoshiyuki (*34)	MIKI Nobuharu (*48)
NAKASHIMA Yoshitane (*10)	NAKAMURA Hiroo	OIKAWA Akira
OKUNO Kiyoshi	ONOZUKA Masanori (*27)	OSANO Katsuharu (*5)

OZAKI Fumio (*48)	SAJI Gen	SATO Kouichi (*1)
SHIBANUMA Kiyoshi	SUGIHARA Masayoshi	
TAKAHASHI Kenji (*27)	TAKIGAMI Hiroyuki (*48)	TANAKA Shigeru
YAMADA Masao (*27)	YAMAMOTO Shin	YONEKAWA Izuru
YOSHIDA Hiroshi	YOSHIDA Kiyoshi	
YOSHIMURA Kunihiro (*48)		

Home Team Design Group

TSUNEMATSU Toshihide (Leader)

ARAKI Masanori	HASHIMOTO Masayoshi (*10)	ITOH Yutaka (*6)
KITAMURA Kazunori	KOIZUMI Koichi	MIURA Hidenori (*19)
MIYAMOTO Masanori (*18)	ODAJIMA Kazuo	OHMORI Jyunji (*48)
OHNO Isamu (*10)	OHKAWA Yoshinao	OZAWA Yoshihiro (*6)
SENDA Ikuo (*48)	SHIRAI Tetsuo (*44)	SHOJI Teruaki
TADO Shigeru (*26)	TAKASE Haruhiko (*48)	YAGENJI Akira (*4)

Safety Evaluation Group

INABE Teruo (Leader)

ARAKI Takao (*48)	MARUO Takeshi	MITSUI Jin (*42)

*1 Atomic Data Service Corp.
*2 Ecole Polytechnique (France)
*3 Fuji Electric Co., Ltd.
*4 Hazama-gumi Ltd.
*5 Hitachi Information Systems, Ltd.
*6 Hitachi Ltd.
*7 Hitachi Nuclear Engineering Co., Ltd
*8 Institute of Plasma Physics Academia Sinica (China)
*9 Ioffe Physical-Technical Institute (Russia)
*10 Ishikawajima-Harima Heavy Industries, Ltd.
*11 JAERI Fellowship
*12 Japan Expert Clone Corp.
*13 Japan Steel Works Ltd.
*14 JST Fellowship
*15 Kaihatsu Denki Co.
*16 Kajima Corporation
*17 Kaken Co.
*18 Kandenko Corp.
*19 Kawasaki Heavy Industries, Ltd.
*20 Kobe Steel Ltd.
*21 Korea Atomic Energy Research Institute (Korea)
*22 Kumagai-gumi Ltd.
*23 Kurchatov Institute (Russia)
*24 Kyushu University
*25 Mito Software Engineering Co.
*26 Mitsubishi Electric Co., Ltd.
*27 Mitsubishi Heavy Industries, Ltd.
*28 Nippon Advanced Technology Co., Ltd.
*29 Nissei Sangyo Co., Ltd.
*30 Nissin Electric Co., Ltd.
*31 Research Organization for Information Science Technology
*32 Nuclear Engineering Co., Ltd.
*33 Nuclear Information Service Co.

*34 Obayashi Corp.
*35 Osaka Vacuum Ltd.
*36 Post-Doctoral Fellow
*37 Princeton Plasma Physics Laboratory (USA)
*38 Shimizu Corparation
*39 Shinryo Corporation
*40 Southwestern Institute of Physics (China)
*41 STA Fellowship
*42 Sumitomo Heavy Industries, Ltd.
*43 Taisei Corp.
*44 Takenaka Corp.
*45 The Graduate University for Advanced Studies
*46 Troitsk Institute (Russia)
*47 Tomoe Shokai
*48 Toshiba Corp.
*49 University of Science and Technology (China)

This is a blank page.

国際単位系（SI）と換算表

表1　SI基本単位および補助単位

量	名称	記号
長さ	メートル	m
質量	キログラム	kg
時間	秒	s
電流	アンペア	A
熱力学温度	ケルビン	K
物質量	モル	mol
光度	カンデラ	cd
平面角	ラジアン	rad
立体角	ステラジアン	sr

表2　SIと併用される単位

名称	記号
分，時，日	min，h，d
度，分，秒	°，′，″
リットル	l，L
トン	t
電子ボルト	eV
原子質量単位	u

1 eV=1.60218×10^{-19}J

1 u=1.66054×10^{-27}kg

表5　SI接頭語

倍数	接頭語	記号
10^{18}	エクサ	E
10^{15}	ペタ	P
10^{12}	テラ	T
10^{9}	ギガ	G
10^{6}	メガ	M
10^{3}	キロ	k
10^{2}	ヘクト	h
10^{1}	デカ	da
10^{-1}	デシ	d
10^{-2}	センチ	c
10^{-3}	ミリ	m
10^{-6}	マイクロ	μ
10^{-9}	ナノ	n
10^{-12}	ピコ	p
10^{-15}	フェムト	f
10^{-18}	アト	a

表3　固有の名称をもつSI組立単位

量	名称	記号	他のSI単位による表現
周波数	ヘルツ	Hz	s^{-1}
力	ニュートン	N	$m\cdot kg/s^2$
圧力，応力	パスカル	Pa	N/m^2
エネルギー，仕事，熱量	ジュール	J	N·m
工率，放射束	ワット	W	J/s
電気量，電荷	クーロン	C	A·s
電位，電圧，起電力	ボルト	V	W/A
静電容量	ファラド	F	C/V
電気抵抗	オーム	Ω	V/A
コンダクタンス	ジーメンス	S	A/V
磁束	ウェーバ	Wb	V·s
磁束密度	テスラ	T	Wb/m^2
インダクタンス	ヘンリー	H	Wb/A
セルシウス温度	セルシウス度	℃	
光束	ルーメン	lm	cd·sr
照度	ルクス	lx	lm/m^2
放射能	ベクレル	Bq	s^{-1}
吸収線量	グレイ	Gy	J/kg
線量等量	シーベルト	Sv	J/kg

表4　SIと共に暫定的に維持される単位

名称	記号
オングストローム	Å
バーン	b
バール	bar
ガル	Gal
キュリー	Ci
レントゲン	R
ラド	rad
レム	rem

1 Å=0.1nm=10^{-10}m

1 b=100fm^2=10^{-28}m^2

1 bar=0.1MPa=10^5Pa

1 Gal=1cm/s^2=10^{-2}m/s^2

1 Ci=3.7×10^{10}Bq

1 R=2.58×10^{-4}C/kg

1 rad=1cGy=10^{-2}Gy

1 rem=1cSv=10^{-2}Sv

(注)

1．表1－5は「国際単位系」第5版，国際度量衡局1985年刊行による。ただし，1 eVおよび1 uの値はCODATAの1986年推奨値によった。

2．表4には海里，ノット，アール，ヘクタールも含まれているが日常の単位なのでここでは省略した。

3．barは，JISでは流体の圧力を表わす場合に限り表2のカテゴリーに分類されている。

4．EC閣僚理事会指令ではbar，barnおよび「血圧の単位」mmHgを表2のカテゴリーに入れている。

換算表

力	N(=10^5dyn)	kgf	lbf
	1	0.101972	0.224809
	9.80665	1	2.20462
	4.44822	0.453592	1

粘度　1 Pa·s(N·s/m^2)=10 P(ポアズ)(g/(cm·s))

動粘度　1m^2/s=10^4St(ストークス)(cm^2/s)

圧力	MPa(=10bar)	kgf/cm^2	atm	mmHg(Torr)	lbf/in^2(psi)
	1	10.1972	9.86923	7.50062×10^3	145.038
	0.0980665	1	0.967841	735.559	14.2233
	0.101325	1.03323	1	760	14.6959
	1.33322×10^{-4}	1.35951×10^{-3}	1.31579×10^{-3}	1	1.93368×10^{-2}
	6.89476×10^{-3}	7.03070×10^{-2}	6.80460×10^{-2}	51.7149	1

エネルギー・仕事・熱量	J(=10^7 erg)	kgf·m	kW·h	cal(計量法)	Btu	ft·lbf	eV
	1	0.101972	2.77778×10^{-7}	0.238889	9.47813×10^{-4}	0.737562	6.24150×10^{18}
	9.80665	1	2.72407×10^{-6}	2.34270	9.29487×10^{-3}	7.23301	6.12082×10^{19}
	3.6×10^6	3.67098×10^5	1	8.59999×10^5	3412.13	2.65522×10^6	2.24694×10^{25}
	4.18605	0.426858	1.16279×10^{-6}	1	3.96759×10^{-3}	3.08747	2.61272×10^{19}
	1055.06	107.586	2.93072×10^{-4}	252.042	1	778.172	6.58515×10^{21}
	1.35582	0.138255	3.76616×10^{-7}	0.323890	1.28506×10^{-3}	1	8.46233×10^{18}
	1.60218×10^{-19}	1.63377×10^{-20}	4.45050×10^{-26}	3.82743×10^{-20}	1.51857×10^{-22}	1.18171×10^{-19}	1

1 cal= 4.18605J（計量法）

= 4.184J（熱化学）

= 4.1855J（15℃）

= 4.1868J（国際蒸気表）

仕事率　1 PS(仏馬力)

= 75 kgf·m/s

= 735.499W

放射能	Bq	Ci
	1	2.70270×10^{-11}
	3.7×10^{10}	1

吸収線量	Gy	rad
	1	100
	0.01	1

照射線量	C/kg	R
	1	3876
	2.58×10^{-4}	1

線量当量	Sv	rem
	1	100
	0.01	1

(86年12月26日現在)

ANNUAL REPORT OF NAKA FUSION RESEARCH ESTABLISHMENT FROM APRIL 1, 1997 TO MARCH 31, 1998